## Supplemental Figures

Figure S1: Frequencies of lethal events under monthly and hourly data during past (1980-2000) climate and the predicted change in the future (2080-2099). Data are presented for nests laid at a depth of 3 cm under different shade conditions. White areas represent locations for which no heat events were predicted. Color scales are the same for figures S1-S4 to enable visual comparison between depths.

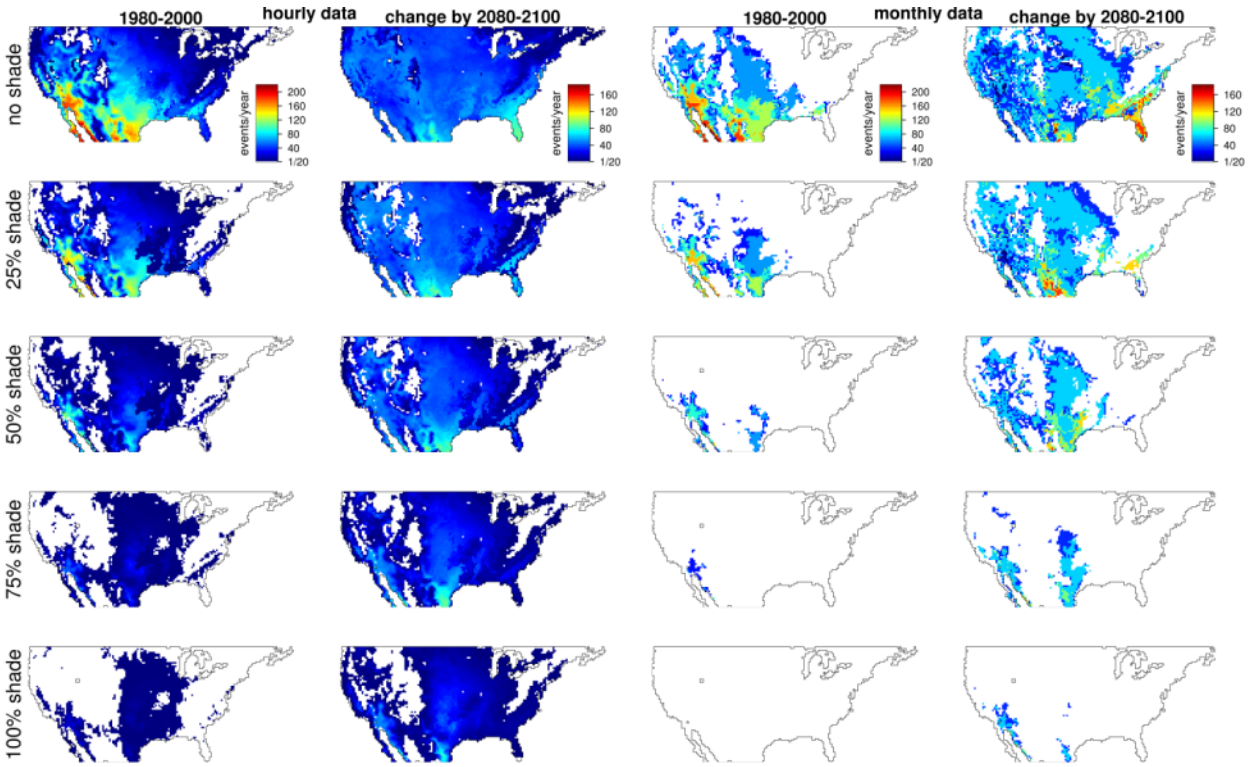

Figure S2: Frequencies of lethal events under monthly and hourly data during past (1980-2000) climate and the predicted change in the future (2080-2099). Data are presented for nests at a depth of 6 cm under different shade conditions. White areas represent locations for which no heat events were predicted. Color scales are the same for figures S1-S4 to enable visual comparison between depths.

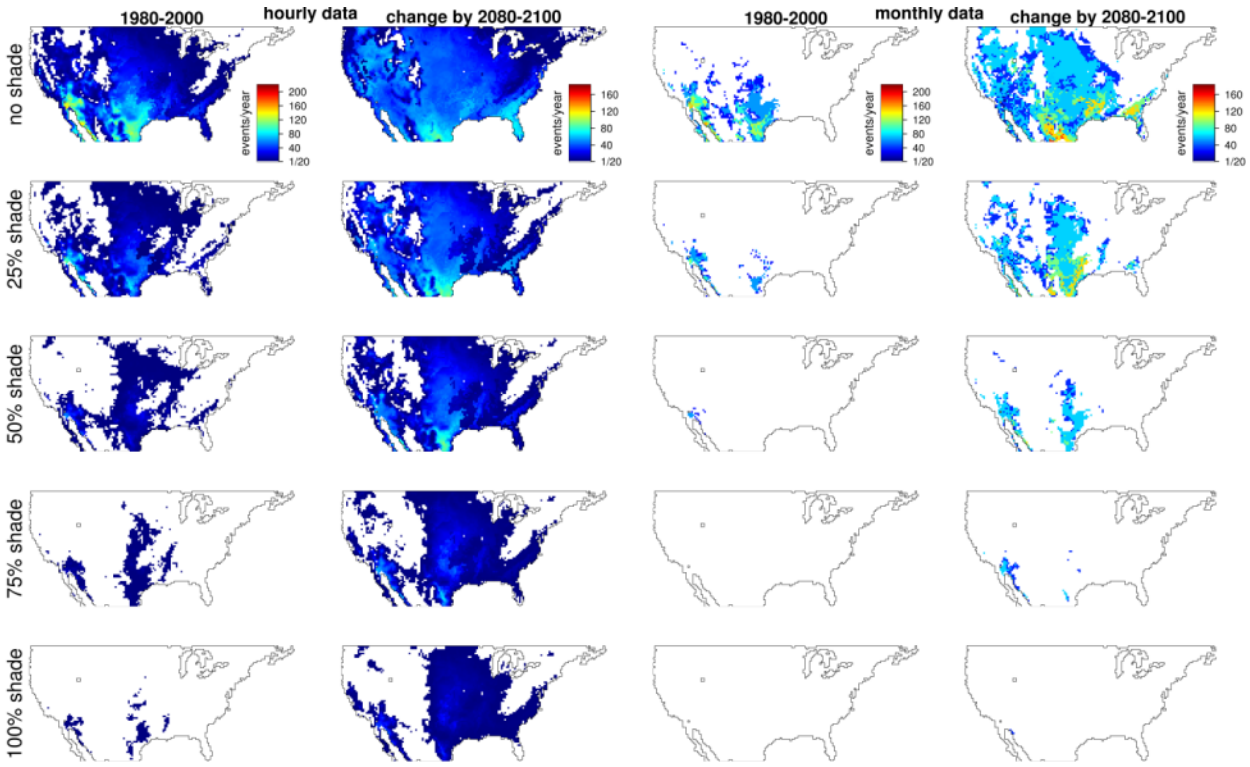

Figure S3: Frequencies of lethal events under monthly and hourly data during past (1980-2000) climate and the predicted change in the future (2080-2099). Data are presented for nests at a depth of 9 cm under different shade conditions. White areas represent locations for which no heat events were predicted. Color scales are the same for figures S1-S4 to enable visual comparison between depths.

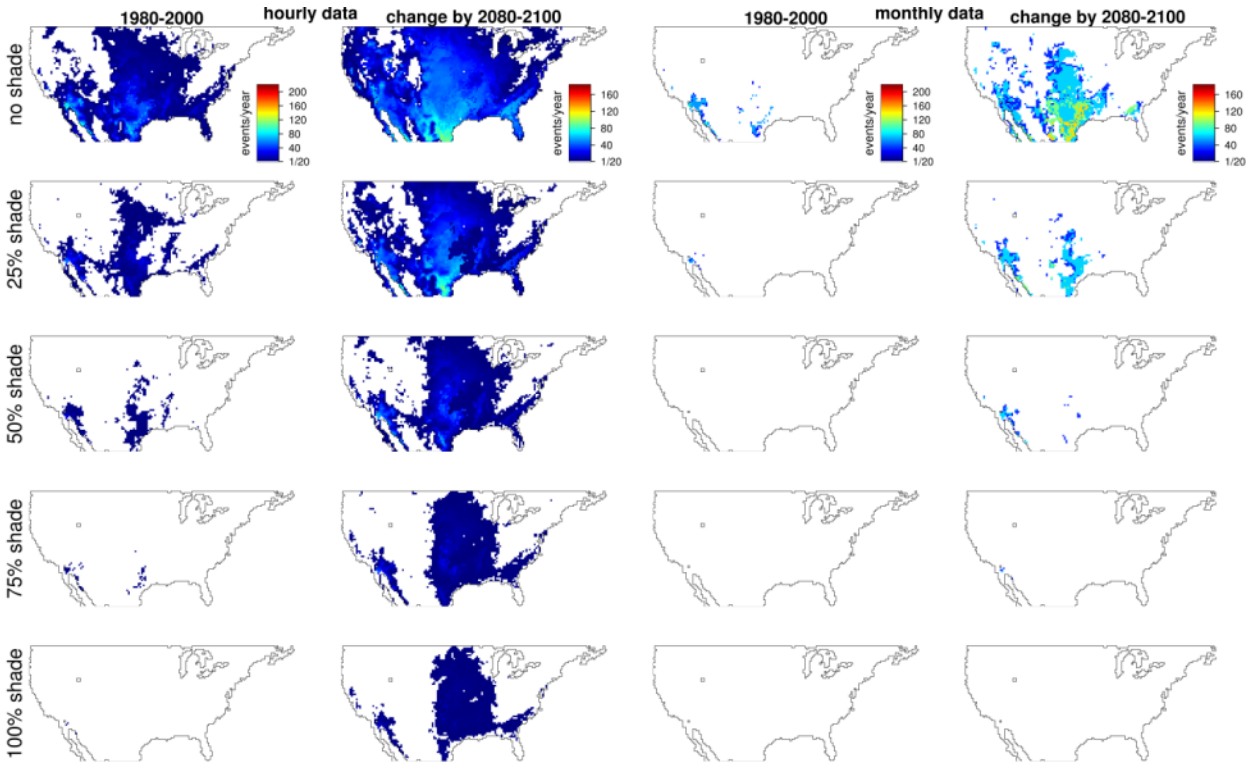

Figure S4: Frequencies of lethal events under monthly and hourly data during past (1980-2000) climate and the predicted change in the future (2080-2099). Data are presented for nests at a depth of 12 cm under different shade conditions. White areas represent locations for which no heat events were predicted. Color scales are the same for figures S1-S4 to enable visual comparison between depths.

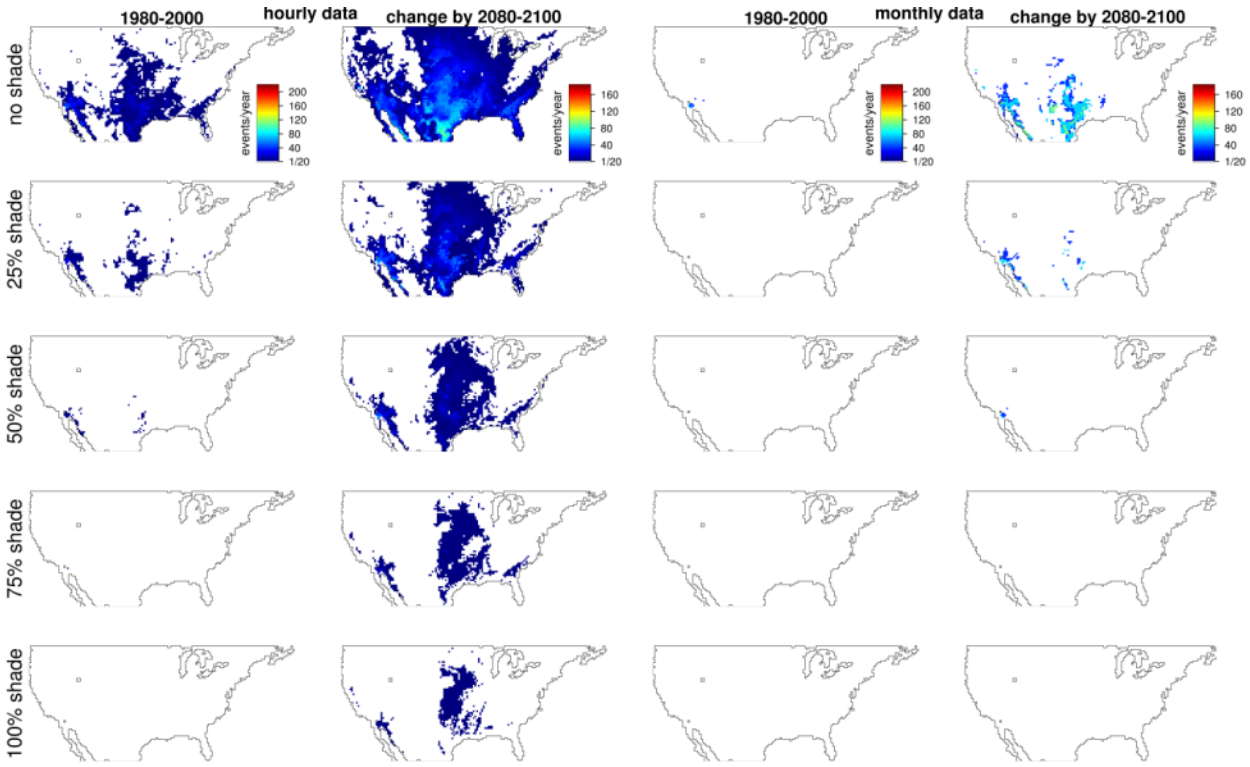

Figure S5: Predictions of embryonic survival rates in the period of 1980-2000 and the predicted change in the future (2080-2100) for embryos that were laid in April at 3 cm depth. Predictions are shown for a scale of shade conditions above the nest and for both hourly and monthly climate resolutions. White areas represent locations for which climate conditions did not enable enough activity to promote reproduction. Color scales are the same for figures S5-S32 to enable visual comparison between different combinations of oviposition months and nests depths.

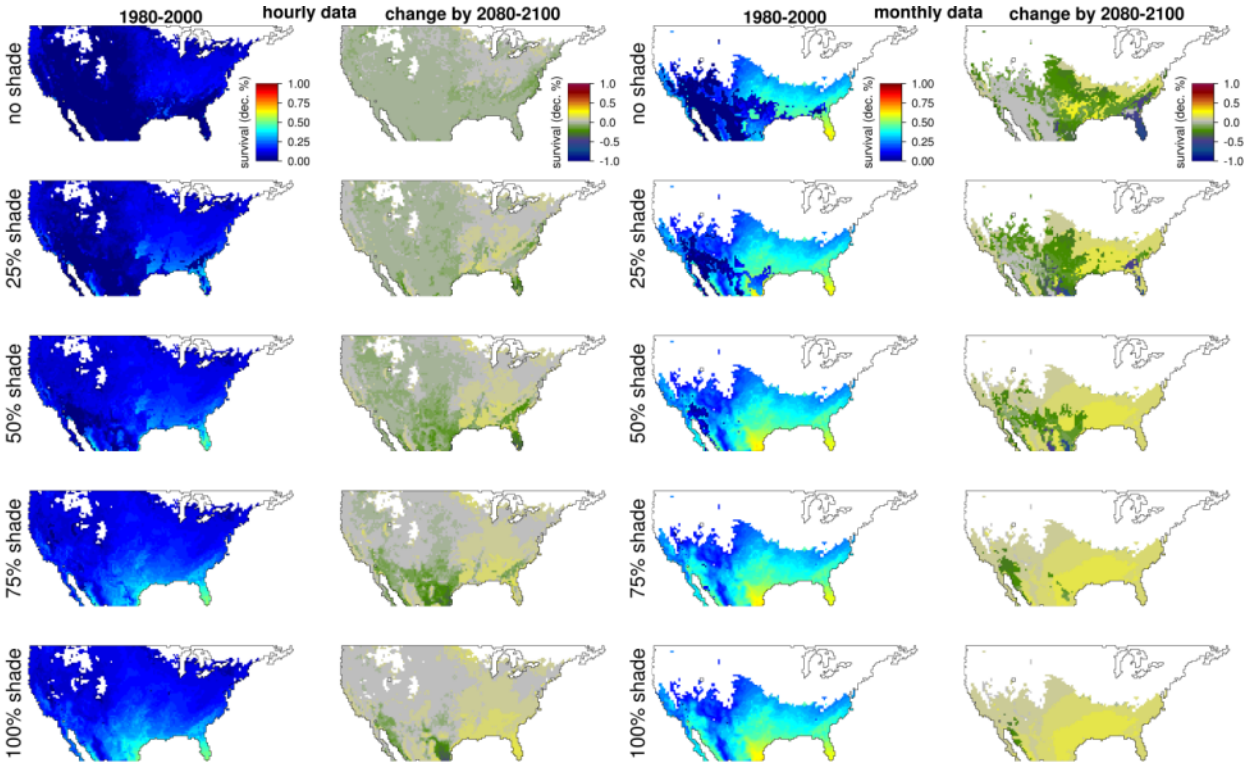

Figure S6: Predictions of embryonic survival rates in the period of 1980-2000 and the predicted change in the future (2080-2100) for embryos that were laid in April at 6 cm depth. Predictions are shown for a scale of shade conditions above the nest and for both hourly and monthly climate resolutions. White areas represent locations for which climate conditions did not enable enough activity to promote reproduction. Color scales are the same for figures S5-S32 to enable visual comparison between different combinations of oviposition months and nests depths.

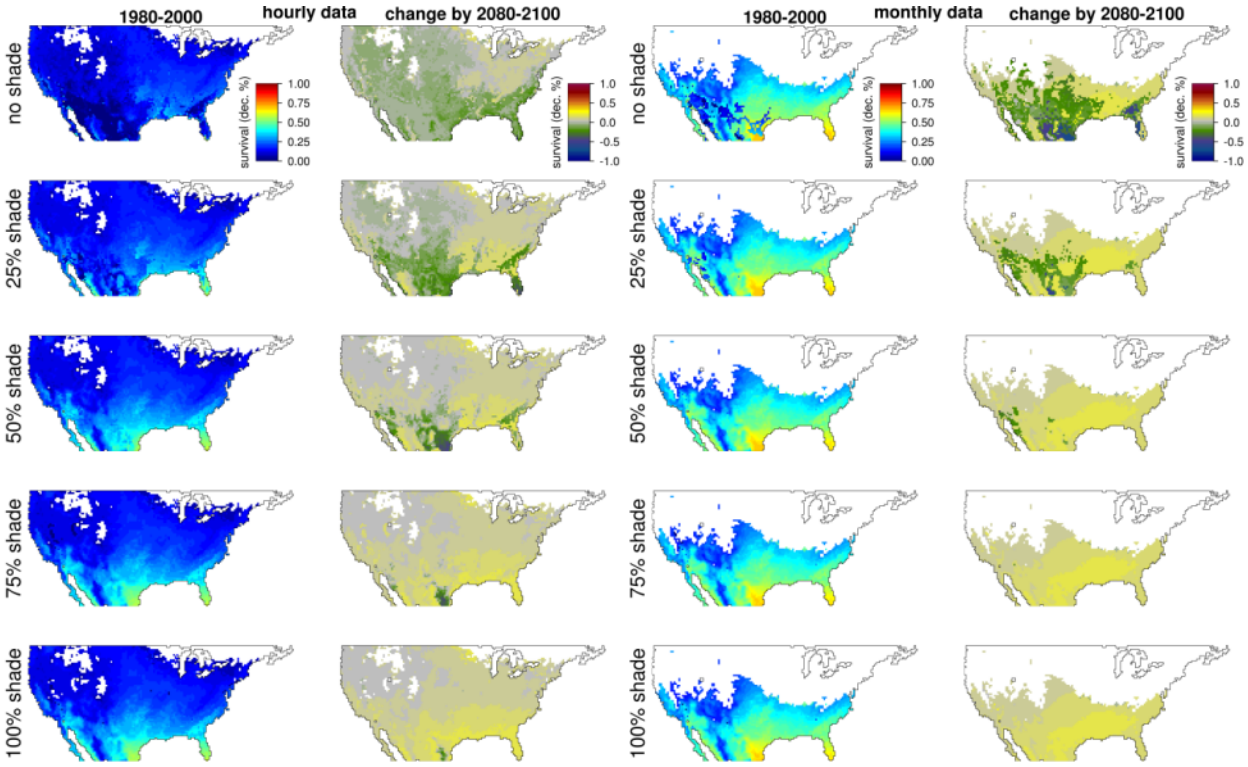

Figure S7: Predictions of embryonic survival rates in the period of 1980-2000 and the predicted change in the future (2080-2100) for embryos that were laid in April at 9 cm depth. Predictions are shown for a scale of shade conditions above the nest and for both hourly and monthly climate resolutions. White areas represent locations for which climate conditions did not enable enough activity to promote reproduction. Color scales are the same for figures S5-S32 to enable visual comparison between different combinations of oviposition months and nests depths.

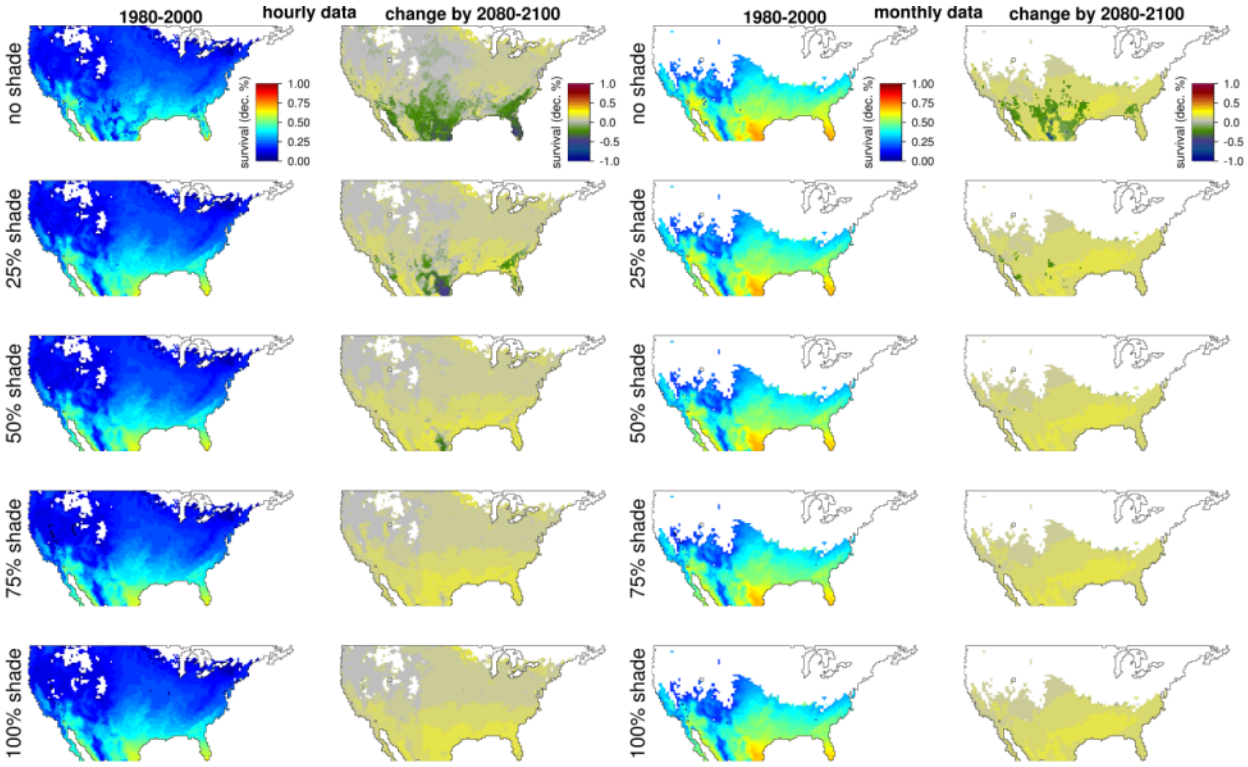

Figure S8: Predictions of embryonic survival rates in the period of 1980-2000 and the predicted change in the future (2080-2100) for embryos that were laid in April at 12 cm depth. Predictions are shown for a scale of shade conditions above the nest and for both hourly and monthly climate resolutions. White areas represent locations for which climate conditions did not enable enough activity to promote reproduction. Color scales are the same for figures S5-S32 to enable visual comparison between different combinations of oviposition months and nests depths.

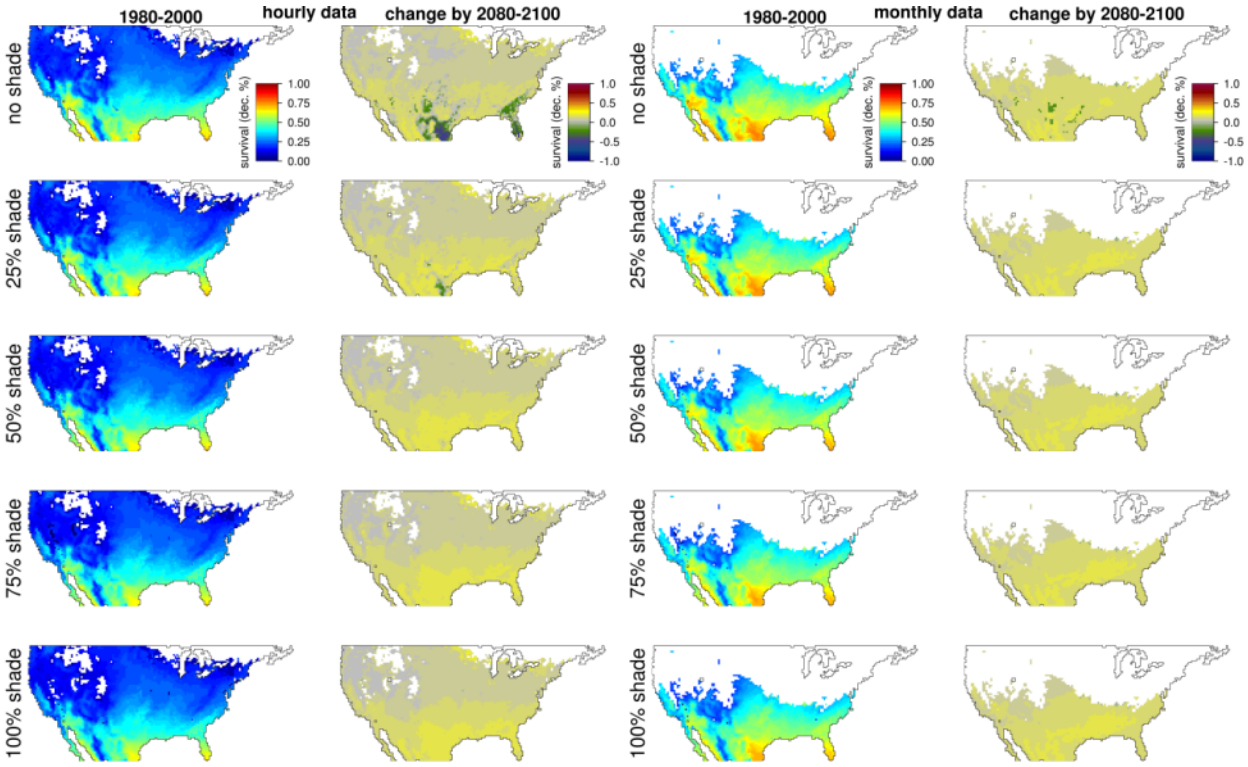

Figure S9: Predictions of embryonic survival rates in the period of 1980-2000 and the predicted change in the future (2080-2100) for embryos that were laid in May at 3 cm depth. Predictions are shown for a scale of shade conditions above the nest and for both hourly and monthly climate resolutions. White areas represent locations for which climate conditions did not enable enough activity to promote reproduction. Color scales are the same for figures S5-S32 to enable visual comparison between different combinations of oviposition months and nests depths.

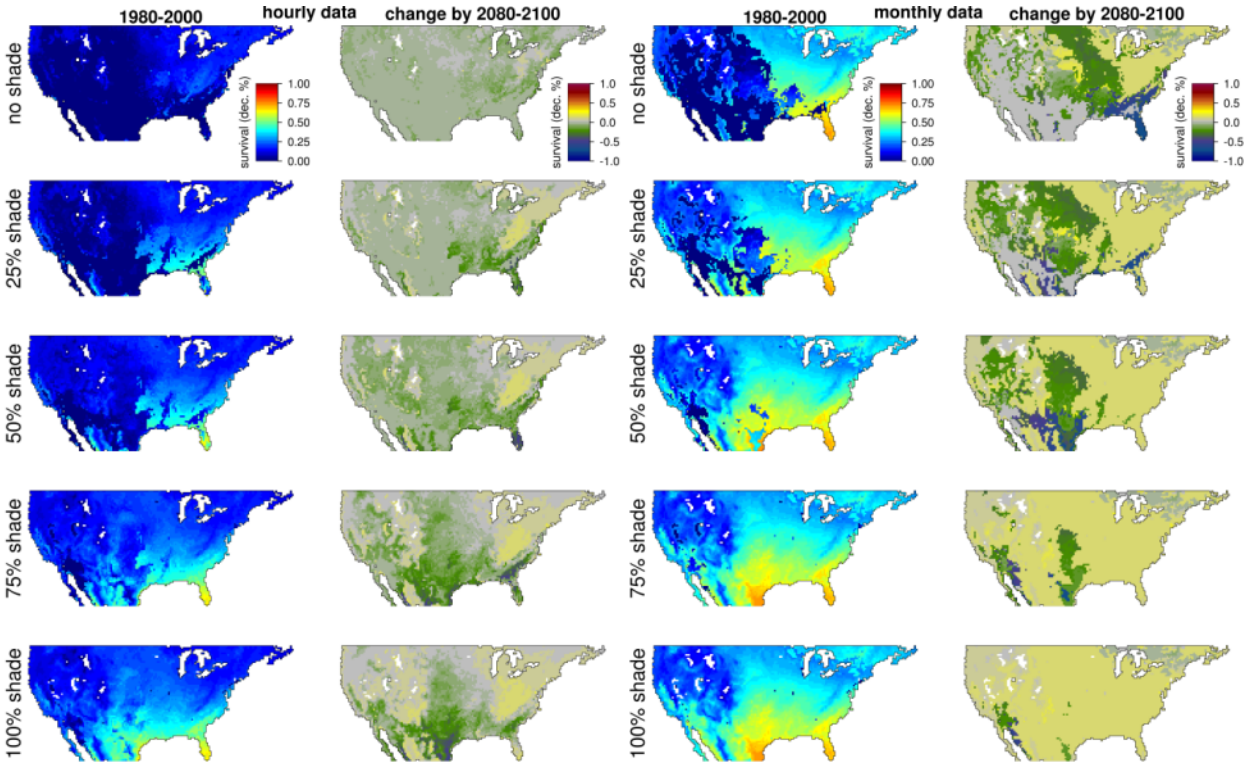

Figure S10: Predictions of embryonic survival rates in the period of 1980-2000 and the predicted change in the future (2080-2100) for embryos that were laid in May at 6 cm depth. Predictions are shown for a scale of shade conditions above the nest and for both hourly and monthly climate resolutions. White areas represent locations for which climate conditions did not enable enough activity to promote reproduction. Color scales are the same for figures S5-S32 to enable visual comparison between different combinations of oviposition months and nests depths.

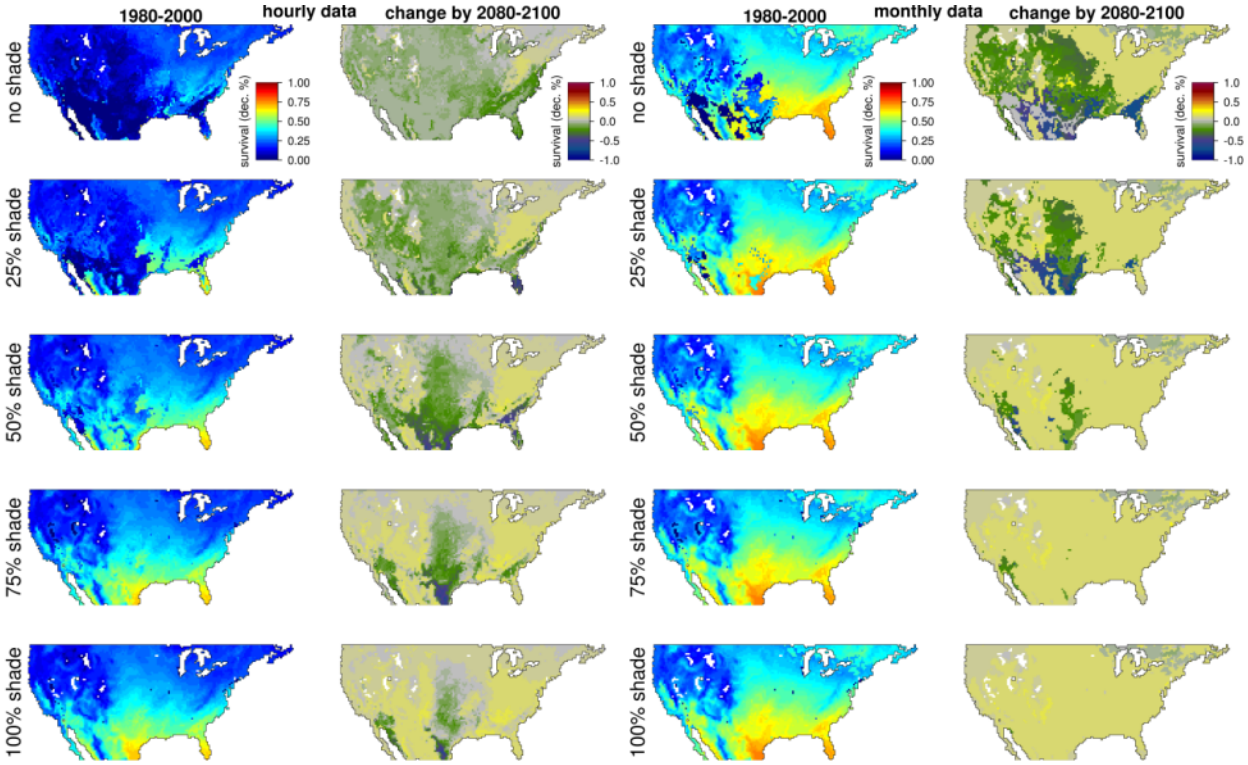

Figure S11: Predictions of embryonic survival rates in the period of 1980-2000 and the predicted change in the future (2080-2100) for embryos that were laid in May at 9 cm depth. Predictions are shown for a scale of shade conditions above the nest and for both hourly and monthly climate resolutions. Color scales are the same for figures S5-S32 to enable visual comparison between different combinations of oviposition months and nests depths.

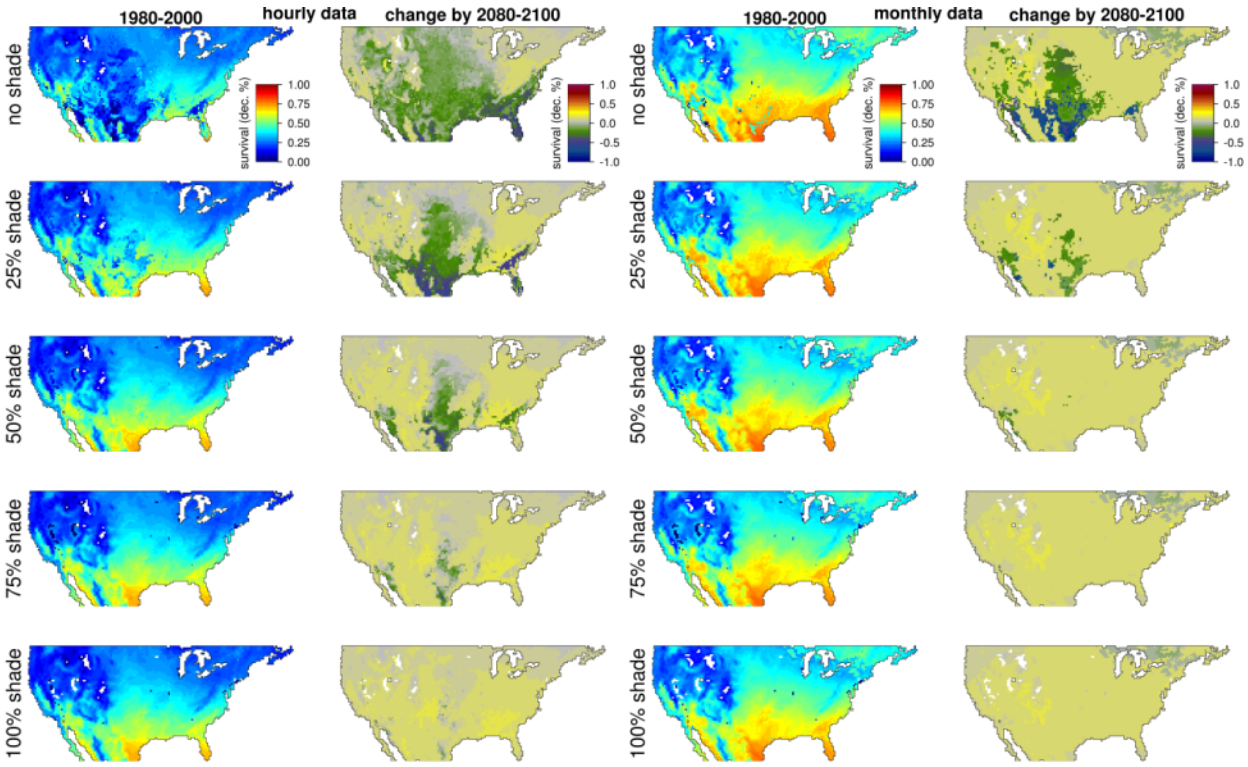

Figure S12: Predictions of embryonic survival rates in the period of 1980-2000 and the predicted change in the future (2080-2100) for embryos that were laid in May at 12 cm depth. Predictions are shown for a scale of shade conditions above the nest and for both hourly and monthly climate resolutions. Color scales are the same for figures S5-S32 to enable visual comparison between different combinations of oviposition months and nests depths.

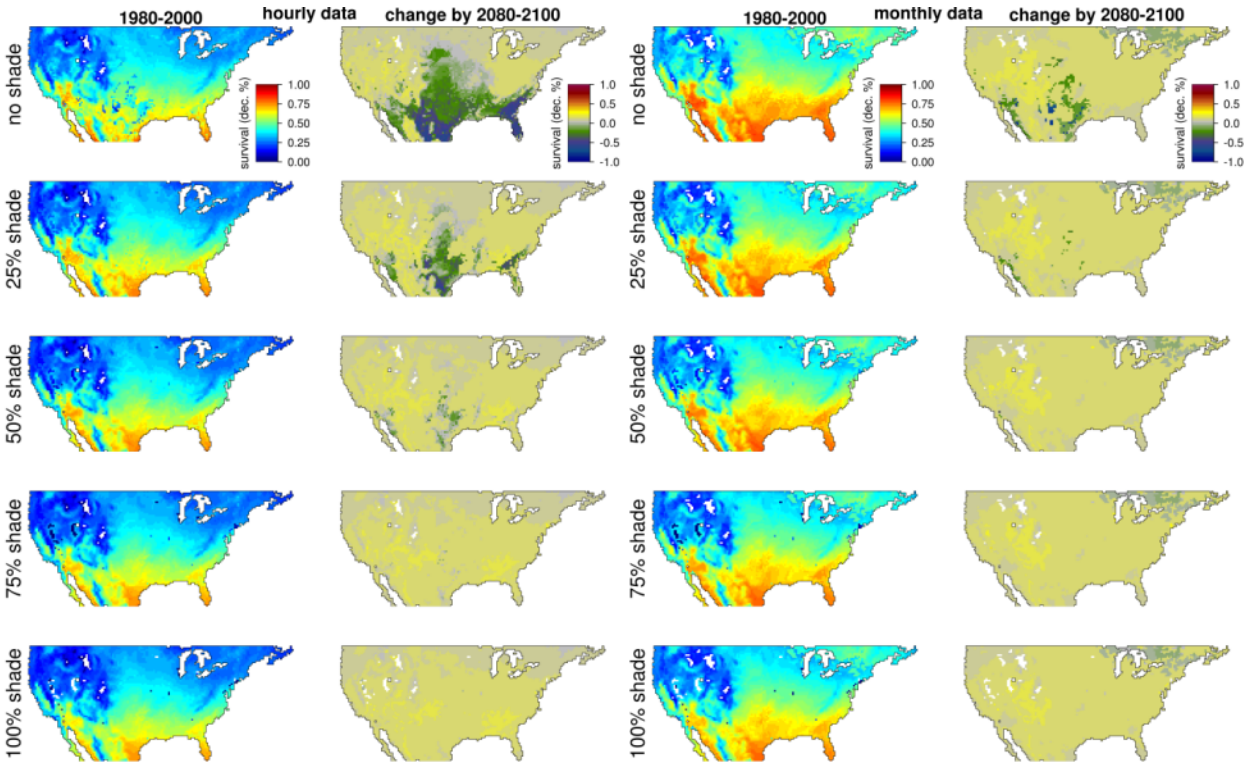

Figure S13: Predictions of embryonic survival rates in the period of 1980-2000 and the predicted change in the future (2080-2100) for embryos that were laid in June at 3 cm depth. Predictions are shown for a scale of shade conditions above the nest and for both hourly and monthly climate resolutions. Color scales are the same for figures S5-S32 to enable visual comparison between different combinations of oviposition months and nests depths.

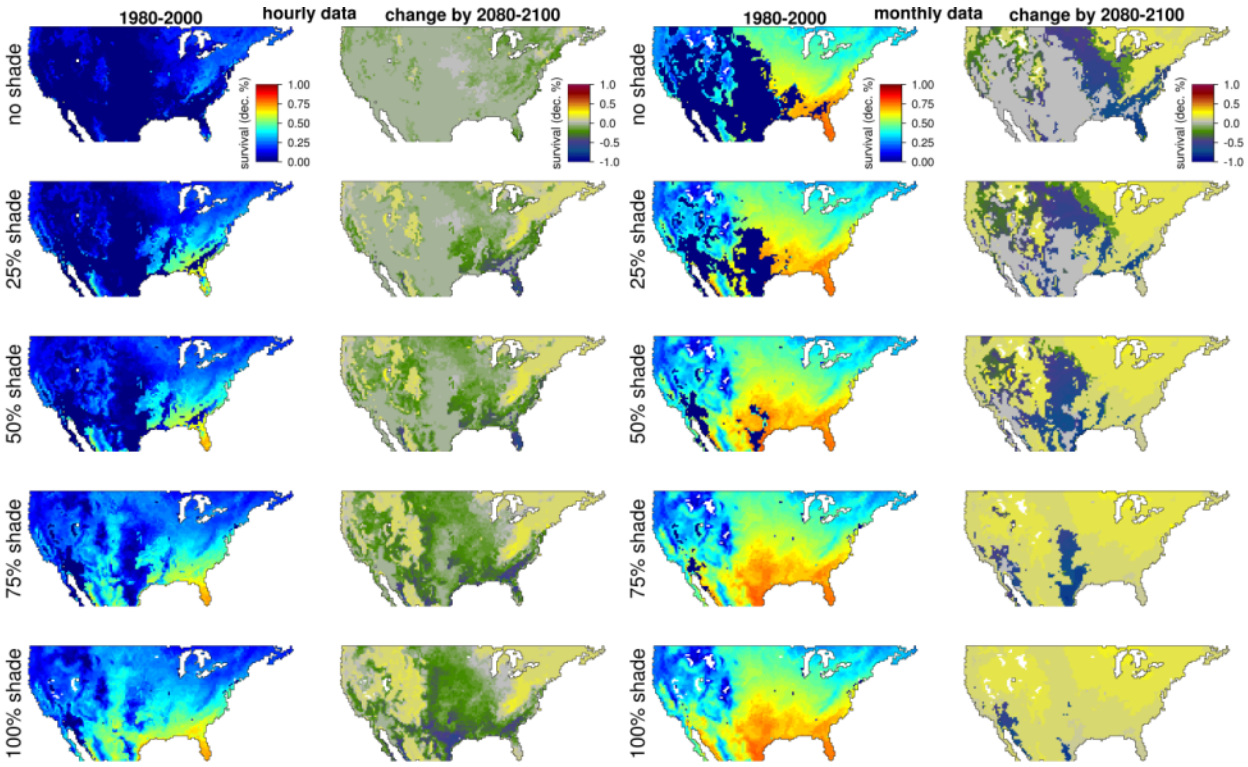

Figure S14: Predictions of embryonic survival rates in the period of 1980-2000 and the predicted change in the future (2080-2100) for embryos that were laid in June at 6 cm depth. Predictions are shown for a scale of shade conditions above the nest and for both hourly and monthly climate resolutions. Color scales are the same for figures S5-S32 to enable visual comparison between different combinations of oviposition months and nests depths.

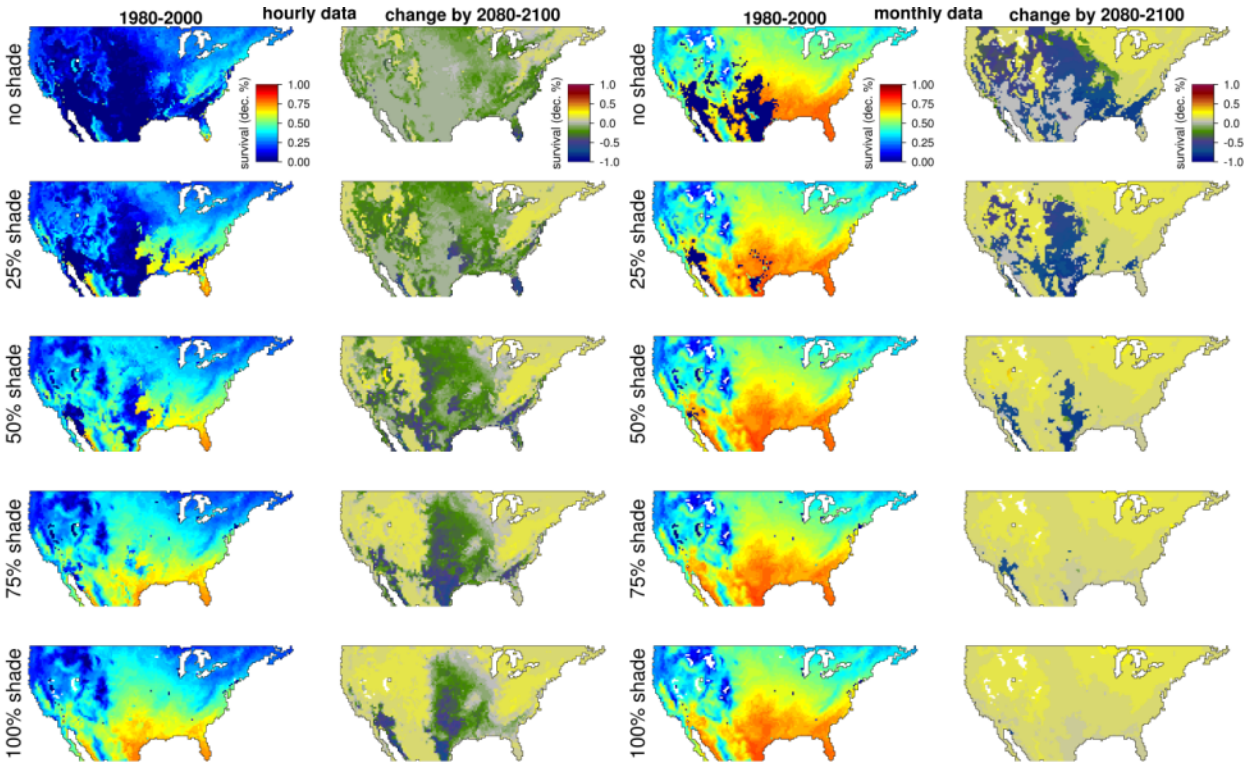

Figure S15: Predictions of embryonic survival rates in the period of 1980-2000 and the predicted change in the future (2080-2100) for embryos that were laid in June at 9 cm depth. Predictions are shown for a scale of shade conditions above the nest and for both hourly and monthly climate resolutions. Color scales are the same for figures S5-S32 to enable visual comparison between different combinations of oviposition months and nests depths.

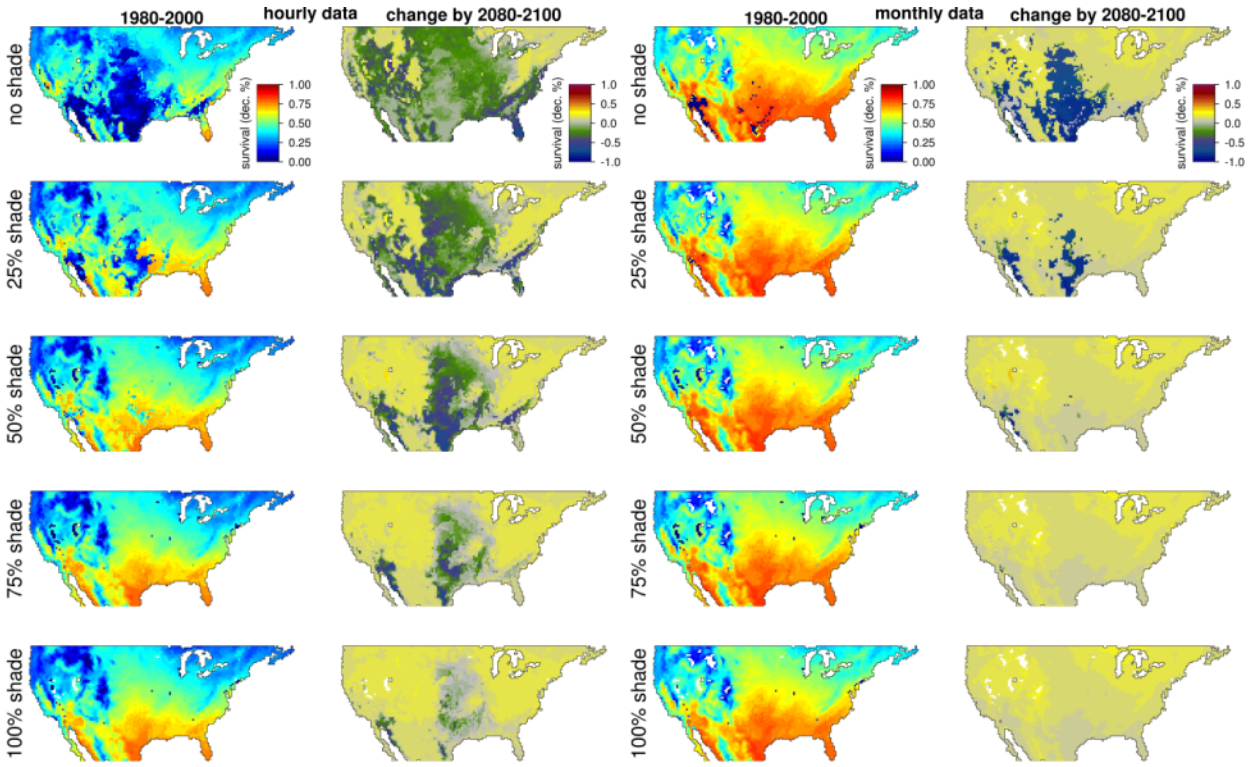

Figure S16: Predictions of embryonic survival rates in the period of 1980-2000 and the predicted change in the future (2080-2100) for embryos that were laid in June at 12 cm depth. Predictions are shown for a scale of shade conditions above the nest and for both hourly and monthly climate resolutions. Color scales are the same for figures S5-S32 to enable visual comparison between different combinations of oviposition months and nests depths.

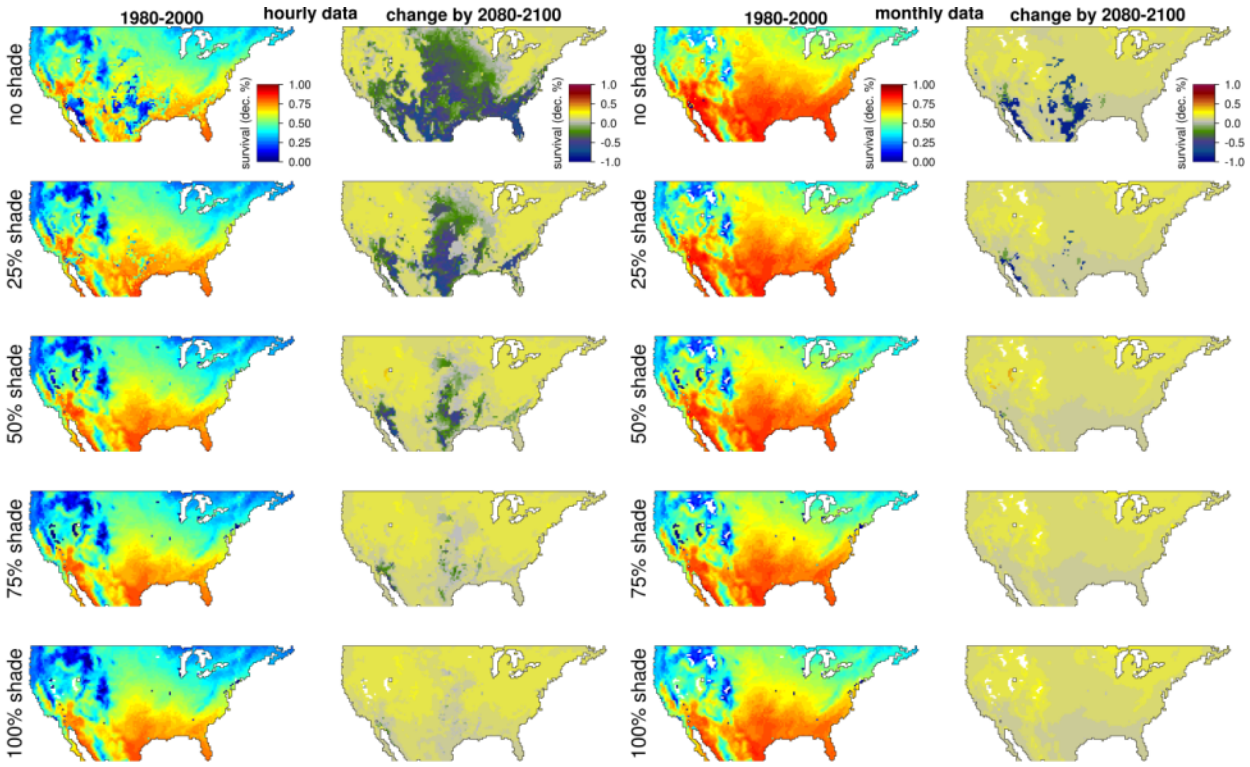

Figure S17: Predictions of embryonic survival rates in the period of 1980-2000 and the predicted change in the future (2080-2100) for embryos that were laid in July at 3 cm depth. Predictions are shown for a scale of shade conditions above the nest and for both hourly and monthly climate resolutions. Color scales are the same for figures S5-S32 to enable visual comparison between different combinations of oviposition months and nests depths.

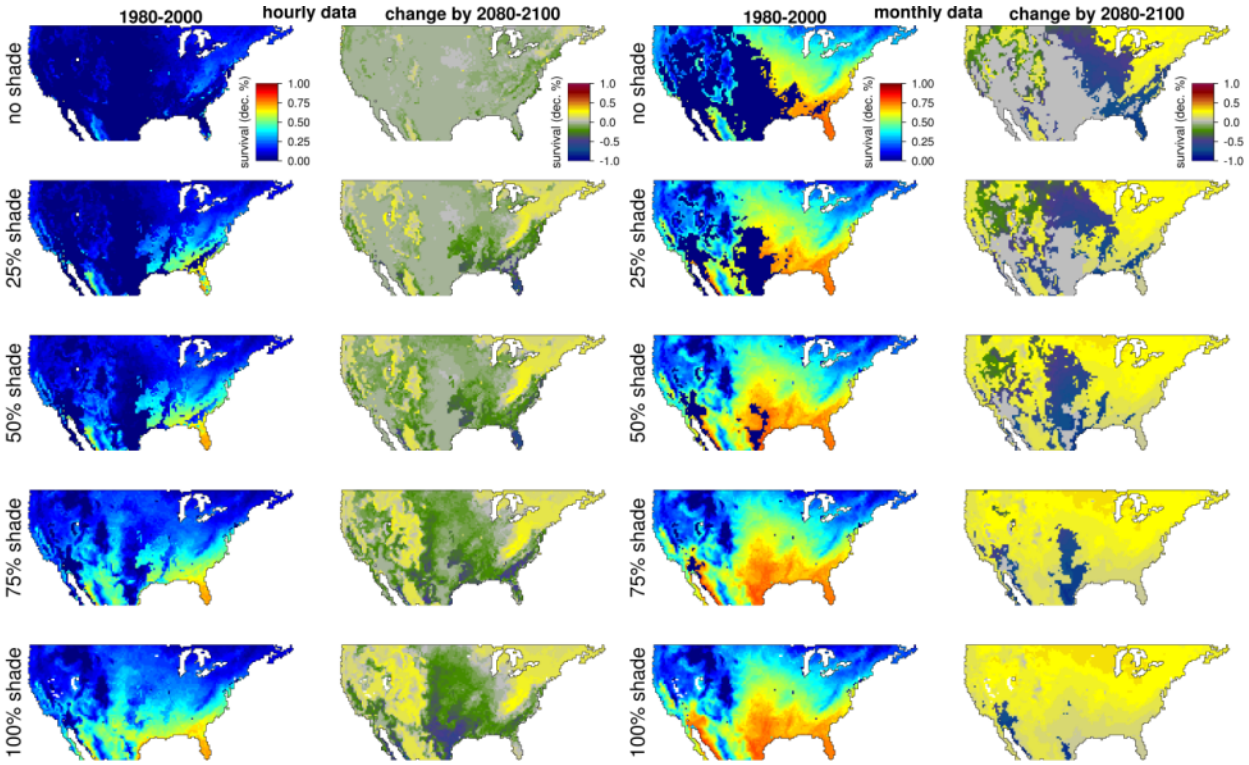

Figure S18: Predictions of embryonic survival rates in the period of 1980-2000 and the predicted change in the future (2080-2100) for embryos that were laid in July at 6 cm depth. Predictions are shown for a scale of shade conditions above the nest and for both hourly and monthly climate resolutions. Color scales are the same for figures S5-S32 to enable visual comparison between different combinations of oviposition months and nests depths.

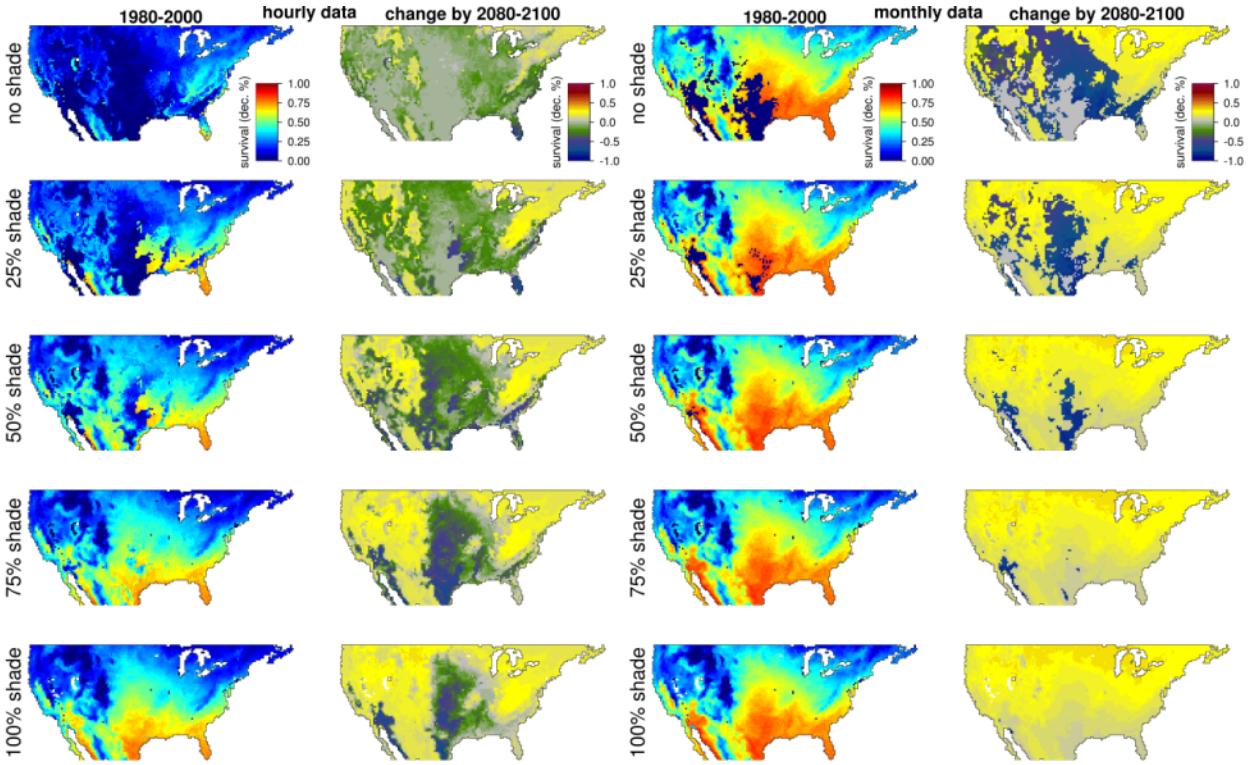

Figure S19: Predictions of embryonic survival rates in the period of 1980-2000 and the predicted change in the future (2080-2100) for embryos that were laid in July at 9 cm depth. Predictions are shown for a scale of shade conditions above the nest and for both hourly and monthly climate resolutions. Color scales are the same for figures S5-S32 to enable visual comparison between different combinations of oviposition months and nests depths.

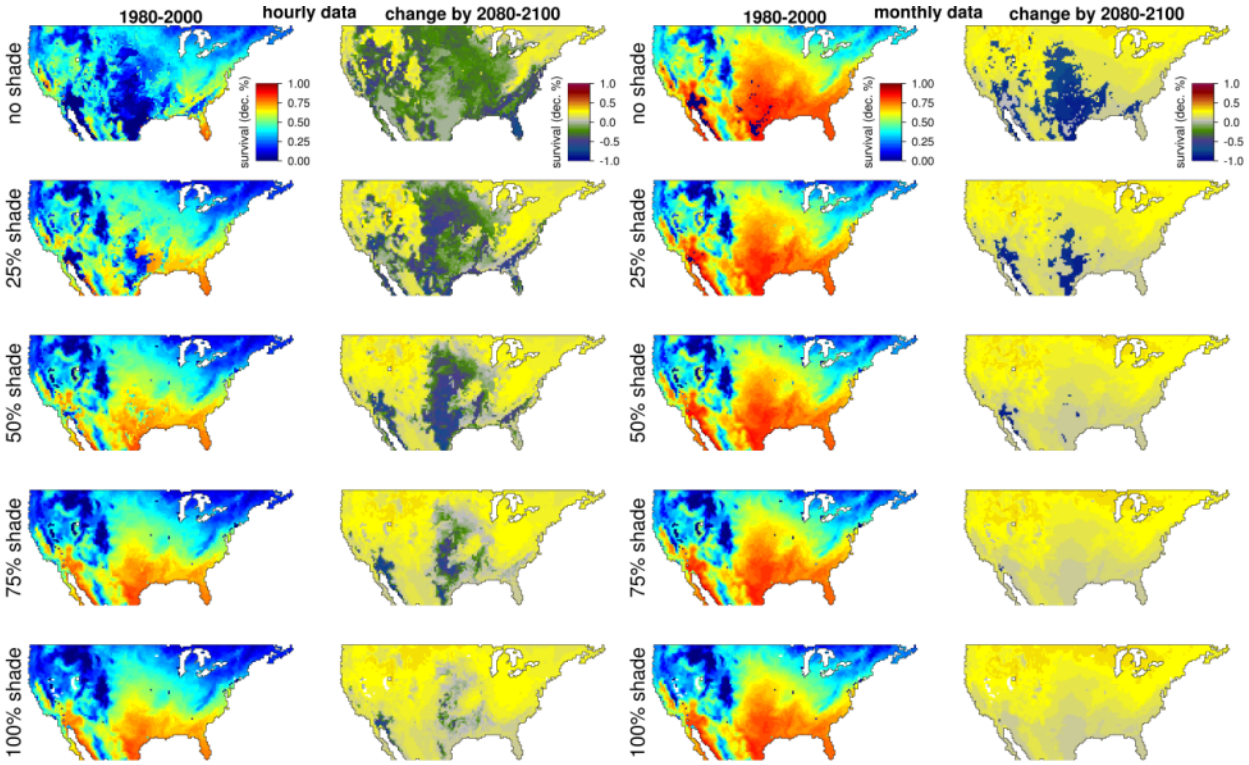

Figure S20: Predictions of embryonic survival rates in the period of 1980-2000 and the predicted change in the future (2080-2100) for embryos that were laid in July at 12 cm depth. Predictions are shown for a scale of shade conditions above the nest and for both hourly and monthly climate resolutions. Color scales are the same for figures S5-S32 to enable visual comparison between different combinations of oviposition months and nests depths.

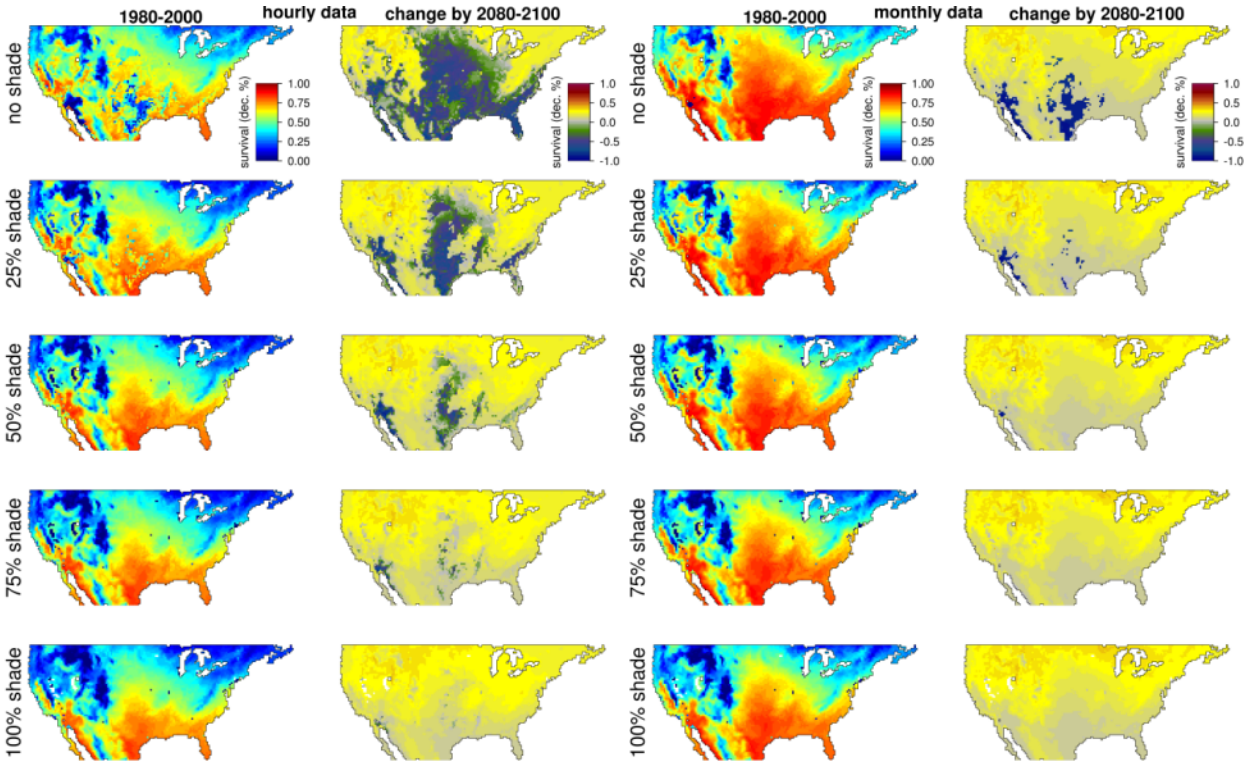

Figure S21: Predictions of embryonic survival rates in the period of 1980-2000 and the predicted change in the future (2080-2100) for embryos that were laid in August at 3 cm depth. Predictions are shown for a scale of shade conditions above the nest and for both hourly and monthly climate resolutions. Color scales are the same for figures S5-S32 to enable visual comparison between different combinations of oviposition months and nests depths.

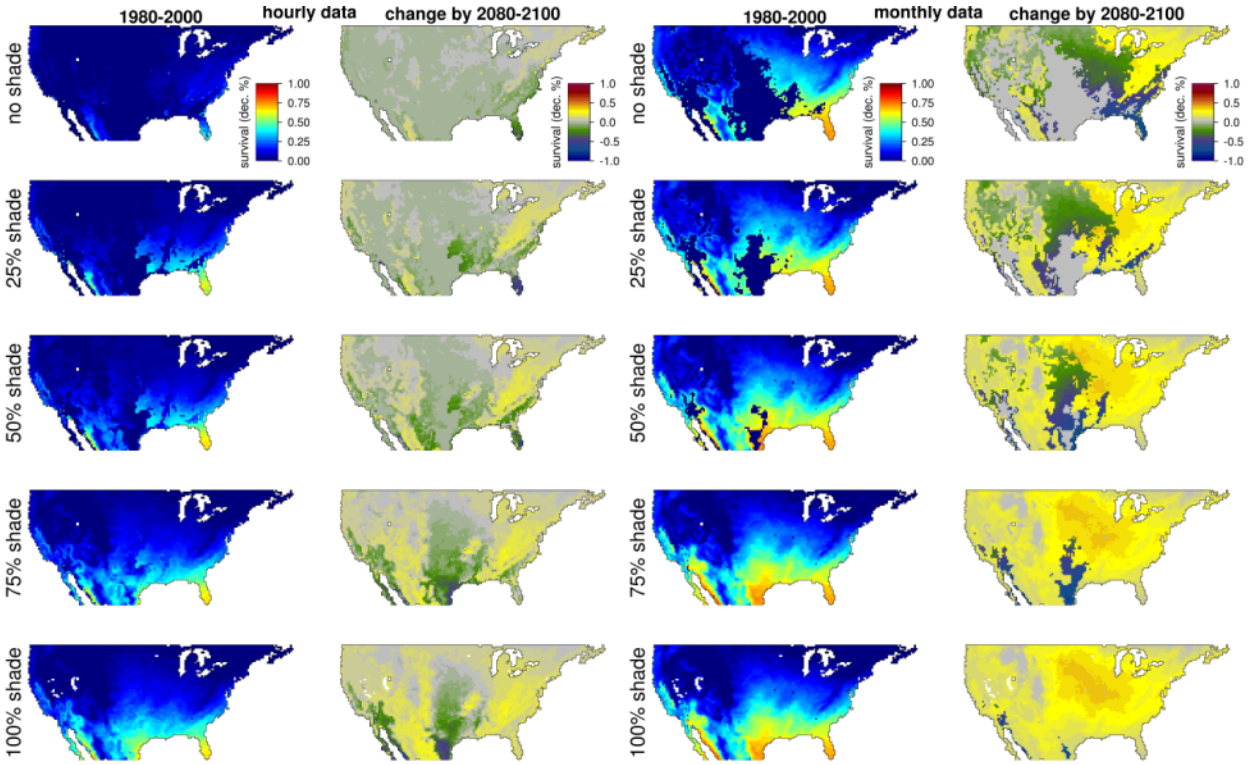

Figure S22: Predictions of embryonic survival rates in the period of 1980-2000 and the predicted change in the future (2080-2100) for embryos that were laid in August at 6 cm depth. Predictions are shown for a scale of shade conditions above the nest and for both hourly and monthly climate resolutions. Color scales are the same for figures S5-S32 to enable visual comparison between different combinations of oviposition months and nests depths.

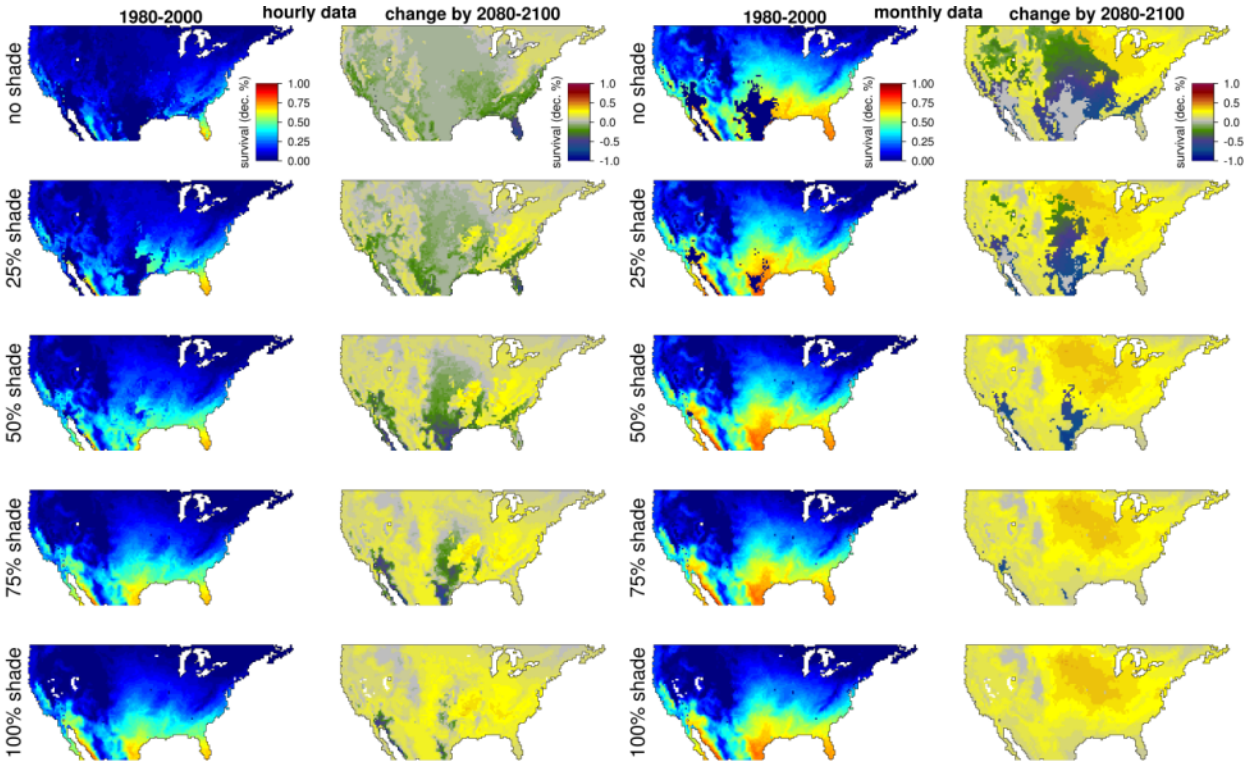

Figure S23: Predictions of embryonic survival rates in the period of 1980-2000 and the predicted change in the future (2080-2100) for embryos that were laid in August at 9 cm depth. Predictions are shown for a scale of shade conditions above the nest and for both hourly and monthly climate resolutions. Color scales are the same for figures S5-S32 to enable visual comparison between different combinations of oviposition months and nests depths.

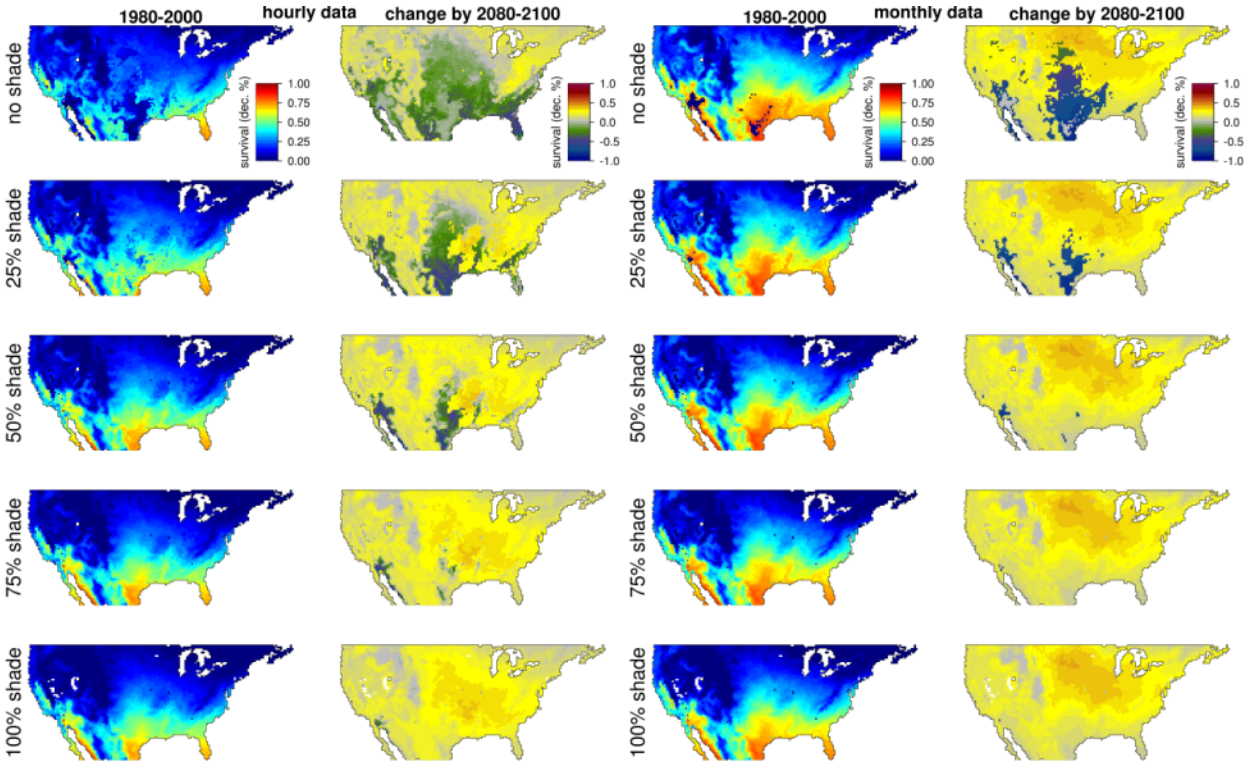

Figure S24: Predictions of embryonic survival rates in the period of 1980-2000 and the predicted change in the future (2080-2100) for embryos that were laid in August at 12 cm depth. Predictions are shown for a scale of shade conditions above the nest and for both hourly and monthly climate resolutions. Color scales are the same for figures S5-S32 to enable visual comparison between different combinations of oviposition months and nests depths.

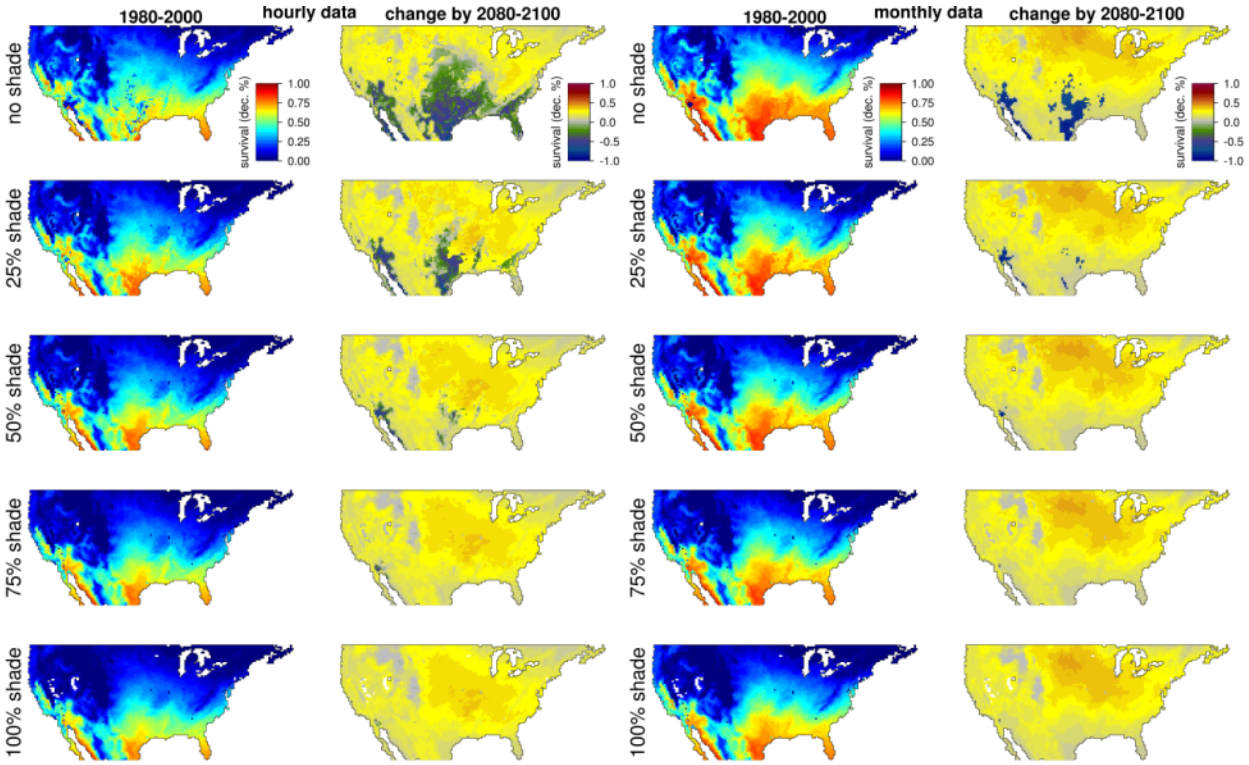

Figure S25: Predictions of embryonic survival rates in the period of 1980-2000 and the predicted change in the future (2080-2100) for embryos that were laid in September at 3 cm depth. Predictions are shown for a scale of shade conditions above the nest and for both hourly and monthly climate resolutions. Color scales are the same for figures S5-S32 to enable visual comparison between different combinations of oviposition months and nests depths.

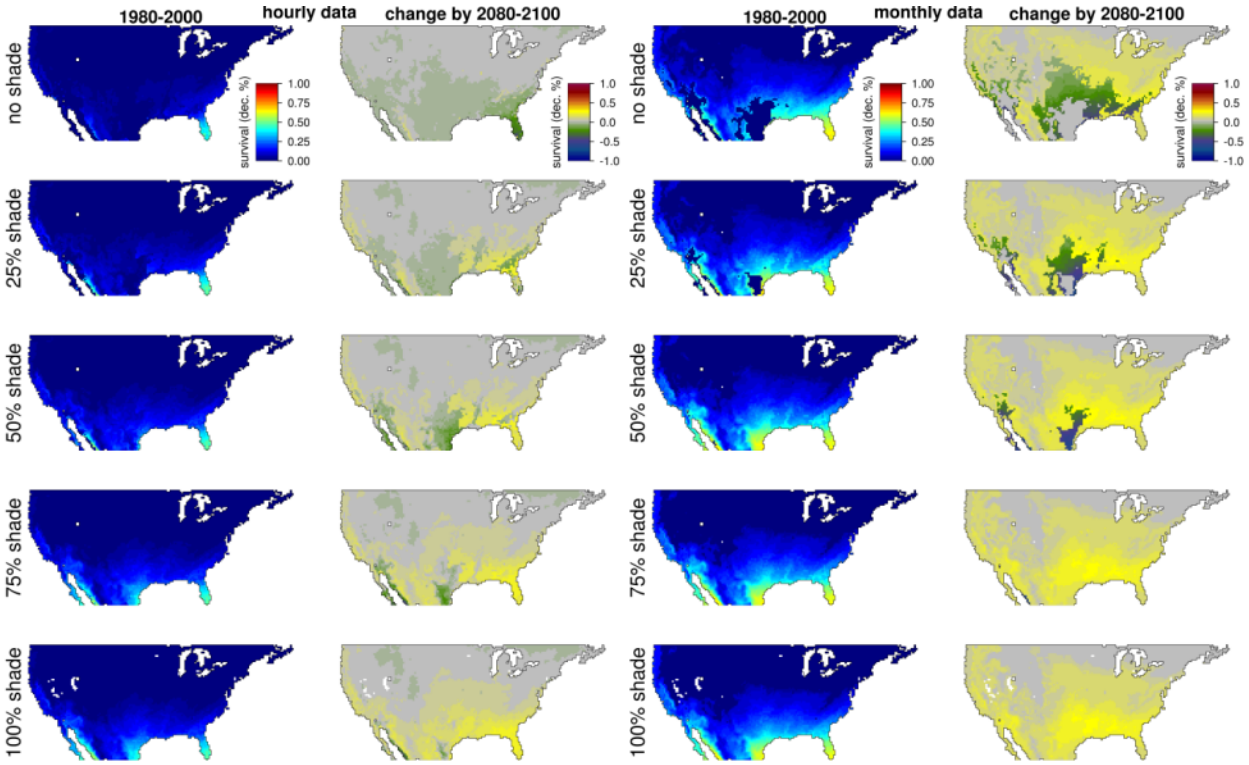

Figure S26: Predictions of embryonic survival rates in the period of 1980-2000 and the predicted change in the future (2080-2100) for embryos that were laid in September at 6 cm depth. Predictions are shown for a scale of shade conditions above the nest and for both hourly and monthly climate resolutions. Color scales are the same for figures S5-S32 to enable visual comparison between different combinations of oviposition months and nests depths.

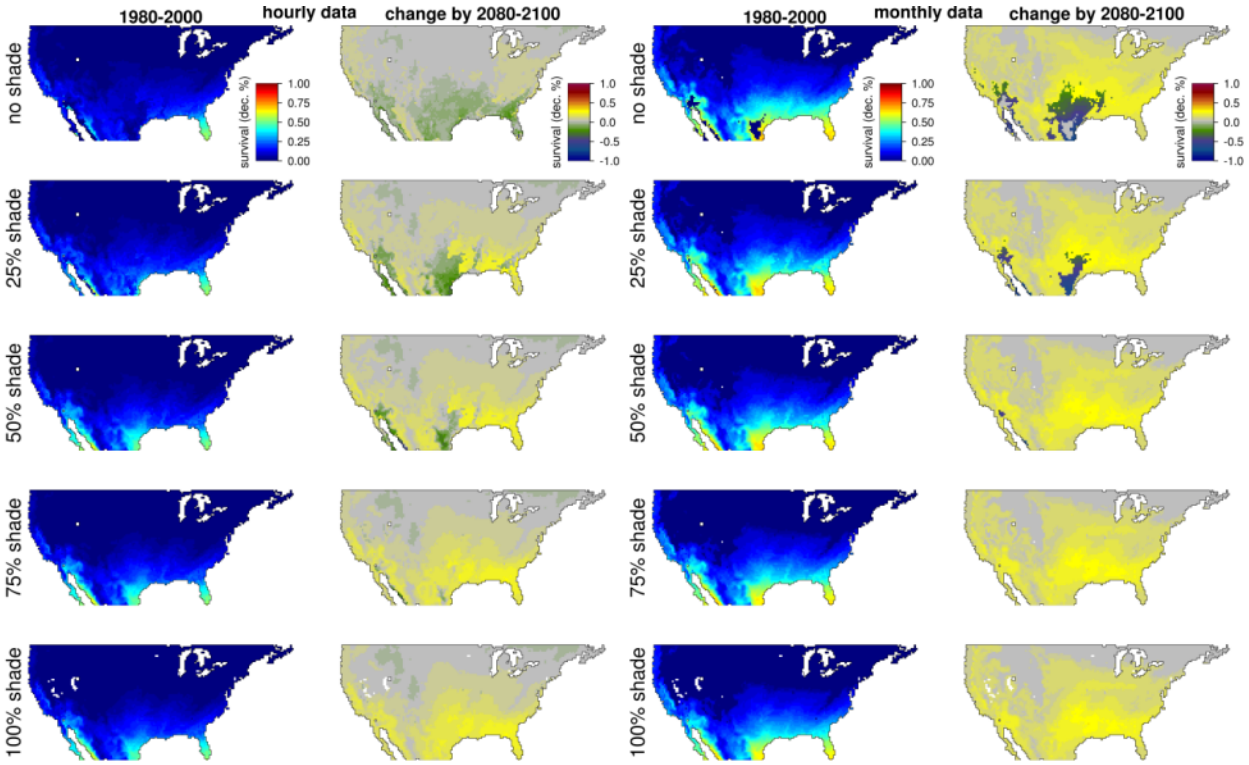

Figure S27: Predictions of embryonic survival rates in the period of 1980-2000 and the predicted change in the future (2080-2100) for embryos that were laid in September at 9 cm depth. Predictions are shown for a scale of shade conditions above the nest and for both hourly and monthly climate resolutions. Color scales are the same for figures S5-S32 to enable visual comparison between different combinations of oviposition months and nests depths.

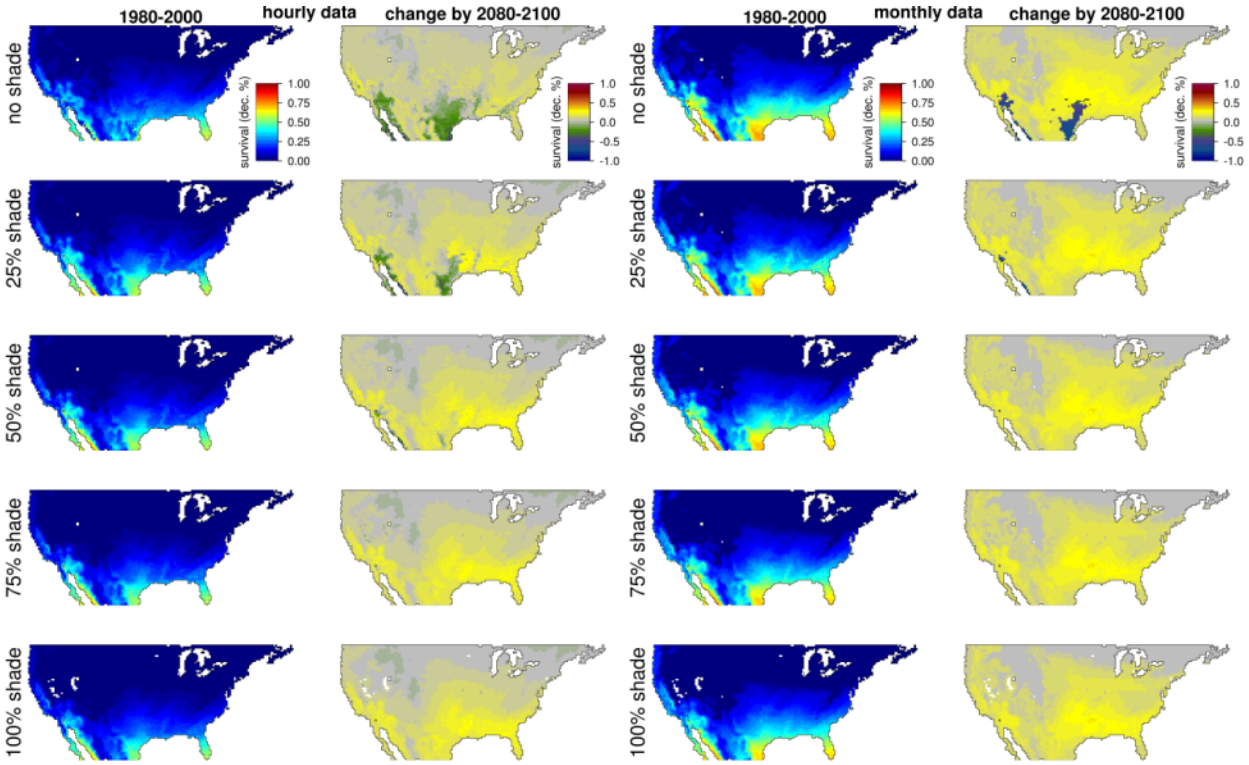

Figure S28: Predictions of embryonic survival rates in the period of 1980-2000 and the predicted change in the future (2080-2100) for embryos that were laid in September at 12 cm depth. Predictions are shown for a scale of shade conditions above the nest and for both hourly and monthly climate resolutions. Color scales are the same for figures S5-S32 to enable visual comparison between different combinations of oviposition months and nests depths.

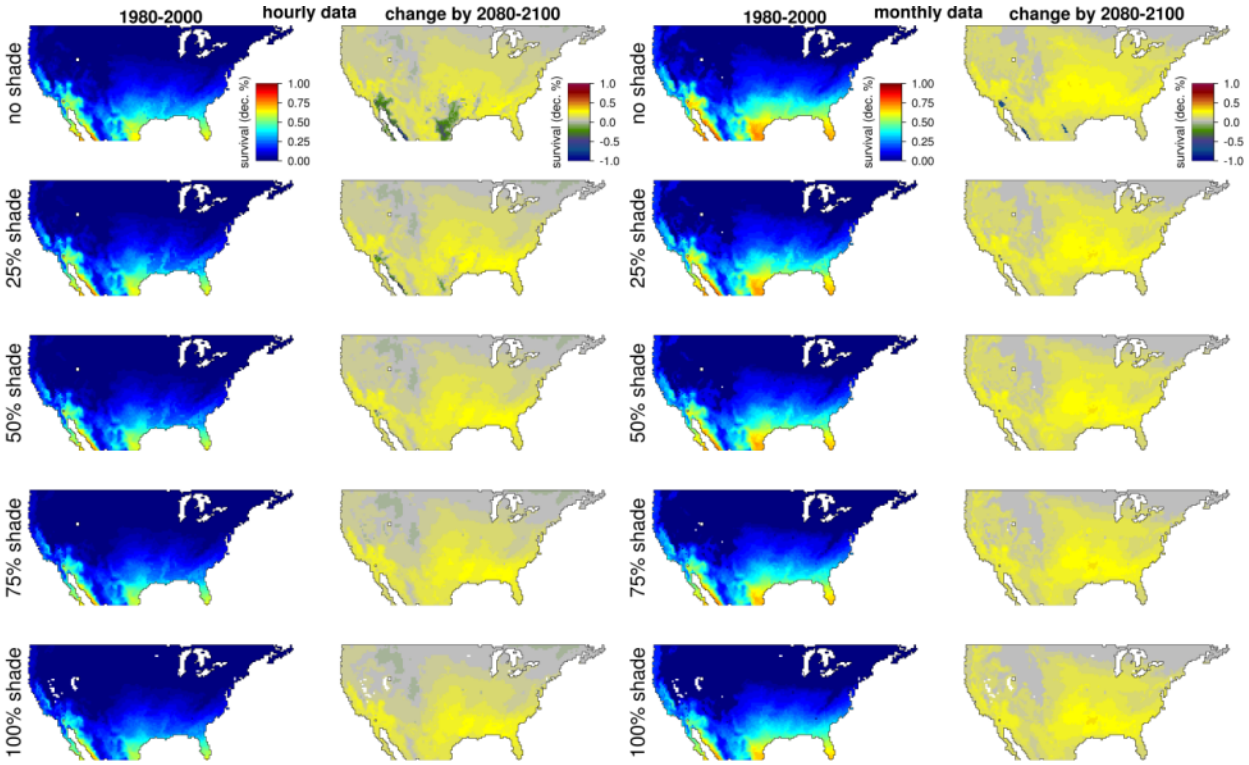

Figure S29: Predictions of embryonic survival rates in the period of 1980-2000 and the predicted change in the future (2080-2100) for embryos that were laid in October at 3 cm depth. Predictions are shown for a scale of shade conditions above the nest and for both hourly and monthly climate resolutions. White areas represent locations for which climate conditions did not enable enough activity to promote reproduction. Color scales are the same for figures S5-S32 to enable visual comparison between different combinations of oviposition months and nests depths.

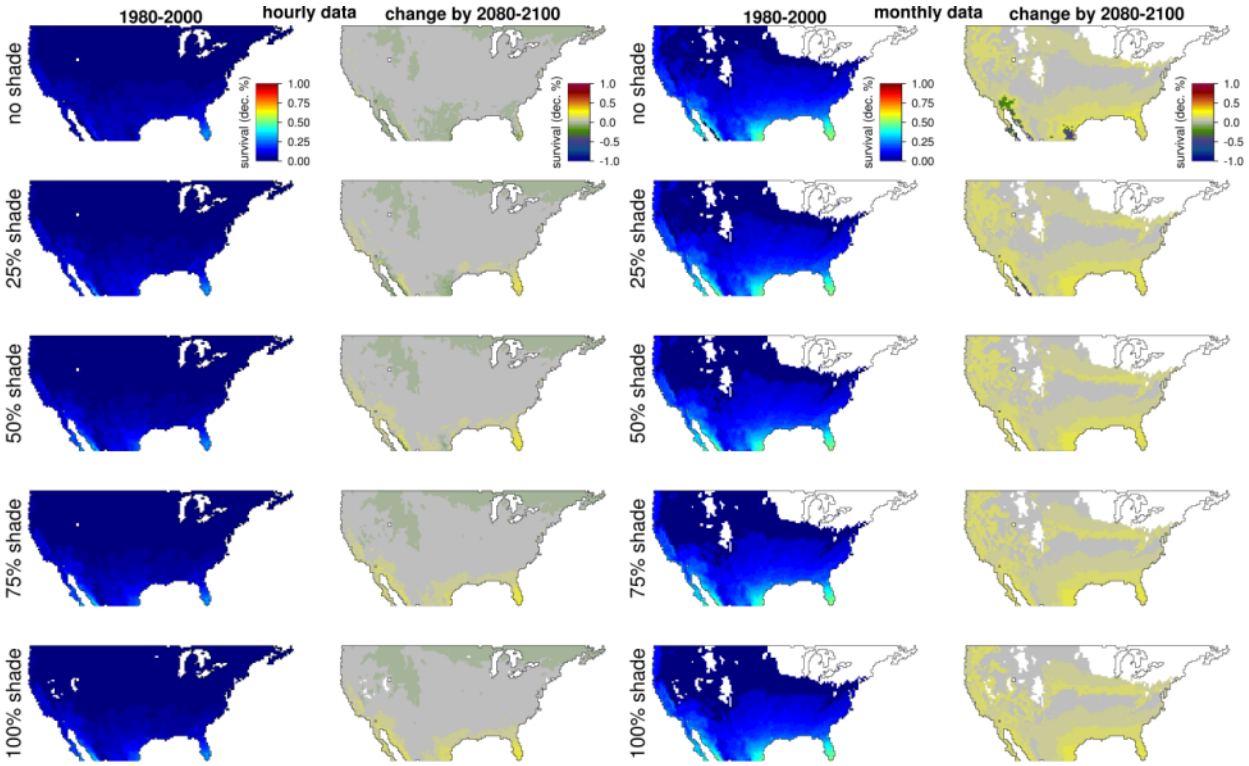

Figure S30: Predictions of embryonic survival rates in the period of 1980-2000 and the predicted change in the future (2080-2100) for embryos that were laid in October at 6 cm depth. Predictions are shown for a scale of shade conditions above the nest and for both hourly and monthly climate resolutions. White areas represent locations for which climate conditions did not enable enough activity to promote reproduction. Color scales are the same for figures S5-S32 to enable visual comparison between different combinations of oviposition months and nests depths.

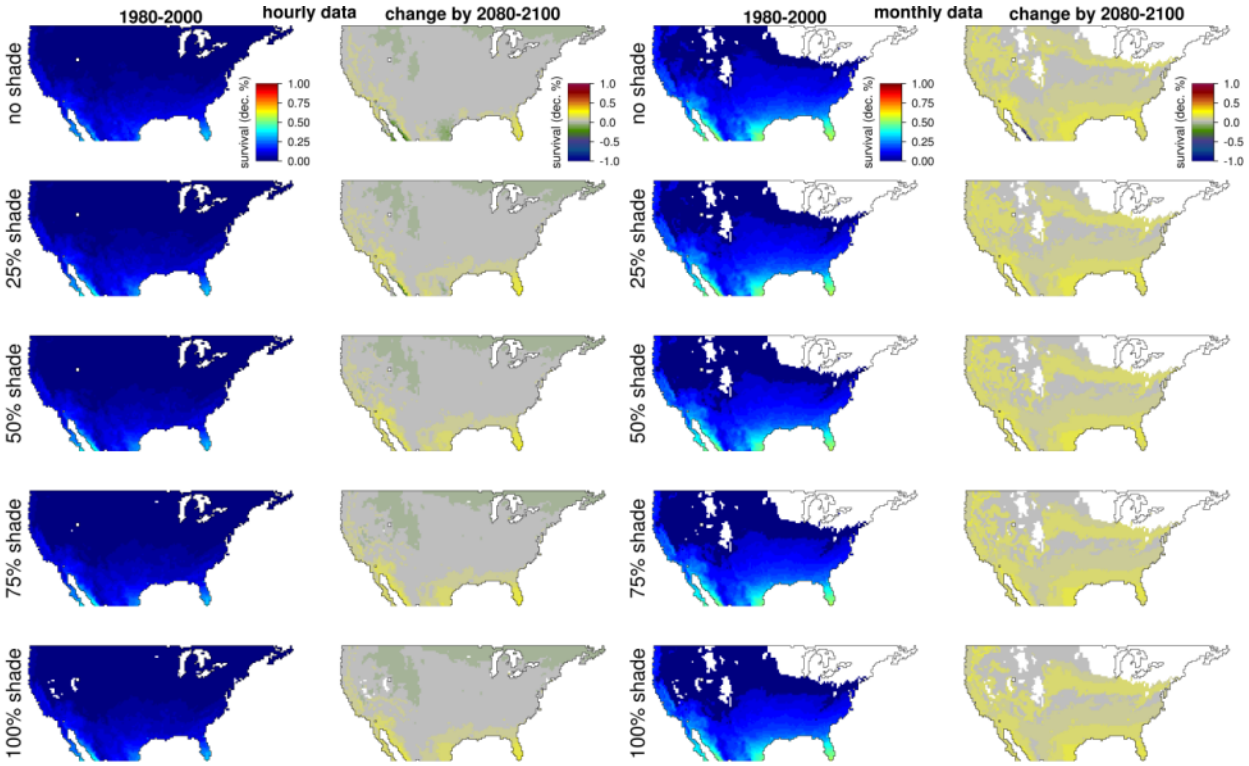

Figure S31: Predictions of embryonic survival rates in the period of 1980-2000 and the predicted change in the future (2080-2100) for embryos that were laid in October at 9 cm depth. Predictions are shown for a scale of shade conditions above the nest and for both hourly and monthly climate resolutions. White areas represent locations for which climate conditions did not enable enough activity to promote reproduction. Color scales are the same for figures S5-S32 to enable visual comparison between different combinations of oviposition months and nests depths.

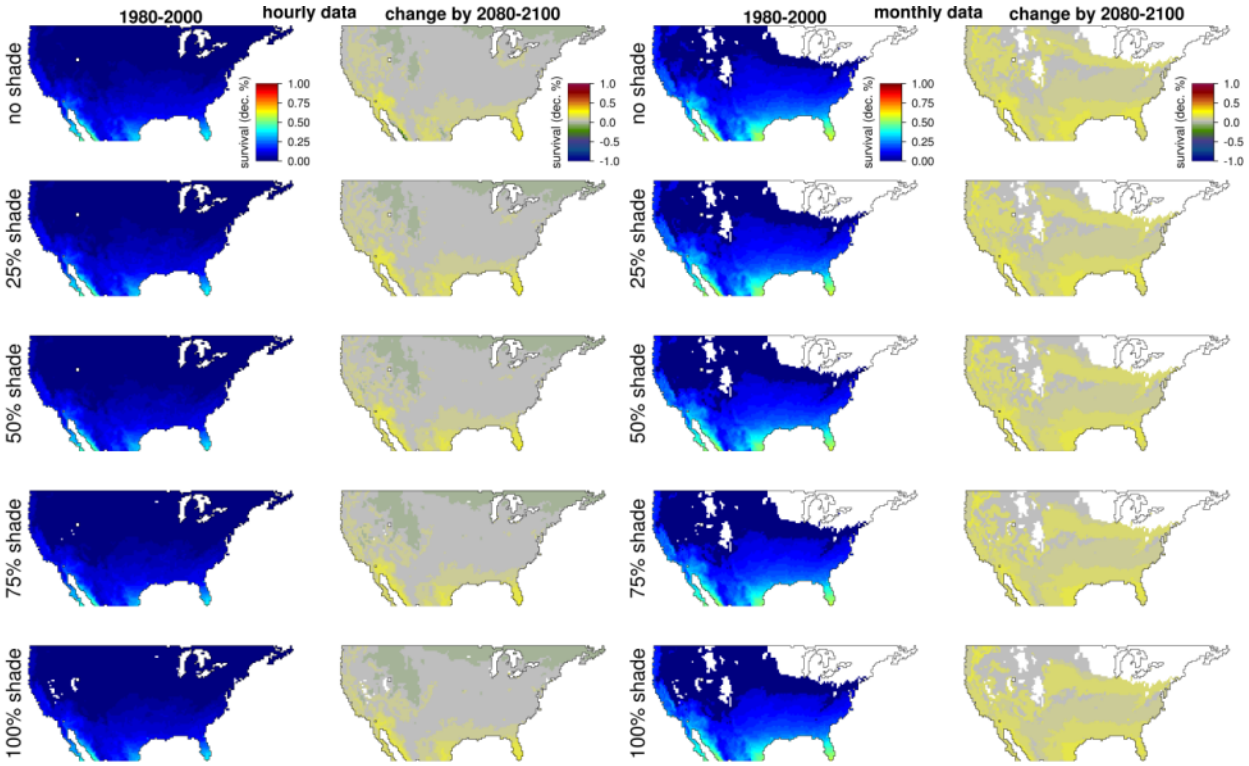

Figure S32: Predictions of embryonic survival rates in the period of 1980-2000 and the predicted change in the future (2080-2100) for embryos that were laid in October at 12 cm depth. Predictions are shown for a scale of shade conditions above the nest and for both hourly and monthly climate resolutions. White areas represent locations for which climate conditions did not enable enough activity to promote reproduction. Color scales are the same for figures S5-S32 to enable visual comparison between different combinations of oviposition months and nests depths.

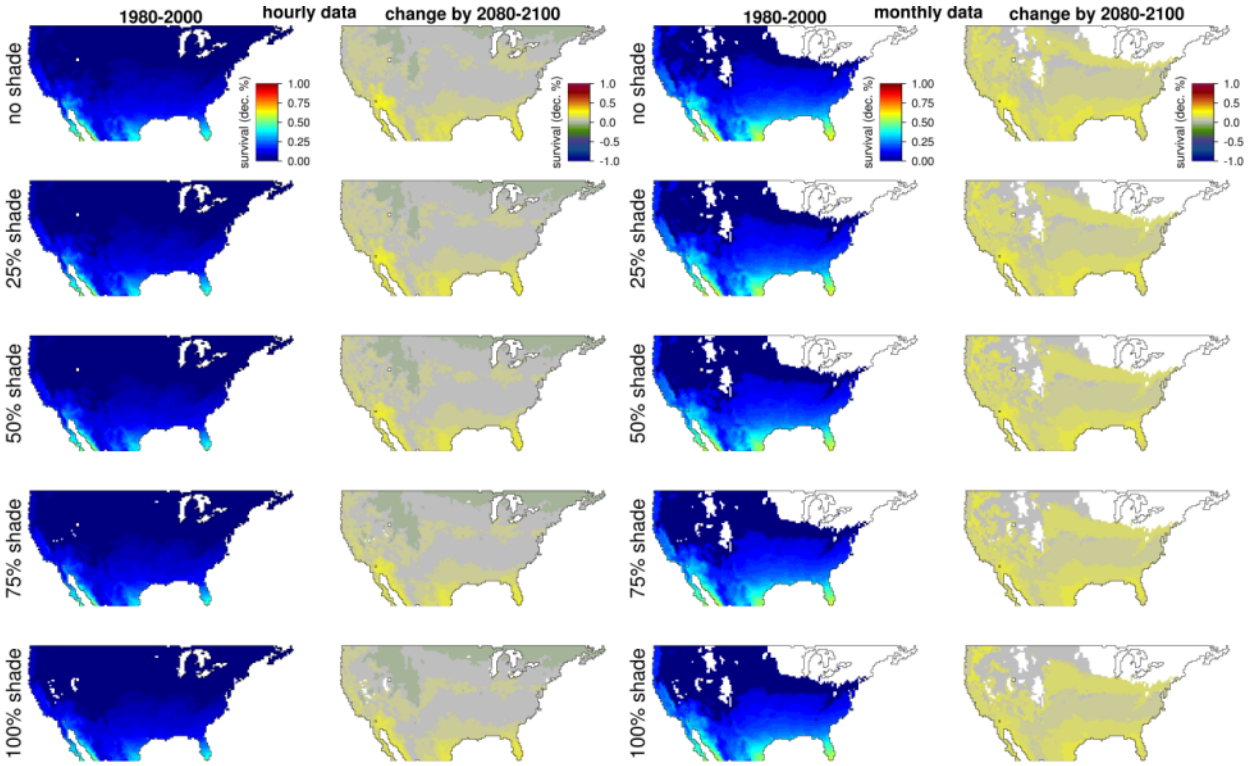

Figure S33: The shade conditions that maximize embryonic survival vary across space and time. Here, we show the optimal levels of shade for eggs laid at a maximal depth of 3 cm during the month of April in the period of 1980-2000 (a). We also show the optimal change in shade between the periods of 1980-2000 and 2080-2100 (b), and (c) the distribution of optimal shade conditions at both periods. The remaining plots depict the maximal soil temperatures (d-f), maximal survival rates (g-i), incubation period (k-l), and time between hatching and the first day of winter (m-o), assuming that mothers construct nests with the optimal level of shade. White areas represent locations for which climate conditions did not enable enough activity to promote reproduction or maximal survival rate was lower than 1%. Color scales are the same for figures S33-S60 to enable visual comparison between different combinations of oviposition months and nests depths.

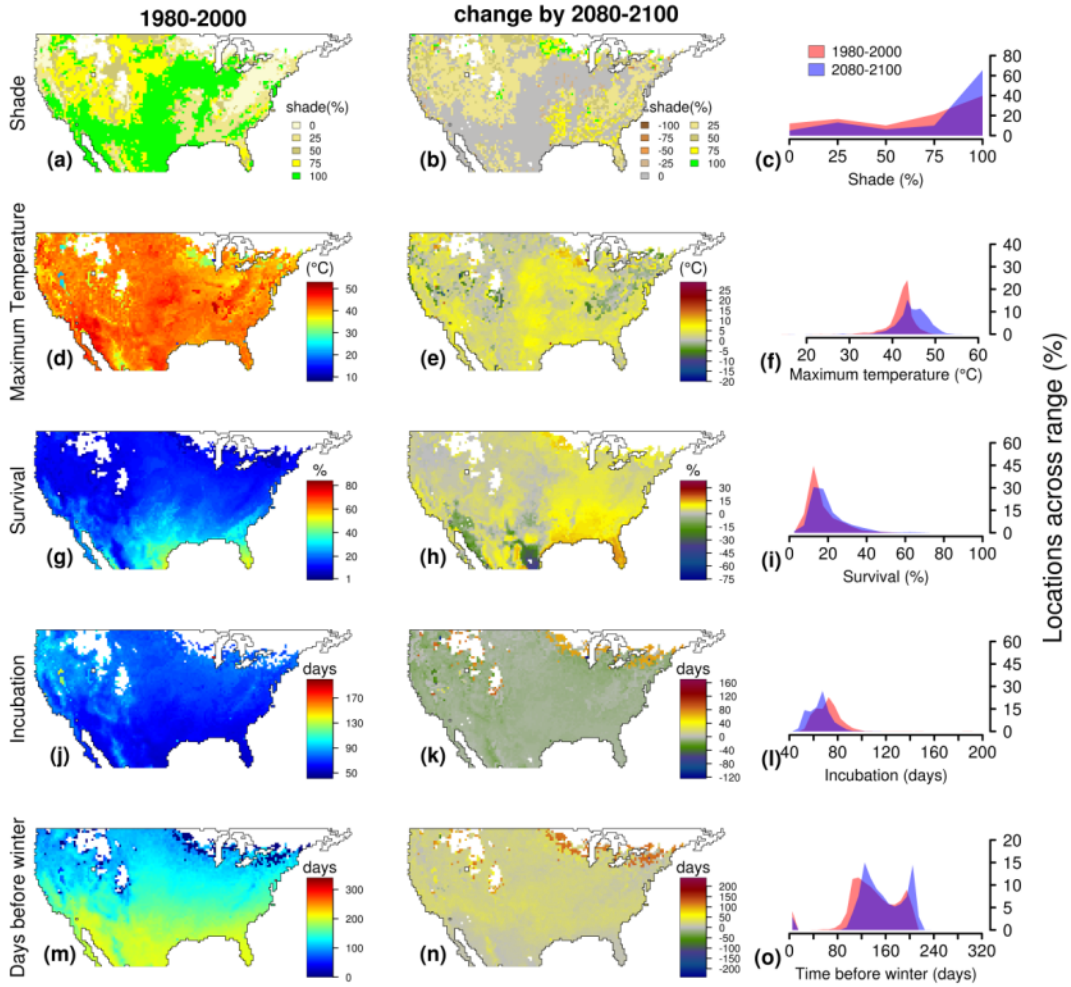

Figure S34: The shade conditions that maximize embryonic survival vary across space and time. Here, we show the optimal levels of shade for eggs laid at a maximal depth of 6 cm during the month of April in the period of 1980-2000 (a). We also show the optimal change in shade between the periods of 1980-2000 and 2080-2100 (b), and (c) the distribution of optimal shade conditions at both periods. The remaining plots depict the maximal soil temperatures (d-f), maximal survival rates (g-i), incubation period (k-l), and time between hatching and the first day of winter (m-o), assuming that mothers construct nests with the optimal level of shade. White areas represent locations for which climate conditions did not enable enough activity to promote reproduction or maximal survival rate was lower than 1%. Color scales are the same for figures S33-S60 to enable visual comparison between different combinations of oviposition months and nests depths.

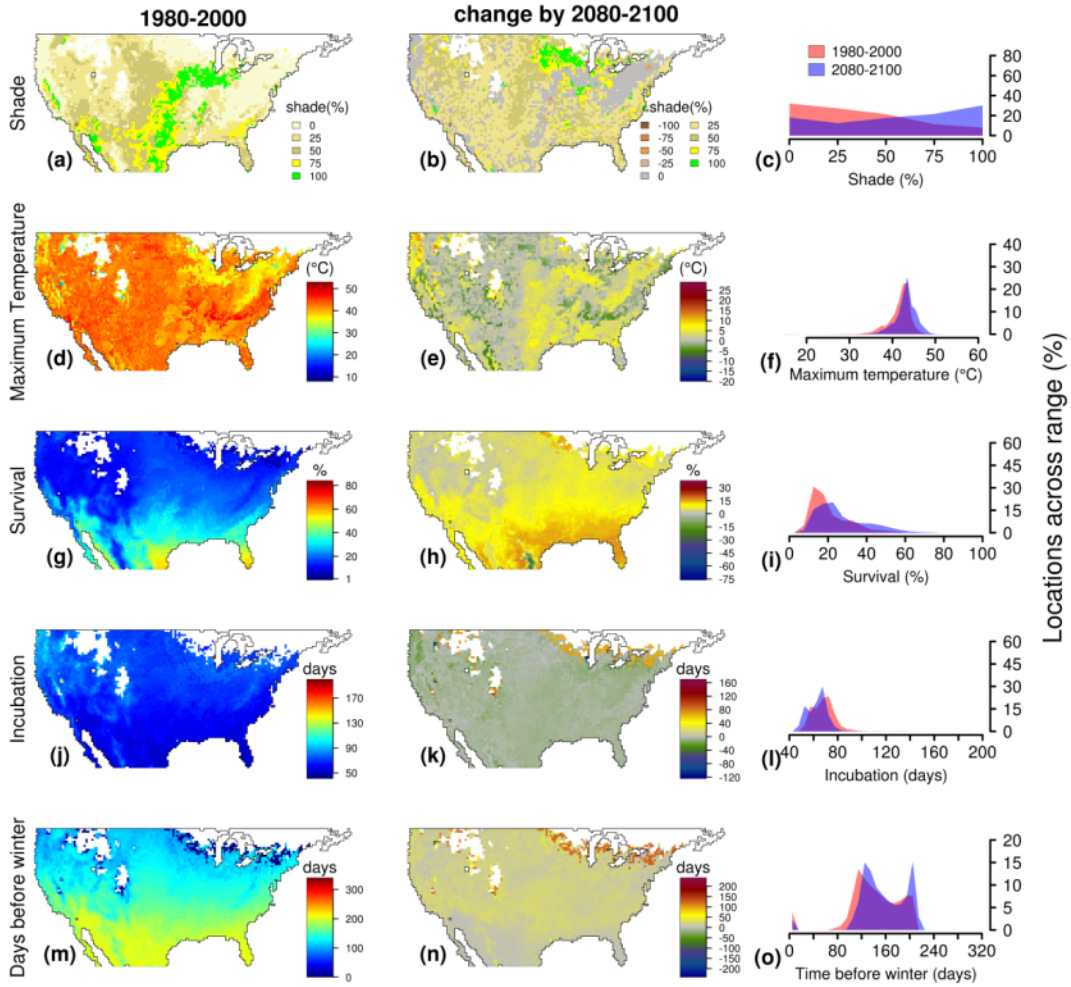

Figure S35: The shade conditions that maximize embryonic survival vary across space and time. Here, we show the optimal levels of shade for eggs laid at a maximal depth of 9 cm during the month of April in the period of 1980-2000 (a). We also show the optimal change in shade between the periods of 1980-2000 and 2080-2100 (b), and (c) the distribution of optimal shade conditions at both periods. The remaining plots depict the maximal soil temperatures (d-f), maximal survival rates (g-i), incubation period (k-l), and time between hatching and the first day of winter (m-o), assuming that mothers construct nests with the optimal level of shade. White areas represent locations for which climate conditions did not enable enough activity to promote reproduction or maximal survival rate was lower than 1%. Color scales are the same for figures S33-S60 to enable visual comparison between different combinations of oviposition months and nests depths.

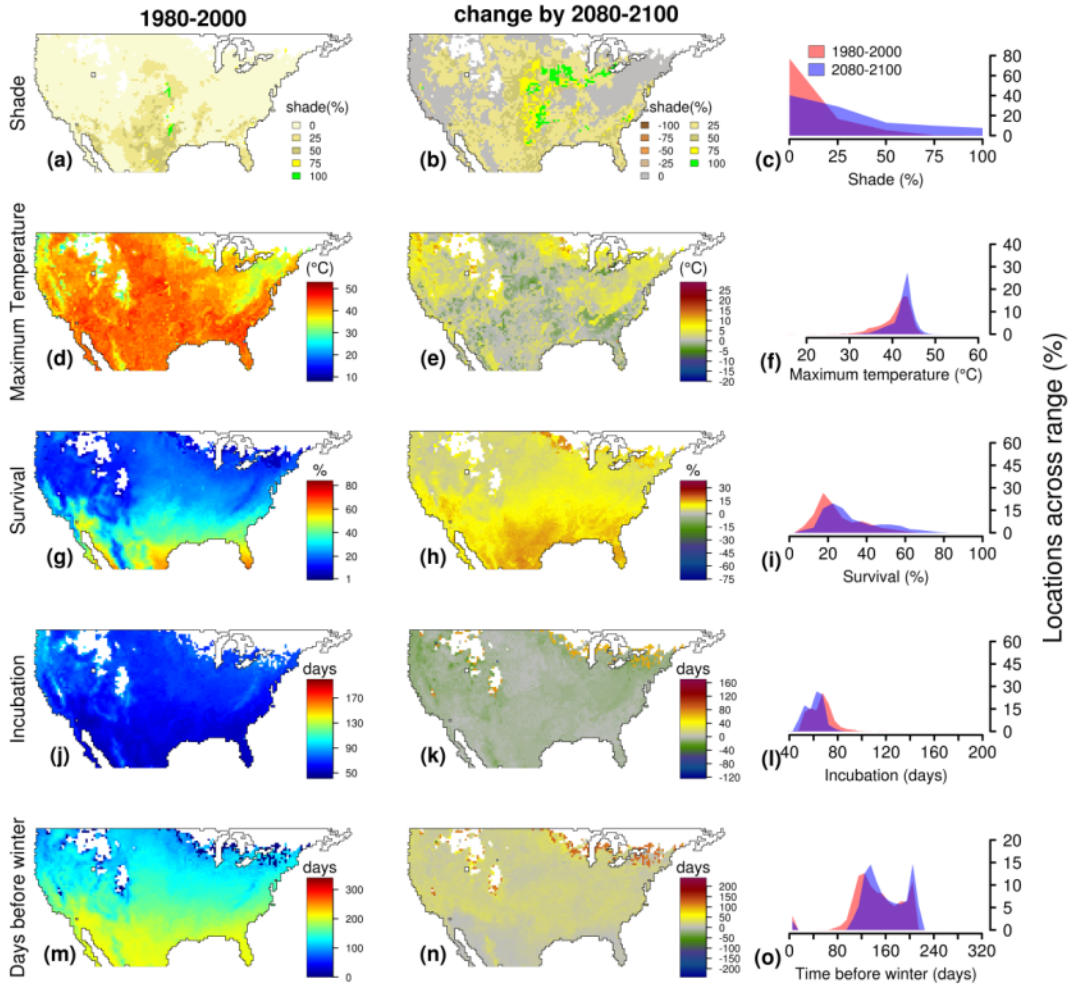

Figure S36: The shade conditions that maximize embryonic survival vary across space and time. Here, we show the optimal levels of shade for eggs laid at a maximal depth of 12 cm during the month of April in the period of 1980-2000 (a). We also show the optimal change in shade between the periods of 1980-2000 and 2080-2100 (b), and (c) the distribution of optimal shade conditions at both periods. The remaining plots depict the maximal soil temperatures (d-f), maximal survival rates (g-i), incubation period (k-l), and time between hatching and the first day of winter (m-o), assuming that mothers construct nests with the optimal level of shade. White areas represent locations for which climate conditions did not enable enough activity to promote reproduction or maximal survival rate was lower than 1%. Color scales are the same for figures S33-S60 to enable visual comparison between different combinations of oviposition months and nests depths.

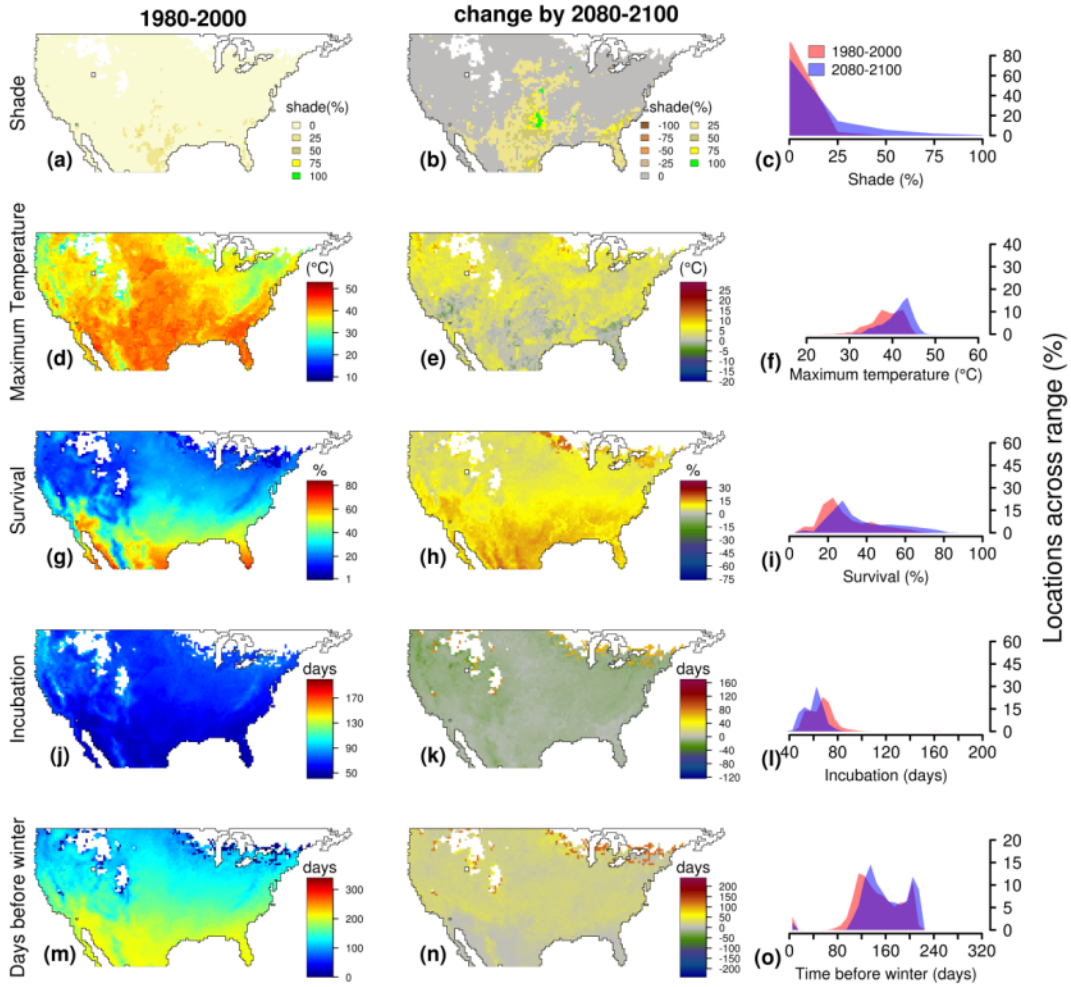

Figure S37: The shade conditions that maximize embryonic survival vary across space and time. Here, we show the optimal levels of shade for eggs laid at a maximal depth of 3 cm during the month of May in the period of 1980-2000 (a). We also show the optimal change in shade between the periods of 1980-2000 and 2080-2100 (b), and (c) the distribution of optimal shade conditions at both periods. The remaining plots depict the maximal soil temperatures (d-f), maximal survival rates (g-i), incubation period (k-l), and time between hatching and the first day of winter (m-o), assuming that mothers construct nests with the optimal level of shade. White areas represent locations for which climate conditions did not enable enough activity to promote reproduction or maximal survival rate was lower than 1%. Color scales are the same for figures S33-S60 to enable visual comparison between different combinations of oviposition months and nests depths.

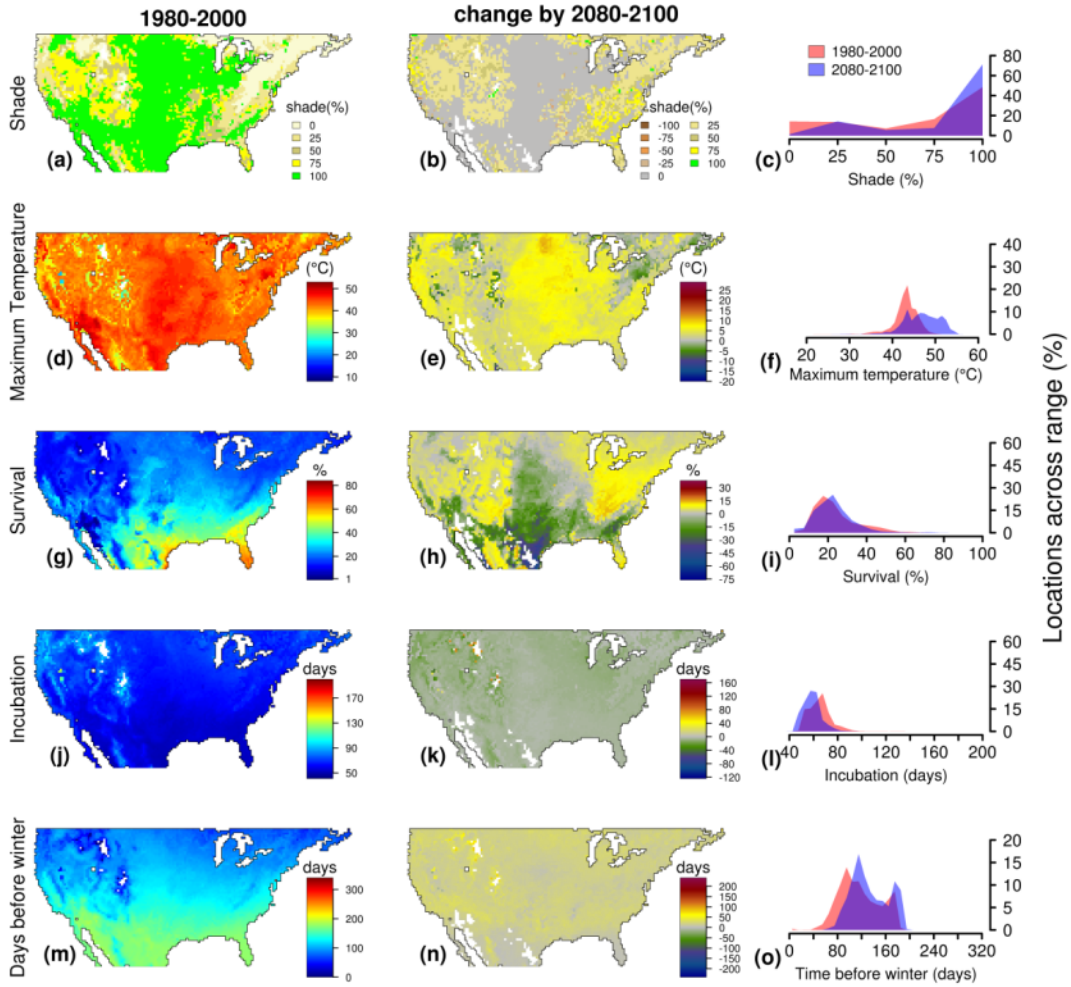

Figure S38: The shade conditions that maximize embryonic survival vary across space and time. Here, we show the optimal levels of shade for eggs laid at a maximal depth of 6 cm during the month of May in the period of 1980-2000 (a). We also show the optimal change in shade between the periods of 1980-2000 and 2080-2100 (b), and (c) the distribution of optimal shade conditions at both periods. The remaining plots depict the maximal soil temperatures (d-f), maximal survival rates (g-i), incubation period (k-l), and time between hatching and the first day of winter (m-o), assuming that mothers construct nests with the optimal level of shade. Color scales are the same for figures S33-S60 to enable visual comparison between different combinations of oviposition months and nests depths.

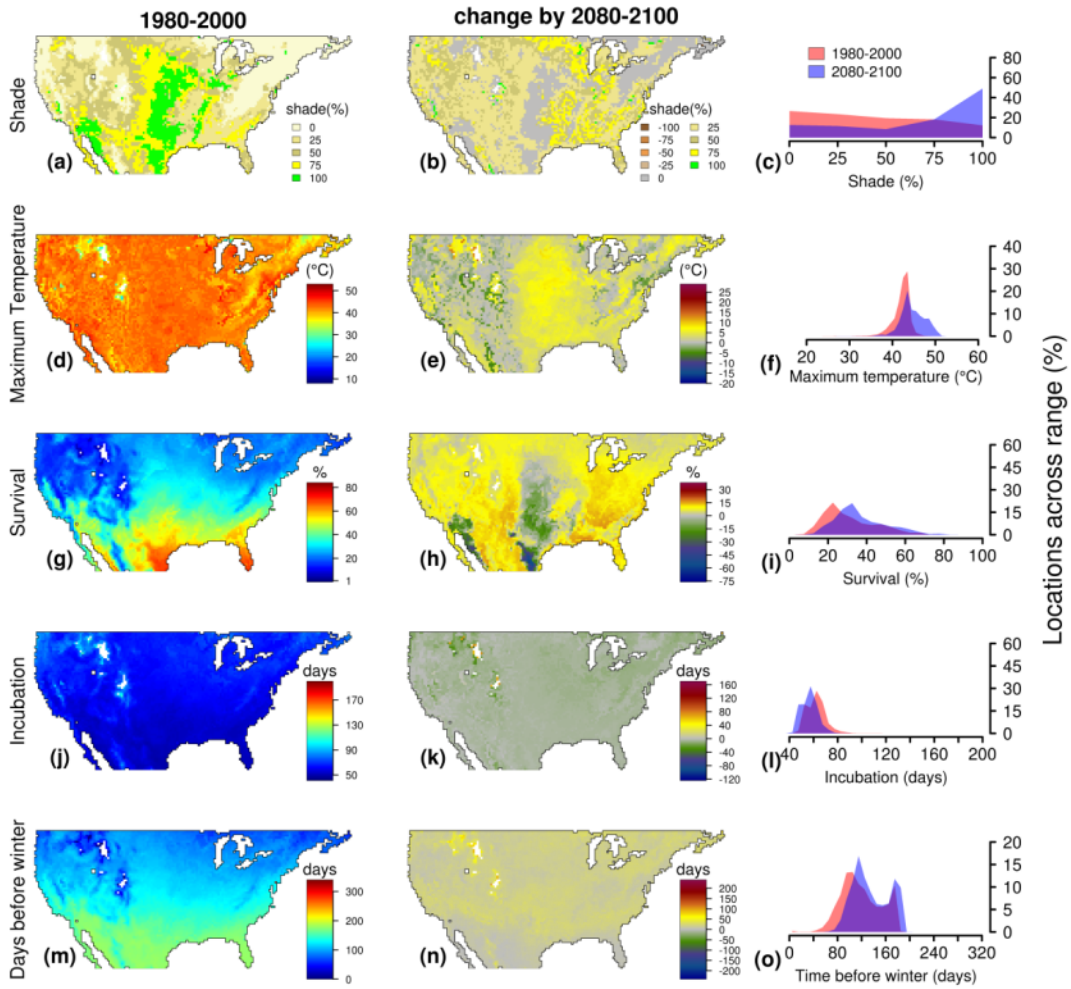

Figure S39: The shade conditions that maximize embryonic survival vary across space and time. Here, we show the optimal levels of shade for eggs laid at a maximal depth of 9 cm during the month of May in the period of 1980-2000 (a). We also show the optimal change in shade between the periods of 1980-2000 and 2080-2100 (b), and (c) the distribution of optimal shade conditions at both periods. The remaining plots depict the maximal soil temperatures (d-f), maximal survival rates (g-i), incubation period (k-l), and time between hatching and the first day of winter (m-o), assuming that mothers construct nests with the optimal level of shade. Color scales are the same for figures S33-S60 to enable visual comparison between different combinations of oviposition months and nests depths.

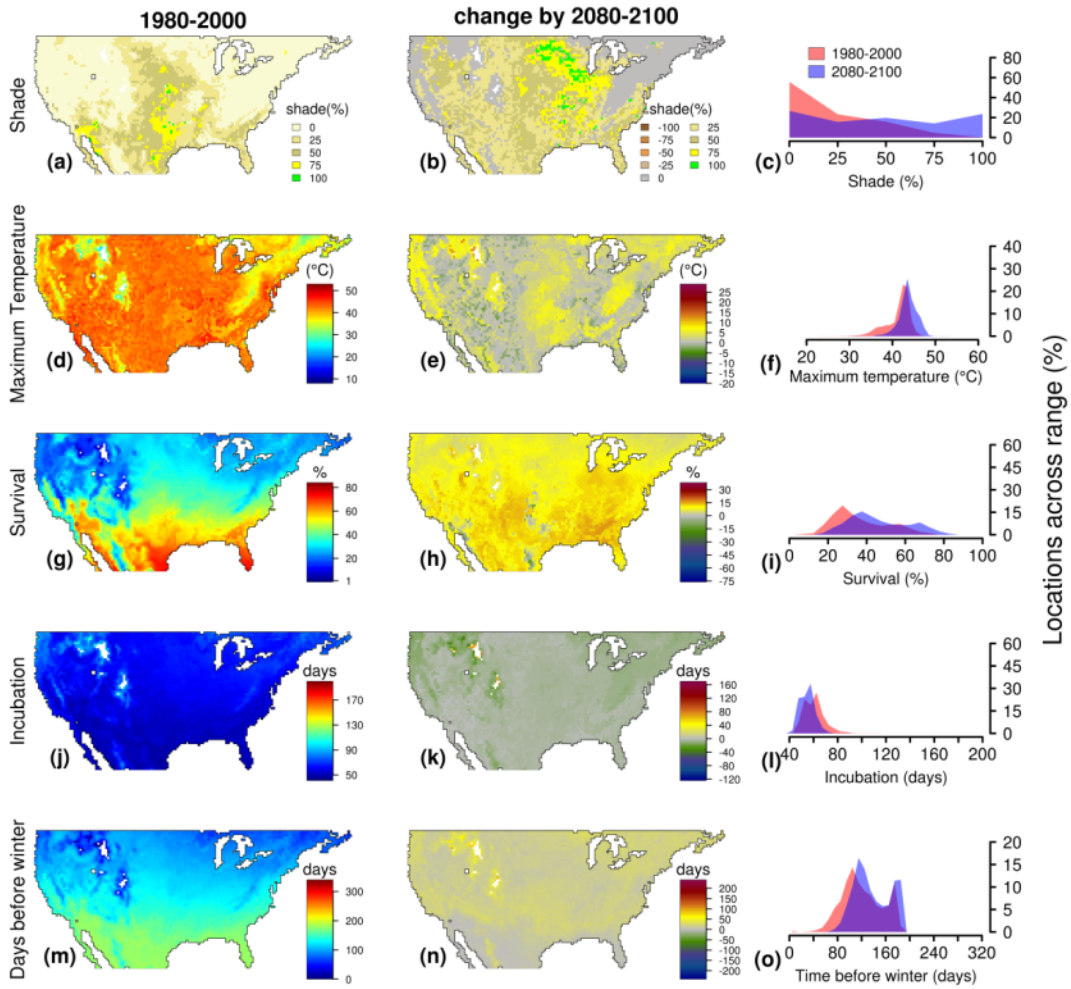

Figure S40: The shade conditions that maximize embryonic survival vary across space and time. Here, we show the optimal levels of shade for eggs laid at a maximal depth of 12 cm during the month of May in the period of 1980-2000 (a). We also show the optimal change in shade between the periods of 1980-2000 and 2080-2100 (b), and (c) the distribution of optimal shade conditions at both periods. The remaining plots depict the maximal soil temperatures (d-f), maximal survival rates (g-i), incubation period (k-l), and time between hatching and the first day of winter (m-o), assuming that mothers construct nests with the optimal level of shade. Color scales are the same for figures S33-S60 to enable visual comparison between different combinations of oviposition months and nests depths.

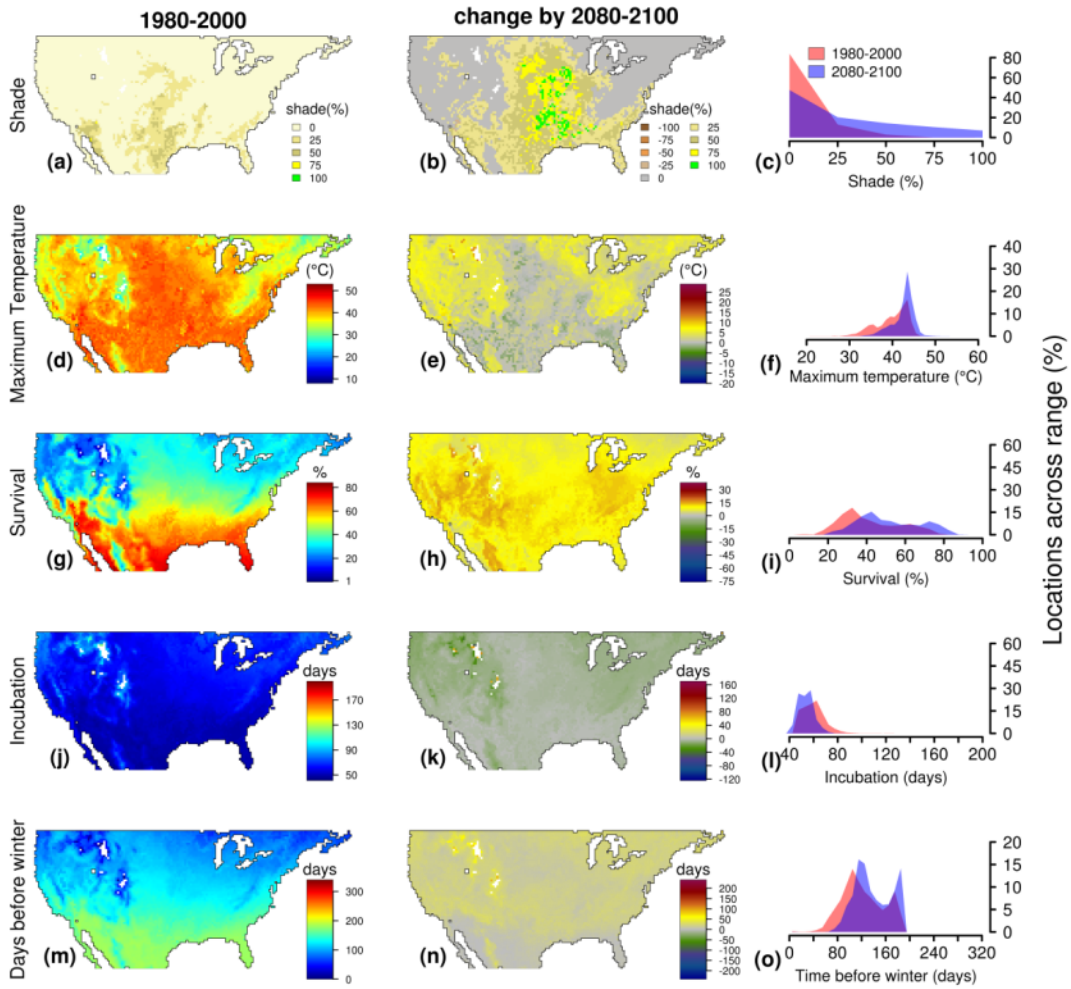

Figure S41: The shade conditions that maximize embryonic survival vary across space and time. Here, we show the optimal levels of shade for eggs laid at a maximal depth of 3 cm during the month of June in the period of 1980-2000 (a). We also show the optimal change in shade between the periods of 1980-2000 and 2080-2100 (b), and (c) the distribution of optimal shade conditions at both periods. The remaining plots depict the maximal soil temperatures (d-f), maximal survival rates (g-i), incubation period (k-l), and time between hatching and the first day of winter (m-o), assuming that mothers construct nests with the optimal level of shade. White areas represent locations for which climate conditions did not enable enough activity to promote reproduction or maximal survival rate was lower than 1%. Color scales are the same for figures S33-S60 to enable visual comparison between different combinations of oviposition months and nests depths.

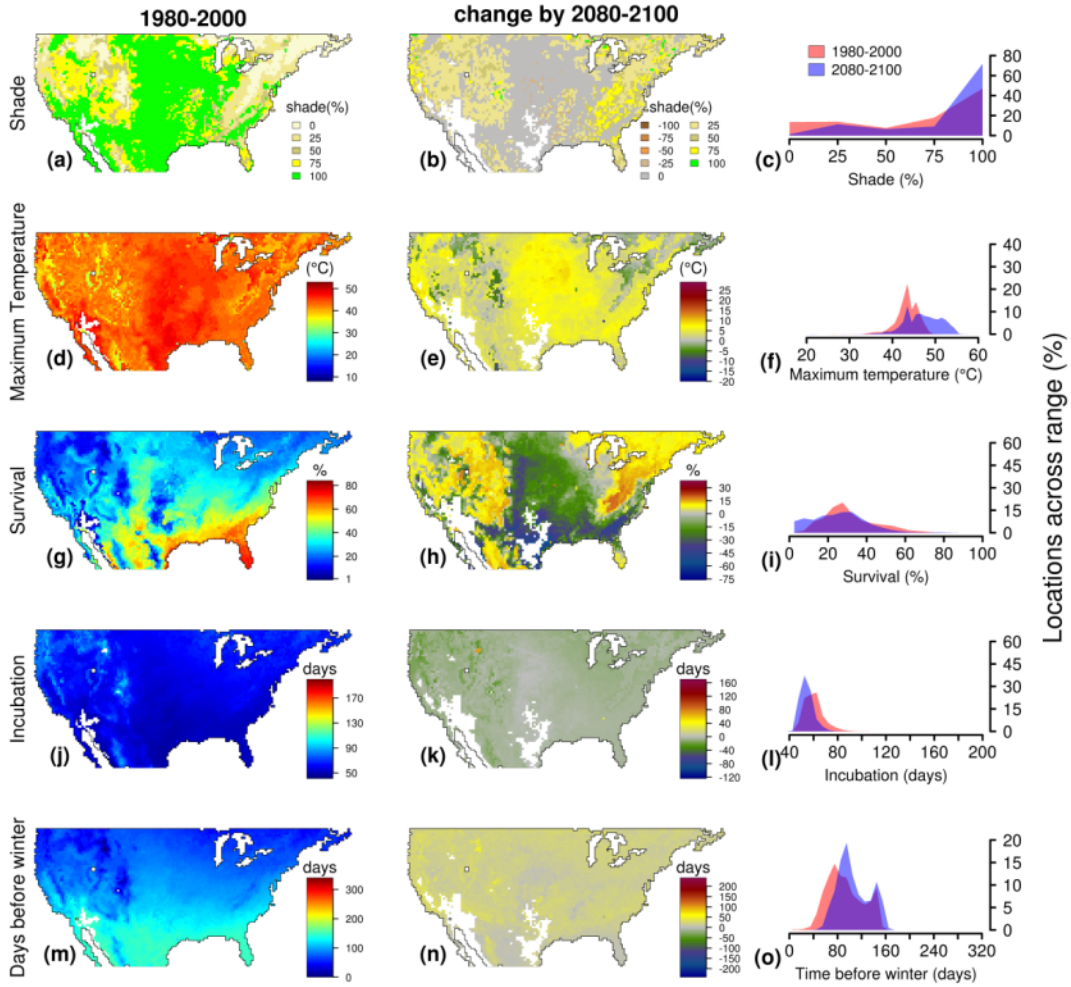

Figure S42: The shade conditions that maximize embryonic survival vary across space and time. Here, we show the optimal levels of shade for eggs laid at a maximal depth of 6 cm during the month of June in the period of 1980-2000 (a). We also show the optimal change in shade between the periods of 1980-2000 and 2080-2100 (b), and (c) the distribution of optimal shade conditions at both periods. The remaining plots depict the maximal soil temperatures (d-f), maximal survival rates (g-i), incubation period (k-l), and time between hatching and the first day of winter (m-o), assuming that mothers construct nests with the optimal level of shade. Color scales are the same for figures S33-S60 to enable visual comparison between different combinations of oviposition months and nests depths.

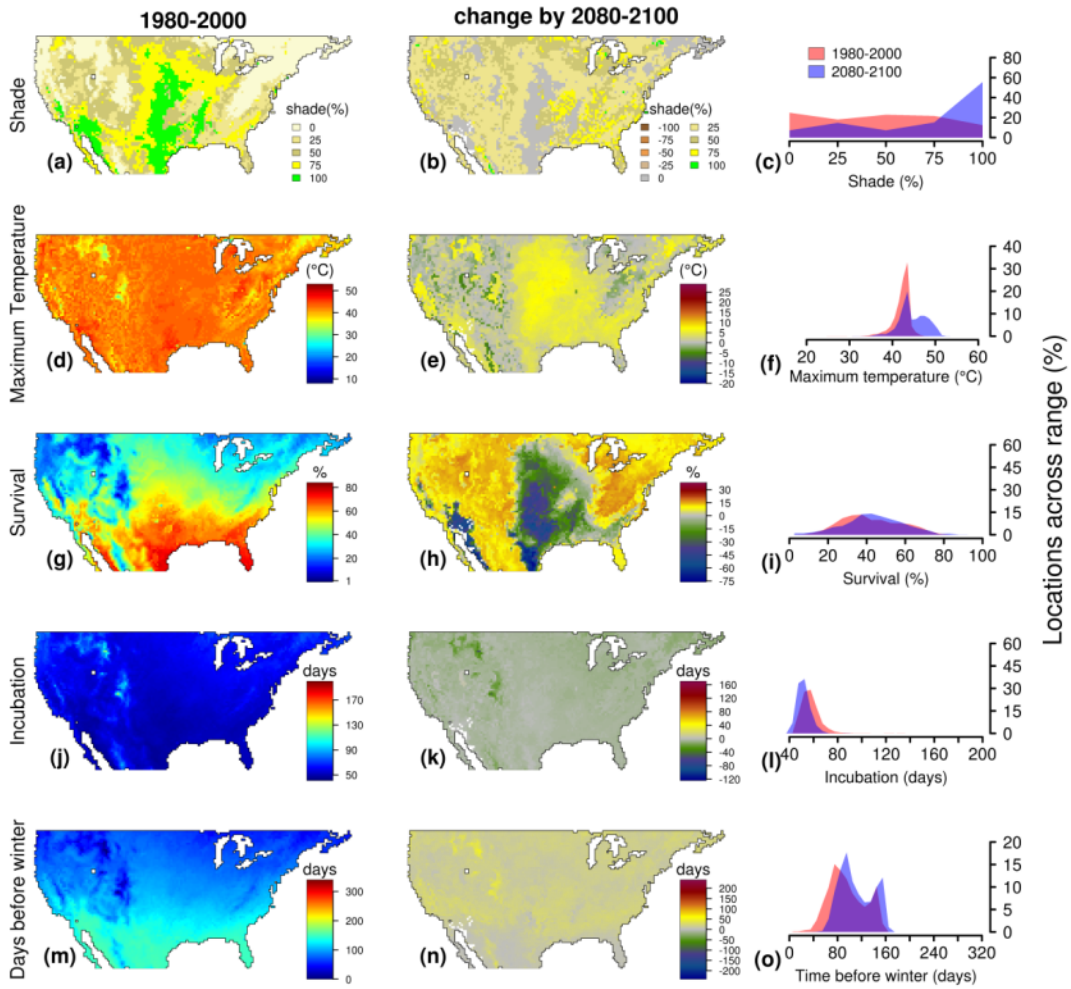

Figure S43: The shade conditions that maximize embryonic survival vary across space and time. Here, we show the optimal levels of shade for eggs laid at a maximal depth of 9 cm during the month of June in the period of 1980-2000 (a). We also show the optimal change in shade between the periods of 1980-2000 and 2080-2100 (b), and (c) the distribution of optimal shade conditions at both periods. The remaining plots depict the maximal soil temperatures (d-f), maximal survival rates (g-i), incubation period (k-l), and time between hatching and the first day of winter (m-o), assuming that mothers construct nests with the optimal level of shade. Color scales are the same for figures S33-S60 to enable visual comparison between different combinations of oviposition months and nests depths.

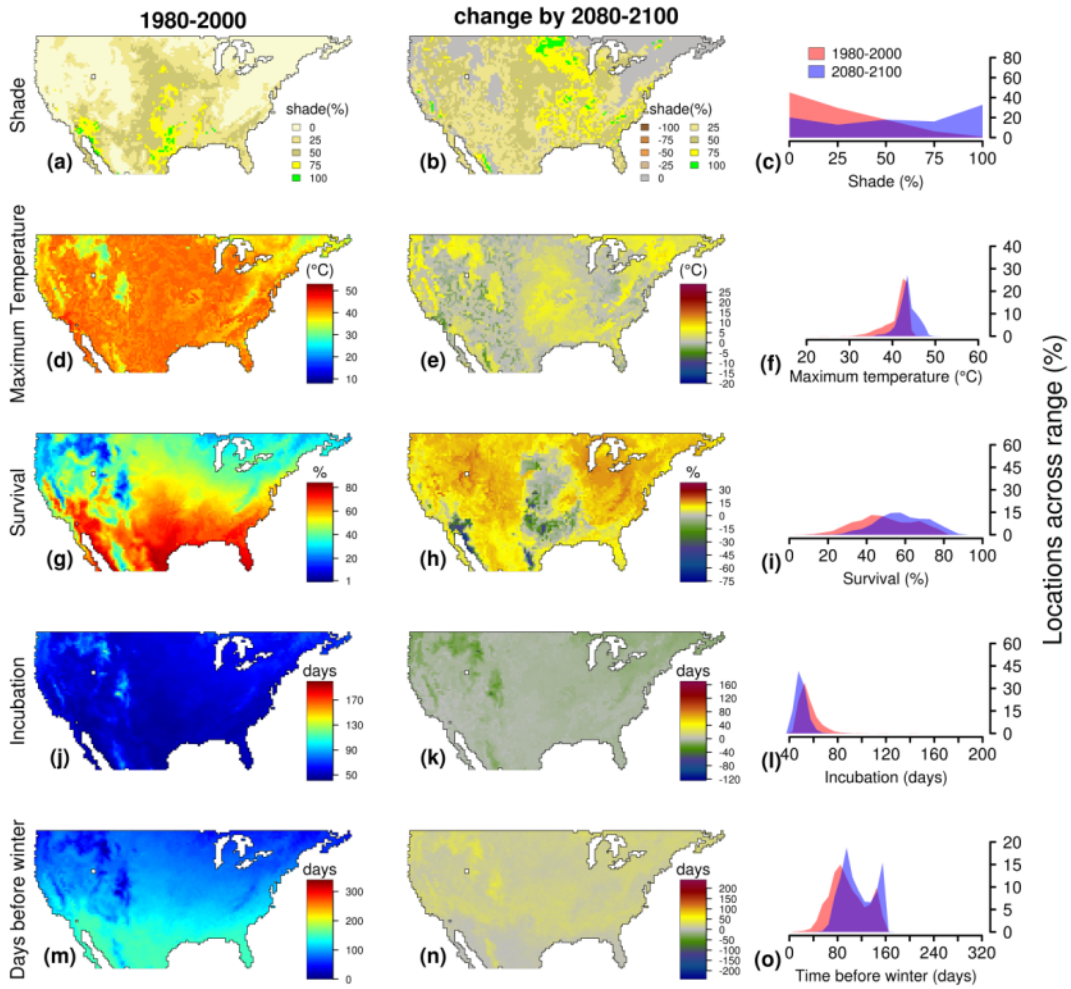

Figure S44: The shade conditions that maximize embryonic survival vary across space and time. Here, we show the optimal levels of shade for eggs laid at a maximal depth of 12 cm during the month of June in the period of 1980-2000 (a). We also show the optimal change in shade between the periods of 1980-2000 and 2080-2100 (b), and (c) the distribution of optimal shade conditions at both periods. The remaining plots depict the maximal soil temperatures (d-f), maximal survival rates (g-i), incubation period (k-l), and time between hatching and the first day of winter (m-o), assuming that mothers construct nests with the optimal level of shade. White areas represent locations for which climate conditions did not enable enough activity to promote reproduction or maximal survival rate was lower than 1%. Color scales are the same for figures S33-S60 to enable visual comparison between different combinations of oviposition months and nests depths.

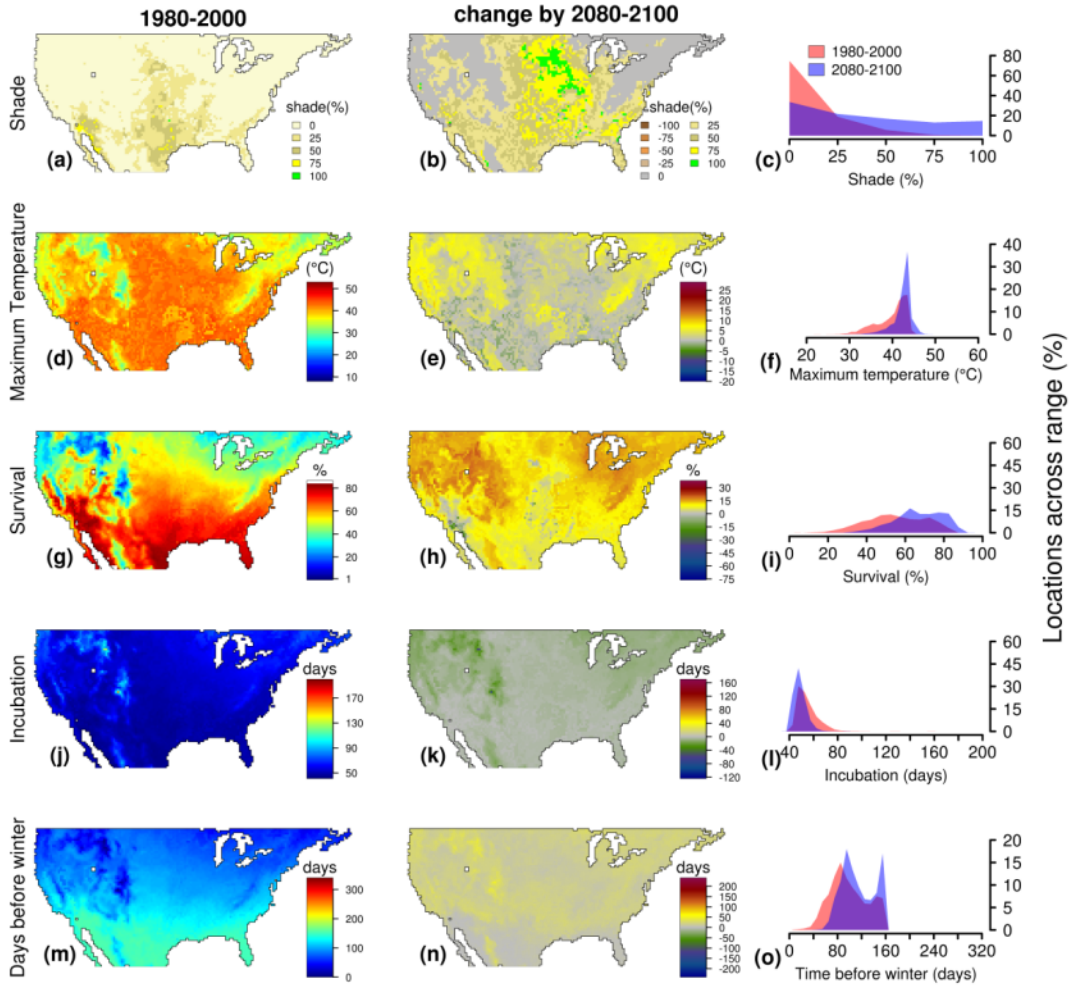

Figure S45: The shade conditions that maximize embryonic survival vary across space and time. Here, we show the optimal levels of shade for eggs laid at a maximal depth of 3 cm during the month of July in the period of 1980-2000 (a). We also show the optimal change in shade between the periods of 1980-2000 and 2080-2100 (b), and (c) the distribution of optimal shade conditions at both periods. The remaining plots depict the maximal soil temperatures (d-f), maximal survival rates (g-i), incubation period (k-l), and time between hatching and the first day of winter (m-o), assuming that mothers construct nests with the optimal level of shade. White areas represent locations for which climate conditions did not enable enough activity to promote reproduction or maximal survival rate was lower than 1%. Color scales are the same for figures S33-S60 to enable visual comparison between different combinations of oviposition months and nests depths.

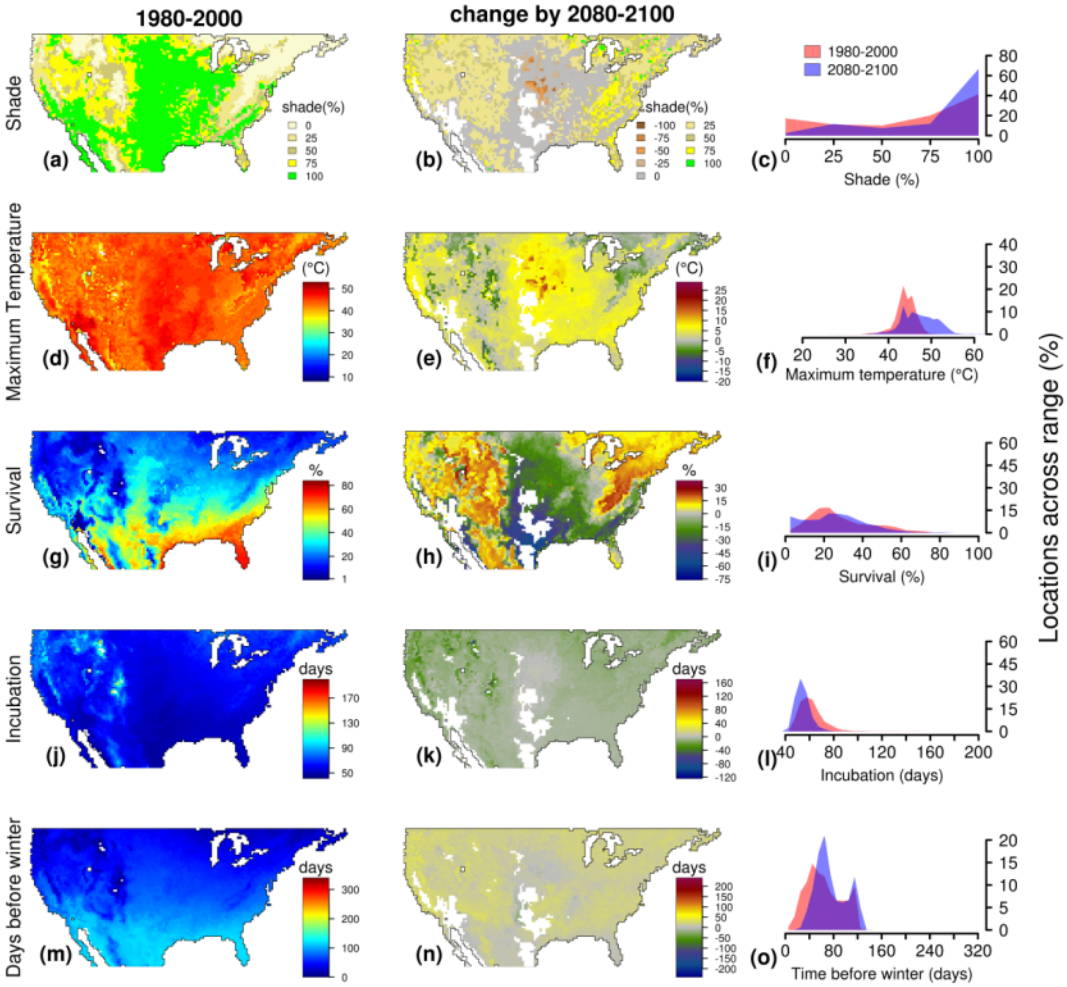

Figure S46: The shade conditions that maximize embryonic survival vary across space and time. Here, we show the optimal levels of shade for eggs laid at a maximal depth of 6 cm during the month of July in the period of 1980-2000 (a). We also show the optimal change in shade between the periods of 1980-2000 and 2080-2100 (b), and (c) the distribution of optimal shade conditions at both periods. The remaining plots depict the maximal soil temperatures (d-f), maximal survival rates (g-i), incubation period (k-l), and time between hatching and the first day of winter (m-o), assuming that mothers construct nests with the optimal level of shade. White areas represent locations for which climate conditions did not enable enough activity to promote reproduction or maximal survival rate was lower than 1%. Color scales are the same for figures S33-S60 to enable visual comparison between different combinations of oviposition months and nests depths.

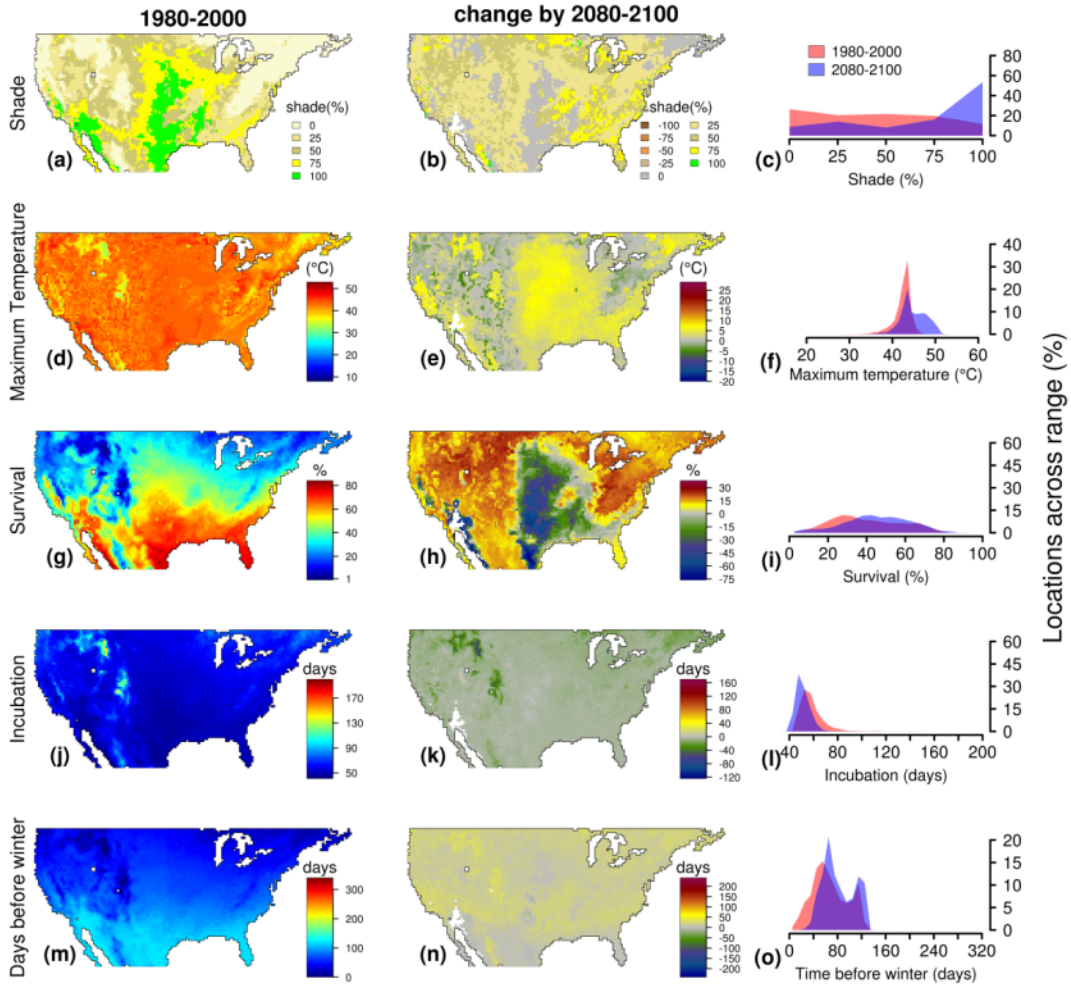

Figure S47: The shade conditions that maximize embryonic survival vary across space and time. Here, we show the optimal levels of shade for eggs laid at a maximal depth of 9 cm during the month of July in the period of 1980-2000 (a). We also show the optimal change in shade between the periods of 1980-2000 and 2080-2100 (b), and (c) the distribution of optimal shade conditions at both periods. The remaining plots depict the maximal soil temperatures (d-f), maximal survival rates (g-i), incubation period (k-l), and time between hatching and the first day of winter (m-o), assuming that mothers construct nests with the optimal level of shade. White areas represent locations for which climate conditions did not enable enough activity to promote reproduction or maximal survival rate was lower than 1%. Color scales are the same for figures S33-S60 to enable visual comparison between different combinations of oviposition months and nests depths.

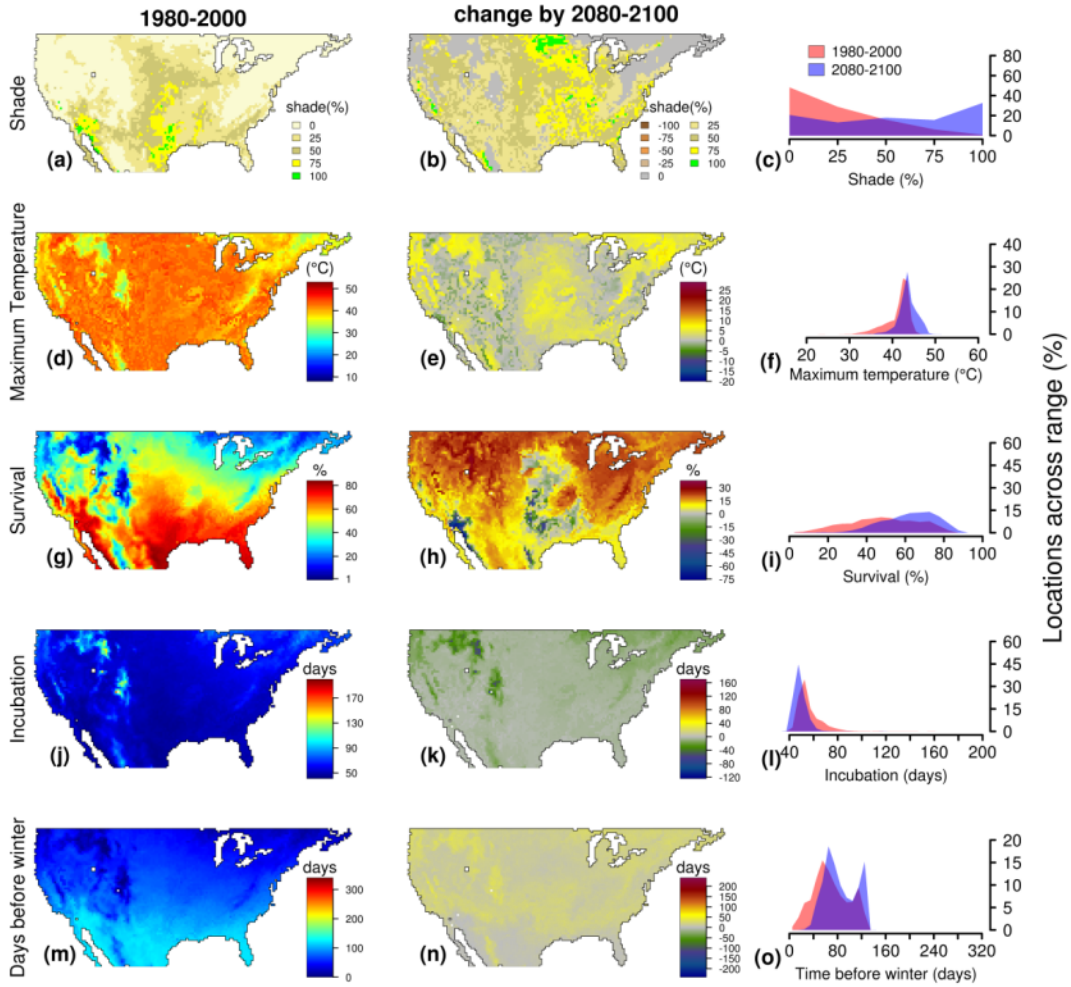

Figure S48: The shade conditions that maximize embryonic survival vary across space and time. Here, we show the optimal levels of shade for eggs laid at a maximal depth of 12 cm during the month of July in the period of 1980-2000 (a). We also show the optimal change in shade between the periods of 1980-2000 and 2080-2100 (b), and (c) the distribution of optimal shade conditions at both periods. The remaining plots depict the maximal soil temperatures (d-f), maximal survival rates (g-i), incubation period (k-l), and time between hatching and the first day of winter (m-o), assuming that mothers construct nests with the optimal level of shade. White areas represent locations for which climate conditions did not enable enough activity to promote reproduction or maximal survival rate was lower than 1%. Color scales are the same for figures S33-S60 to enable visual comparison between different combinations of oviposition months and nests depths.

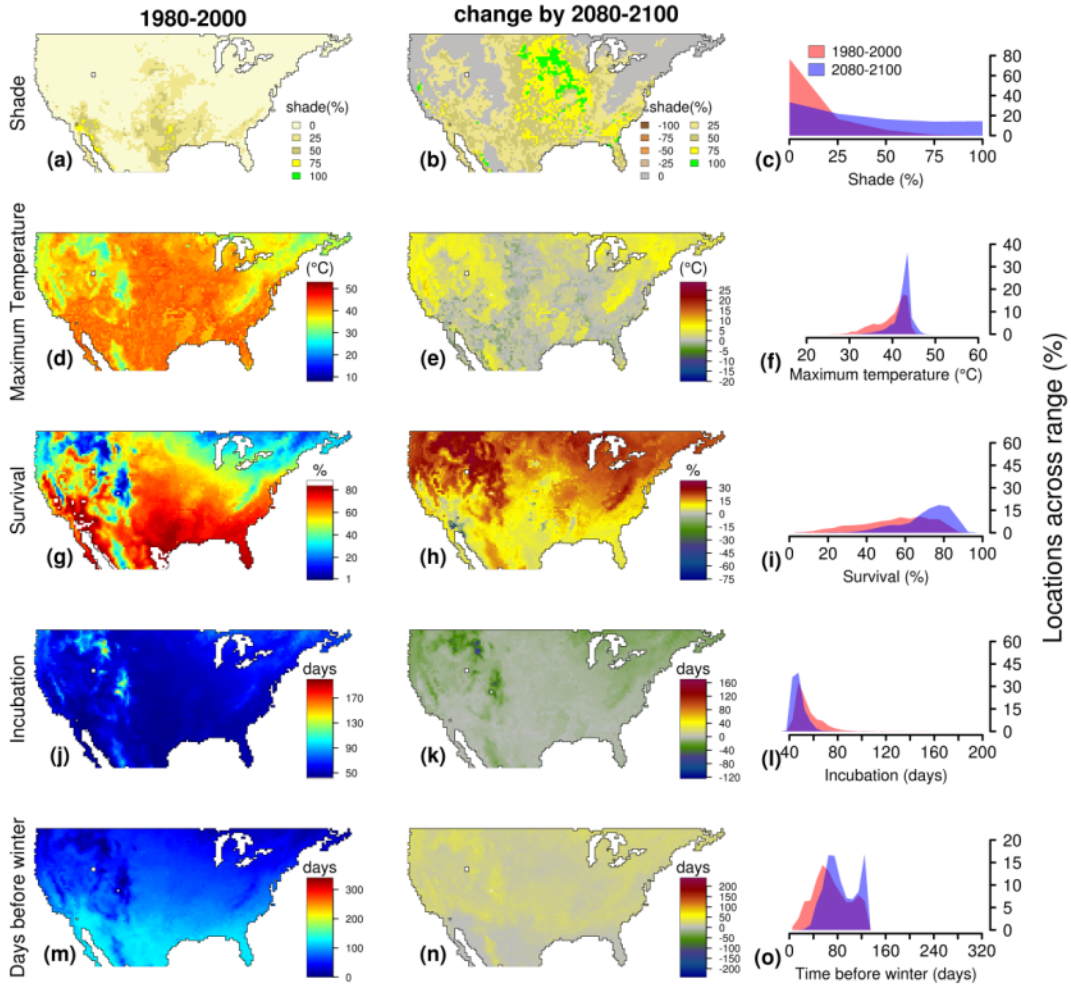

Figure S49: The shade conditions that maximize embryonic survival vary across space and time. Here, we show the optimal levels of shade for eggs laid at a maximal depth of 3 cm during the month of August in the period of 1980-2000 (a). We also show the optimal change in shade between the periods of 1980-2000 and 2080-2100 (b), and (c) the distribution of optimal shade conditions at both periods. The remaining plots depict the maximal soil temperatures (d-f), maximal survival rates (g-i), incubation period (k-l), and time between hatching and the first day of winter (m-o), assuming that mothers construct nests with the optimal level of shade. White areas represent locations for which climate conditions did not enable enough activity to promote reproduction or maximal survival rate was lower than 1%. Color scales are the same for figures S33-S60 to enable visual comparison between different combinations of oviposition months and nests depths.

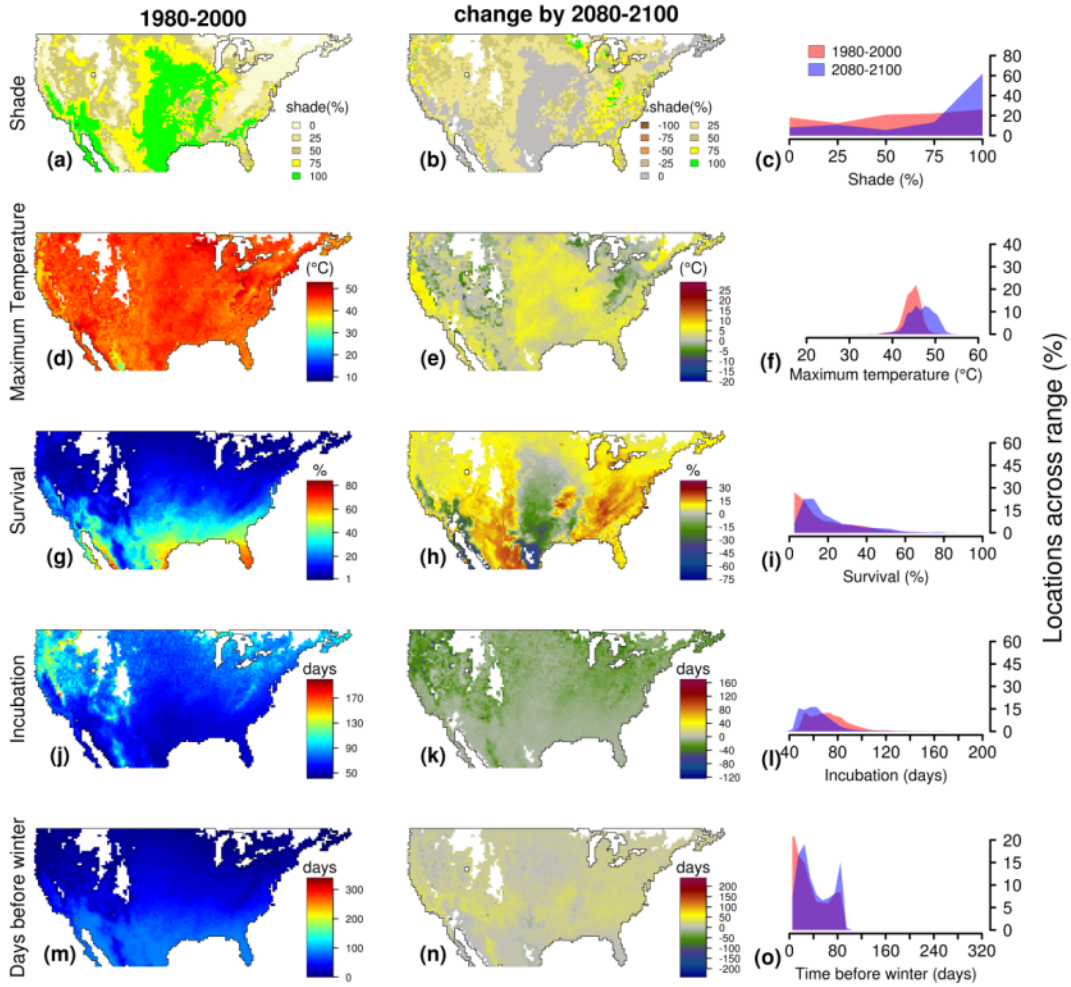

Figure S50: The shade conditions that maximize embryonic survival vary across space and time. Here, we show the optimal levels of shade for eggs laid at a maximal depth of 6 cm during the month of August in the period of 1980-2000 (a). We also show the optimal change in shade between the periods of 1980-2000 and 2080-2100 (b), and (c) the distribution of optimal shade conditions at both periods. The remaining plots depict the maximal soil temperatures (d-f), maximal survival rates (g-i), incubation period (k-l), and time between hatching and the first day of winter (m-o), assuming that mothers construct nests with the optimal level of shade. White areas represent locations for which climate conditions did not enable enough activity to promote reproduction or maximal survival rate was lower than 1%. Color scales are the same for figures S33-S60 to enable visual comparison between different combinations of oviposition months and nests depths.

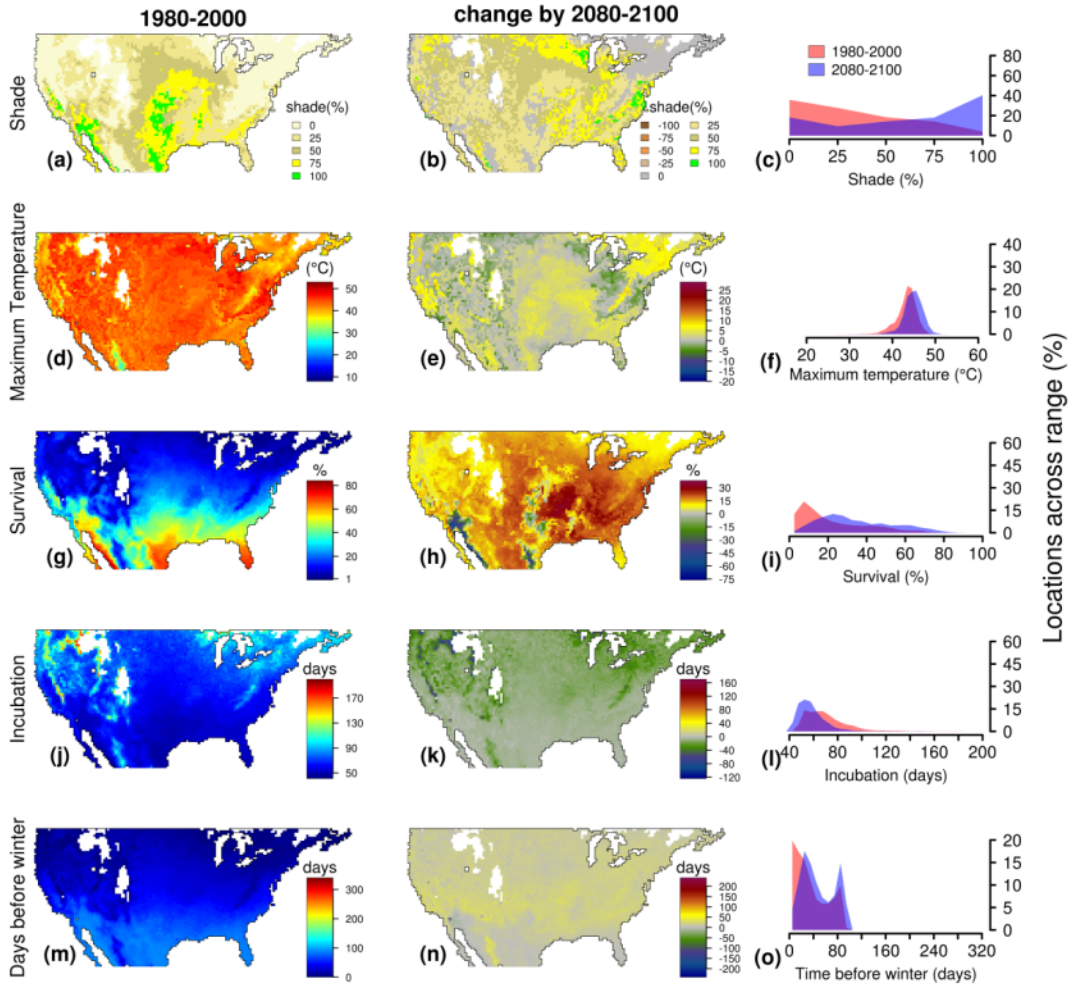

Figure S51: The shade conditions that maximize embryonic survival vary across space and time. Here, we show the optimal levels of shade for eggs laid at a maximal depth of 9 cm during the month of August in the period of 1980-2000 (a). We also show the optimal change in shade between the periods of 1980-2000 and 2080-2100 (b), and (c) the distribution of optimal shade conditions at both periods. The remaining plots depict the maximal soil temperatures (d-f), maximal survival rates (g-i), incubation period (k-l), and time between hatching and the first day of winter (m-o), assuming that mothers construct nests with the optimal level of shade. White areas represent locations for which climate conditions did not enable enough activity to promote reproduction or maximal survival rate was lower than 1%. Color scales are the same for figures S33-S60 to enable visual comparison between different combinations of oviposition months and nests depths.

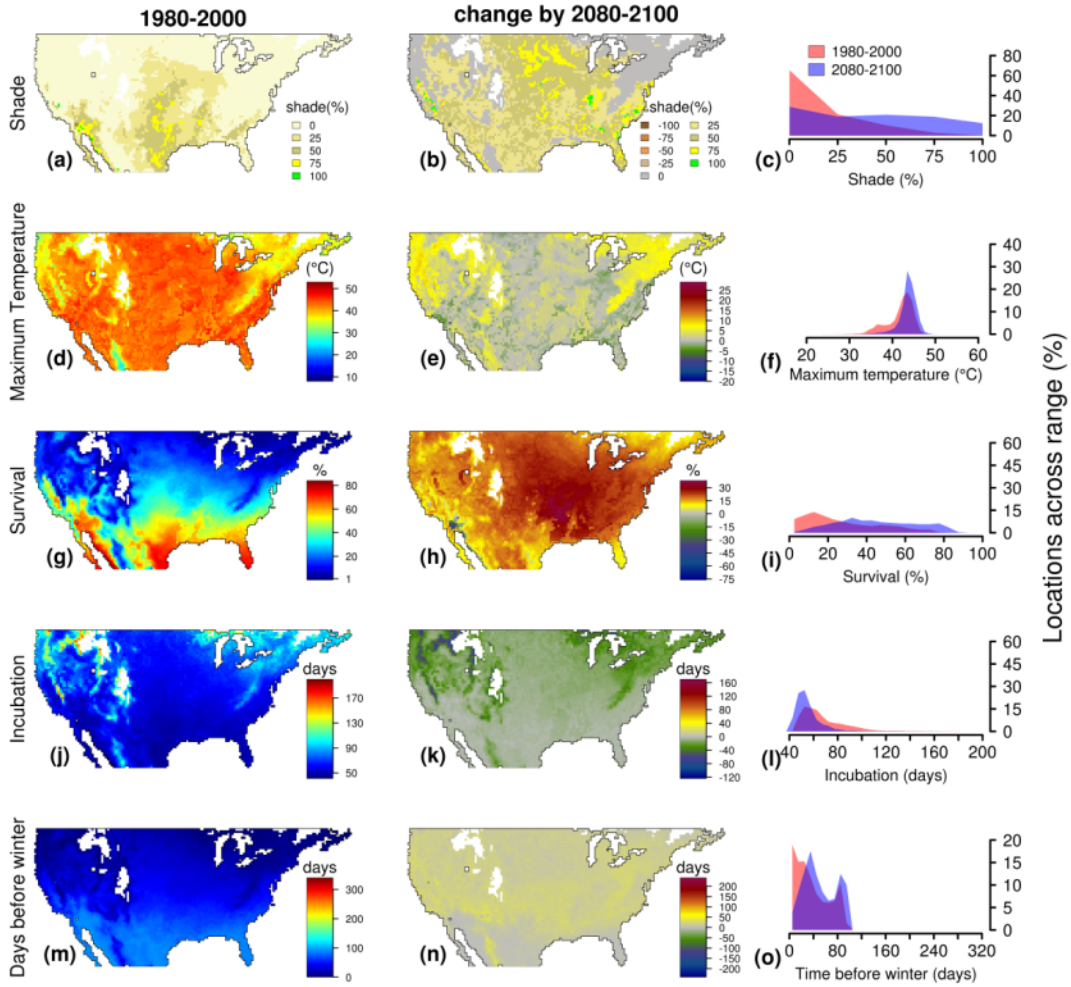

Figure S52: The shade conditions that maximize embryonic survival vary across space and time. Here, we show the optimal levels of shade for eggs laid at a maximal depth of 12 cm during the month of August in the period of 1980-2000 (a). We also show the optimal change in shade between the periods of 1980-2000 and 2080-2100 (b), and (c) the distribution of optimal shade conditions at both periods. The remaining plots depict the maximal soil temperatures (d-f), maximal survival rates (g-i), incubation period (k-l), and time between hatching and the first day of winter (m-o), assuming that mothers construct nests with the optimal level of shade. White areas represent locations for which climate conditions did not enable enough activity to promote reproduction or maximal survival rate was lower than 1%. Color scales are the same for figures S33-S60 to enable visual comparison between different combinations of oviposition months and nests depths.

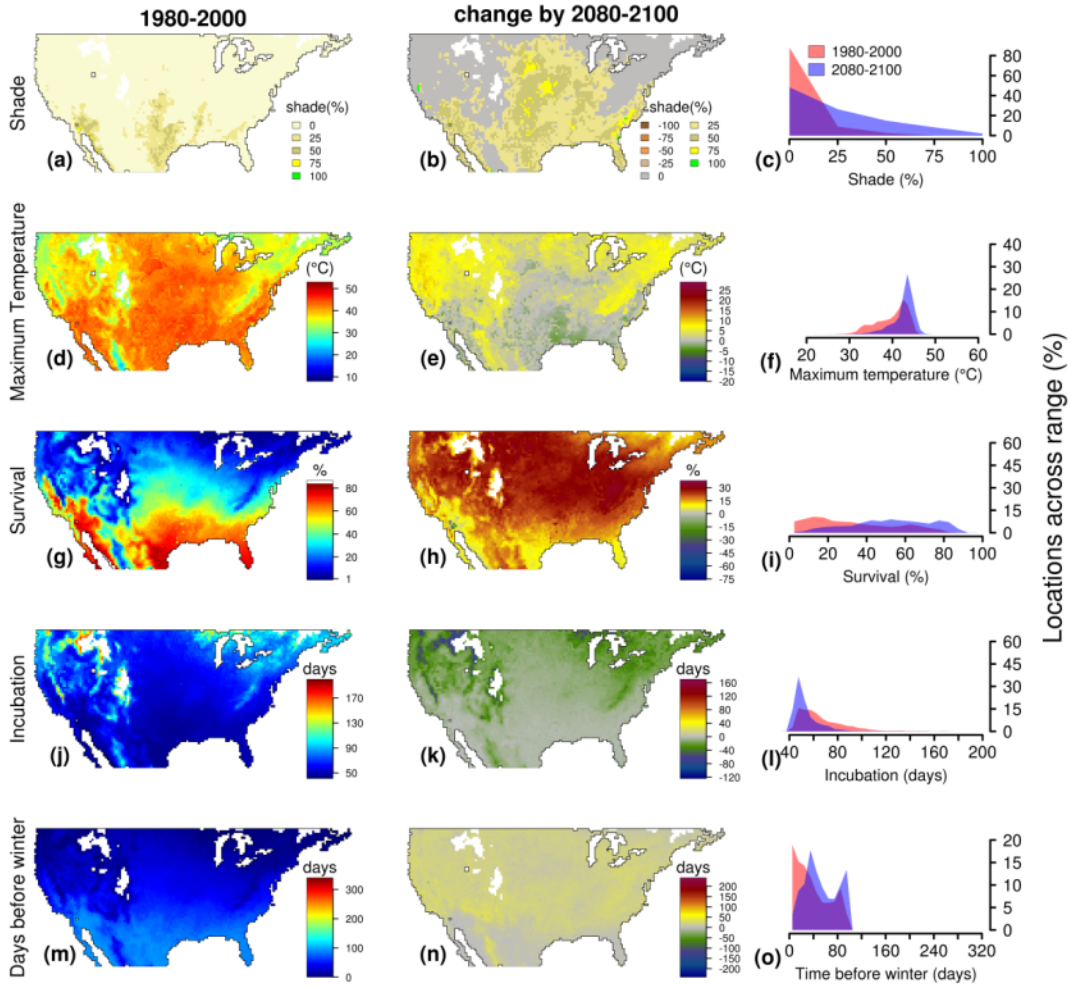

Figure S53: The shade conditions that maximize embryonic survival vary across space and time. Here, we show the optimal levels of shade for eggs laid at a maximal depth of 3 cm during the month of September in the period of 1980-2000 (a). We also show the optimal change in shade between the periods of 1980-2000 and 2080-2100 (b), and (c) the distribution of optimal shade conditions at both periods. The remaining plots depict the maximal soil temperatures (d-f), maximal survival rates (g-i), incubation period (k-l), and time between hatching and the first day of winter (m-o), assuming that mothers construct nests with the optimal level of shade. White areas represent locations for which climate conditions did not enable enough activity to promote reproduction or maximal survival rate was lower than 1%. Color scales are the same for figures S33-S60 to enable visual comparison between different combinations of oviposition months and nests depths.

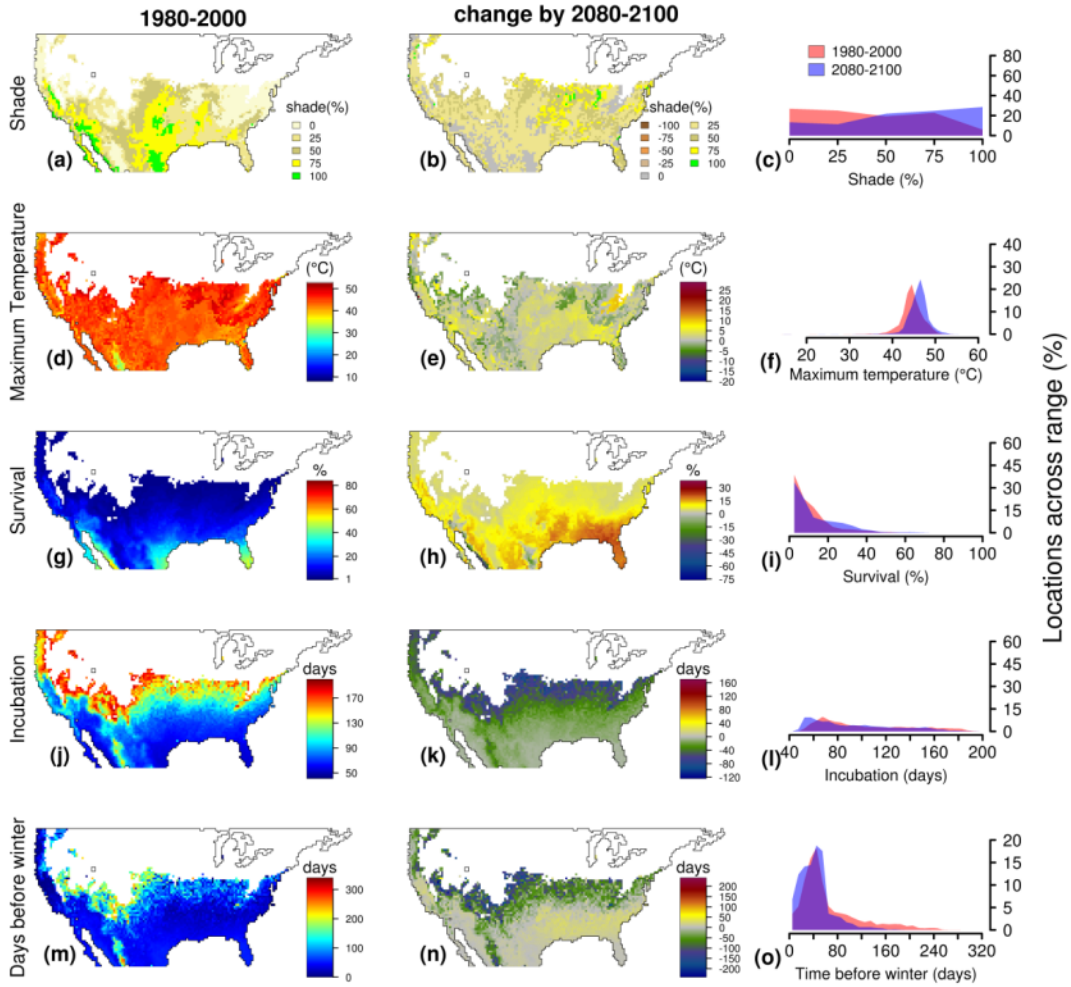

Figure S54: The shade conditions that maximize embryonic survival vary across space and time. Here, we show the optimal levels of shade for eggs laid at a maximal depth of 6 cm during the month of September in the period of 1980-2000 (a). We also show the optimal change in shade between the periods of 1980-2000 and 2080-2100 (b), and (c) the distribution of optimal shade conditions at both periods. The remaining plots depict the maximal soil temperatures (d-f), maximal survival rates (g-i), incubation period (k-l), and time between hatching and the first day of winter (m-o), assuming that mothers construct nests with the optimal level of shade. White areas represent locations for which climate conditions did not enable enough activity to promote reproduction or maximal survival rate was lower than 1%. Color scales are the same for figures S33-S60 to enable visual comparison between different combinations of oviposition months and nests depths.

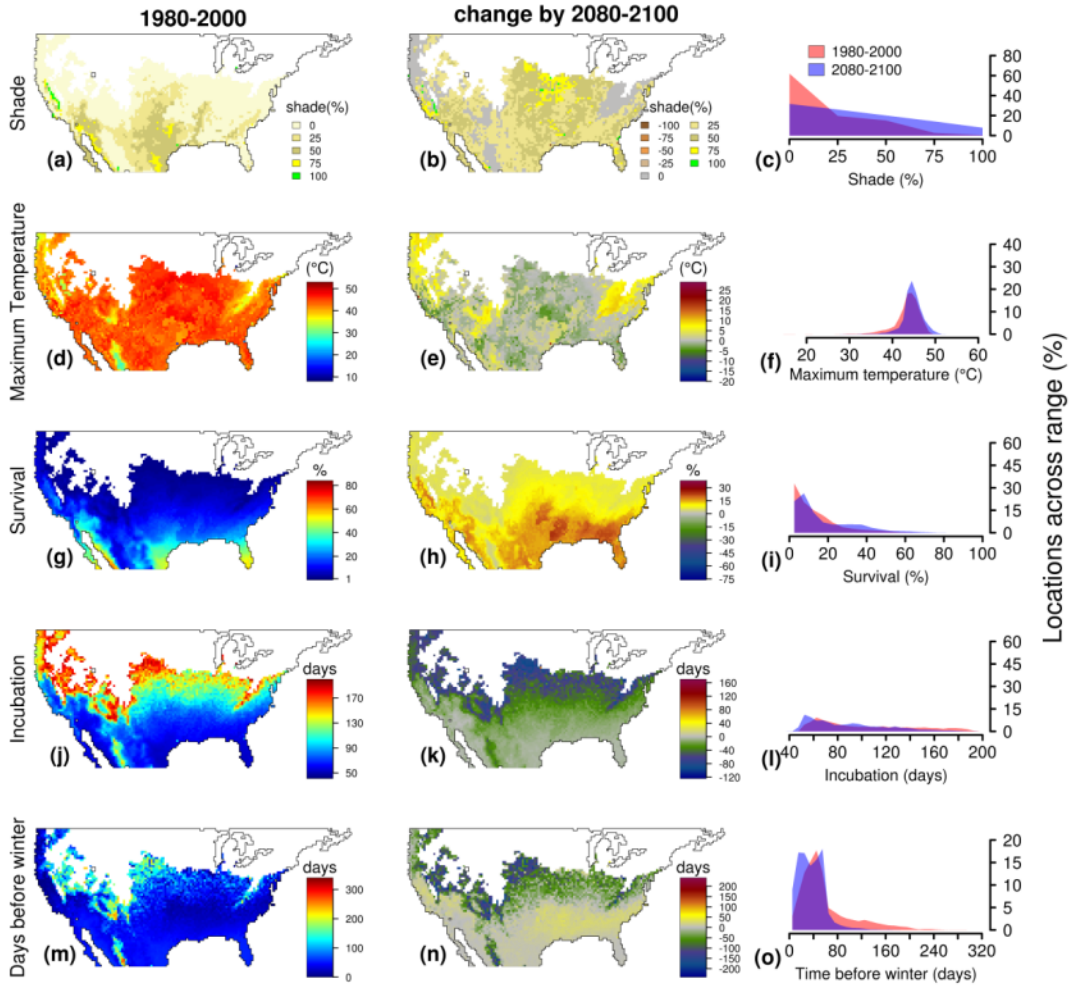

Figure S55: The shade conditions that maximize embryonic survival vary across space and time. Here, we show the optimal levels of shade for eggs laid at a maximal depth of 9 cm during the month of September in the period of 1980-2000 (a). We also show the optimal change in shade between the periods of 1980-2000 and 2080-2100 (b), and (c) the distribution of optimal shade conditions at both periods. The remaining plots depict the maximal soil temperatures (d-f), maximal survival rates (g-i), incubation period (k-l), and time between hatching and the first day of winter (m-o), assuming that mothers construct nests with the optimal level of shade. White areas represent locations for which climate conditions did not enable enough activity to promote reproduction or maximal survival rate was lower than 1%. Color scales are the same for figures S33-S60 to enable visual comparison between different combinations of oviposition months and nests depths.

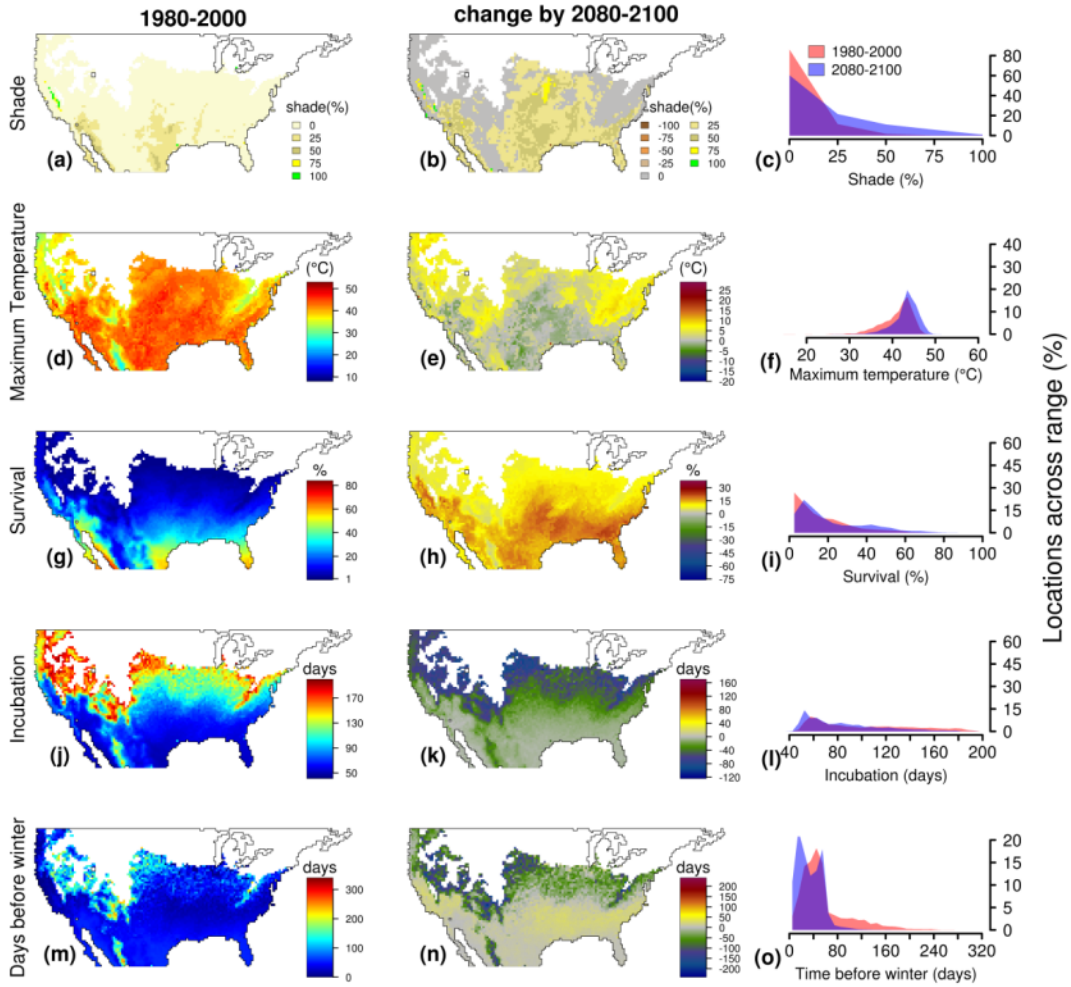

Figure S56: The shade conditions that maximize embryonic survival vary across space and time. Here, we show the optimal levels of shade for eggs laid at a maximal depth of 12 cm during the month of October in the period of 1980-2000 (a). We also show the optimal change in shade between the periods of 1980-2000 and 2080-2100 (b), and (c) the distribution of optimal shade conditions at both periods. The remaining plots depict the maximal soil temperatures (d-f), maximal survival rates (g-i), incubation period (k-l), and time between hatching and the first day of winter (m-o), assuming that mothers construct nests with the optimal level of shade. White areas represent locations for which climate conditions did not enable enough activity to promote reproduction or maximal survival rate was lower than 1%. Color scales are the same for figures S33-S60 to enable visual comparison between different combinations of oviposition months and nests depths.

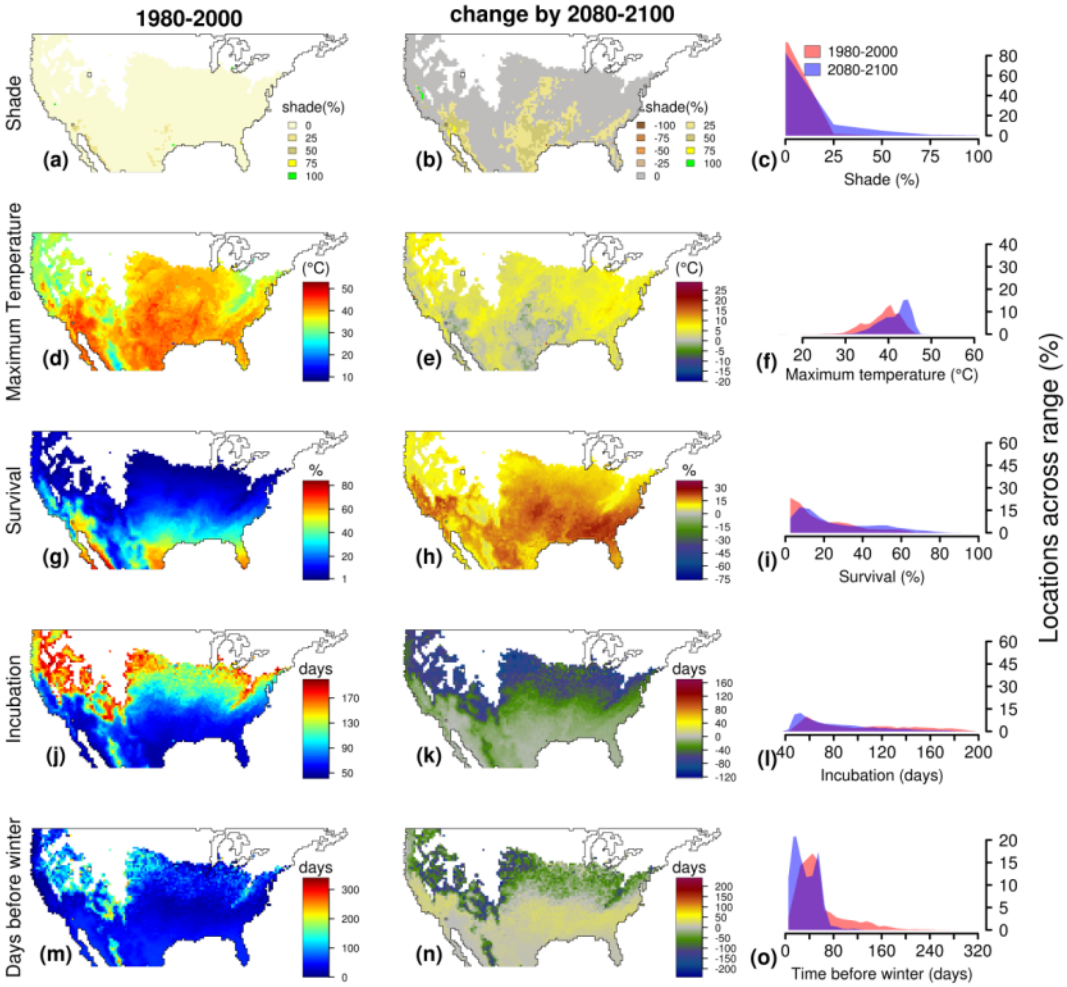

Figure S57: The shade conditions that maximize embryonic survival vary across space and time. Here, we show the optimal levels of shade for eggs laid at a maximal depth of 3 cm during the month of October in the period of 1980-2000 (a). We also show the optimal change in shade between the periods of 1980-2000 and 2080-2100 (b), and (c) the distribution of optimal shade conditions at both periods. The remaining plots depict the maximal soil temperatures (d-f), maximal survival rates (g-i), incubation period (k-l), and time between hatching and the first day of winter (m-o), assuming that mothers construct nests with the optimal level of shade. White areas represent locations for which climate conditions did not enable enough activity to promote reproduction or maximal survival rate was lower than 1%. Color scales are the same for figures S33-S60 to enable visual comparison between different combinations of oviposition months and nests depths.

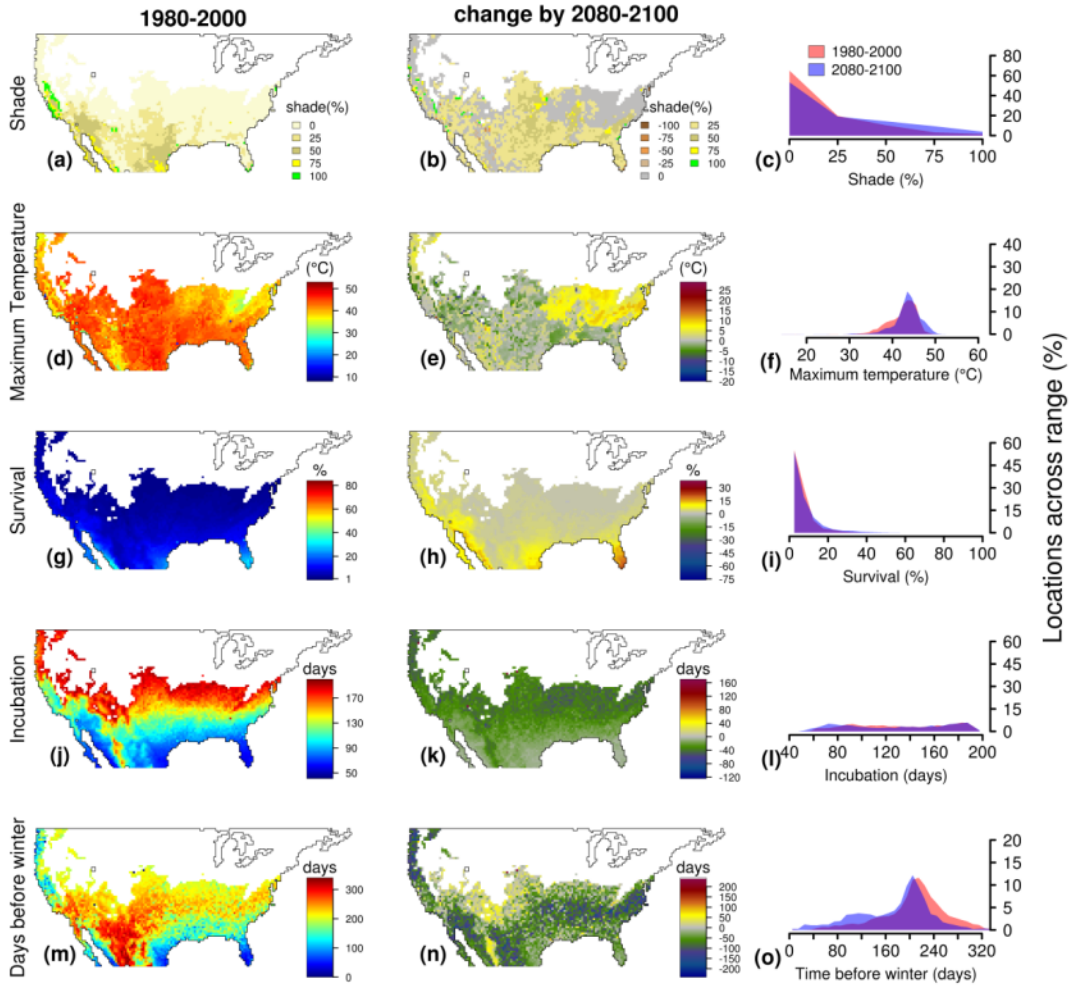

Figure S58: The shade conditions that maximize embryonic survival vary across space and time. Here, we show the optimal levels of shade for eggs laid at a maximal depth of 6 cm during the month of October in the period of 1980-2000 (a). We also show the optimal change in shade between the periods of 1980-2000 and 2080-2100 (b), and (c) the distribution of optimal shade conditions at both periods. The remaining plots depict the maximal soil temperatures (d-f), maximal survival rates (g-i), incubation period (k-l), and time between hatching and the first day of winter (m-o), assuming that mothers construct nests with the optimal level of shade. White areas represent locations for which climate conditions did not enable enough activity to promote reproduction or maximal survival rate was lower than 1%. Color scales are the same for figures S33-S60 to enable visual comparison between different combinations of oviposition months and nests depths.

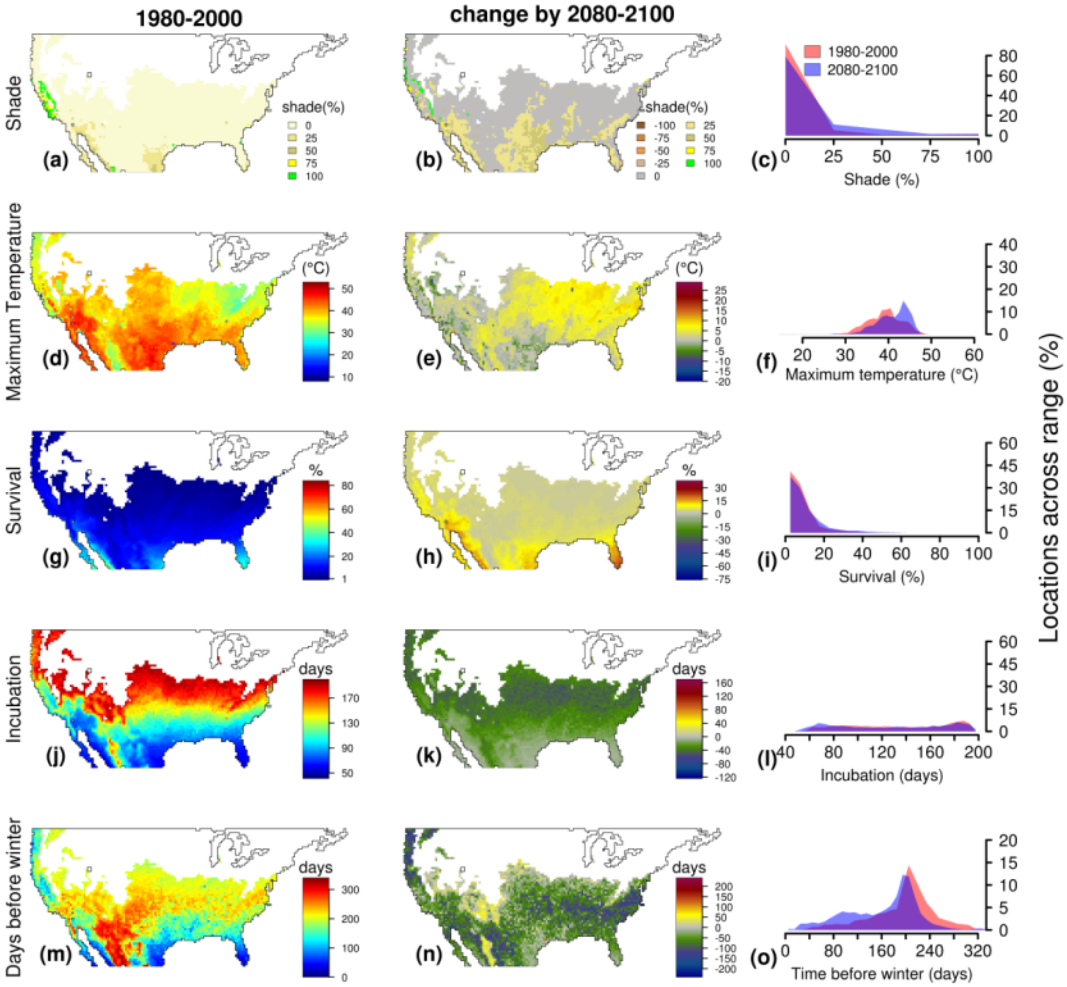

Figure S59: The shade conditions that maximize embryonic survival vary across space and time. Here, we show the optimal levels of shade for eggs laid at a maximal depth of 9 cm during the month of October in the period of 1980-2000 (a). We also show the optimal change in shade between the periods of 1980-2000 and 2080-2100 (b), and (c) the distribution of optimal shade conditions at both periods. The remaining plots depict the maximal soil temperatures (d-f), maximal survival rates (g-i), incubation period (k-l), and time between hatching and the first day of winter (m-o), assuming that mothers construct nests with the optimal level of shade. White areas represent locations for which climate conditions did not enable enough activity to promote reproduction or maximal survival rate was lower than 1%. Color scales are the same for figures S33-S60 to enable visual comparison between different combinations of oviposition months and nests depths.

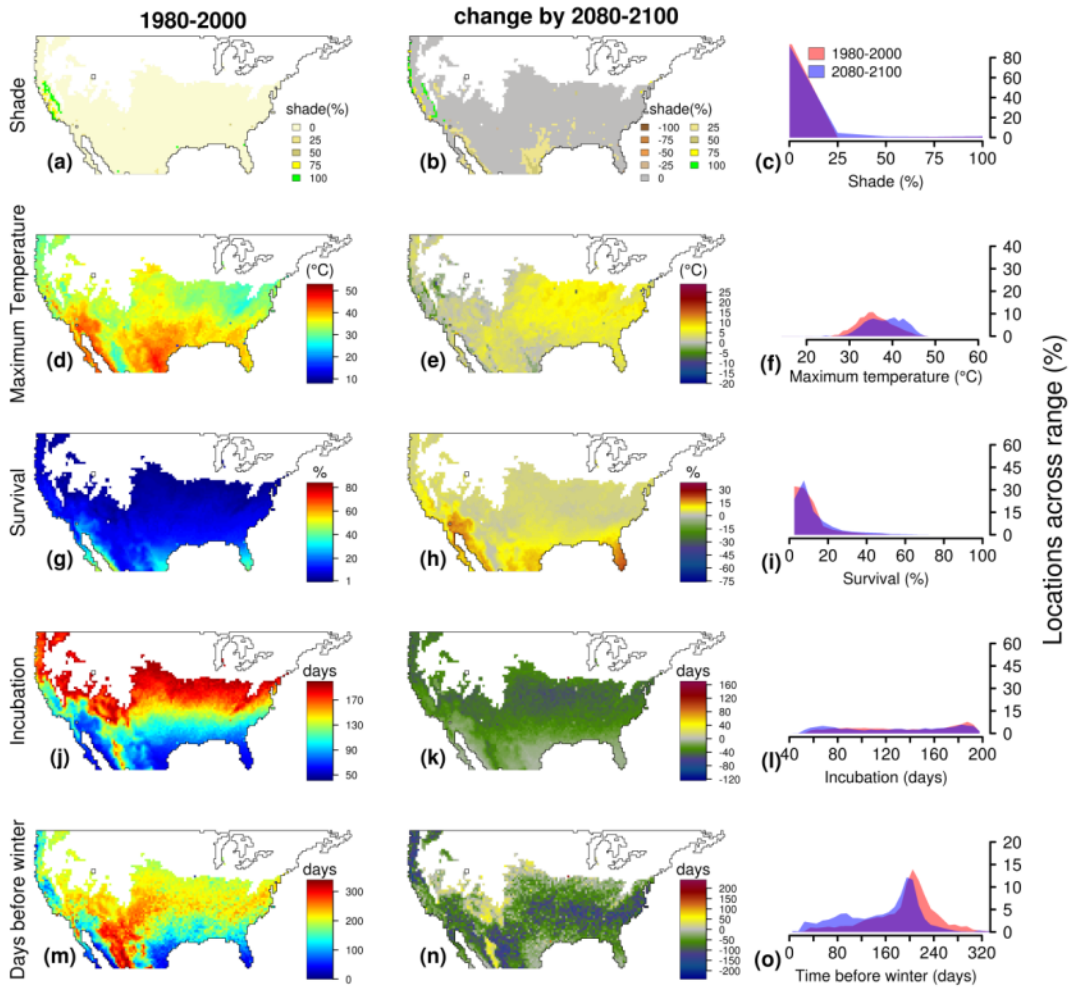

Figure S60: The shade conditions that maximize embryonic survival vary across space and time. Here, we show the optimal levels of shade for eggs laid at a maximal depth of 12 cm during the month of October in the period of 1980-2000 (a). We also show the optimal change in shade between the periods of 1980-2000 and 2080-2100 (b), and (c) the distribution of optimal shade conditions at both periods. The remaining plots depict the maximal soil temperatures (d-f), maximal survival rates (g-i), incubation period (k-l), and time between hatching and the first day of winter (m-o), assuming that mothers construct nests with the optimal level of shade. White areas represent locations for which climate conditions did not enable enough activity to promote reproduction or maximal survival rate was lower than 1%. Color scales are the same for figures S33-S60 to enable visual comparison between different combinations of oviposition months and nests depths.

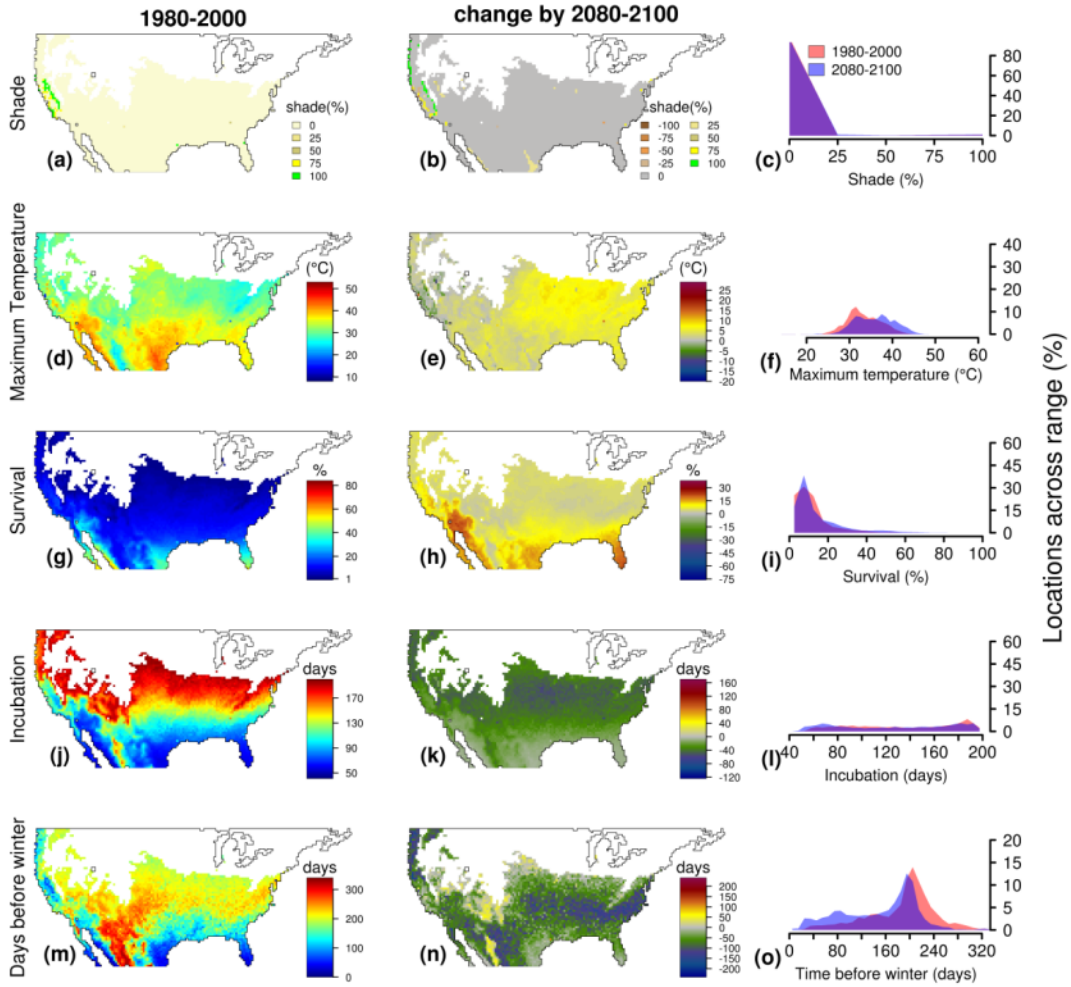

Figure S61: Population growth rates predicted when embryos survival varies with time and location under (a) monthly averages climate and (b) under hourly climate; and when assuming constant embryos survival (c) under monthly averaged climate and (d) under hourly climate. The impact of future climate on populations growth rate when changes in embryos survival are taken into account and when females nesting choice remains the same (e – monthly climate data, f – hourly climate data), or females lay in more shaded locations (g – monthly climate data, h – hourly climate data) or at deeper nests (i – monthly climate data, j – hourly climate data). The impact of future climate on population growth rates when changes in embryos survival rates are ignored (k – monthly climate data, l – hourly climate data). Data is presented for nests at 3 cm depth and 0% shade conditions. Color scales are the same for figures S61-S72 to enable visual comparison between different combinations of nests depths and shade conditions.

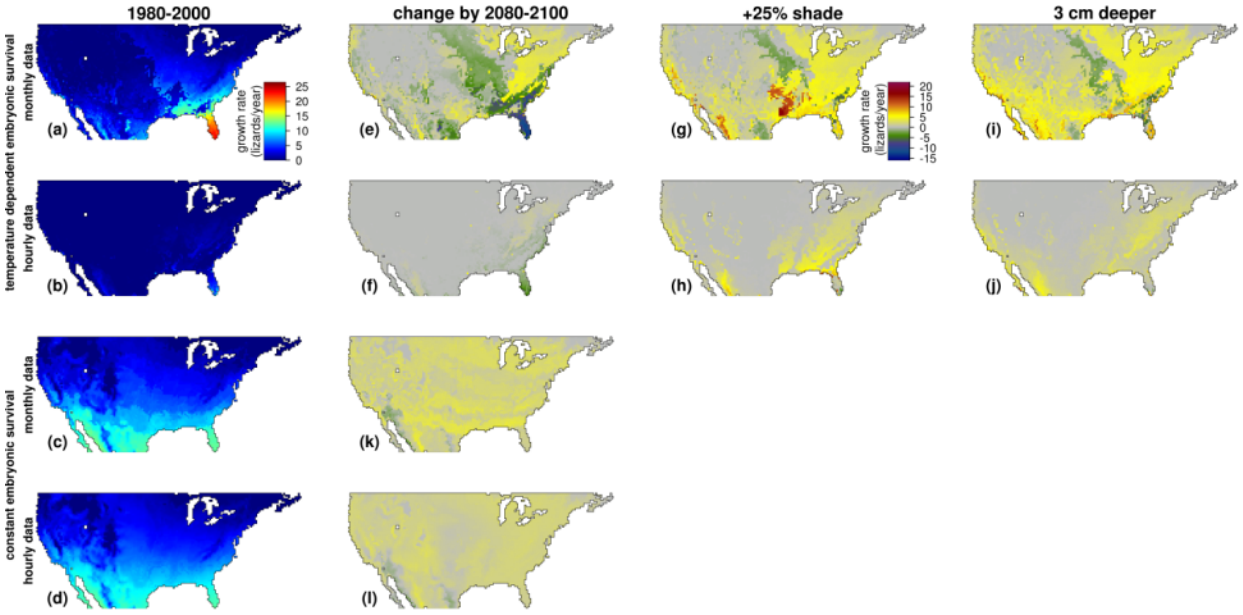

Figure S62: Population growth rates predicted when embryos survival varies with time and location under (a) monthly averages climate and (b) under hourly climate; and when assuming constant embryos survival (c) under monthly averaged climate and (d) under hourly climate. The impact of future climate on populations growth rate when changes in embryos survival are taken into account and when females nesting choice remains the same (e – monthly climate data, f – hourly climate data), or females lay in more shaded locations (g – monthly climate data, h – hourly climate data) or at deeper nests (i – monthly climate data, j – hourly climate data). The impact of future climate on population growth rates when changes in embryos survival rates are ignored (k – monthly climate data, l – hourly climate data). Data is presented for nests at 6 cm depth and 0% shade conditions. Color scales are the same for figures S61-S72 to enable visual comparison between different combinations of nests depths and shade conditions.

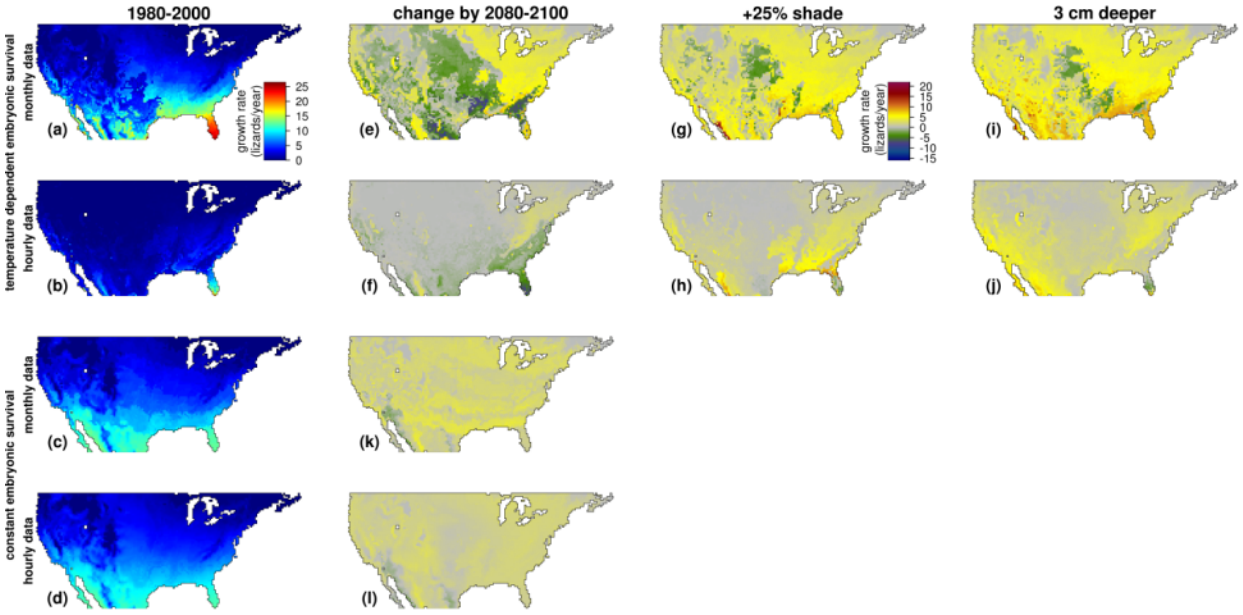

Figure S63: Population growth rates predicted when embryos survival varies with time and location under (a) monthly averages climate and (b) under hourly climate; and when assuming constant embryos survival (c) under monthly averaged climate and (d) under hourly climate. The impact of future climate on populations growth rate when changes in embryos survival are taken into account and when females nesting choice remains the same (e – monthly climate data, f – hourly climate data), or females lay in more shaded locations (g – monthly climate data, h – hourly climate data) or at deeper nests (i – monthly climate data, j – hourly climate data). The impact of future climate on population growth rates when changes in embryos survival rates are ignored (k – monthly climate data, l – hourly climate data). Data is presented for nests at 9 cm depth and 0% shade conditions. Color scales are the same for figures S61-S72 to enable visual comparison between different combinations of nests depths and shade conditions.

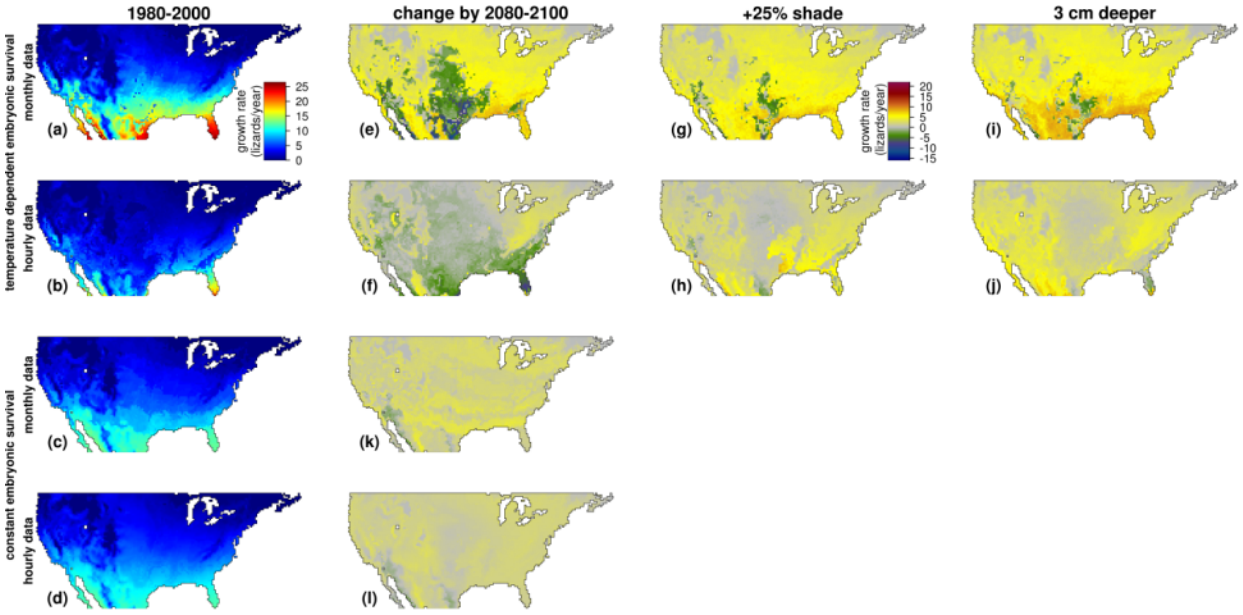

Figure S64: Population growth rates predicted when embryos survival varies with time and location under (a) monthly averages climate and (b) under hourly climate; and when assuming constant embryos survival (c) under monthly averaged climate and (d) under hourly climate. The impact of future climate on populations growth rate when changes in embryos survival are taken into account and when females nesting choice remains the same (e – monthly climate data, f – hourly climate data), or females lay in more shaded locations (g – monthly climate data, h – hourly climate data) or at deeper nests (i – monthly climate data, j – hourly climate data). The impact of future climate on population growth rates when changes in embryos survival rates are ignored (k – monthly climate data, l – hourly climate data). Data is presented for nests at 3 cm depth and 25% shade conditions. Color scales are the same for figures S61-S72 to enable visual comparison between different combinations of nests depths and shade conditions.

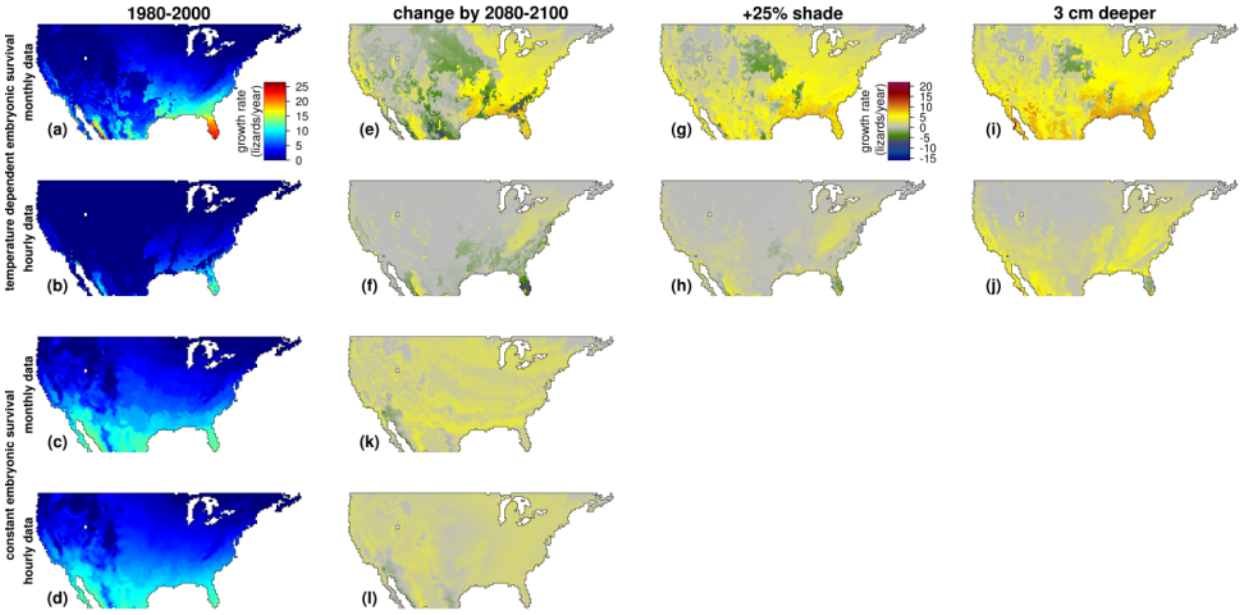

Figure S65: Population growth rates predicted when embryos survival varies with time and location under (a) monthly averages climate and (b) under hourly climate; and when assuming constant embryos survival (c) under monthly averaged climate and (d) under hourly climate. The impact of future climate on populations growth rate when changes in embryos survival are taken into account and when females nesting choice remains the same (e – monthly climate data, f – hourly climate data), or females lay in more shaded locations (g – monthly climate data, h – hourly climate data) or at deeper nests (i – monthly climate data, j – hourly climate data). The impact of future climate on population growth rates when changes in embryos survival rates are ignored (k – monthly climate data, l – hourly climate data). Data is presented for nests at 6 cm depth and 25% shade conditions. Color scales are the same for figures S61-S72 to enable visual comparison between different combinations of nests depths and shade conditions.

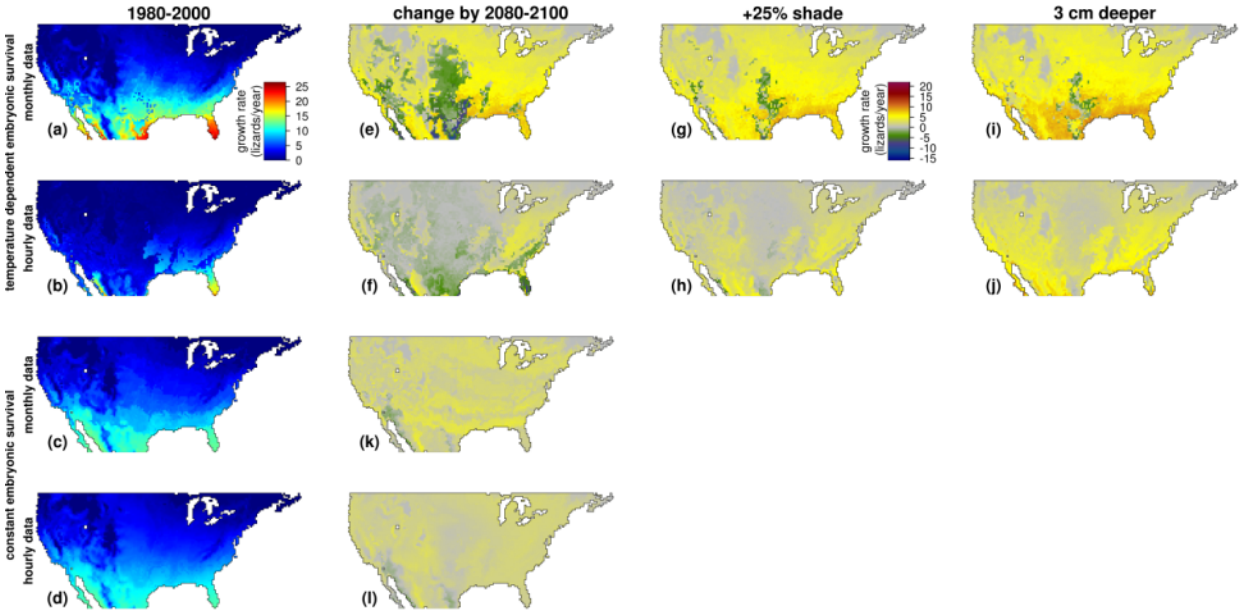

Figure S66: Population growth rates predicted when embryos survival varies with time and location under (a) monthly averages climate and (b) under hourly climate; and when assuming constant embryos survival (c) under monthly averaged climate and (d) under hourly climate. The impact of future climate on populations growth rate when changes in embryos survival are taken into account and when females nesting choice remains the same (e – monthly climate data, f – hourly climate data), or females lay in more shaded locations (g – monthly climate data, h – hourly climate data) or at deeper nests (i – monthly climate data, j – hourly climate data). The impact of future climate on population growth rates when changes in embryos survival rates are ignored (k – monthly climate data, l – hourly climate data). Data is presented for nests at 9 cm depth and 25% shade conditions. Color scales are the same for figures S61-S72 to enable visual comparison between different combinations of nests depths and shade conditions.

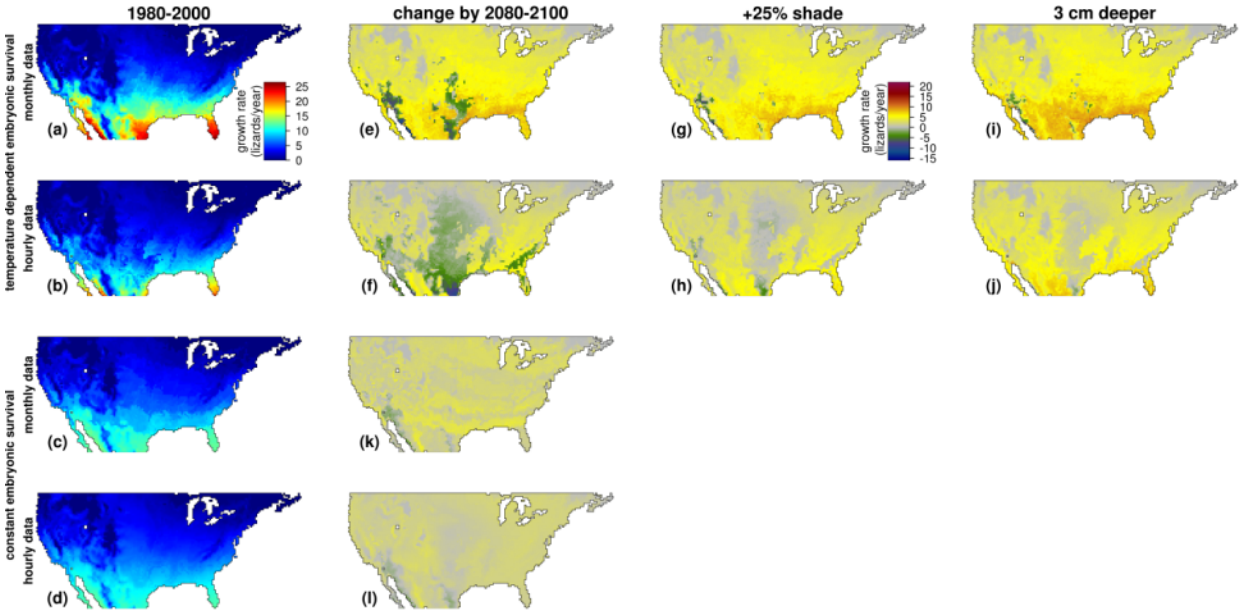

Figure S67: Population growth rates predicted when embryos survival varies with time and location under (a) monthly averages climate and (b) under hourly climate; and when assuming constant embryos survival (c) under monthly averaged climate and (d) under hourly climate. The impact of future climate on populations growth rate when changes in embryos survival are taken into account and when females nesting choice remains the same (e – monthly climate data, f – hourly climate data), or females lay in more shaded locations (g – monthly climate data, h – hourly climate data) or at deeper nests (i – monthly climate data, j – hourly climate data). The impact of future climate on population growth rates when changes in embryos survival rates are ignored (k – monthly climate data, l – hourly climate data). Data is presented for nests at 3 cm depth and 50% shade conditions. Color scales are the same for figures S61-S72 to enable visual comparison between different combinations of nests depths and shade conditions.

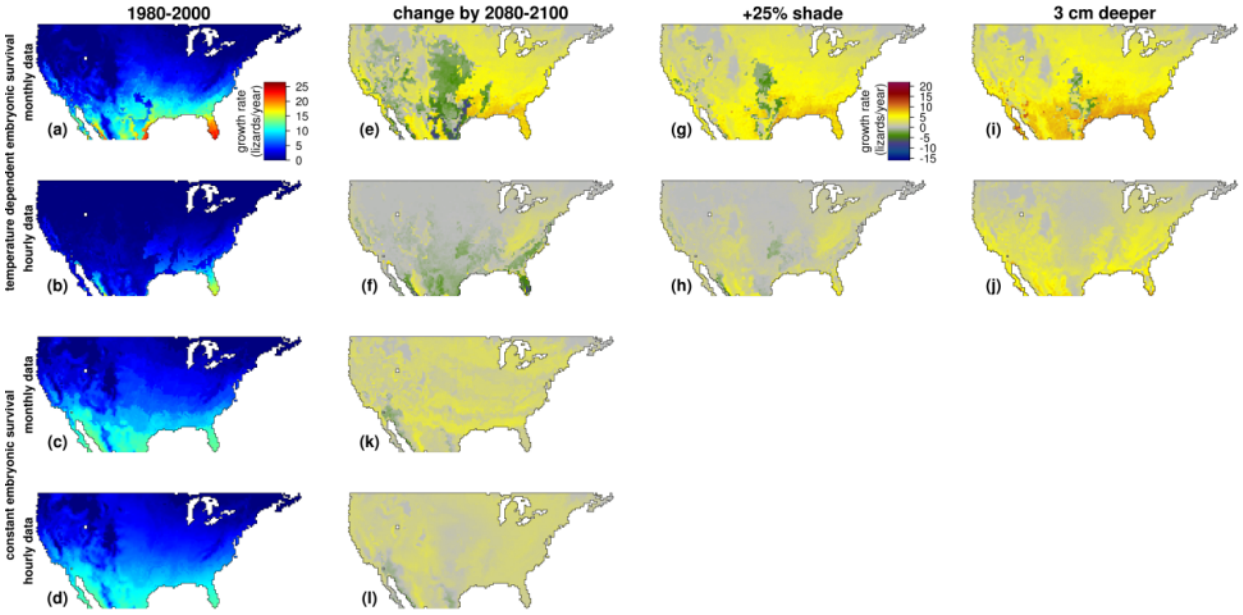

Figure S68: Population growth rates predicted when embryos survival varies with time and location under (a) monthly averages climate and (b) under hourly climate; and when assuming constant embryos survival (c) under monthly averaged climate and (d) under hourly climate. The impact of future climate on populations growth rate when changes in embryos survival are taken into account and when females nesting choice remains the same (e – monthly climate data, f – hourly climate data), or females lay in more shaded locations (g – monthly climate data, h – hourly climate data) or at deeper nests (i – monthly climate data, j – hourly climate data). The impact of future climate on population growth rates when changes in embryos survival rates are ignored (k – monthly climate data, l – hourly climate data). Data is presented for nests at 6 cm depth and 50% shade conditions. Color scales are the same for figures S61-S72 to enable visual comparison between different combinations of nests depths and shade conditions.

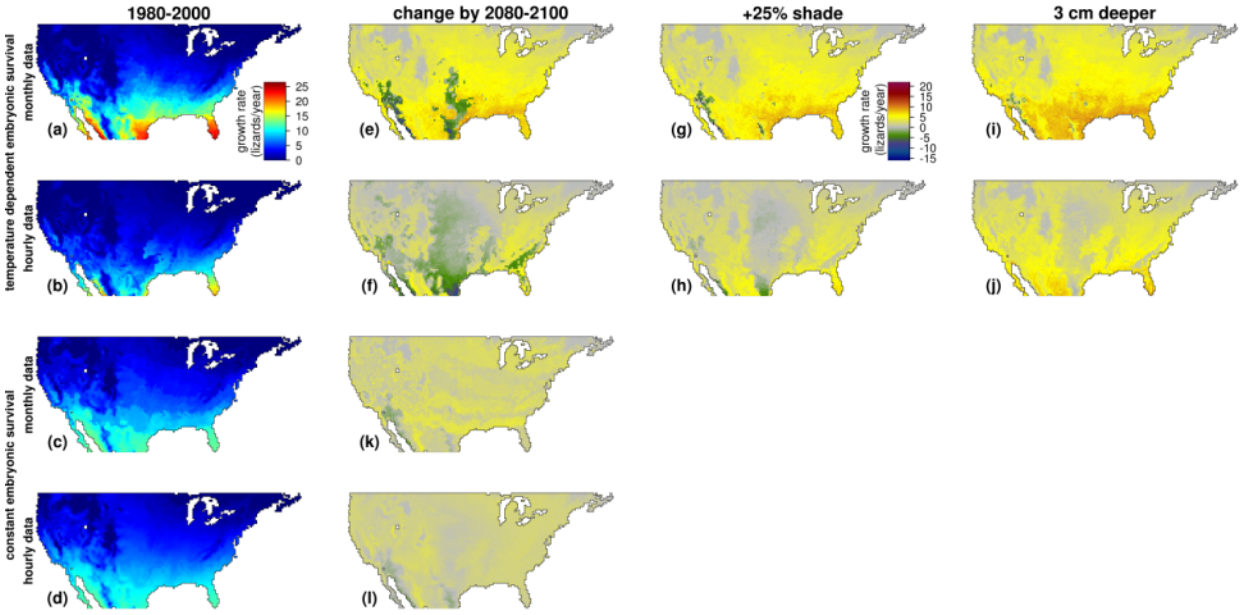

Figure S69: Population growth rates predicted when embryos survival varies with time and location under (a) monthly averages climate and (b) under hourly climate; and when assuming constant embryos survival (c) under monthly averaged climate and (d) under hourly climate. The impact of future climate on populations growth rate when changes in embryos survival are taken into account and when females nesting choice remains the same (e – monthly climate data, f – hourly climate data), or females lay in more shaded locations (g – monthly climate data, h – hourly climate data) or at deeper nests (i – monthly climate data, j – hourly climate data). The impact of future climate on population growth rates when changes in embryos survival rates are ignored (k – monthly climate data, l – hourly climate data). Data is presented for nests at 9 cm depth and 50% shade conditions. Color scales are the same for figures S61-S72 to enable visual comparison between different combinations of nests depths and shade conditions.

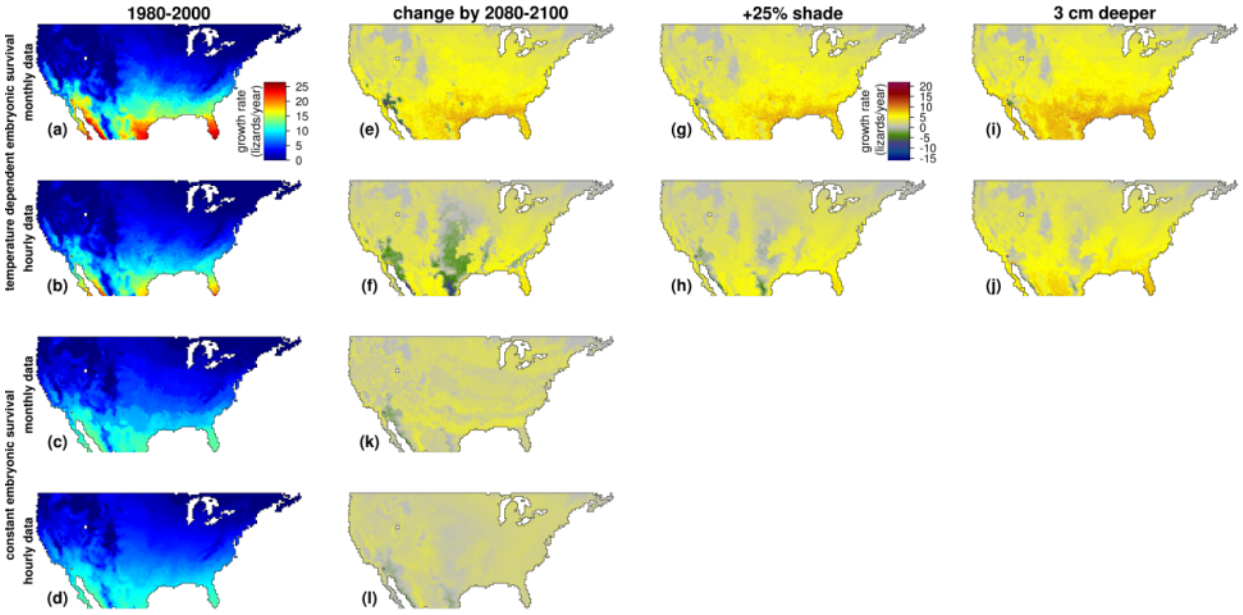

Figure S70: Population growth rates predicted when embryos survival varies with time and location under (a) monthly averages climate and (b) under hourly climate; and when assuming constant embryos survival (c) under monthly averaged climate and (d) under hourly climate. The impact of future climate on populations growth rate when changes in embryos survival are taken into account and when females nesting choice remains the same (e – monthly climate data, f – hourly climate data), or females lay in more shaded locations (g – monthly climate data, h – hourly climate data) or at deeper nests (i – monthly climate data, j – hourly climate data). The impact of future climate on population growth rates when changes in embryos survival rates are ignored (k – monthly climate data, l – hourly climate data). Data is presented for nests at 3 cm depth and 75% shade conditions. Color scales are the same for figures S61-S72 to enable visual comparison between different combinations of nests depths and shade conditions.

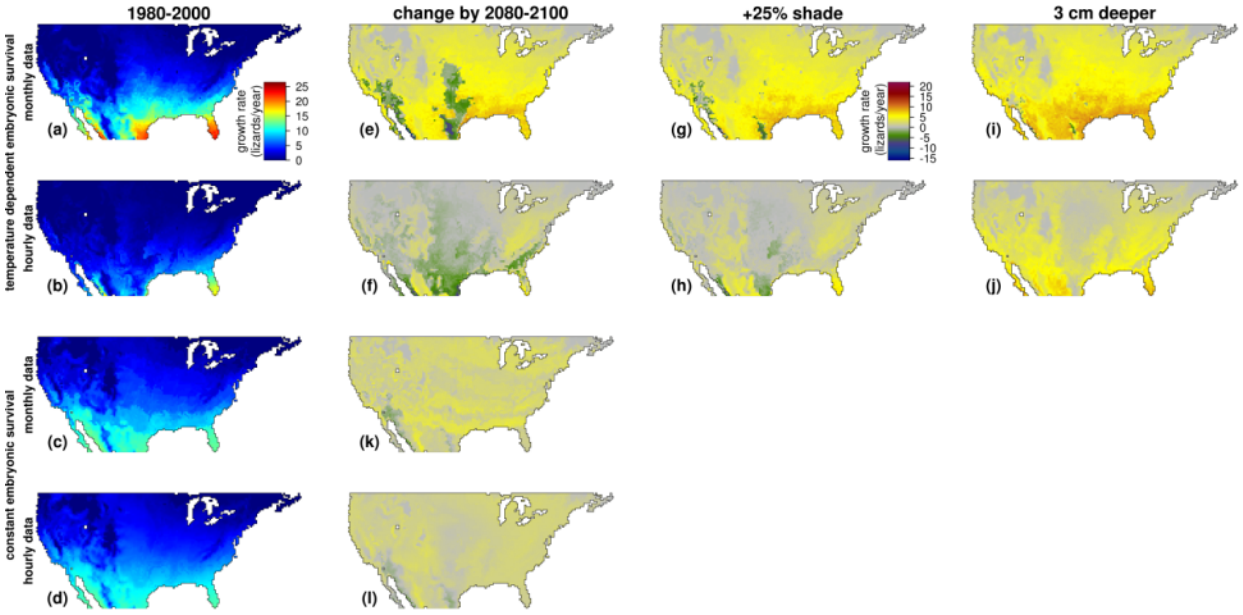

Figure S71: Population growth rates predicted when embryos survival varies with time and location under (a) monthly averages climate and (b) under hourly climate; and when assuming constant embryos survival (c) under monthly averaged climate and (d) under hourly climate. The impact of future climate on populations growth rate when changes in embryos survival are taken into account and when females nesting choice remains the same (e – monthly climate data, f – hourly climate data), or females lay in more shaded locations (g – monthly climate data, h – hourly climate data) or at deeper nests (i – monthly climate data, j – hourly climate data). The impact of future climate on population growth rates when changes in embryos survival rates are ignored (k – monthly climate data, l – hourly climate data). Data is presented for nests at 6 cm depth and 75% shade conditions. Color scales are the same for figures S61-S72 to enable visual comparison between different combinations of nests depths and shade conditions.

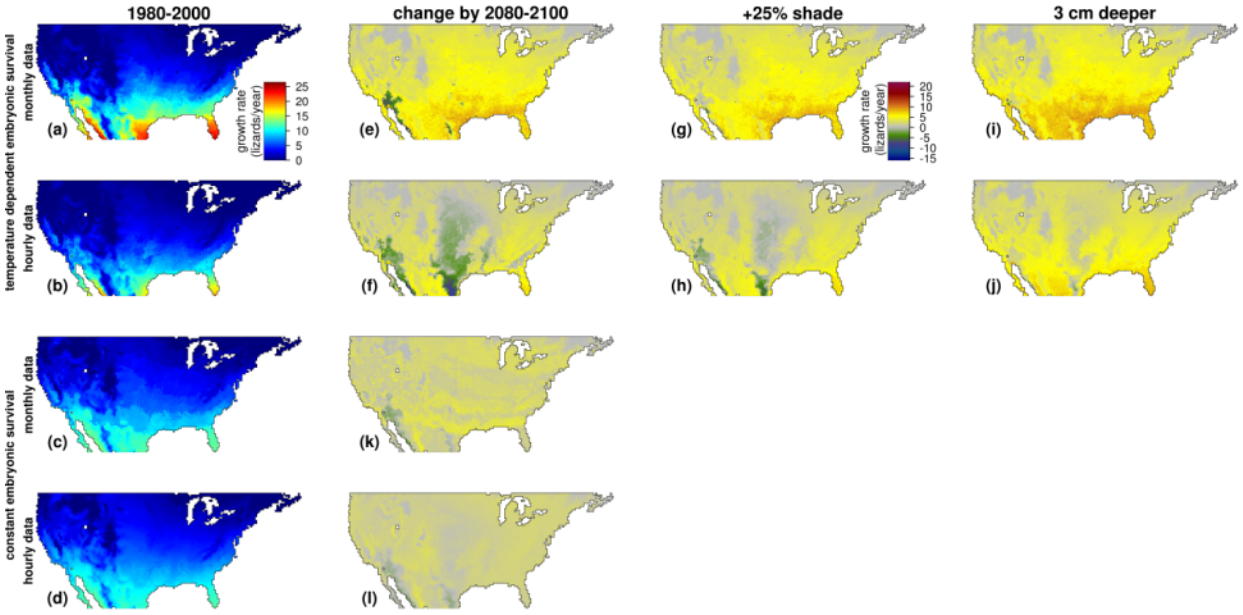

Figure S72: Population growth rates predicted when embryos survival varies with time and location under (a) monthly averages climate and (b) under hourly climate; and when assuming constant embryos survival (c) under monthly averaged climate and (d) under hourly climate. The impact of future climate on populations growth rate when changes in embryos survival are taken into account and when females nesting choice remains the same (e – monthly climate data, f – hourly climate data), or females lay in more shaded locations (g – monthly climate data, h – hourly climate data) or at deeper nests (i – monthly climate data, j – hourly climate data). The impact of future climate on population growth rates when changes in embryos survival rates are ignored (k – monthly climate data, l – hourly climate data). Data is presented for nests at 9 cm depth and 75% shade conditions. Color scales are the same for figures S61-S72 to enable visual comparison between different combinations of nests depths and shade conditions.

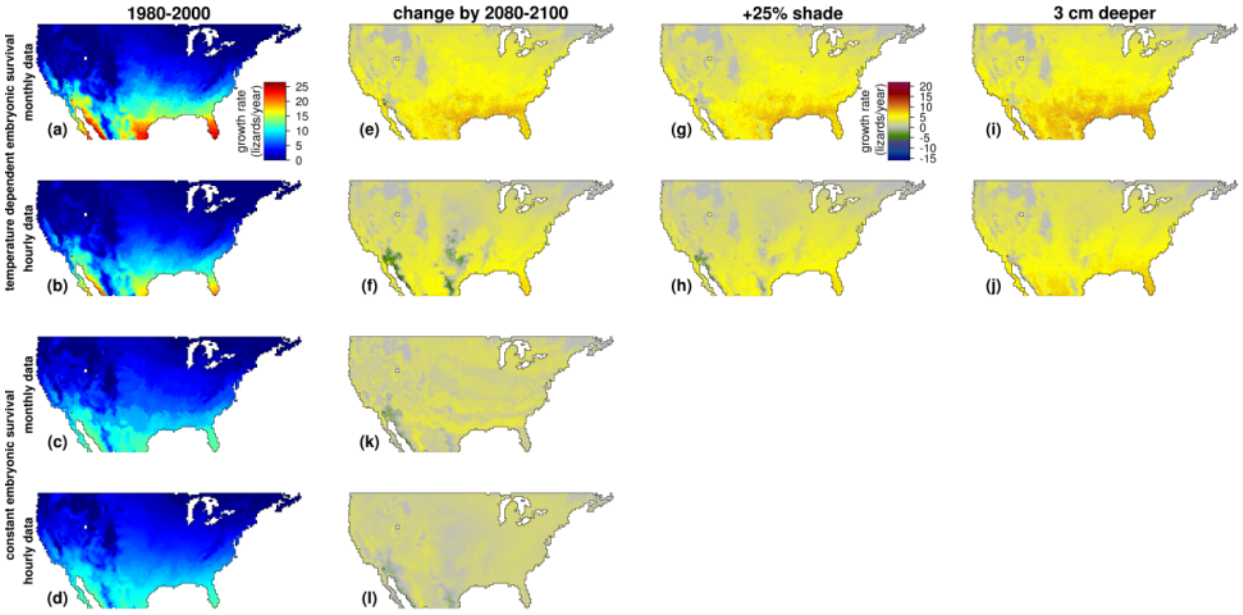

Figure S73: Minimum soil temperature during nesting under monthly and hourly data during past (1980-2000) climate and the predicted change in the future (2080-2099). Data are presented for nests laid in April at a depth of 3 cm under different shade conditions. White areas represent locations for which climate conditions did not enable enough activity to promote reproduction. Color scales are the same for figures S73-S100 to enable visual comparison between different combinations of oviposition months and nests depths.

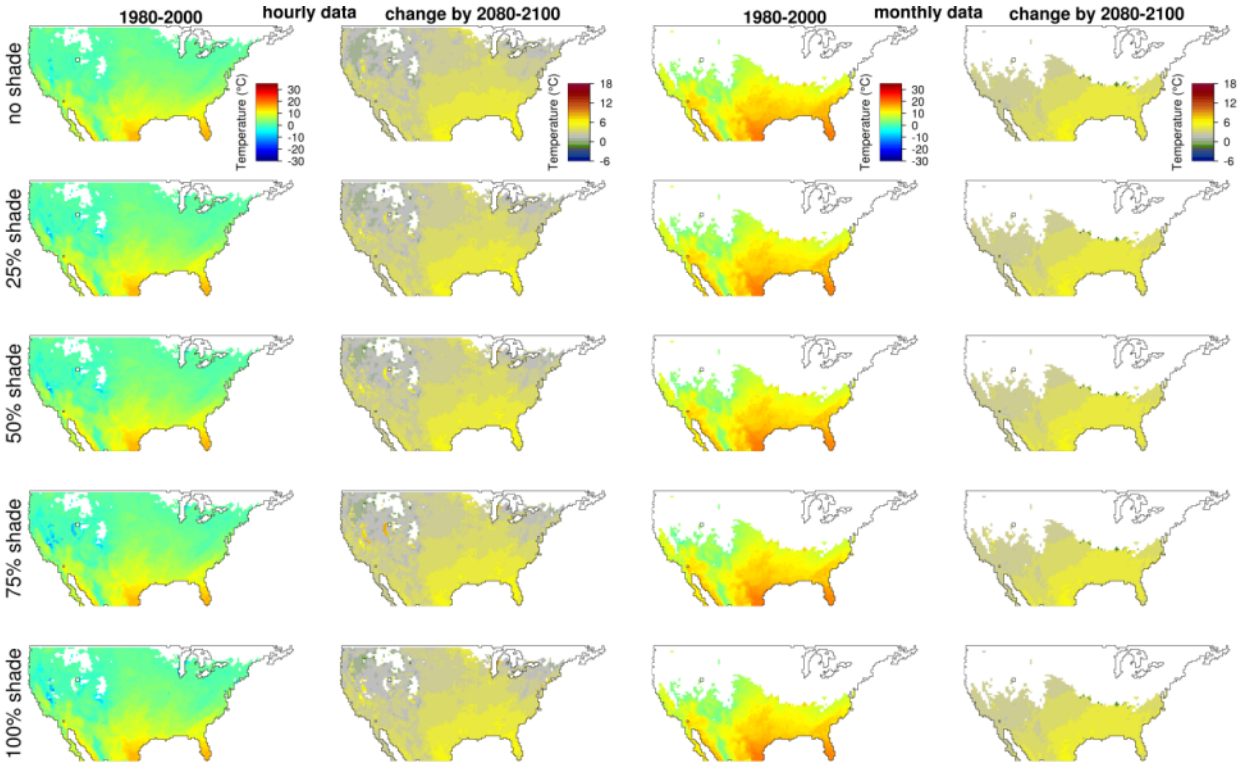

Figure S74: Minimum soil temperature during nesting under monthly and hourly data during past (1980-2000) climate and the predicted change in the future (2080-2099). Data are presented for nests laid in April at a depth of 6 cm under different shade conditions. White areas represent locations for which climate conditions did not enable enough activity to promote reproduction. Color scales are the same for figures S73-S100 to enable visual comparison between different combinations of oviposition months and nests depths.

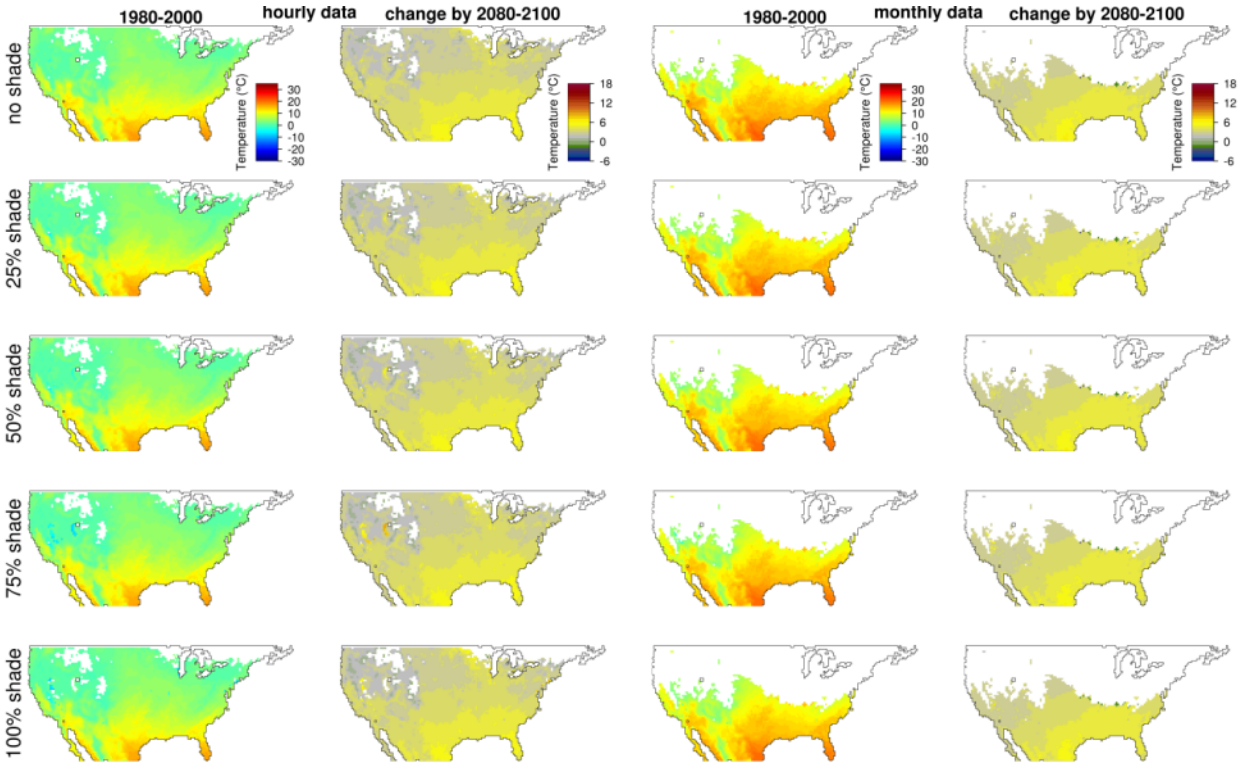

Figure S75: Minimum soil temperature during nesting under monthly and hourly data during past (1980-2000) climate and the predicted change in the future (2080-2099). Data are presented for nests laid in April at a depth of 9 cm under different shade conditions. White areas represent locations for which climate conditions did not enable enough activity to promote reproduction. Color scales are the same for figures S73-S100 to enable visual comparison between different combinations of oviposition months and nests depths.

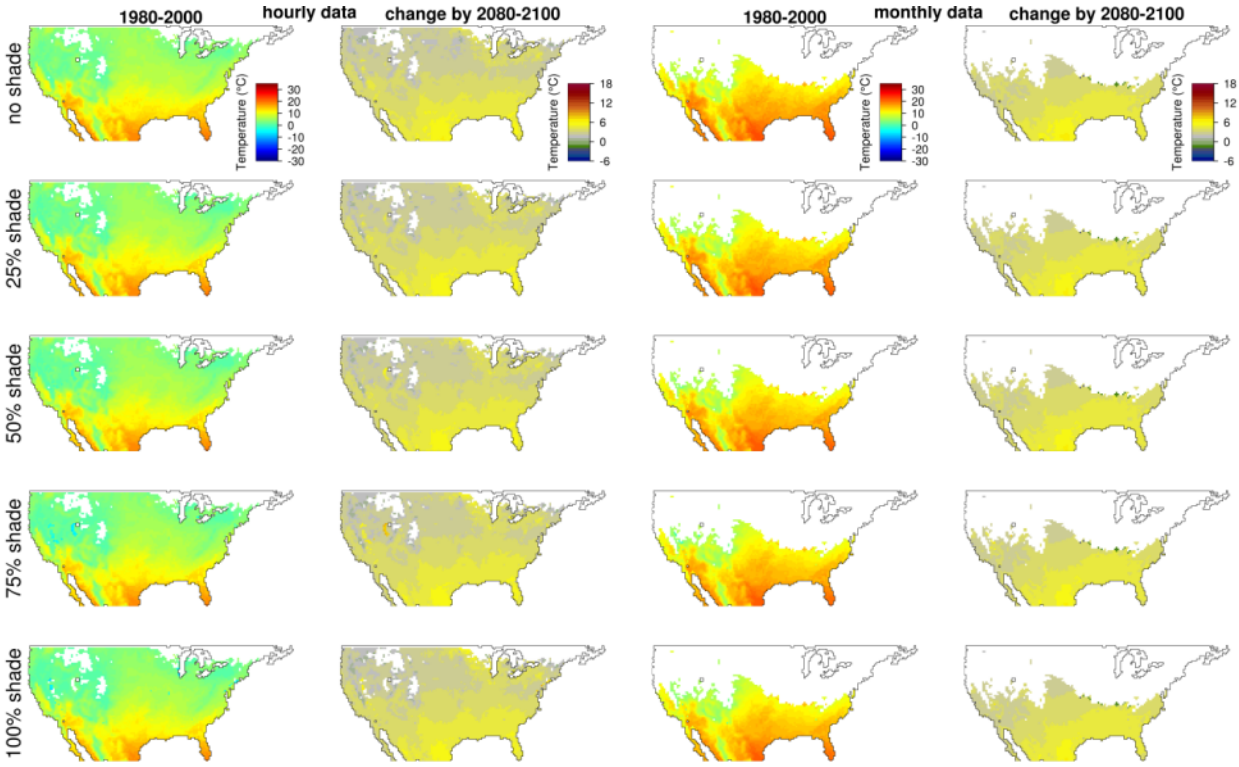

Figure S76: Minimum soil temperature during nesting under monthly and hourly data during past (1980-2000) climate and the predicted change in the future (2080-2099). Data are presented for nests laid in April at a depth of 12 cm under different shade conditions. White areas represent locations for which climate conditions did not enable enough activity to promote reproduction. Color scales are the same for figures S73-S100 to enable visual comparison between different combinations of oviposition months and nests depths.

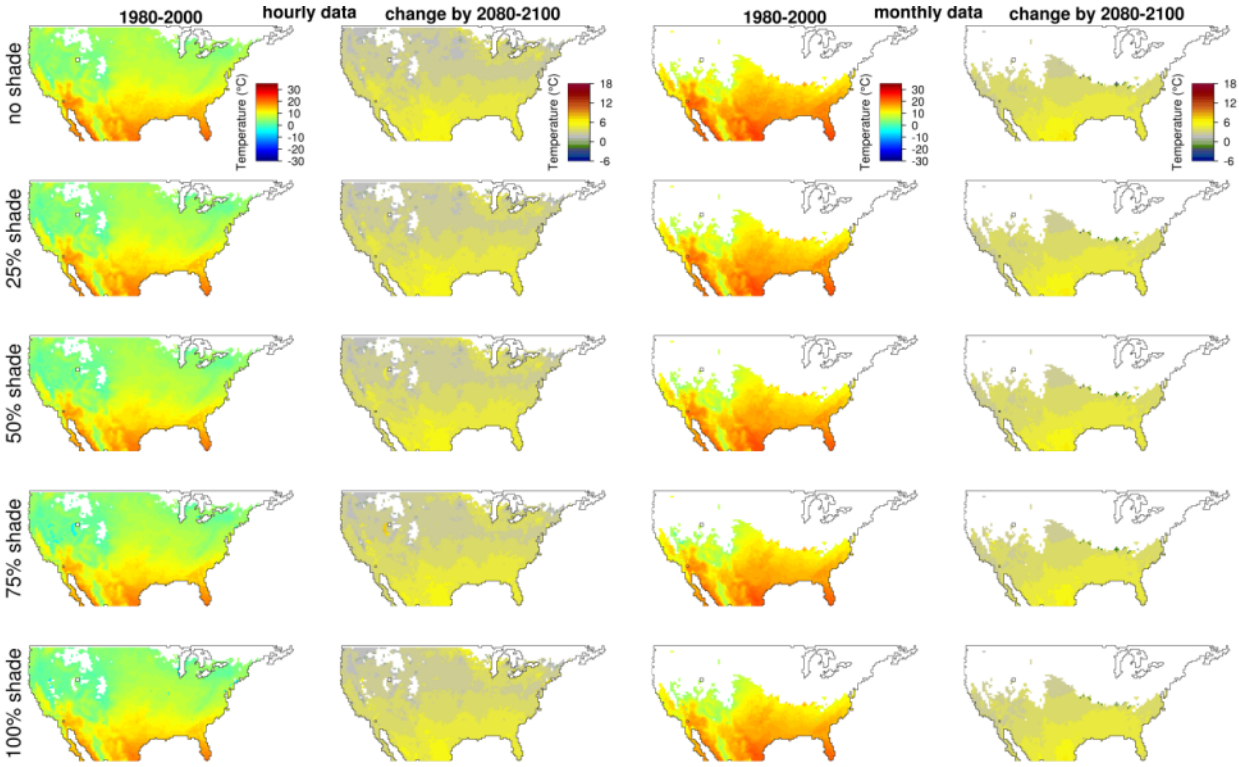

Figure S77: Minimum soil temperature during nesting under monthly and hourly data during past (1980-2000) climate and the predicted change in the future (2080-2099). Data are presented for nests laid in May at a depth of 3 cm under different shade conditions. Color scales are the same for figures S73-S100 to enable visual comparison between different combinations of oviposition months and nests depths.

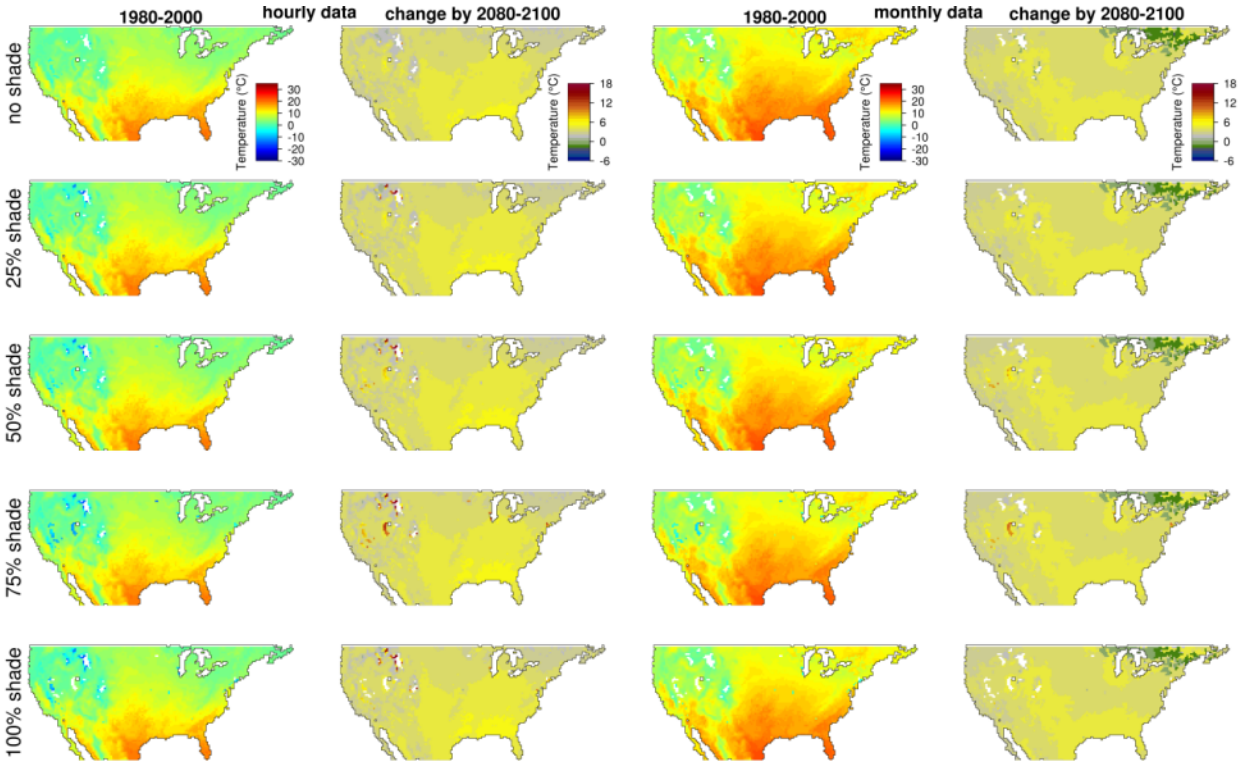

Figure S78: Minimum soil temperature during nesting under monthly and hourly data during past (1980-2000) climate and the predicted change in the future (2080-2099). Data are presented for nests laid in May at a depth of 6 cm under different shade conditions. Color scales are the same for figures S73-S100 to enable visual comparison between different combinations of oviposition months and nests depths.

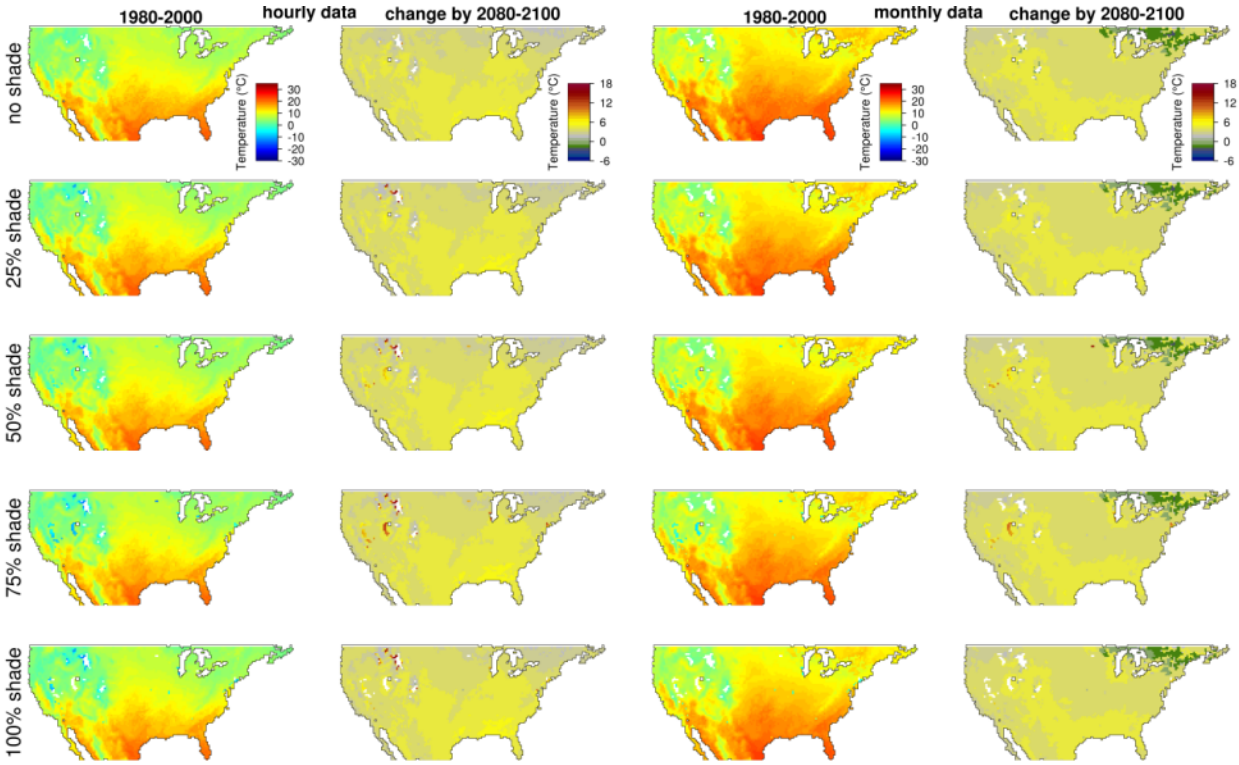

Figure S79: Minimum soil temperature during nesting under monthly and hourly data during past (1980-2000) climate and the predicted change in the future (2080-2099). Data are presented for nests laid in May at a depth of 9 cm under different shade conditions. Color scales are the same for figures S73-S100 to enable visual comparison between different combinations of oviposition months and nests depths.

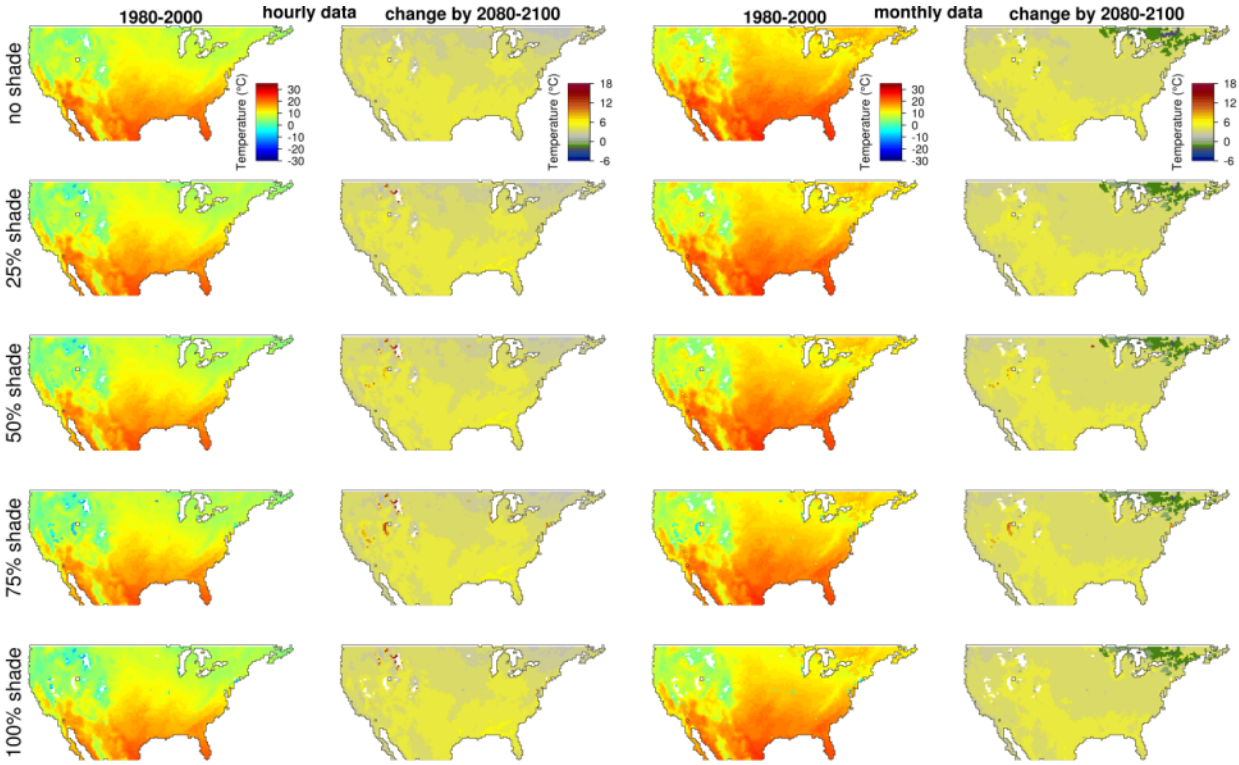

Figure S80: Minimum soil temperature during nesting under monthly and hourly data during past (1980-2000) climate and the predicted change in the future (2080-2099). Data are presented for nests laid in May at a depth of 12 cm under different shade conditions. Color scales are the same for figures S73-S100 to enable visual comparison between different combinations of oviposition months and nests depths.

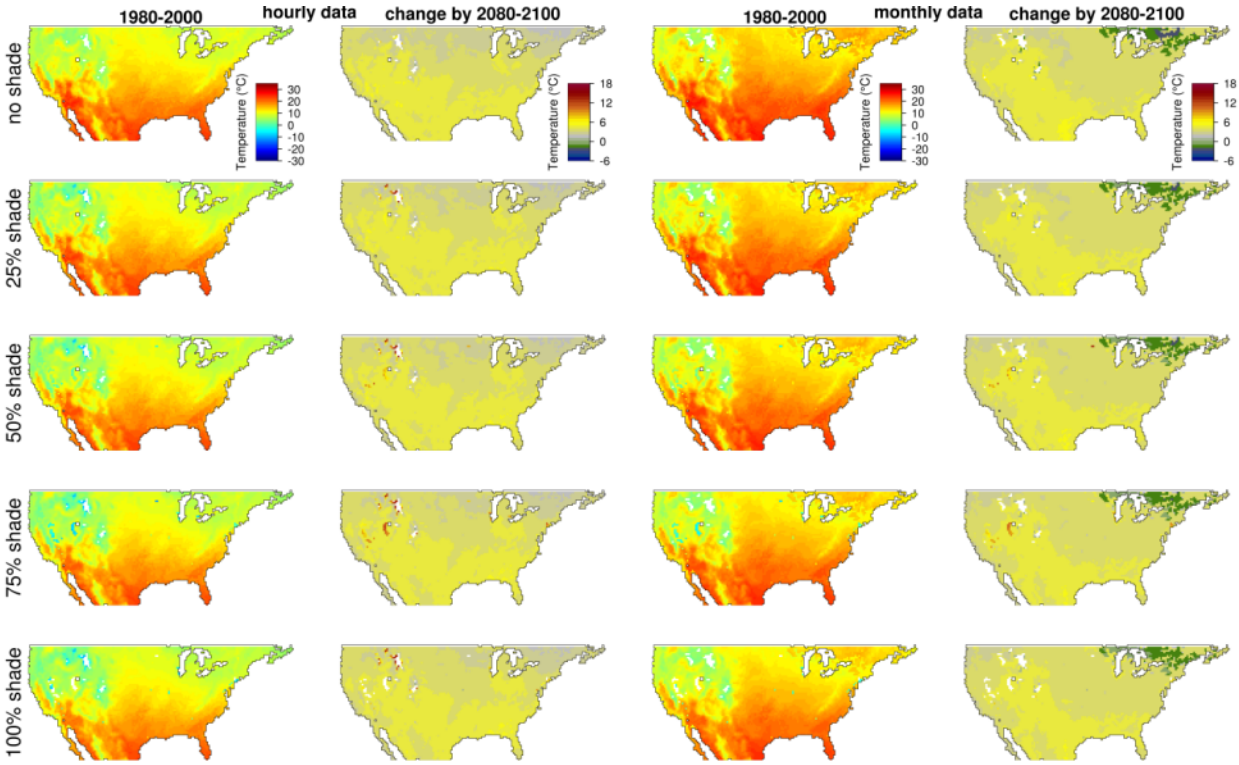

Figure S81: Minimum soil temperature during nesting under monthly and hourly data during past (1980-2000) climate and the predicted change in the future (2080-2099). Data are presented for nests laid in June at a depth of 3 cm under different shade conditions. Color scales are the same for figures S73-S100 to enable visual comparison between different combinations of oviposition months and nests depths.

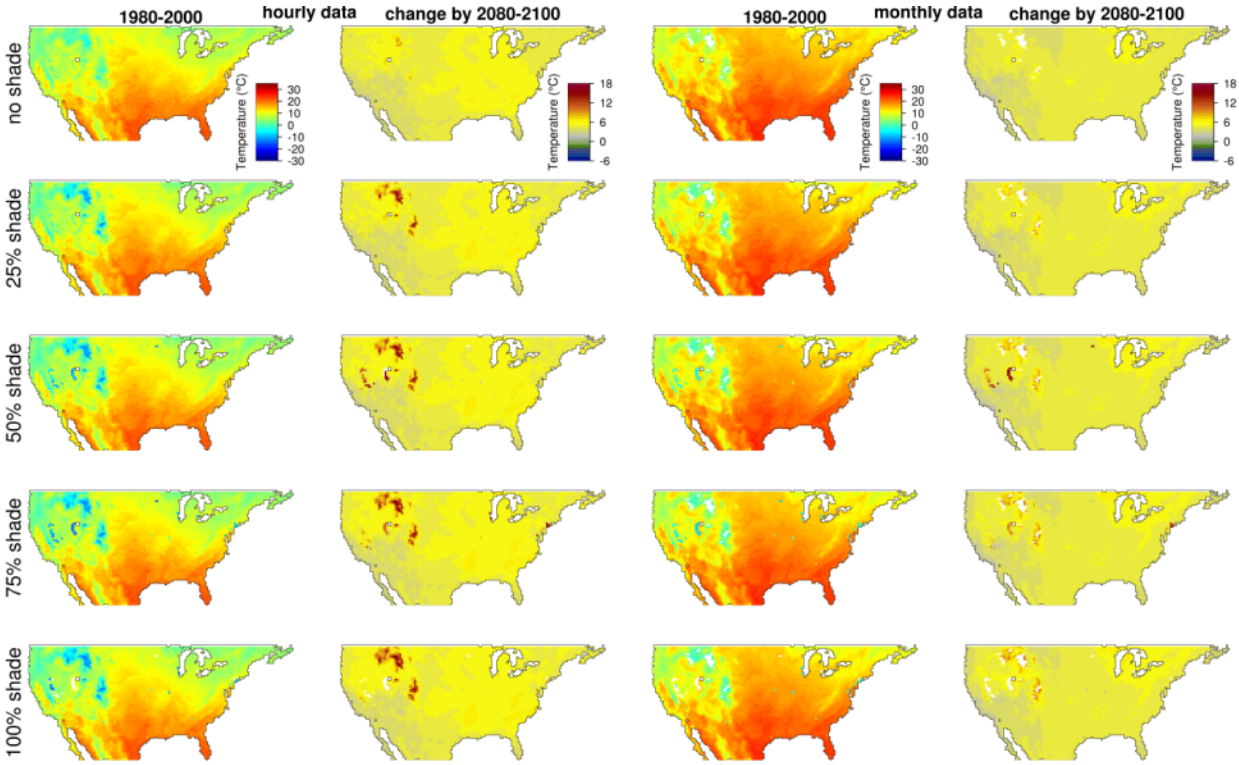

Figure S82: Minimum soil temperature during nesting under monthly and hourly data during past (1980-2000) climate and the predicted change in the future (2080-2099). Data are presented for nests laid in June at a depth of 6 cm under different shade conditions. Color scales are the same for figures S73-S100 to enable visual comparison between different combinations of oviposition months and nests depths.

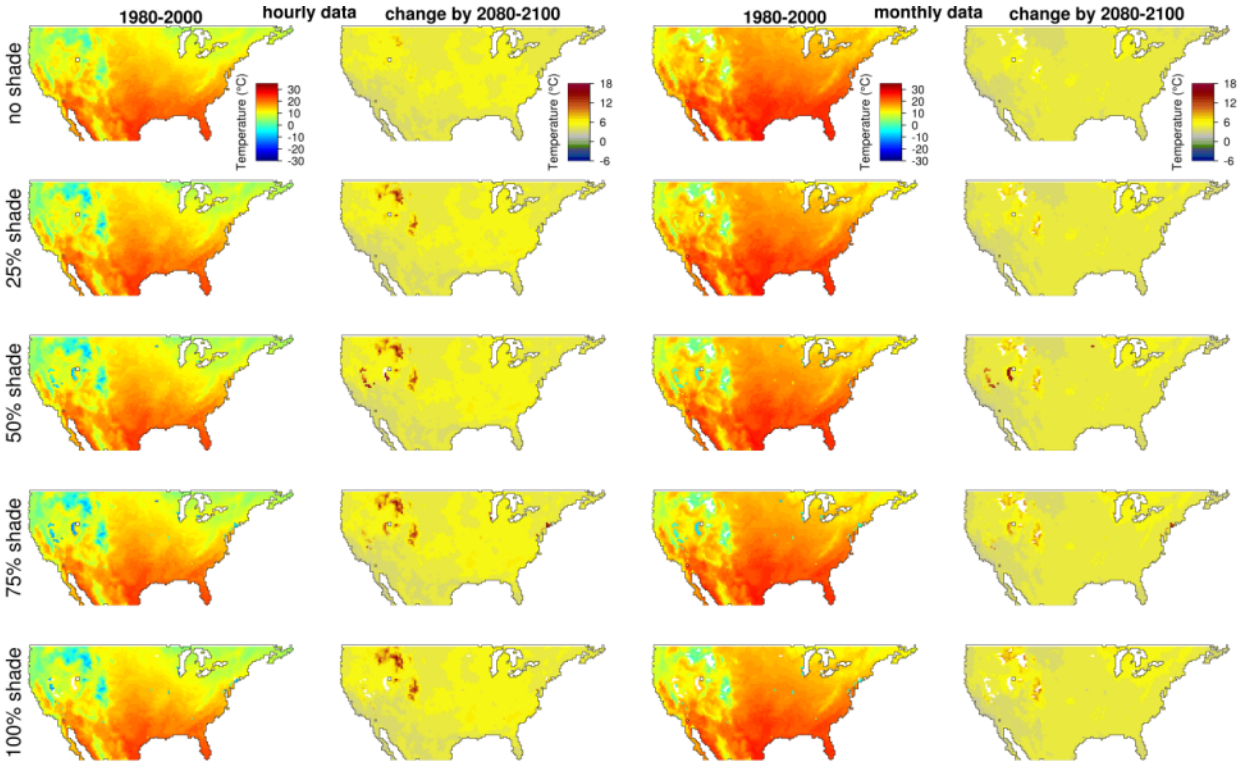

Figure S83: Minimum soil temperature during nesting under monthly and hourly data during past (1980-2000) climate and the predicted change in the future (2080-2099). Data are presented for nests laid in June at a depth of 9 cm under different shade conditions. Color scales are the same for figures S73-S100 to enable visual comparison between different combinations of oviposition months and nests depths.

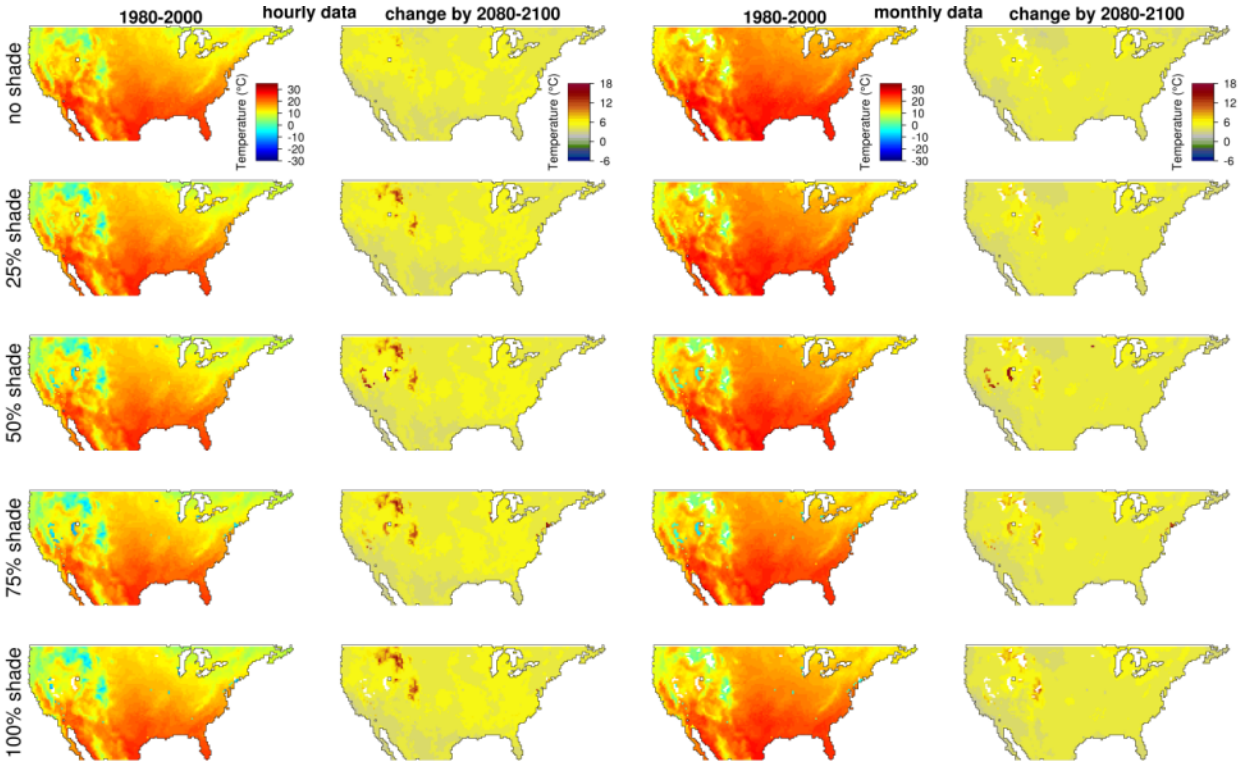

Figure S84: Minimum soil temperature during nesting under monthly and hourly data during past (1980-2000) climate and the predicted change in the future (2080-2099). Data are presented for nests laid in June at a depth of 12 cm under different shade conditions. Color scales are the same for figures S73-S100 to enable visual comparison between different combinations of oviposition months and nests depths.

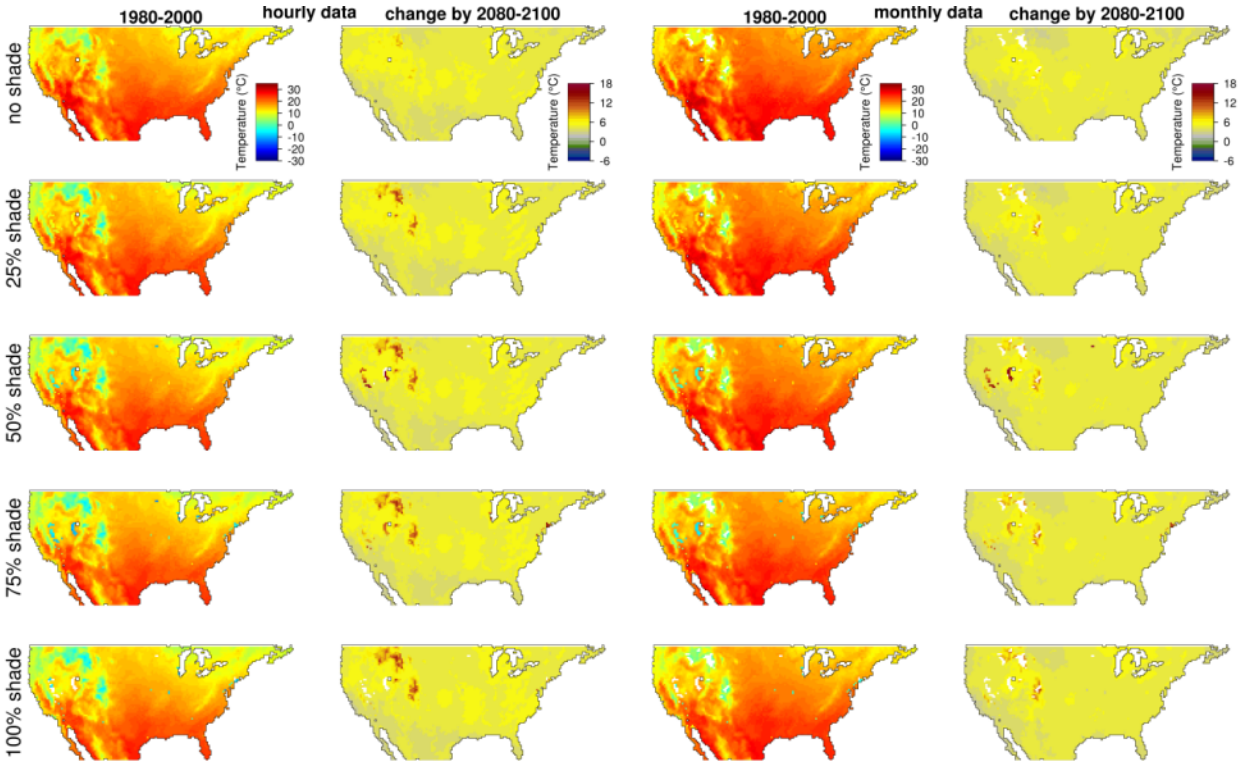

Figure S85: Minimum soil temperature during nesting under monthly and hourly data during past (1980-2000) climate and the predicted change in the future (2080-2099). Data are presented for nests laid in July at a depth of 3 cm under different shade conditions. Color scales are the same for figures S73-S100 to enable visual comparison between different combinations of oviposition months and nests depths.

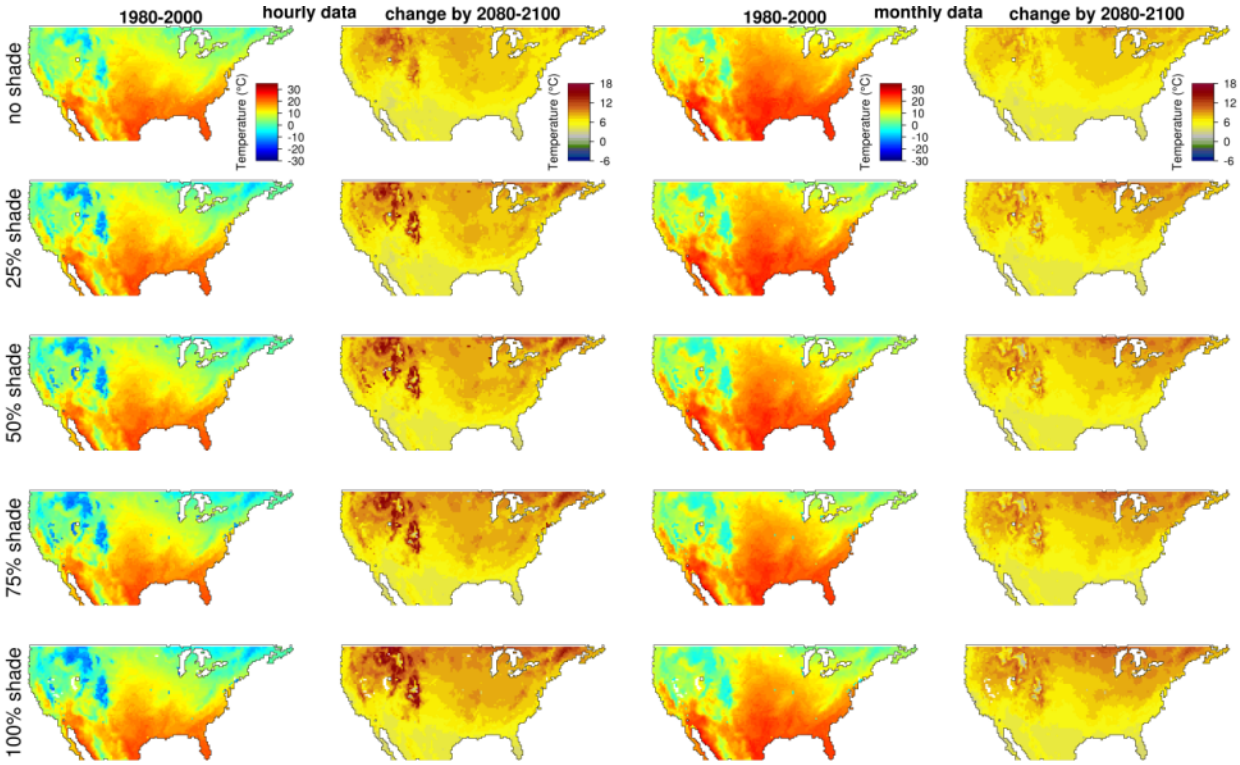

Figure S86: Minimum soil temperature during nesting under monthly and hourly data during past (1980-2000) climate and the predicted change in the future (2080-2099). Data are presented for nests laid in July at a depth of 6 cm under different shade conditions. Color scales are the same for figures S73-S100 to enable visual comparison between different combinations of oviposition months and nests depths.

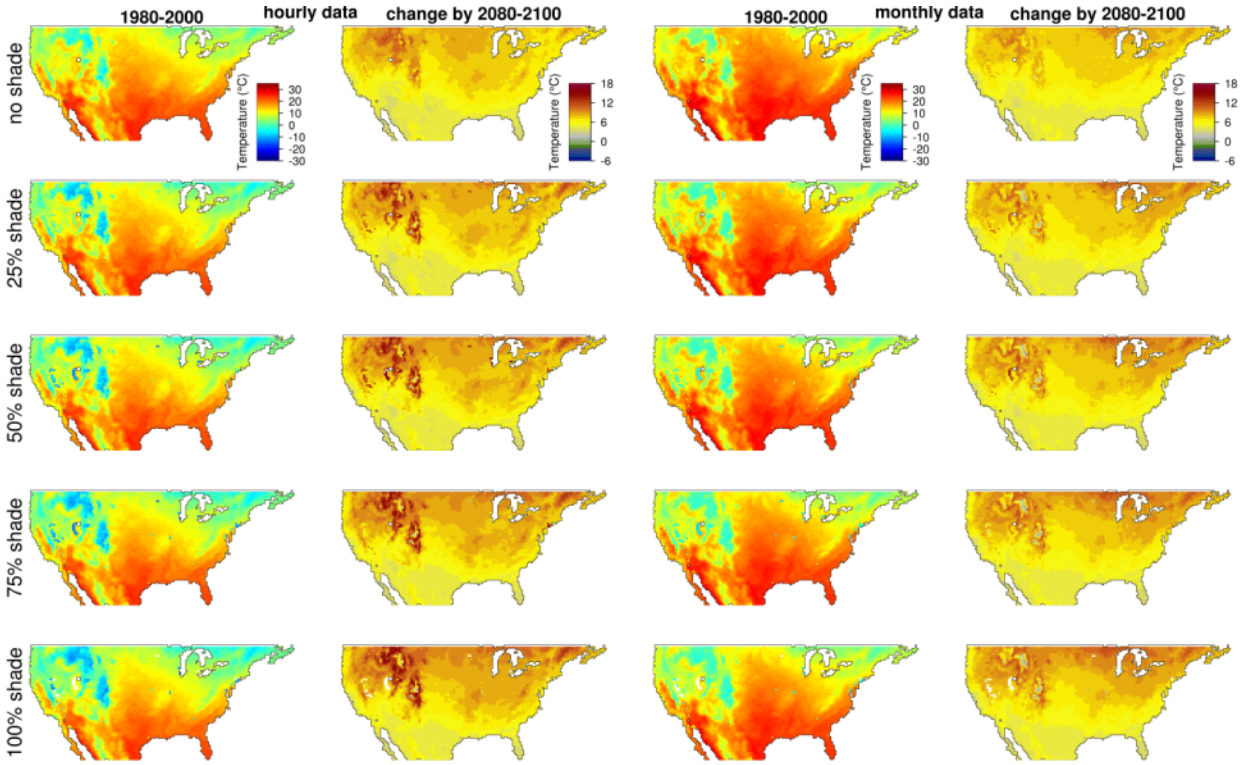

Figure S87: Minimum soil temperature during nesting under monthly and hourly data during past (1980-2000) climate and the predicted change in the future (2080-2099). Data are presented for nests laid in July at a depth of 9 cm under different shade conditions. Color scales are the same for figures S73-S100 to enable visual comparison between different combinations of oviposition months and nests depths.

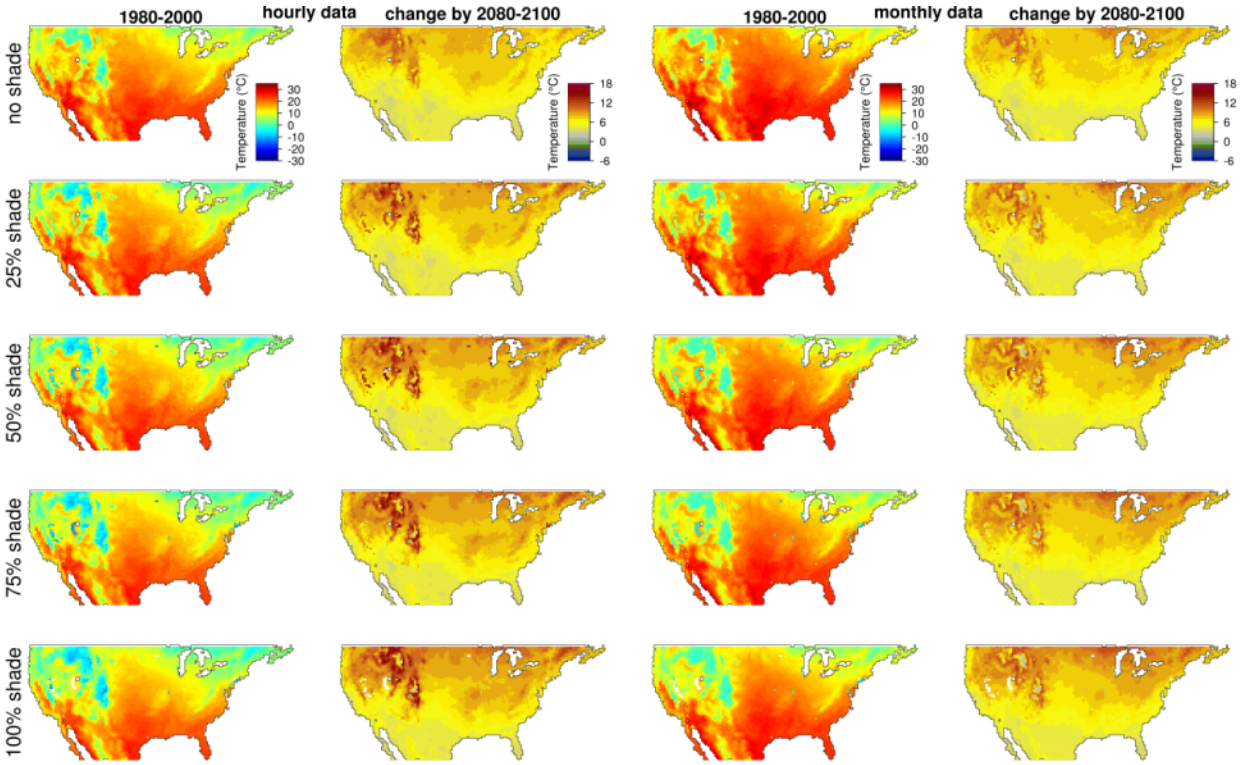

Figure S88: Minimum soil temperature during nesting under monthly and hourly data during past (1980-2000) climate and the predicted change in the future (2080-2099). Data are presented for nests laid in July at a depth of 12 cm under different shade conditions. Color scales are the same for figures S73-S100 to enable visual comparison between different combinations of oviposition months and nests depths.

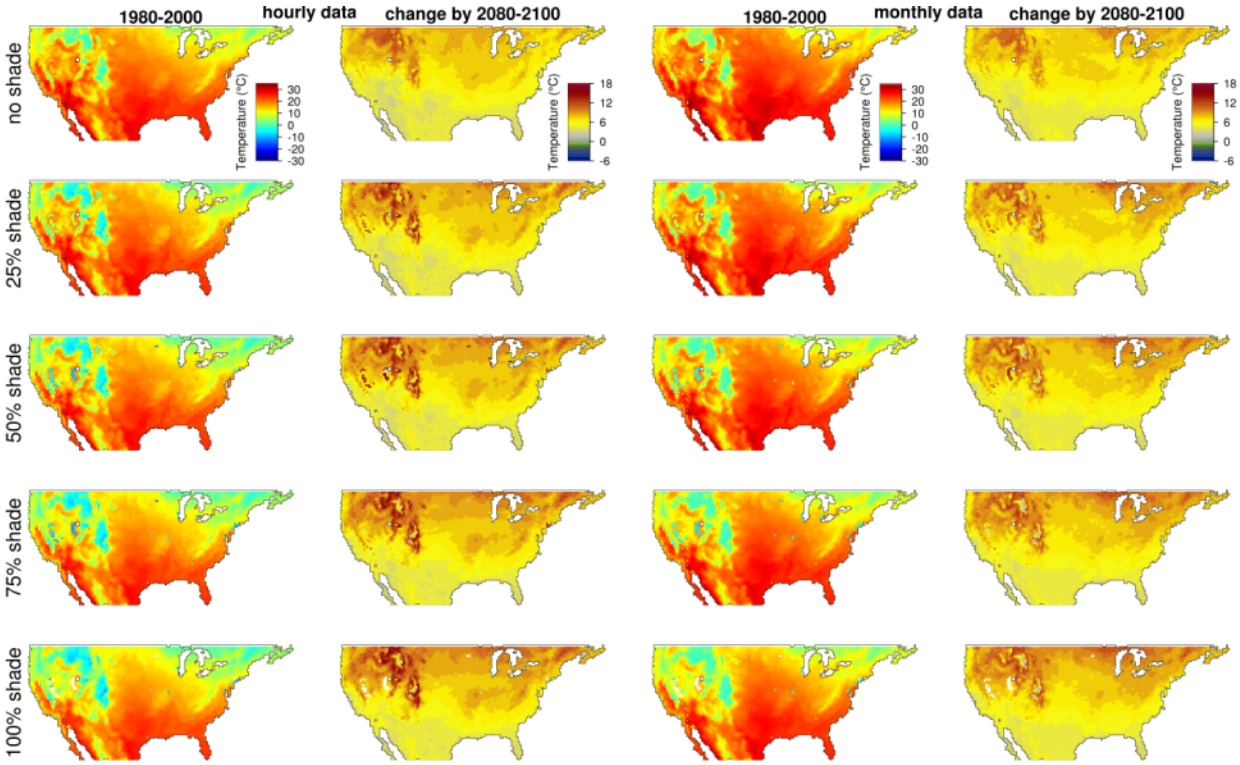

Figure S89: Minimum soil temperature during nesting under monthly and hourly data during past (1980-2000) climate and the predicted change in the future (2080-2099). Data are presented for nests laid in August at a depth of 3 cm under different shade conditions. Color scales are the same for figures S73-S100 to enable visual comparison between different combinations of oviposition months and nests depths.

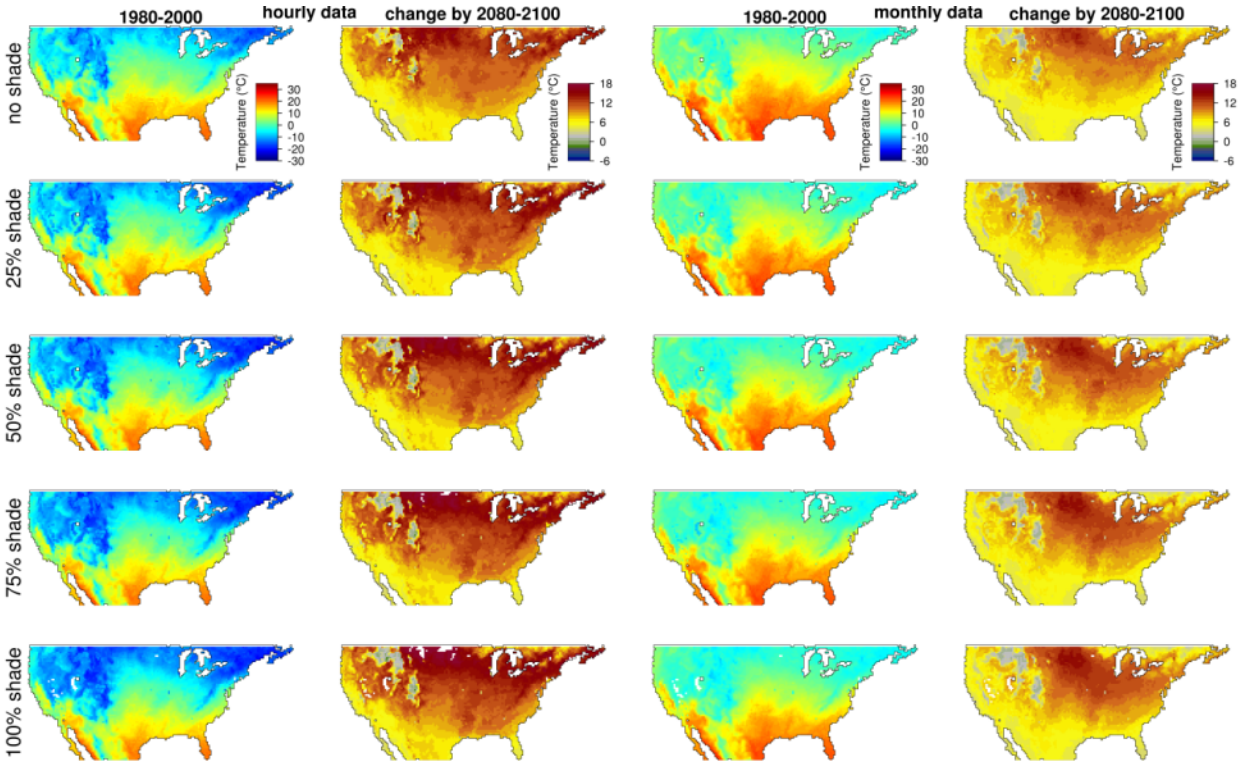

Figure S90: Minimum soil temperature during nesting under monthly and hourly data during past (1980-2000) climate and the predicted change in the future (2080-2099). Data are presented for nests laid in August at a depth of 6 cm under different shade conditions. Color scales are the same for figures S73-S100 to enable visual comparison between different combinations of oviposition months and nests depths.

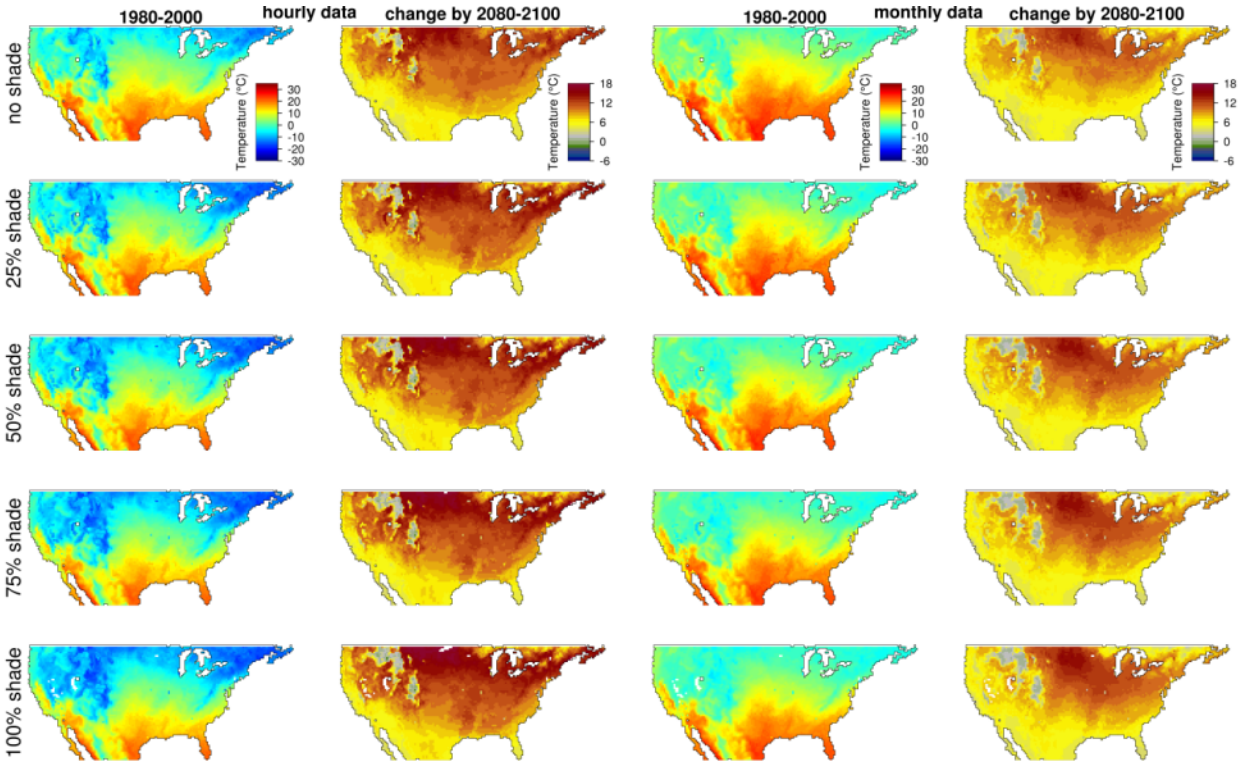

Figure S91: Minimum soil temperature during nesting under monthly and hourly data during past (1980-2000) climate and the predicted change in the future (2080-2099). Data are presented for nests laid in August at a depth of 9 cm under different shade conditions. Color scales are the same for figures S73-S100 to enable visual comparison between different combinations of oviposition months and nests depths.

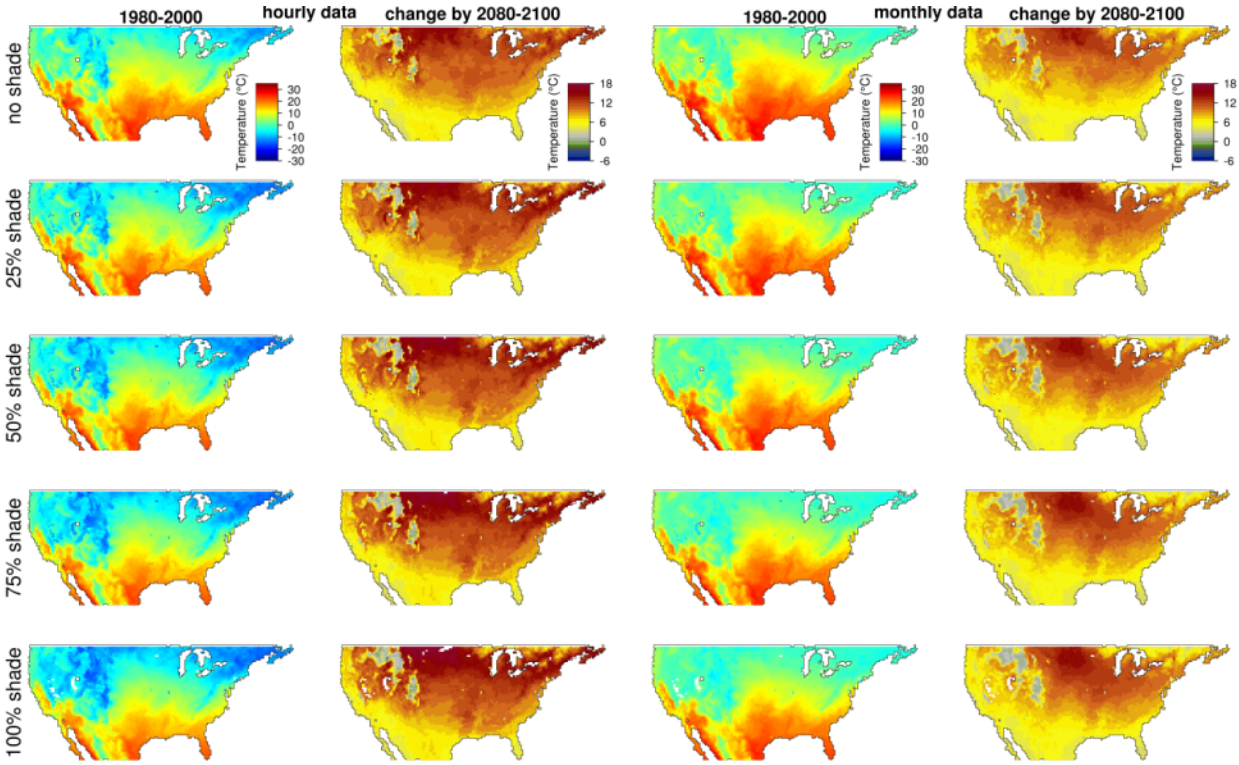

Figure S92: Minimum soil temperature during nesting under monthly and hourly data during past (1980-2000) climate and the predicted change in the future (2080-2099). Data are presented for nests laid in August at a depth of 12 cm under different shade conditions. Color scales are the same for figures S73-S100 to enable visual comparison between different combinations of oviposition months and nests depths.

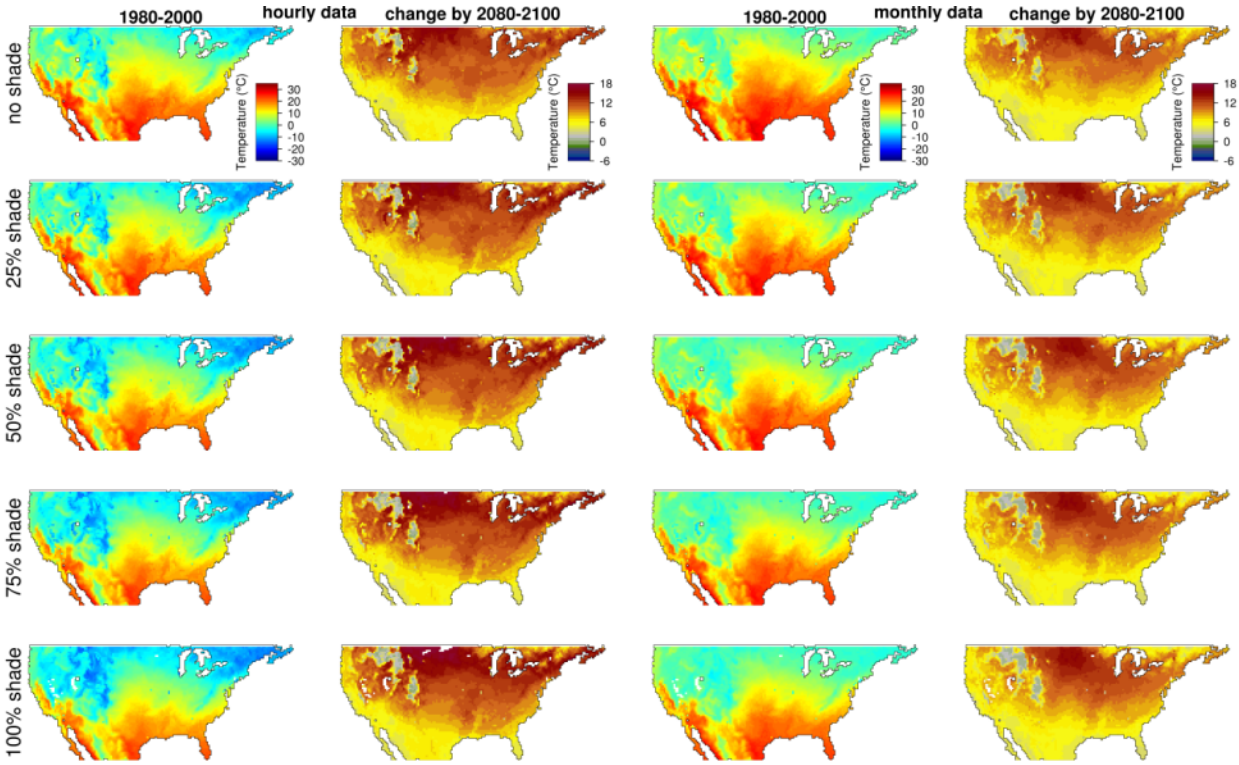

Figure S93: Minimum soil temperature during nesting under monthly and hourly data during past (1980-2000) climate and the predicted change in the future (2080-2099). Data are presented for nests laid in September at a depth of 3 cm under different shade conditions. Color scales are the same for figures S73-S100 to enable visual comparison between different combinations of oviposition months and nests depths.

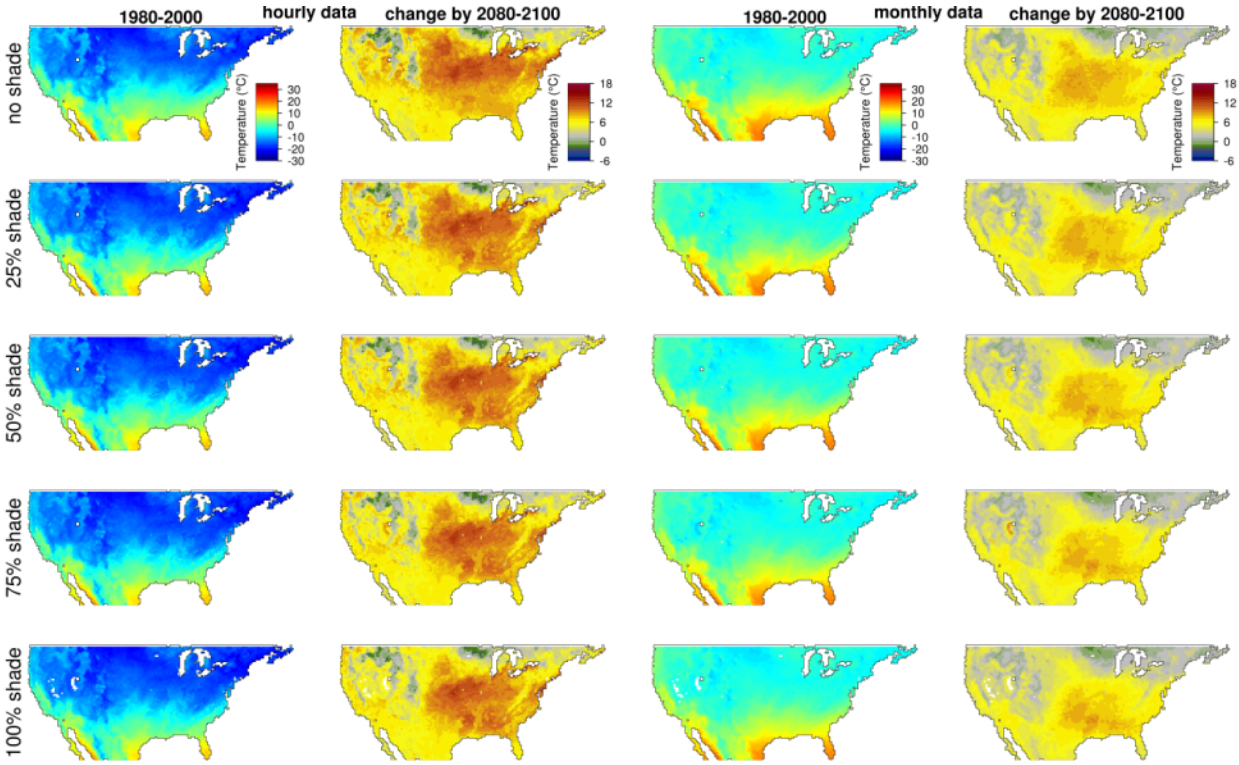

Figure S94: Minimum soil temperature during nesting under monthly and hourly data during past (1980-2000) climate and the predicted change in the future (2080-2099). Data are presented for nests laid in September at a depth of 6 cm under different shade conditions. Color scales are the same for figures S73-S100 to enable visual comparison between different combinations of oviposition months and nests depths.

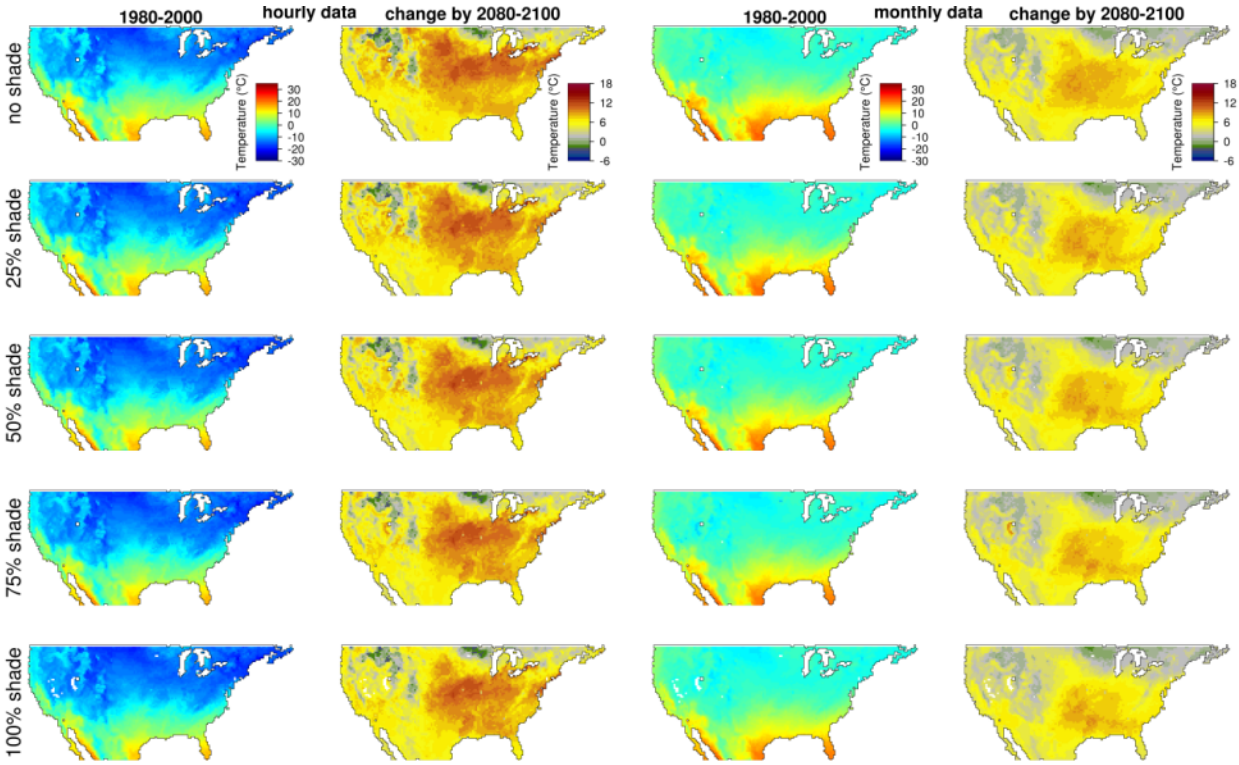

Figure S95: Minimum soil temperature during nesting under monthly and hourly data during past (1980-2000) climate and the predicted change in the future (2080-2099). Data are presented for nests laid in September at a depth of 9 cm under different shade conditions. Color scales are the same for figures S73-S100 to enable visual comparison between different combinations of oviposition months and nests depths.

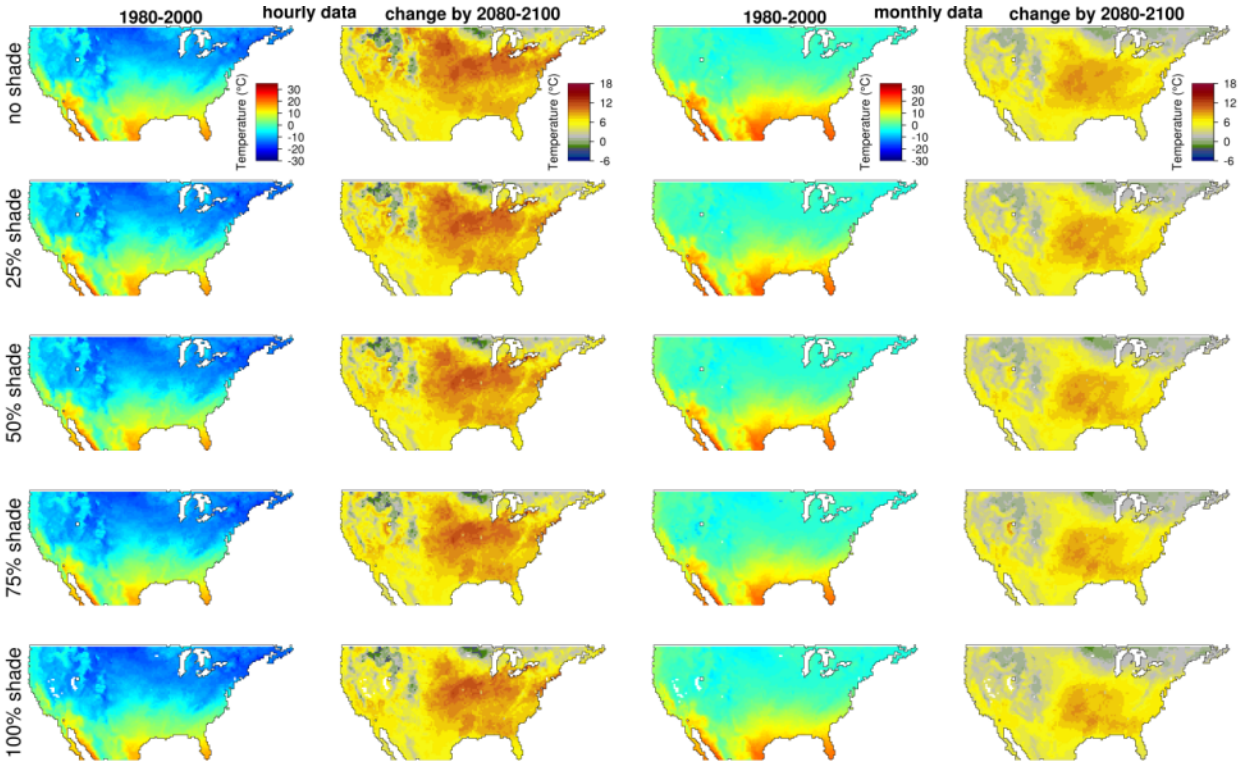

Figure S96: Minimum soil temperature during nesting under monthly and hourly data during past (1980-2000) climate and the predicted change in the future (2080-2099). Data are presented for nests laid in September at a depth of 12 cm under different shade conditions. Color scales are the same for figures S73-S100 to enable visual comparison between different combinations of oviposition months and nests depths.

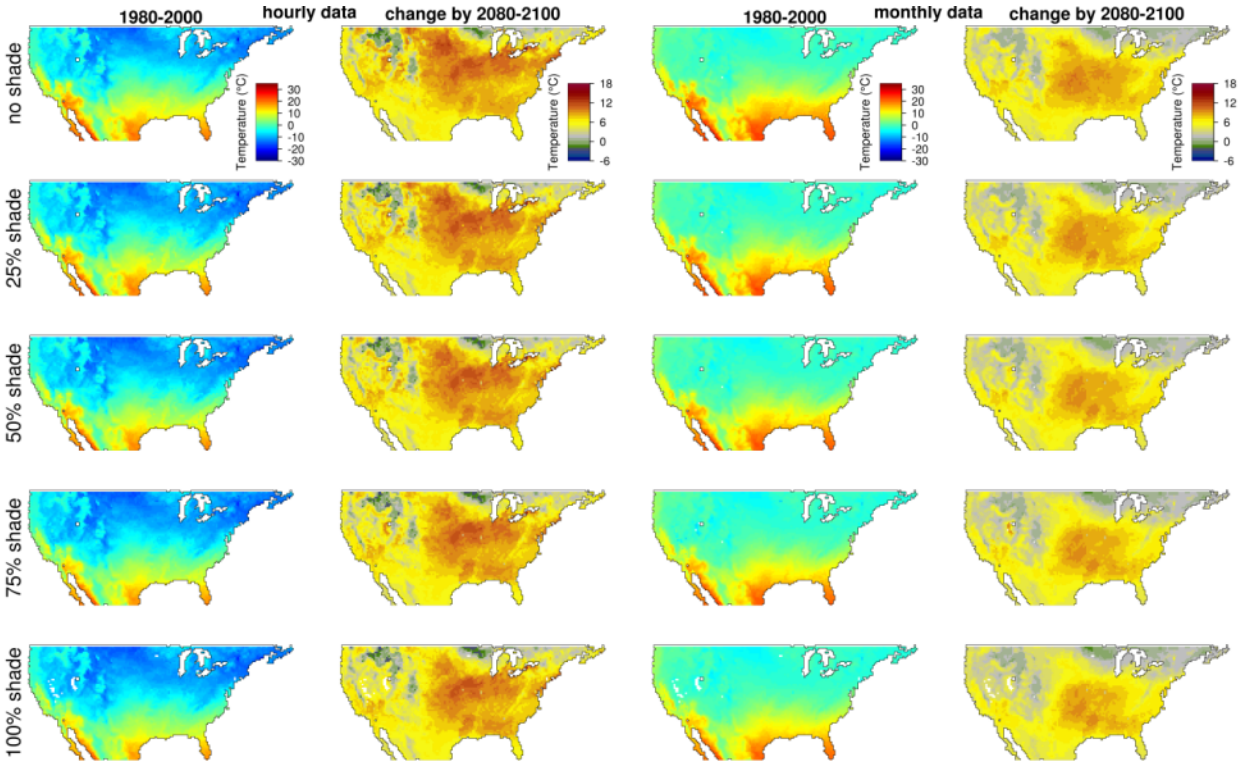

Figure S97: Minimum soil temperature during nesting under monthly and hourly data during past (1980-2000) climate and the predicted change in the future (2080-2099). Data are presented for nests laid in October at a depth of 3 cm under different shade conditions. White areas represent locations for which climate conditions did not enable enough activity to promote reproduction. Color scales are the same for figures S73-S100 to enable visual comparison between different combinations of oviposition months and nests depths.

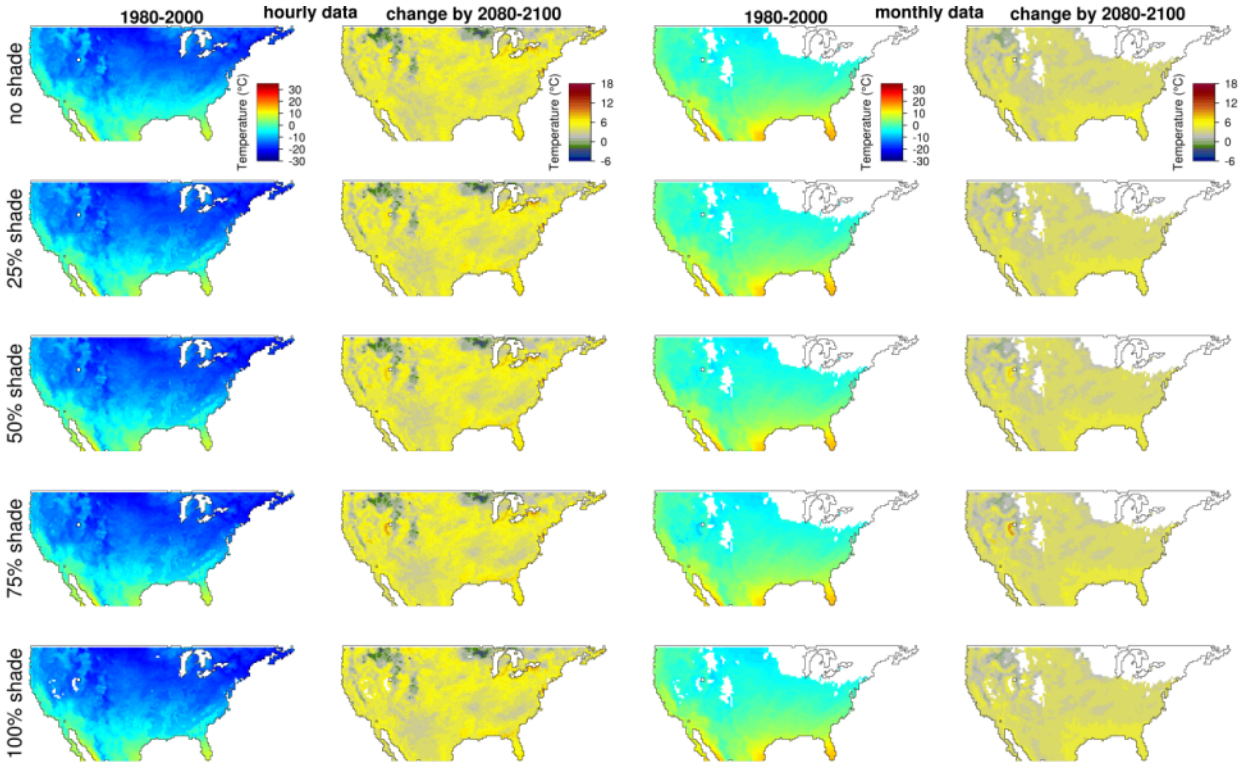

Figure S98: Minimum soil temperature during nesting under monthly and hourly data during past (1980-2000) climate and the predicted change in the future (2080-2099). Data are presented for nests laid in October at a depth of 6 cm under different shade conditions. White areas represent locations for which climate conditions did not enable enough activity to promote reproduction. Color scales are the same for figures S73-S100 to enable visual comparison between different combinations of oviposition months and nests depths.

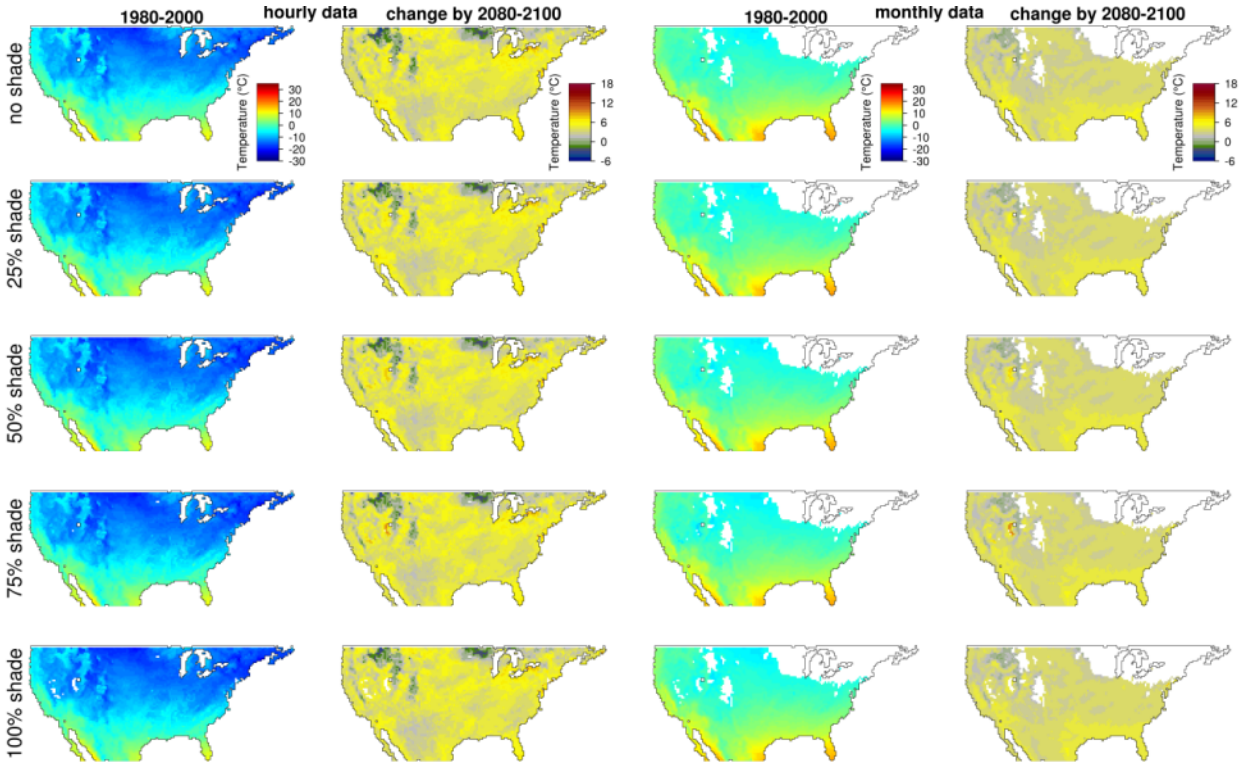

Figure S99: Minimum soil temperature during nesting under monthly and hourly data during past (1980-2000) climate and the predicted change in the future (2080-2099). Data are presented for nests laid in October at a depth of 9 cm under different shade conditions. White areas represent locations for which climate conditions did not enable enough activity to promote reproduction. Color scales are the same for figures S73-S100 to enable visual comparison between different combinations of oviposition months and nests depths.

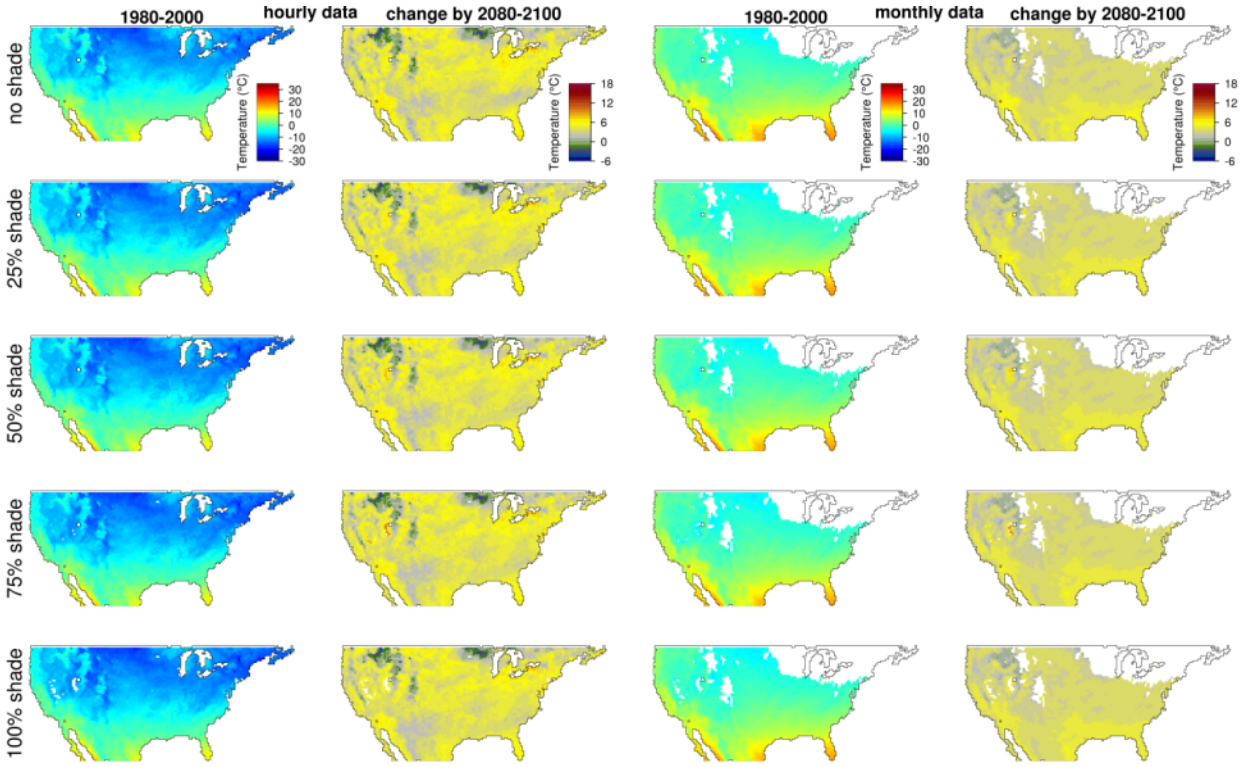

Figure S100: Minimum soil temperature during nesting under monthly and hourly data during past (1980-2000) climate and the predicted change in the future (2080-2099). Data are presented for nests laid in October at a depth of 12 cm under different shade conditions. White areas represent locations for which climate conditions did not enable enough activity to promote reproduction. Color scales are the same for figures S73-S100 to enable visual comparison between different combinations of oviposition months and nests depths.

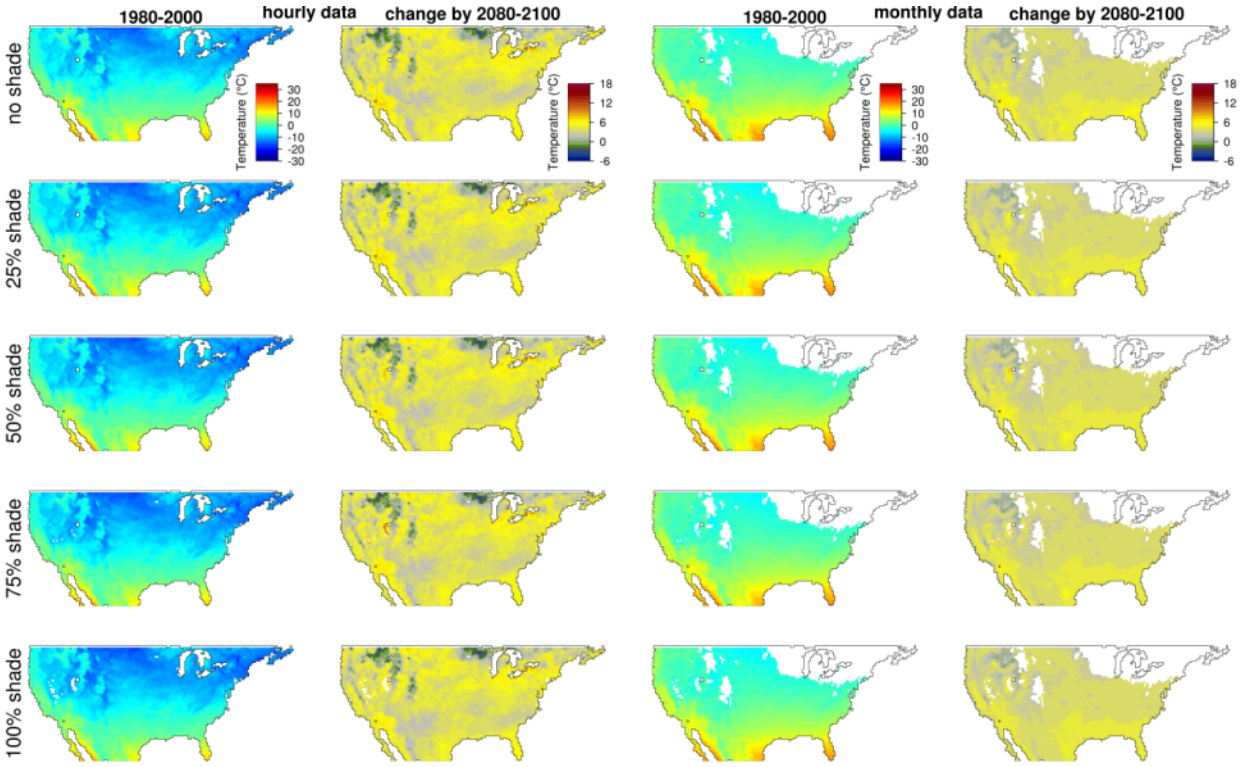

Figure S101: Maximum soil temperature during nesting under monthly and hourly data during past (1980-2000) climate and the predicted change in the future (2080-2099). Data are presented for nests laid in April at a depth of 3 cm under different shade conditions. White areas represent locations for which climate conditions did not enable enough activity to promote reproduction. Color scales are the same for figures S101-S128 to enable visual comparison between different combinations of oviposition months and nests depths.

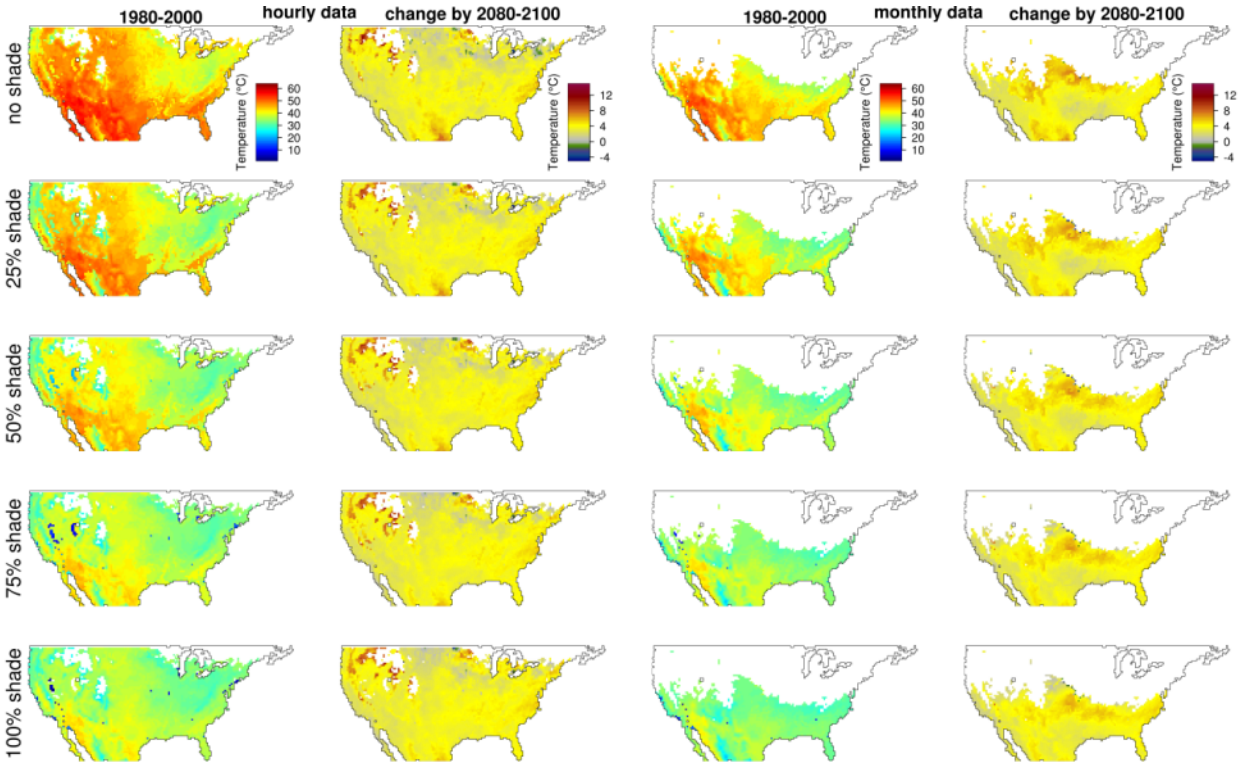

Figure S102: Maximum soil temperature during nesting under monthly and hourly data during past (1980-2000) climate and the predicted change in the future (2080-2099). Data are presented for nests laid in April at a depth of 6 cm under different shade conditions. White areas represent locations for which climate conditions did not enable enough activity to promote reproduction. Color scales are the same for figures S101-S128 to enable visual comparison between different combinations of oviposition months and nests depths.

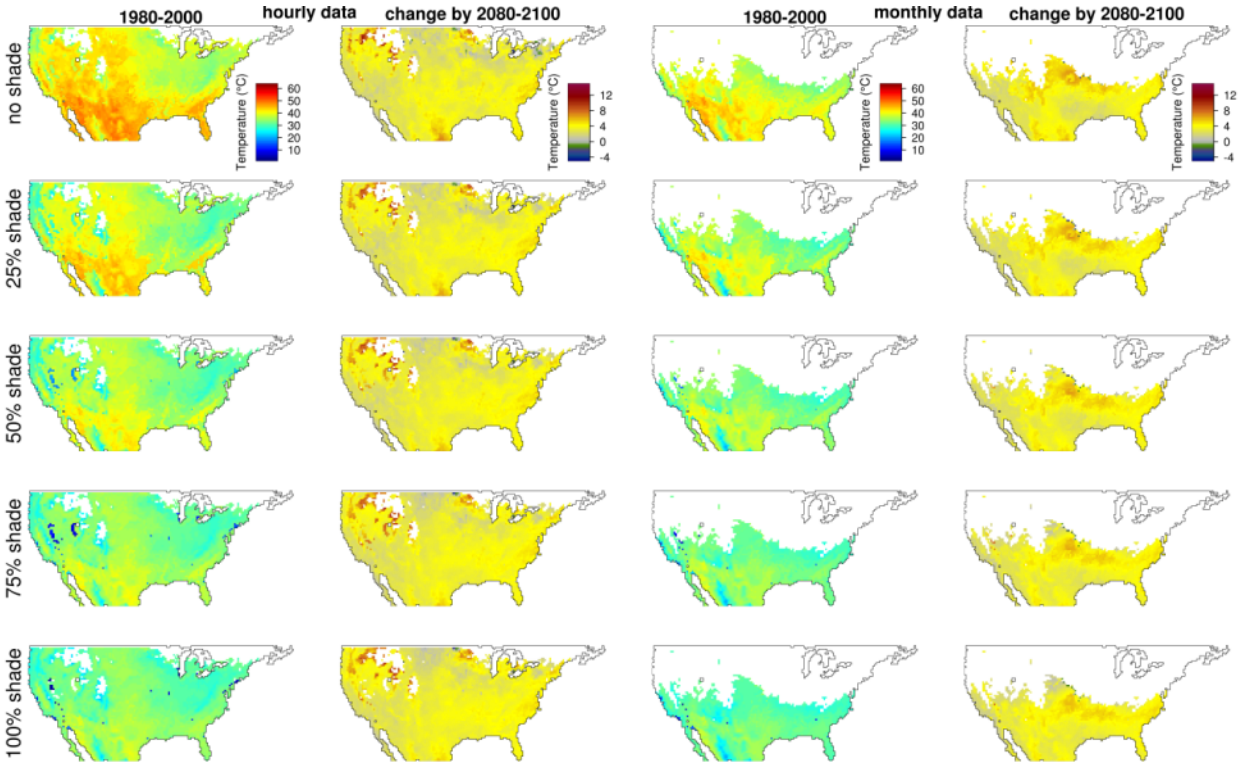

Figure S103: Maximum soil temperature during nesting under monthly and hourly data during past (1980-2000) climate and the predicted change in the future (2080-2099). Data are presented for nests laid in April at a depth of 9 cm under different shade conditions. White areas represent locations for which climate conditions did not enable enough activity to promote reproduction. Color scales are the same for figures S101-S128 to enable visual comparison between different combinations of oviposition months and nests depths.

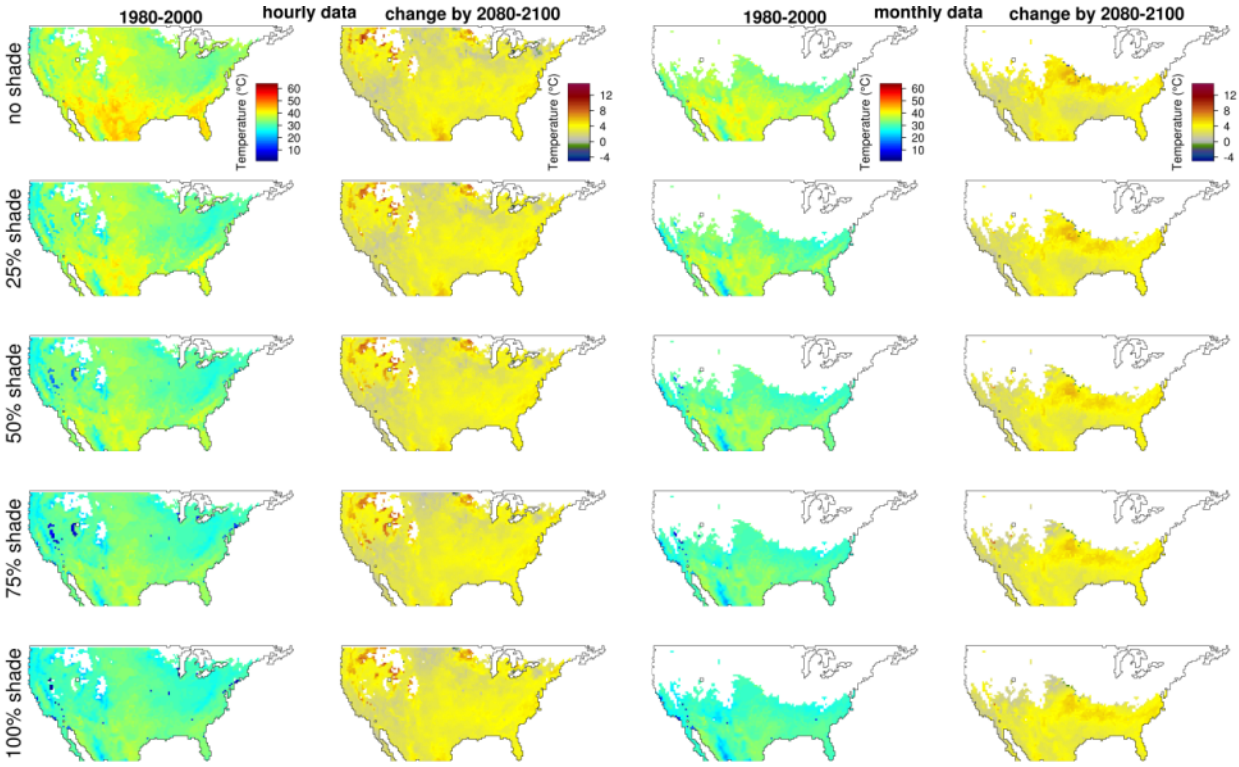

Figure S104: Maximum soil temperature during nesting under monthly and hourly data during past (1980-2000) climate and the predicted change in the future (2080-2099). Data are presented for nests laid in April at a depth of 12 cm under different shade conditions. White areas represent locations for which climate conditions did not enable enough activity to promote reproduction. Color scales are the same for figures S101-S128 to enable visual comparison between different combinations of oviposition months and nests depths.

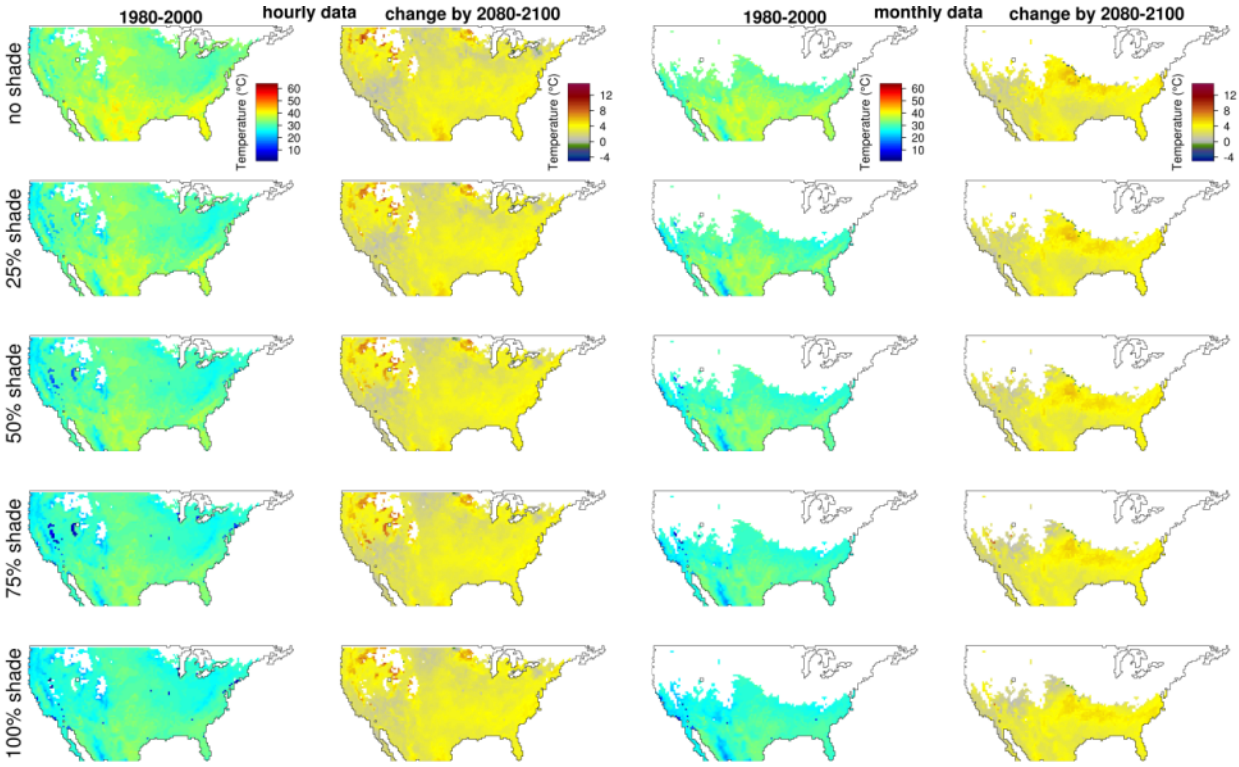

Figure S105: Maximum soil temperature during nesting under monthly and hourly data during past (1980-2000) climate and the predicted change in the future (2080-2099). Data are presented for nests laid in May at a depth of 3 cm under different shade conditions. Color scales are the same for figures S101-S128 to enable visual comparison between different combinations of oviposition months and nests depths.

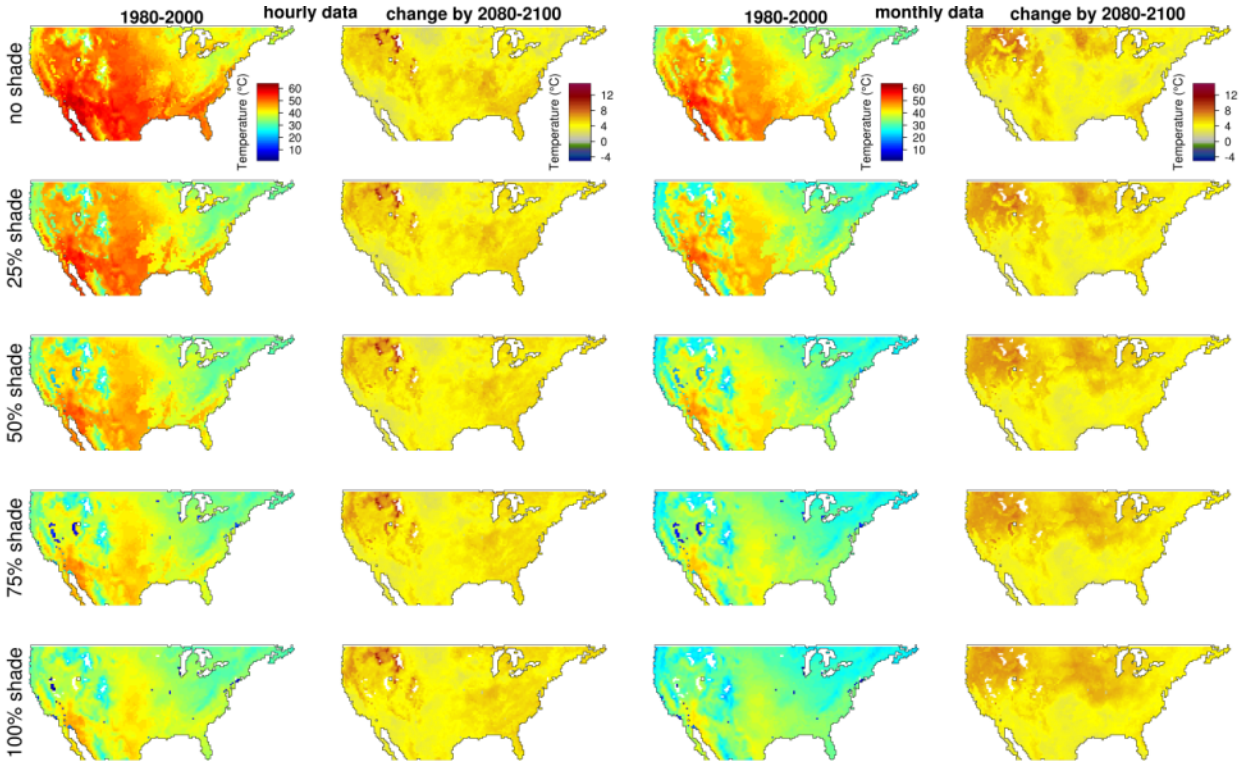

Figure S106: Maximum soil temperature during nesting under monthly and hourly data during past (1980-2000) climate and the predicted change in the future (2080-2099). Data are presented for nests laid in May at a depth of 6 cm under different shade conditions. Color scales are the same for figures S101-S128 to enable visual comparison between different combinations of oviposition months and nests depths.

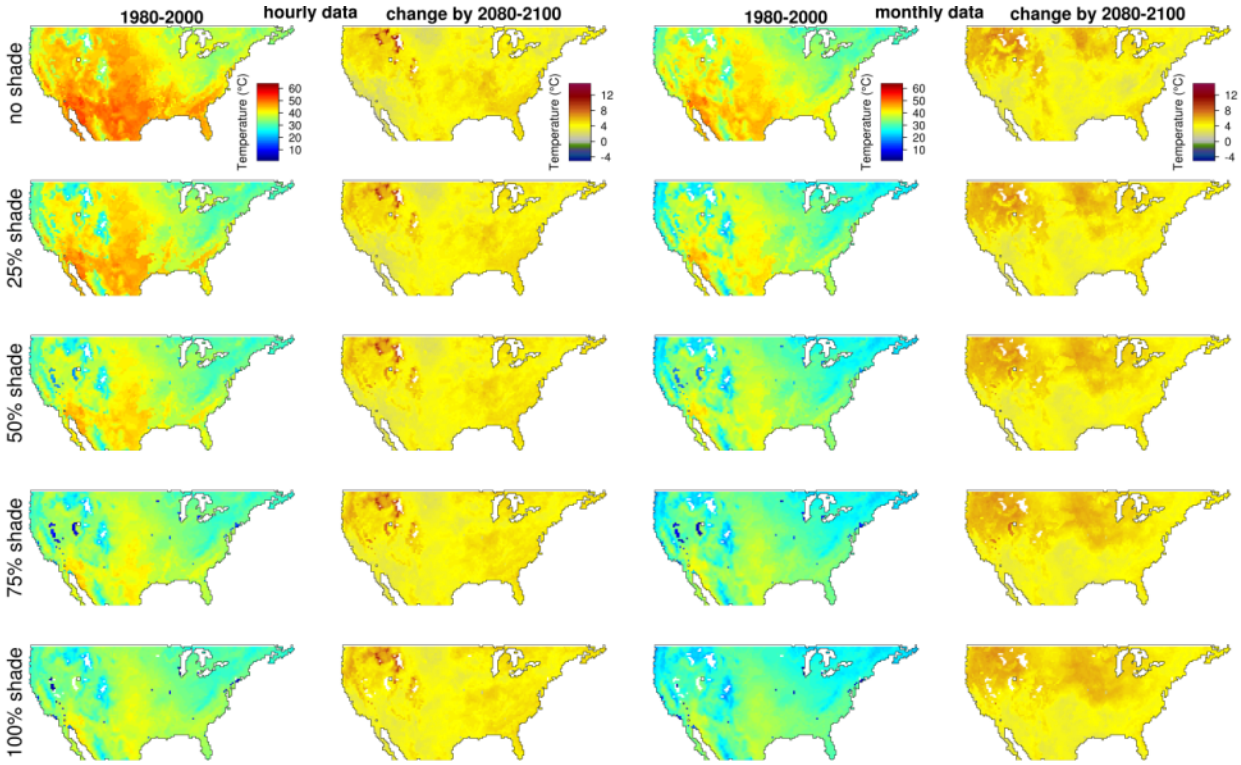

Figure S107: Maximum soil temperature during nesting under monthly and hourly data during past (1980-2000) climate and the predicted change in the future (2080-2099). Data are presented for nests laid in May at a depth of 9 cm under different shade conditions. Color scales are the same for figures S101-S128 to enable visual comparison between different combinations of oviposition months and nests depths.

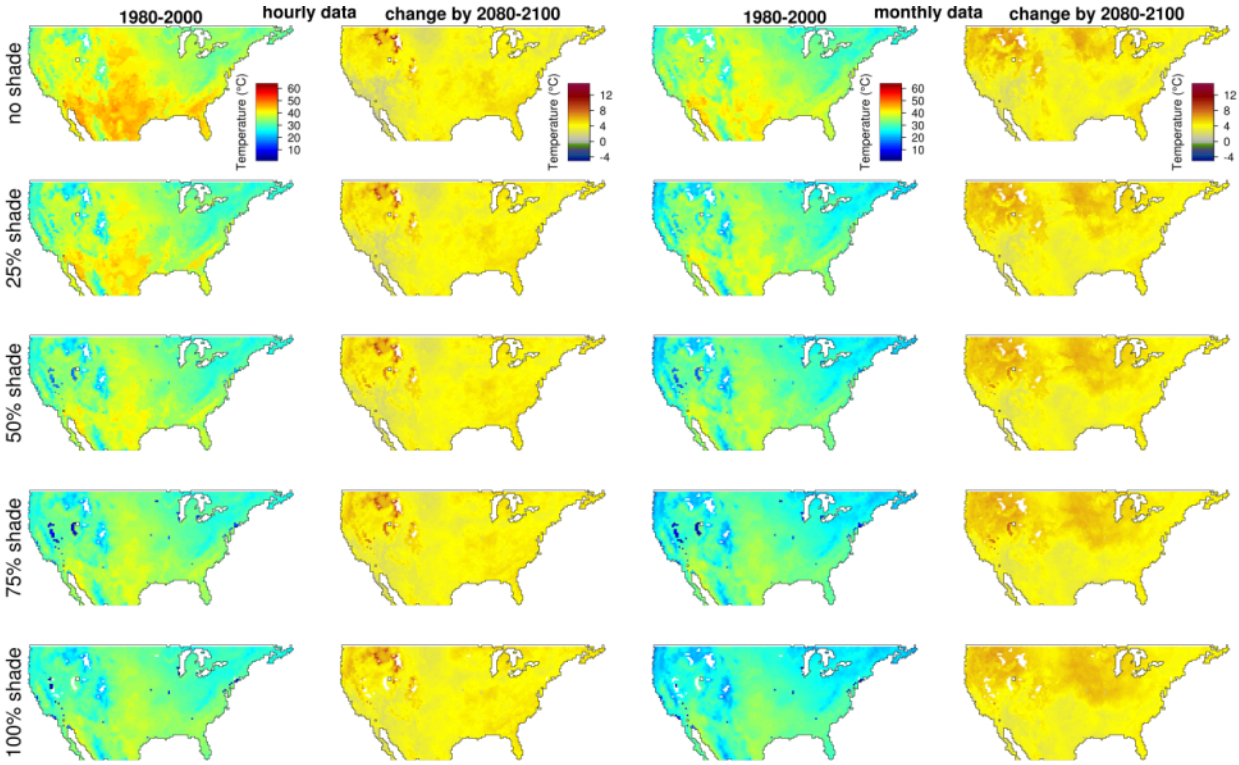

Figure S108: Maximum soil temperature during nesting under monthly and hourly data during past (1980-2000) climate and the predicted change in the future (2080-2099). Data are presented for nests laid in May at a depth of 12 cm under different shade conditions. Color scales are the same for figures S101-S128 to enable visual comparison between different combinations of oviposition months and nests depths.

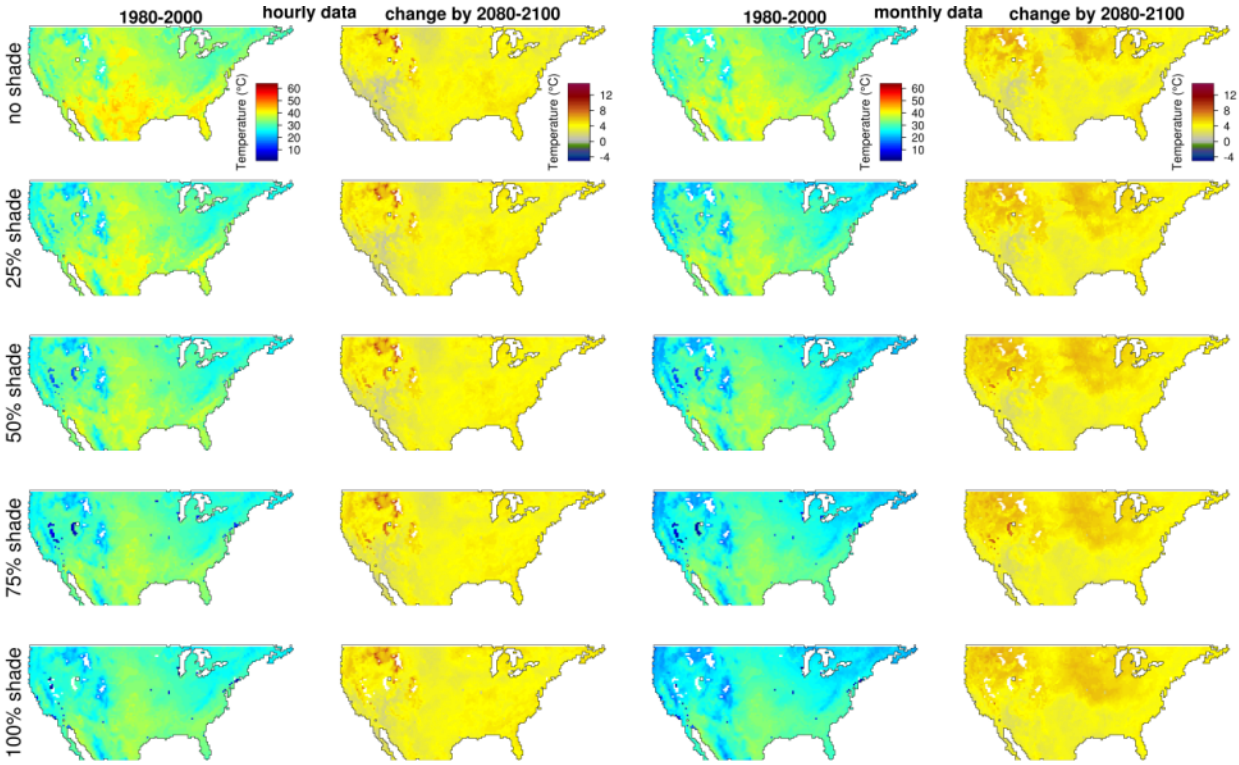

Figure S109: Maximum soil temperature during nesting under monthly and hourly data during past (1980-2000) climate and the predicted change in the future (2080-2099). Data are presented for nests laid in June at a depth of 3 cm under different shade conditions. Color scales are the same for figures S101-S128 to enable visual comparison between different combinations of oviposition months and nests depths.

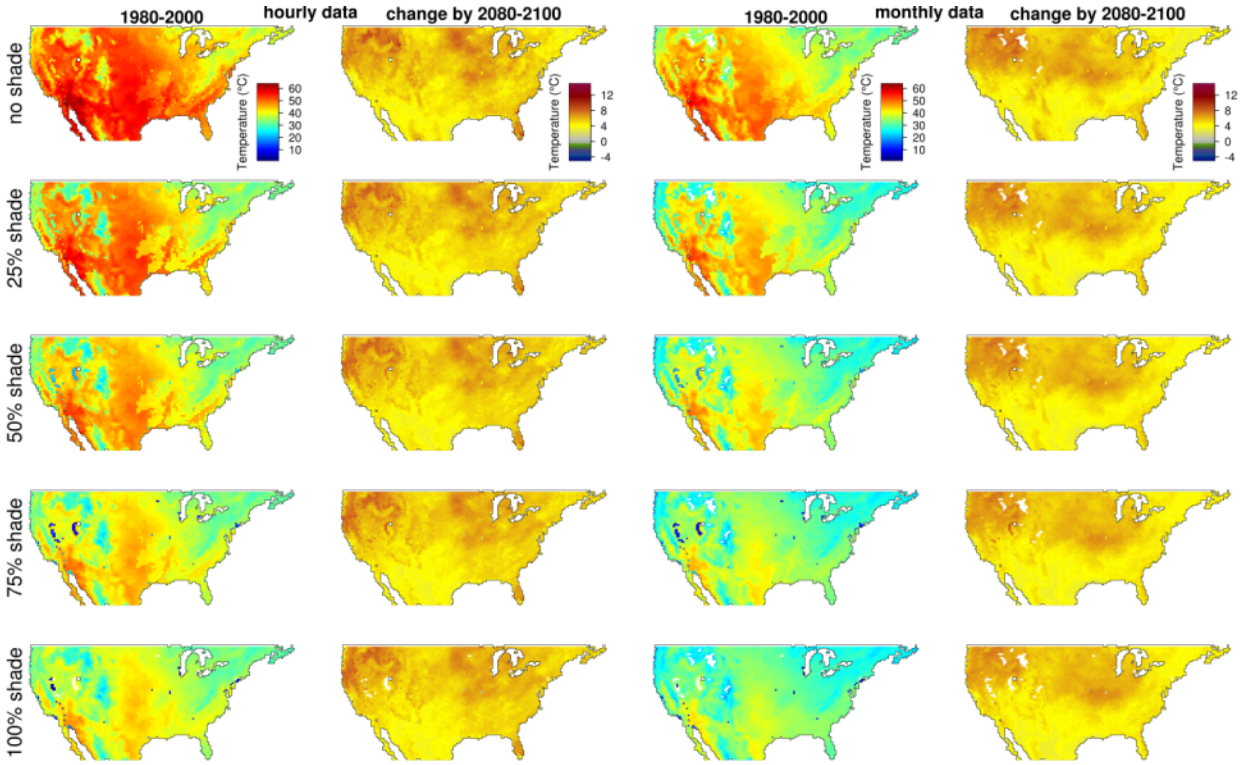

Figure S110: Maximum soil temperature during nesting under monthly and hourly data during past (1980-2000) climate and the predicted change in the future (2080-2099). Data are presented for nests laid in June at a depth of 6 cm under different shade conditions. Color scales are the same for figures S101-S128 to enable visual comparison between different combinations of oviposition months and nests depths.

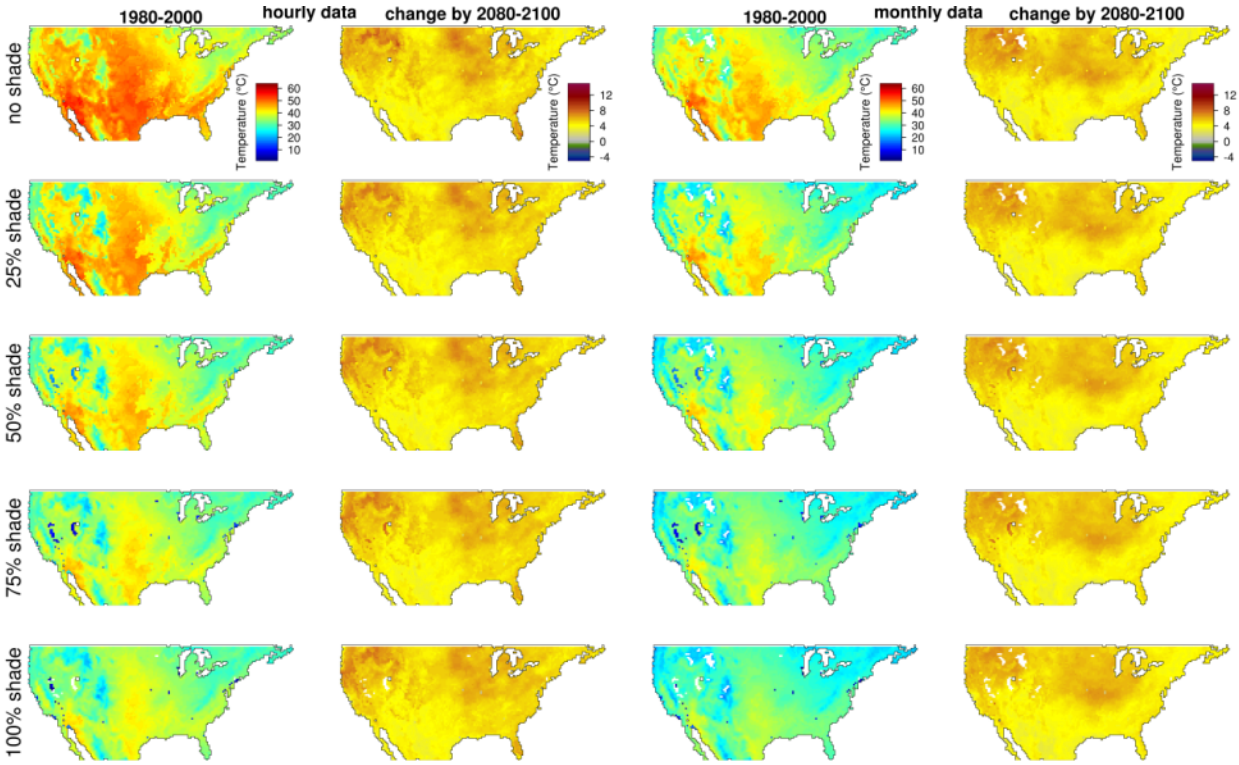

Figure S111: Maximum soil temperature during nesting under monthly and hourly data during past (1980-2000) climate and the predicted change in the future (2080-2099). Data are presented for nests laid in June at a depth of 9 cm under different shade conditions. Color scales are the same for figures S101-S128 to enable visual comparison between different combinations of oviposition months and nests depths.

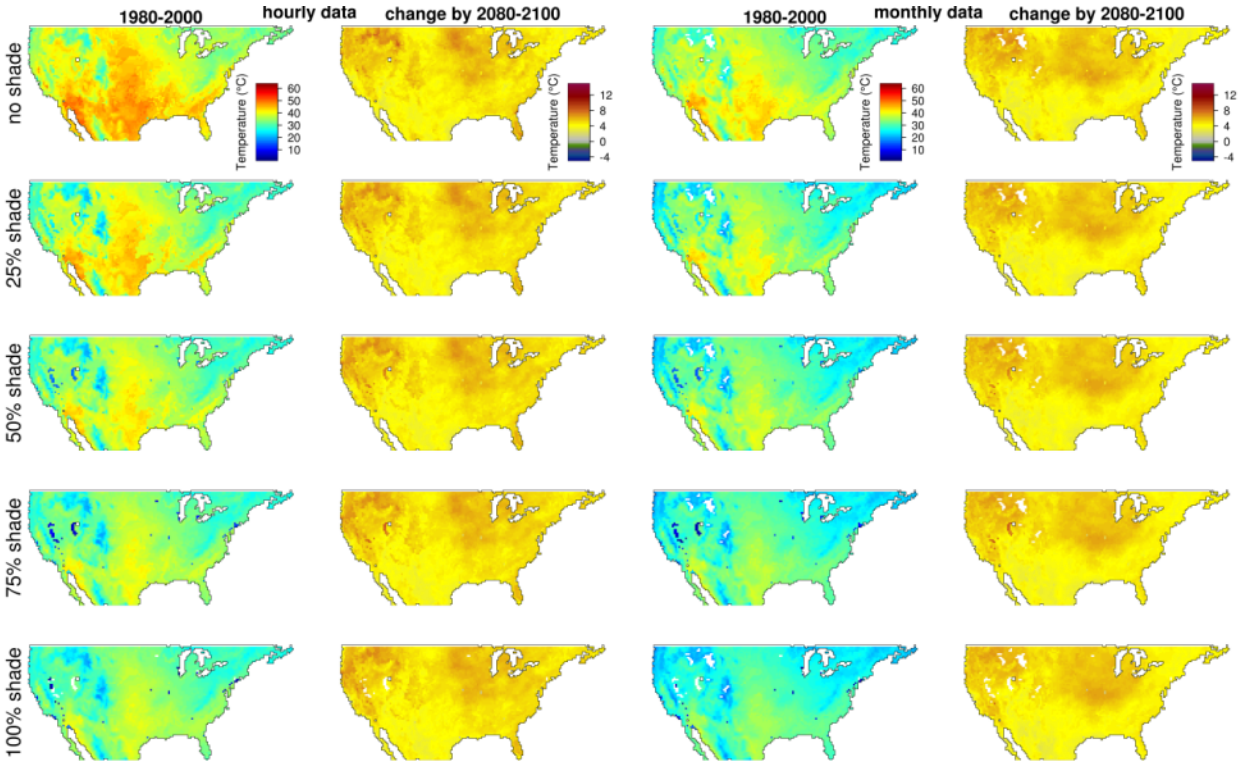

Figure S112: Maximum soil temperature during nesting under monthly and hourly data during past (1980-2000) climate and the predicted change in the future (2080-2099). Data are presented for nests laid in June at a depth of 12 cm under different shade conditions. Color scales are the same for figures S101-S128 to enable visual comparison between different combinations of oviposition months and nests depths.

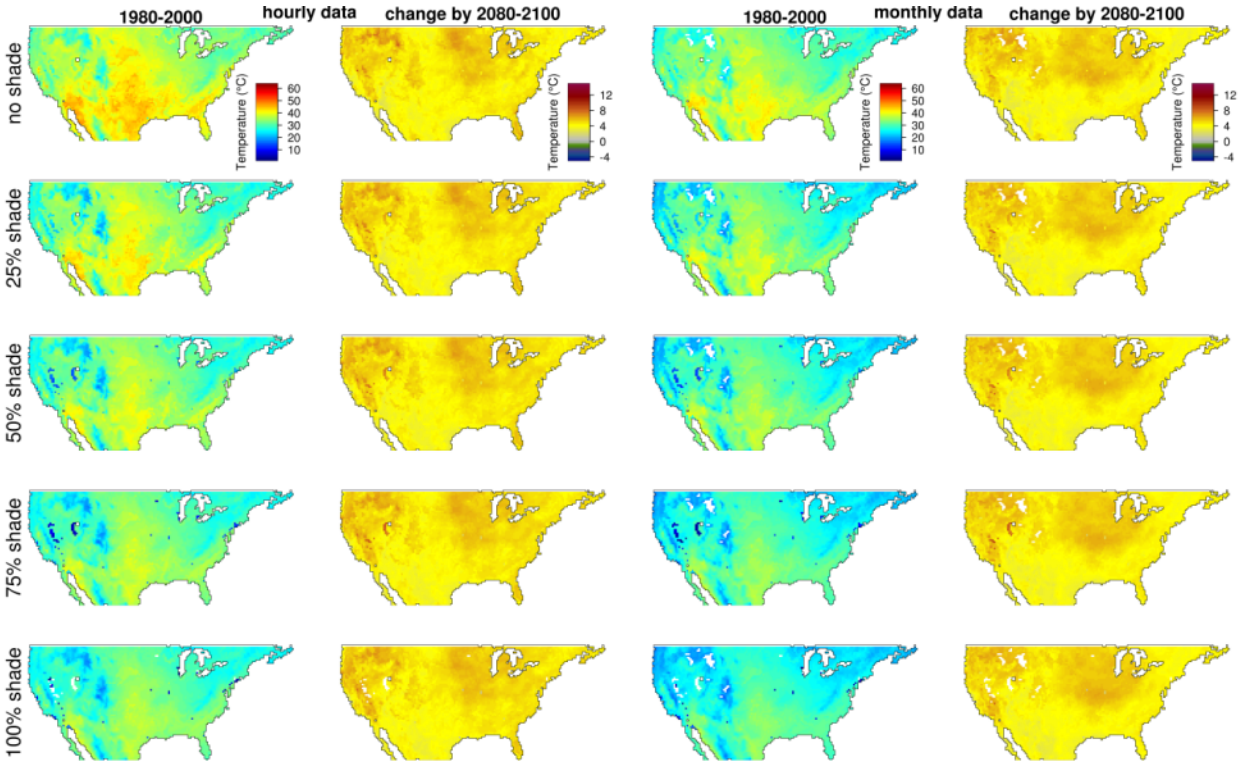

Figure S113: Maximum soil temperature during nesting under monthly and hourly data during past (1980-2000) climate and the predicted change in the future (2080-2099). Data are presented for nests laid in July at a depth of 3 cm under different shade conditions. Color scales are the same for figures S101-S128 to enable visual comparison between different combinations of oviposition months and nests depths.

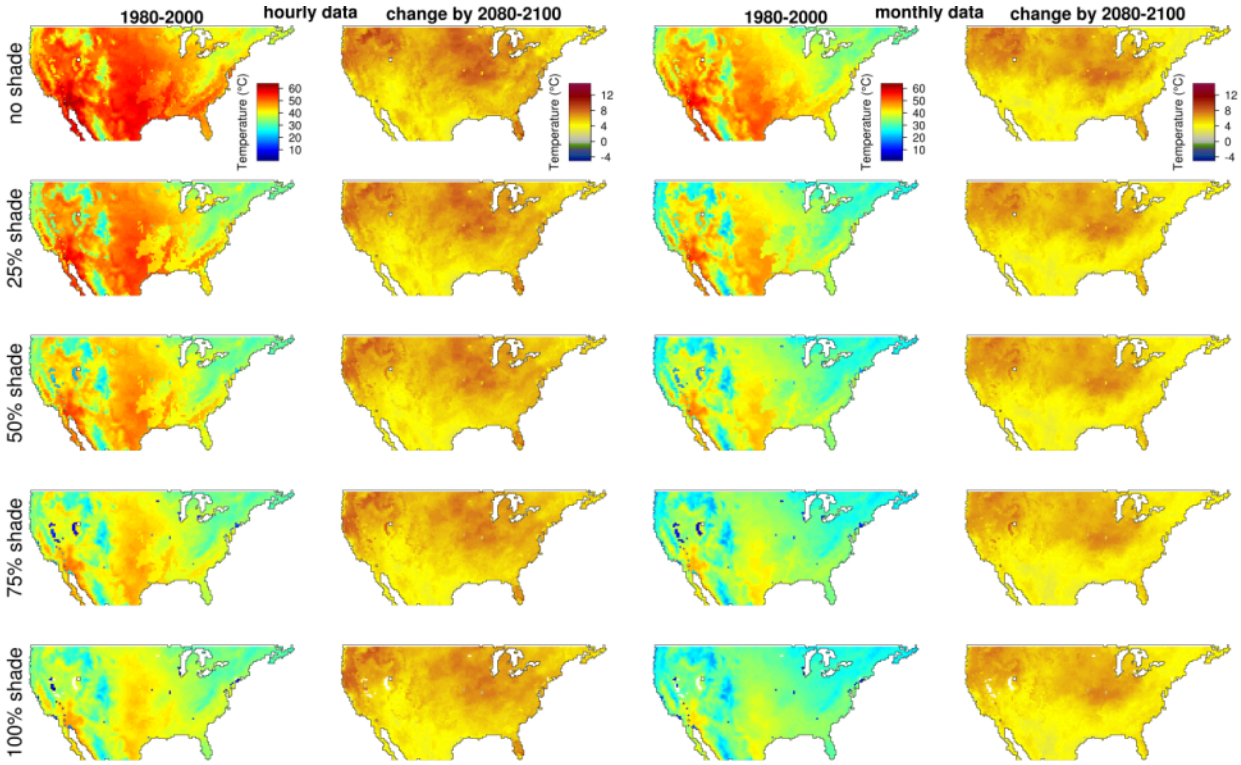

Figure S114: Maximum soil temperature during nesting under monthly and hourly data during past (1980-2000) climate and the predicted change in the future (2080-2099). Data are presented for nests laid in July at a depth of 6 cm under different shade conditions. Color scales are the same for figures S101-S128 to enable visual comparison between different combinations of oviposition months and nests depths.

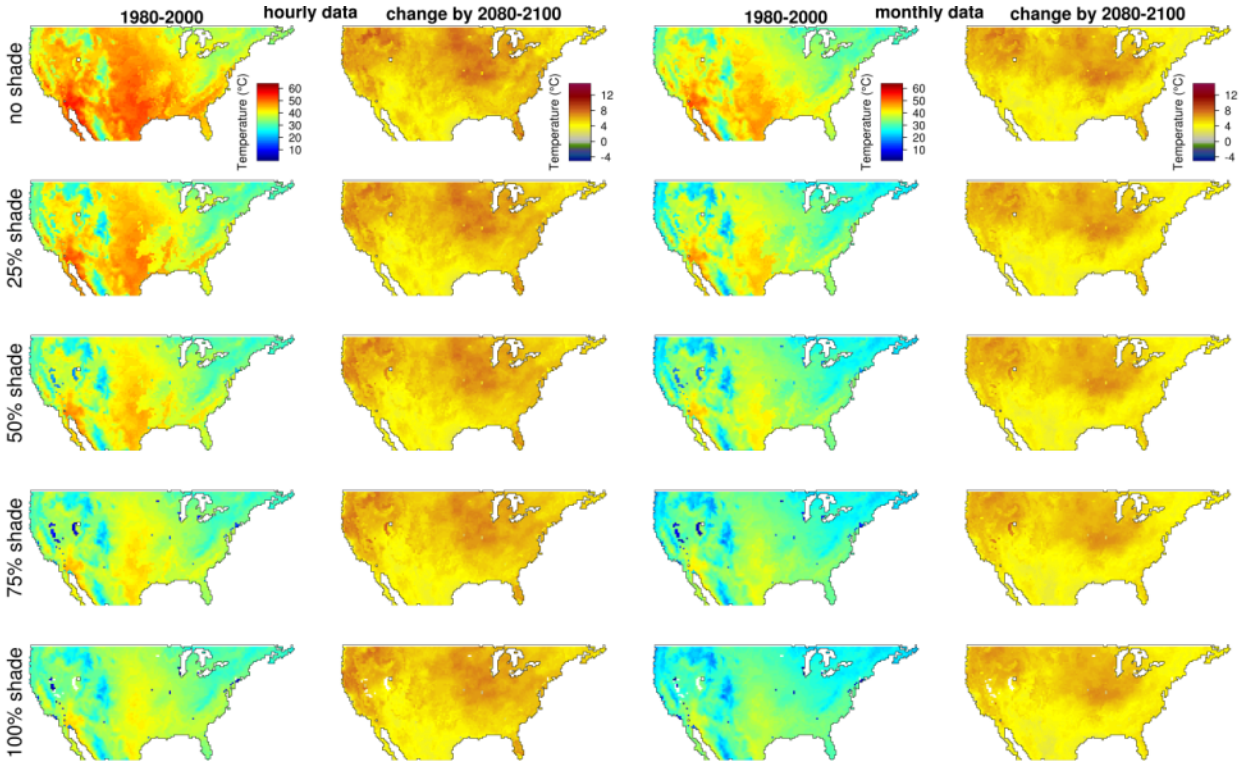

Figure S115: Maximum soil temperature during nesting under monthly and hourly data during past (1980-2000) climate and the predicted change in the future (2080-2099). Data are presented for nests laid in July at a depth of 9 cm under different shade conditions. Color scales are the same for figures S101-S128 to enable visual comparison between different combinations of oviposition months and nests depths.

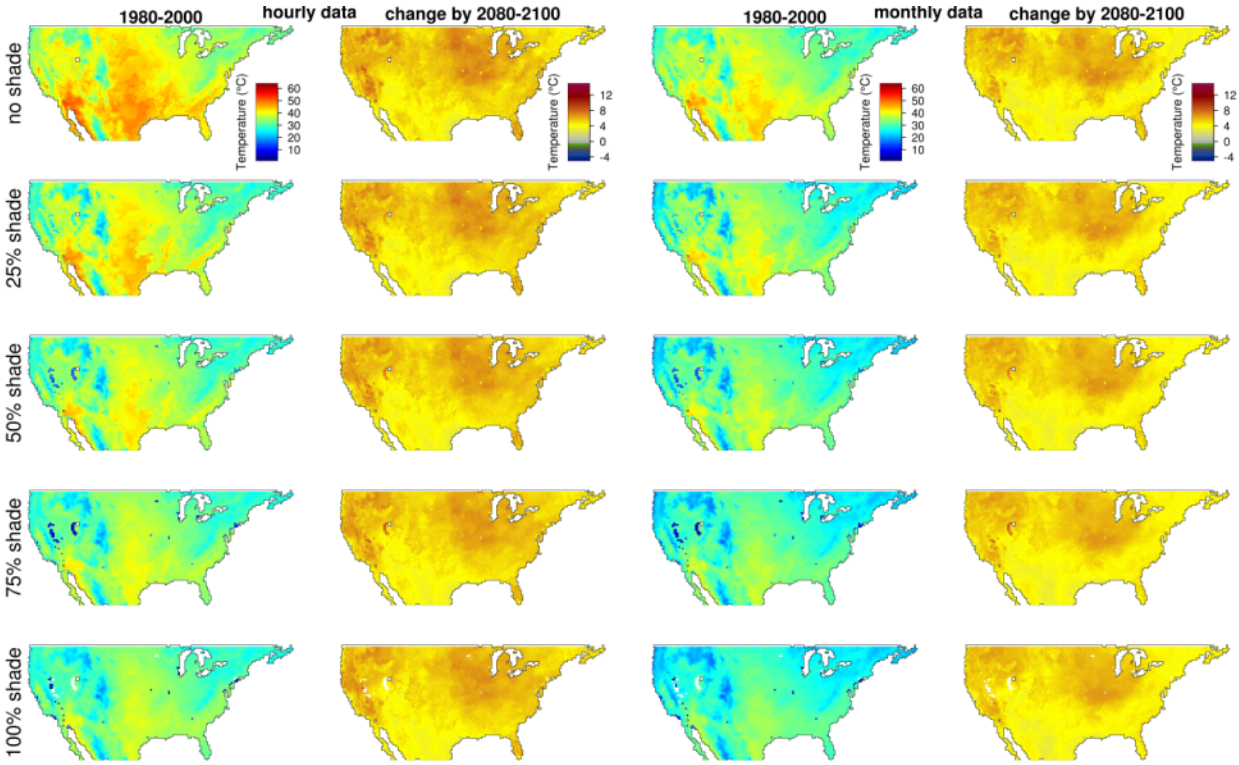

Figure S116: Maximum soil temperature during nesting under monthly and hourly data during past (1980-2000) climate and the predicted change in the future (2080-2099). Data are presented for nests laid in July at a depth of 12 cm under different shade conditions. Color scales are the same for figures S101-S128 to enable visual comparison between different combinations of oviposition months and nests depths.

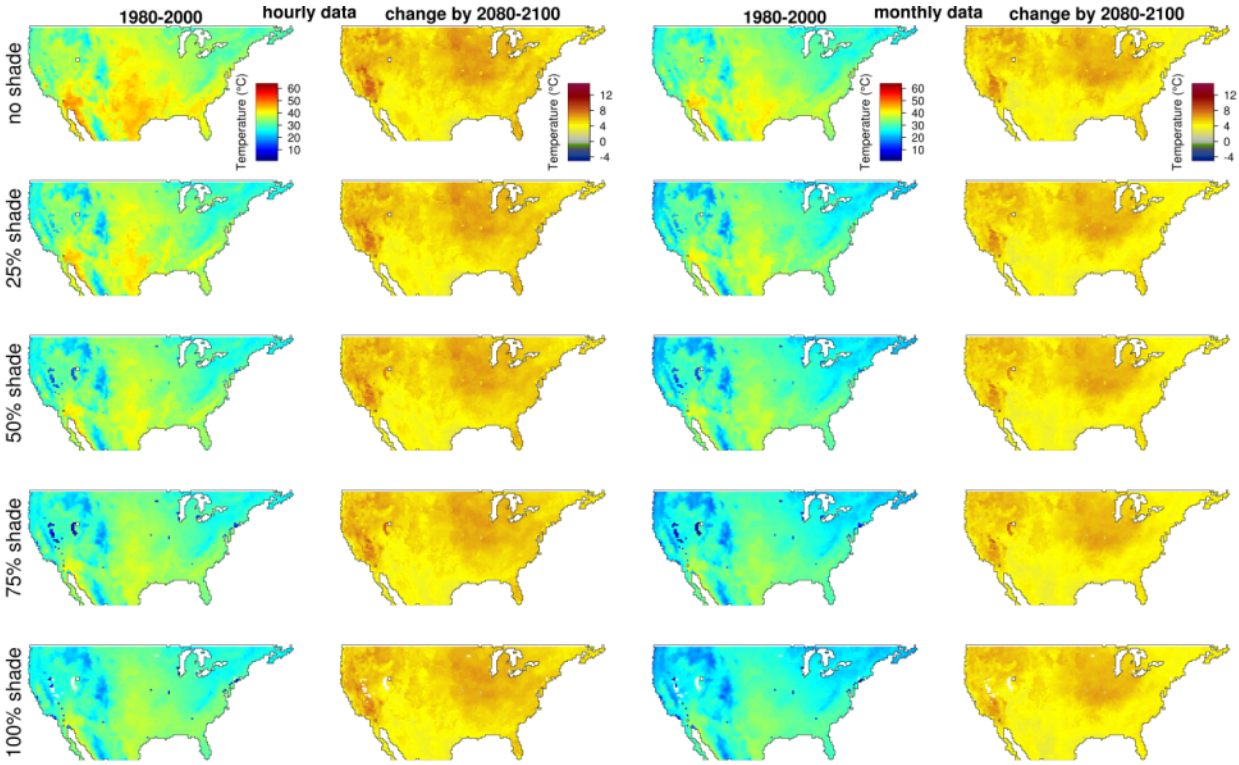

Figure S117: Maximum soil temperature during nesting under monthly and hourly data during past (1980-2000) climate and the predicted change in the future (2080-2099). Data are presented for nests laid in August at a depth of 3 cm under different shade conditions. Color scales are the same for figures S101-S128 to enable visual comparison between different combinations of oviposition months and nests depths.

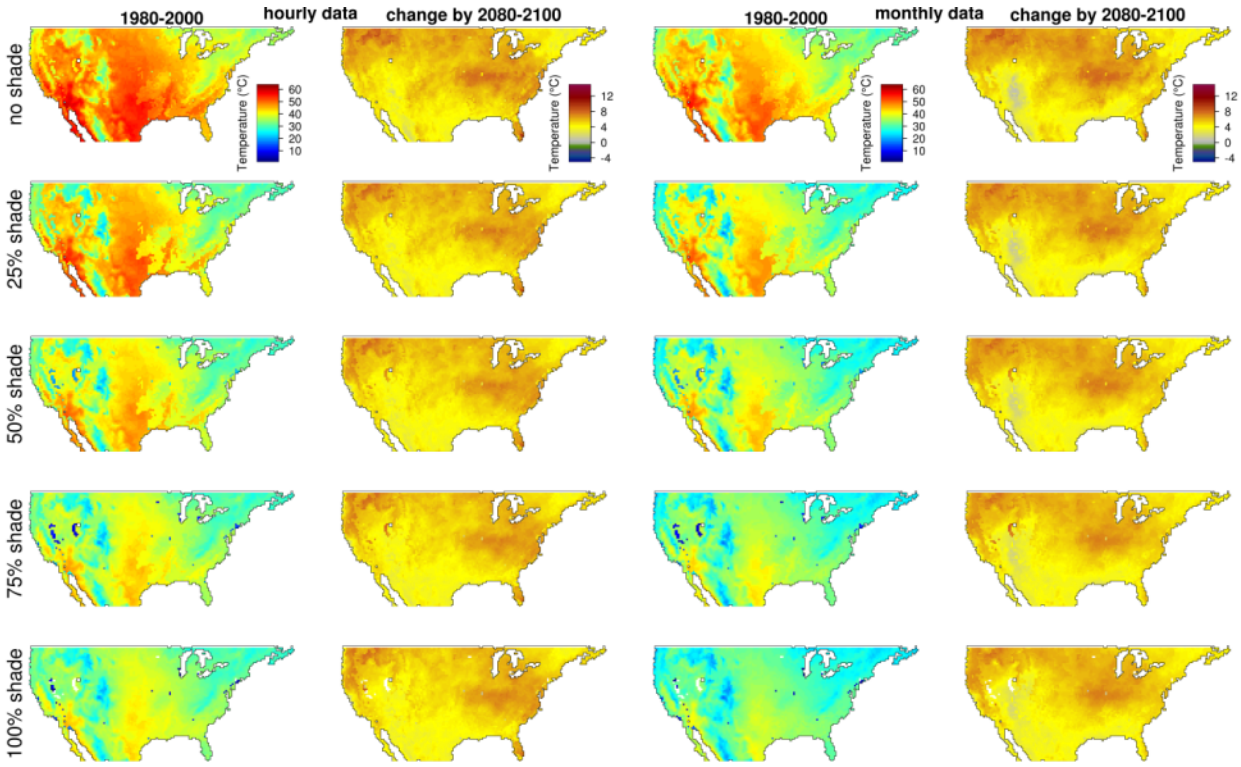

Figure S118: Maximum soil temperature during nesting under monthly and hourly data during past (1980-2000) climate and the predicted change in the future (2080-2099). Data are presented for nests laid in August at a depth of 6 cm under different shade conditions. Color scales are the same for figures S101-S128 to enable visual comparison between different combinations of oviposition months and nests depths.

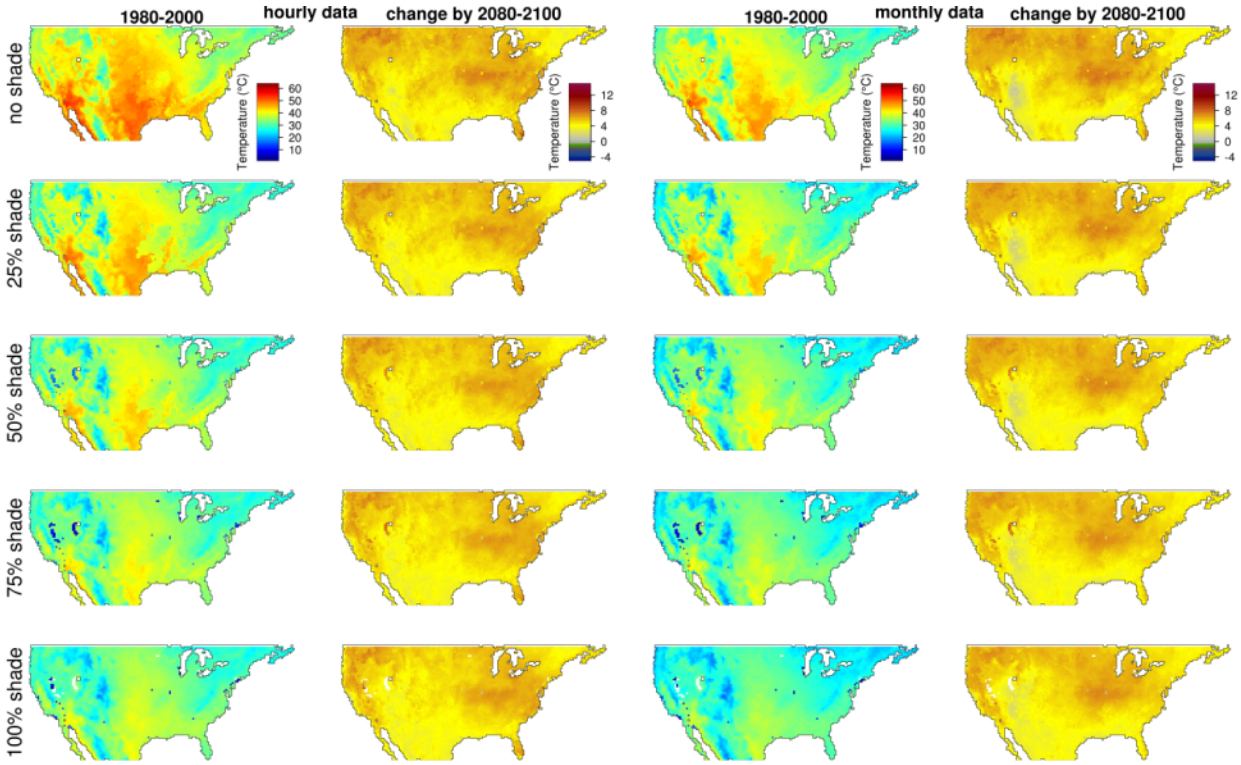

Figure S119: Maximum soil temperature during nesting under monthly and hourly data during past (1980-2000) climate and the predicted change in the future (2080-2099). Data are presented for nests laid in August at a depth of 9 cm under different shade conditions. Color scales are the same for figures S101-S128 to enable visual comparison between different combinations of oviposition months and nests depths.

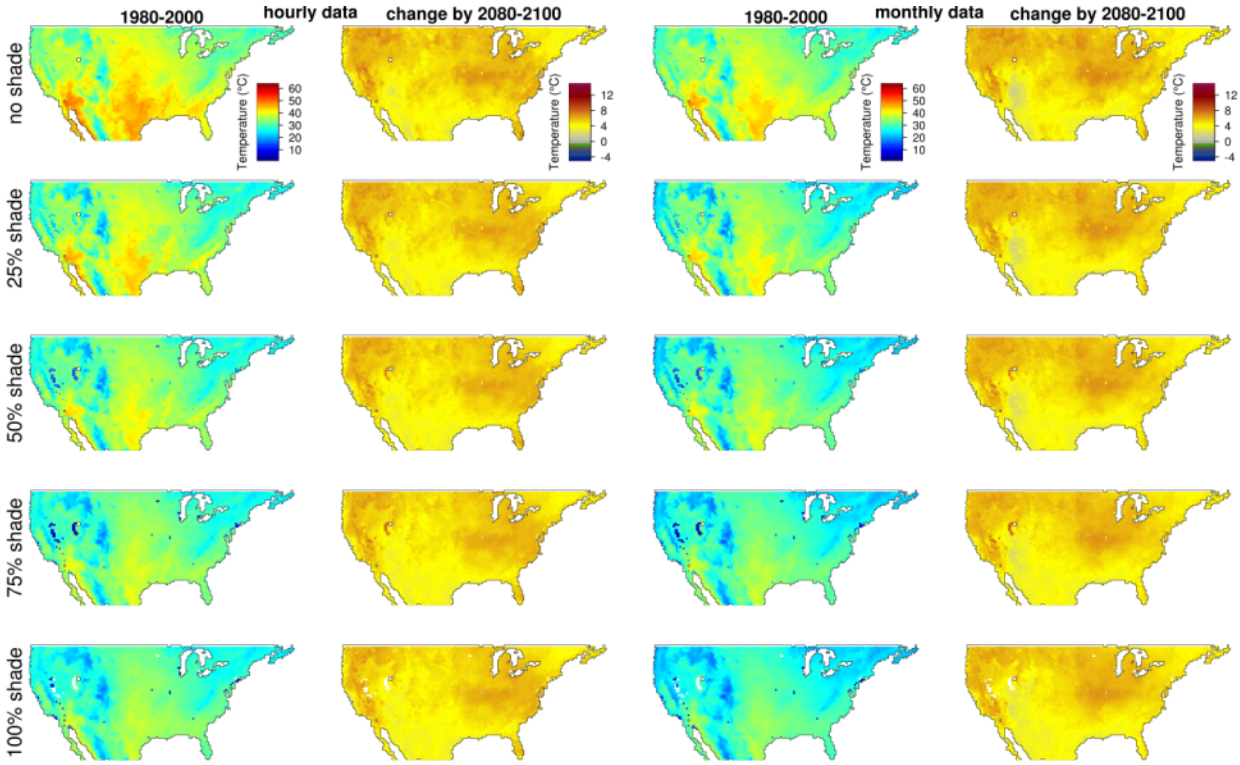

Figure S120: Maximum soil temperature during nesting under monthly and hourly data during past (1980-2000) climate and the predicted change in the future (2080-2099). Data are presented for nests laid in August at a depth of 12 cm under different shade conditions. Color scales are the same for figures S101-S128 to enable visual comparison between different combinations of oviposition months and nests depths.

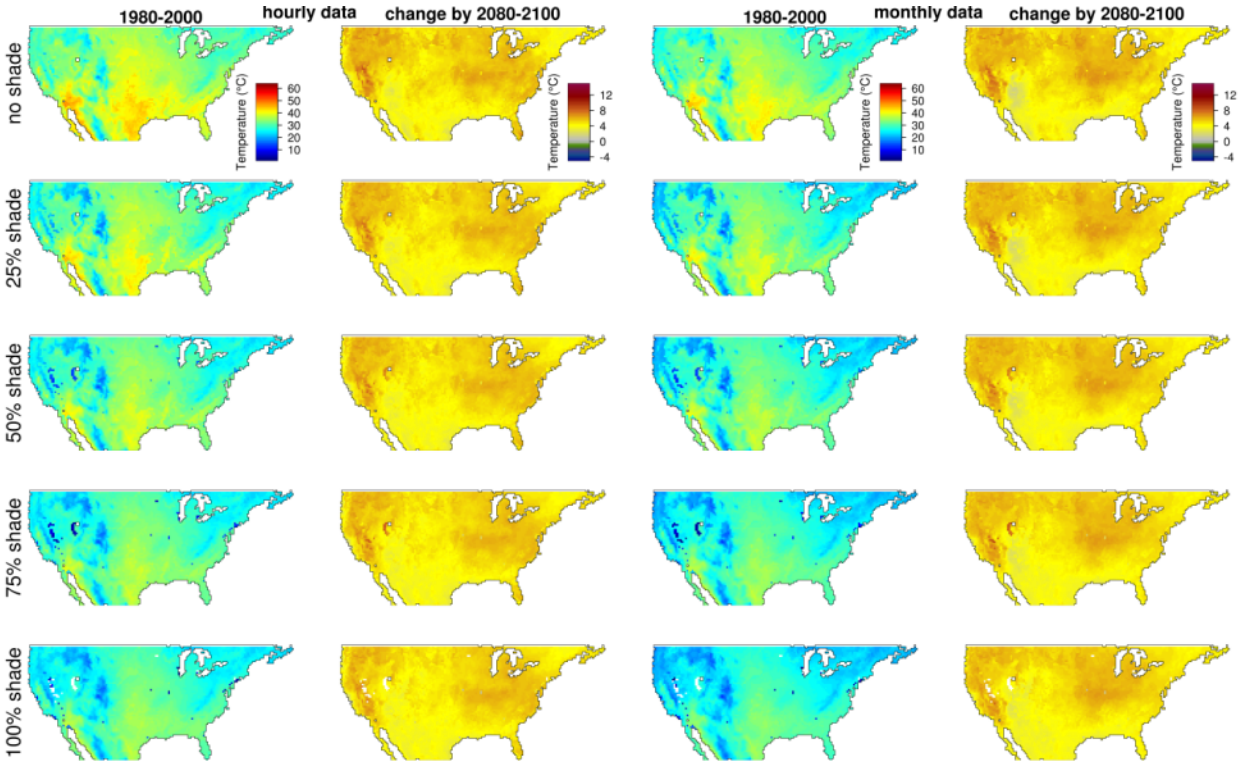

Figure S121: Maximum soil temperature during nesting under monthly and hourly data during past (1980-2000) climate and the predicted change in the future (2080-2099). Data are presented for nests laid in September at a depth of 3 cm under different shade conditions. Color scales are the same for figures S101-S128 to enable visual comparison between different combinations of oviposition months and nests depths.

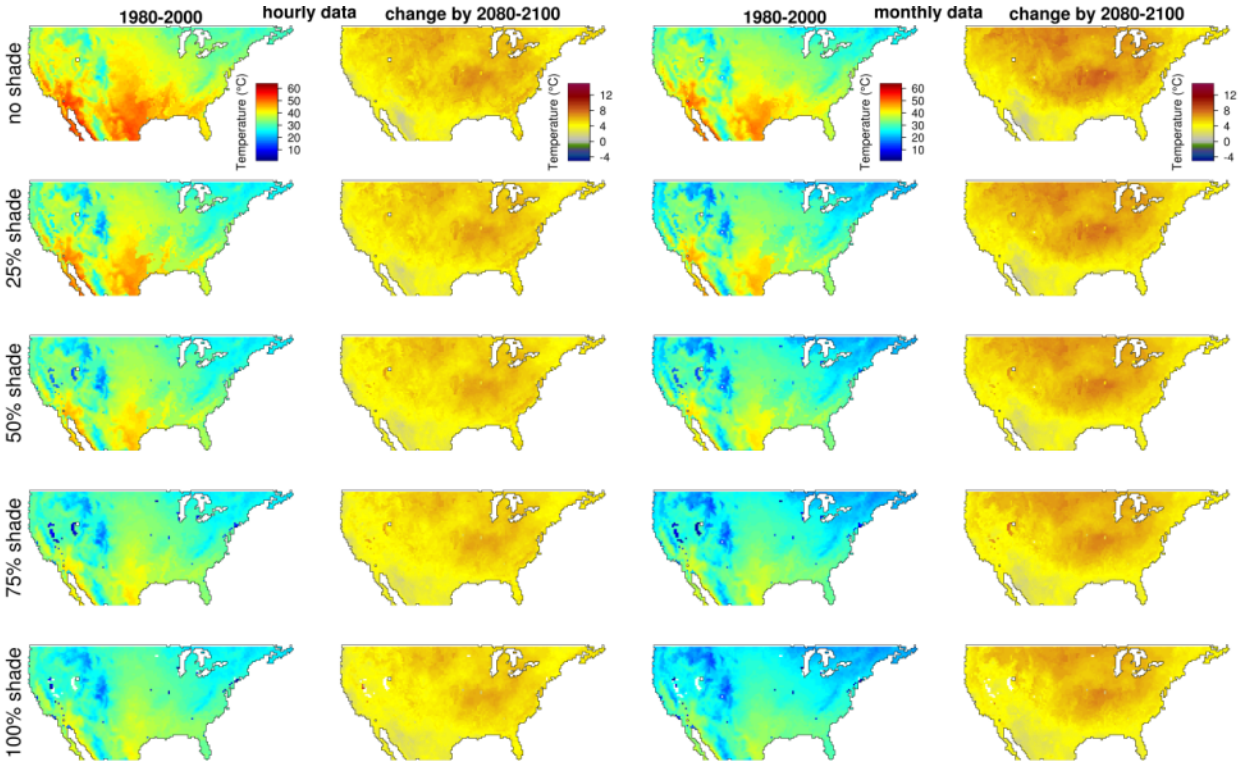

Figure S122: Maximum soil temperature during nesting under monthly and hourly data during past (1980-2000) climate and the predicted change in the future (2080-2099). Data are presented for nests laid in September at a depth of 6 cm under different shade conditions. Color scales are the same for figures S101-S128 to enable visual comparison between different combinations of oviposition months and nests depths.

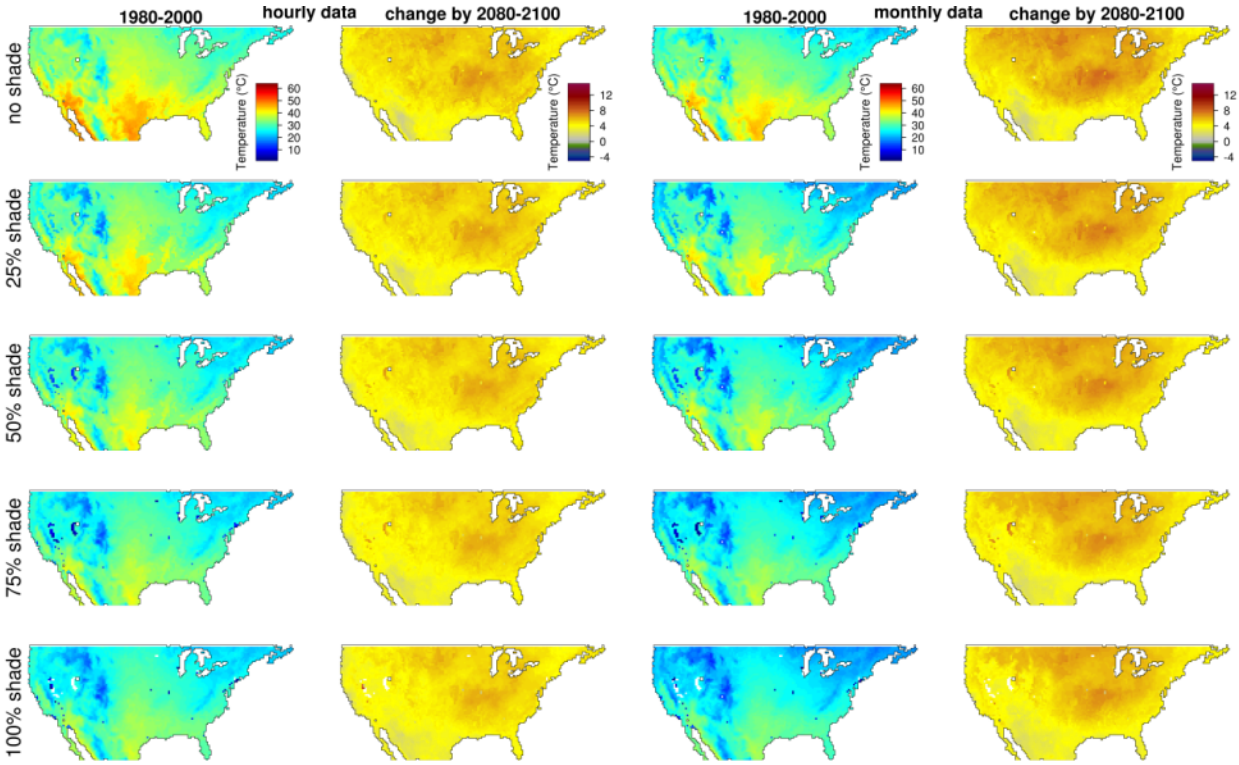

Figure S123: Maximum soil temperature during nesting under monthly and hourly data during past (1980-2000) climate and the predicted change in the future (2080-2099). Data are presented for nests laid in September at a depth of 9 cm under different shade conditions. Color scales are the same for figures S101-S128 to enable visual comparison between different combinations of oviposition months and nests depths.

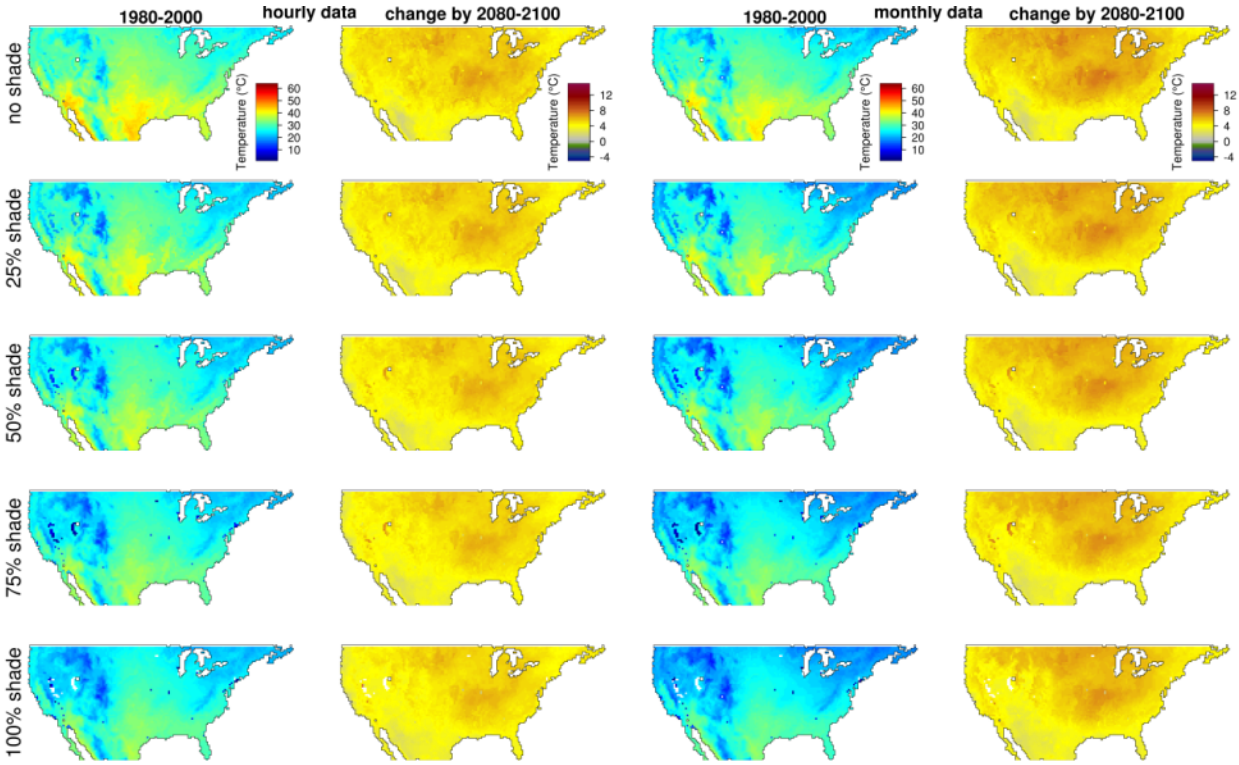

Figure S124: Maximum soil temperature during nesting under monthly and hourly data during past (1980-2000) climate and the predicted change in the future (2080-2099). Data are presented for nests laid in September at a depth of 12 cm under different shade conditions. Color scales are the same for figures S101-S128 to enable visual comparison between different combinations of oviposition months and nests depths.

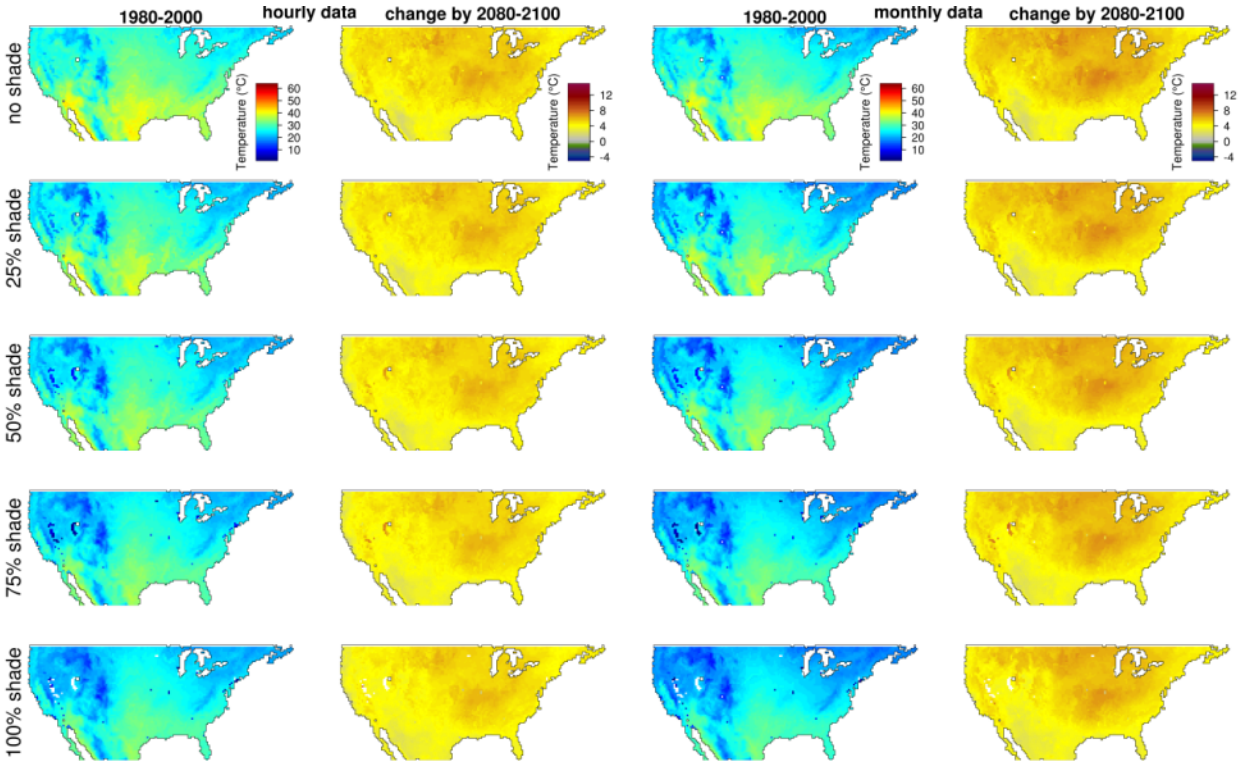

Figure S125: Maximum soil temperature during nesting under monthly and hourly data during past (1980-2000) climate and the predicted change in the future (2080-2099). Data are presented for nests laid in October at a depth of 3 cm under different shade conditions. White areas represent locations for which climate conditions did not enable enough activity to promote reproduction. Color scales are the same for figures S101-S128 to enable visual comparison between different combinations of oviposition months and nests depths.

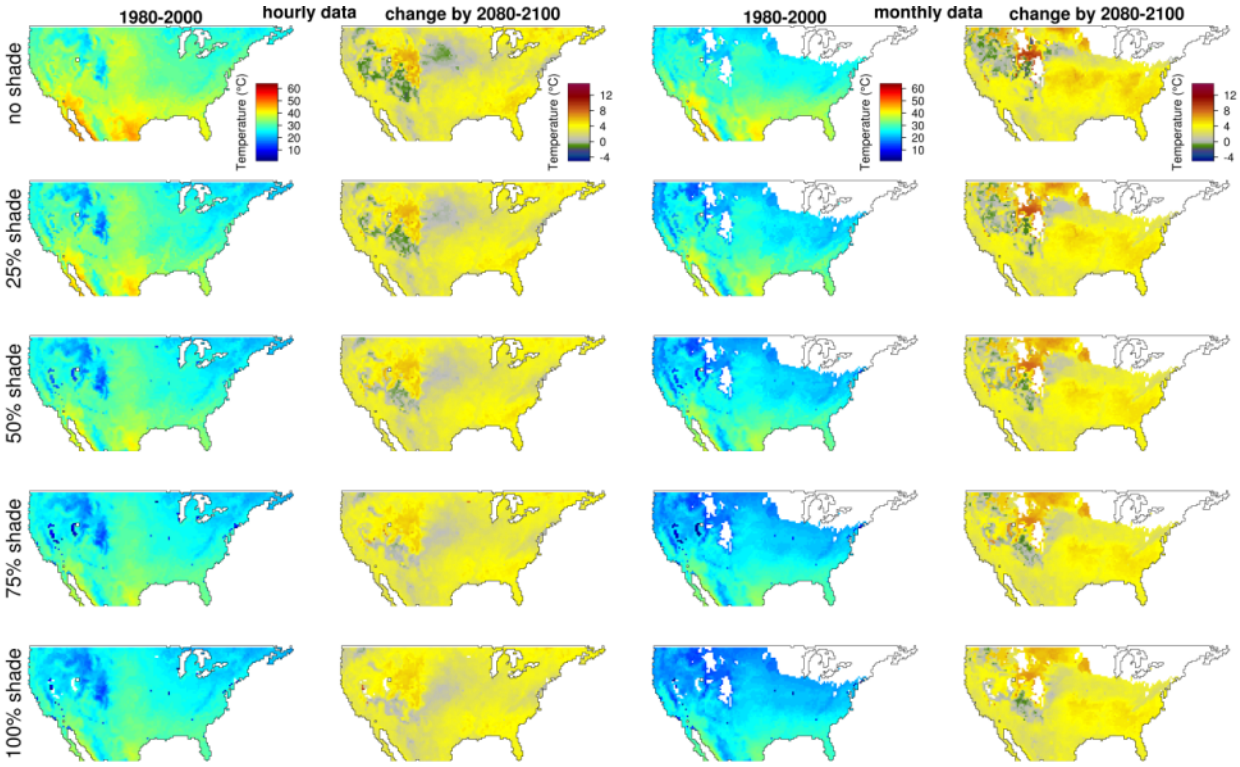

Figure S126: Maximum soil temperature during nesting under monthly and hourly data during past (1980-2000) climate and the predicted change in the future (2080-2099). Data are presented for nests laid in October at a depth of 6 cm under different shade conditions. White areas represent locations for which climate conditions did not enable enough activity to promote reproduction. Color scales are the same for figures S101-S128 to enable visual comparison between different combinations of oviposition months and nests depths.

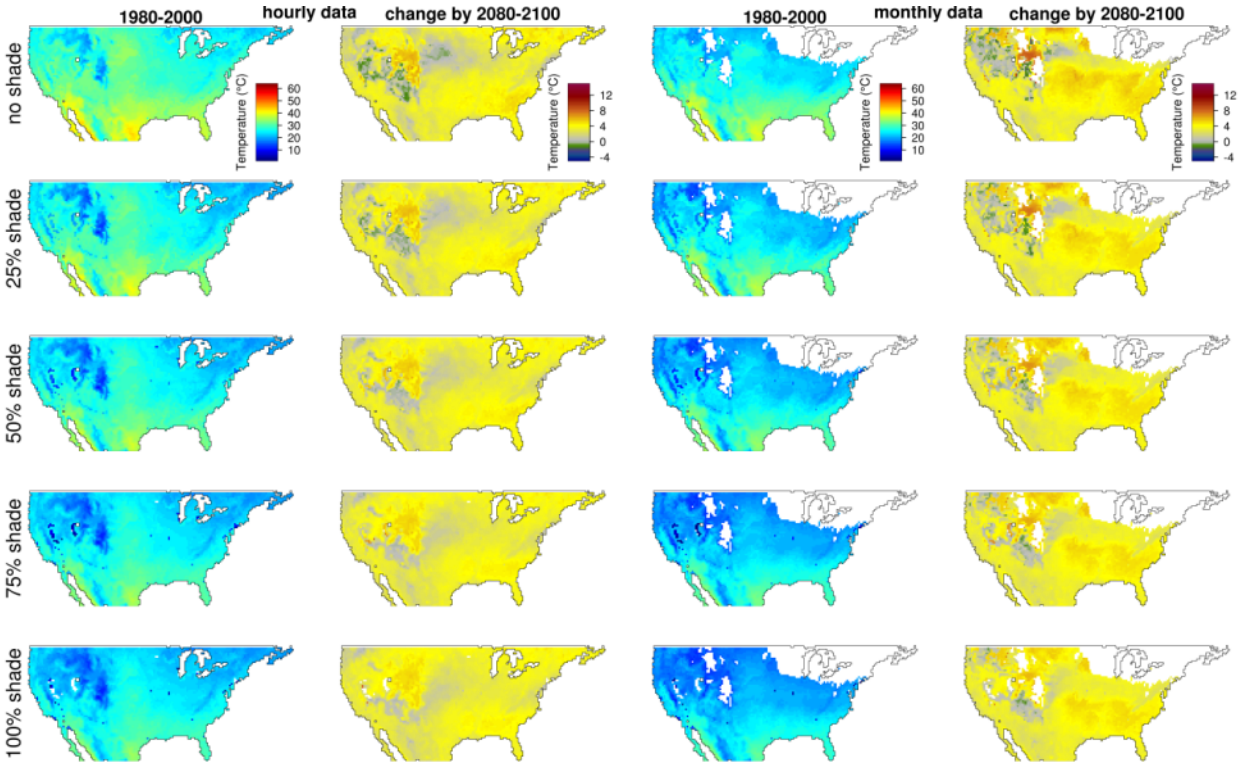

Figure S127: Maximum soil temperature during nesting under monthly and hourly data during past (1980-2000) climate and the predicted change in the future (2080-2099). Data are presented for nests laid in October at a depth of 9 cm under different shade conditions. White areas represent locations for which climate conditions did not enable enough activity to promote reproduction. Color scales are the same for figures S101-S128 to enable visual comparison between different combinations of oviposition months and nests depths.

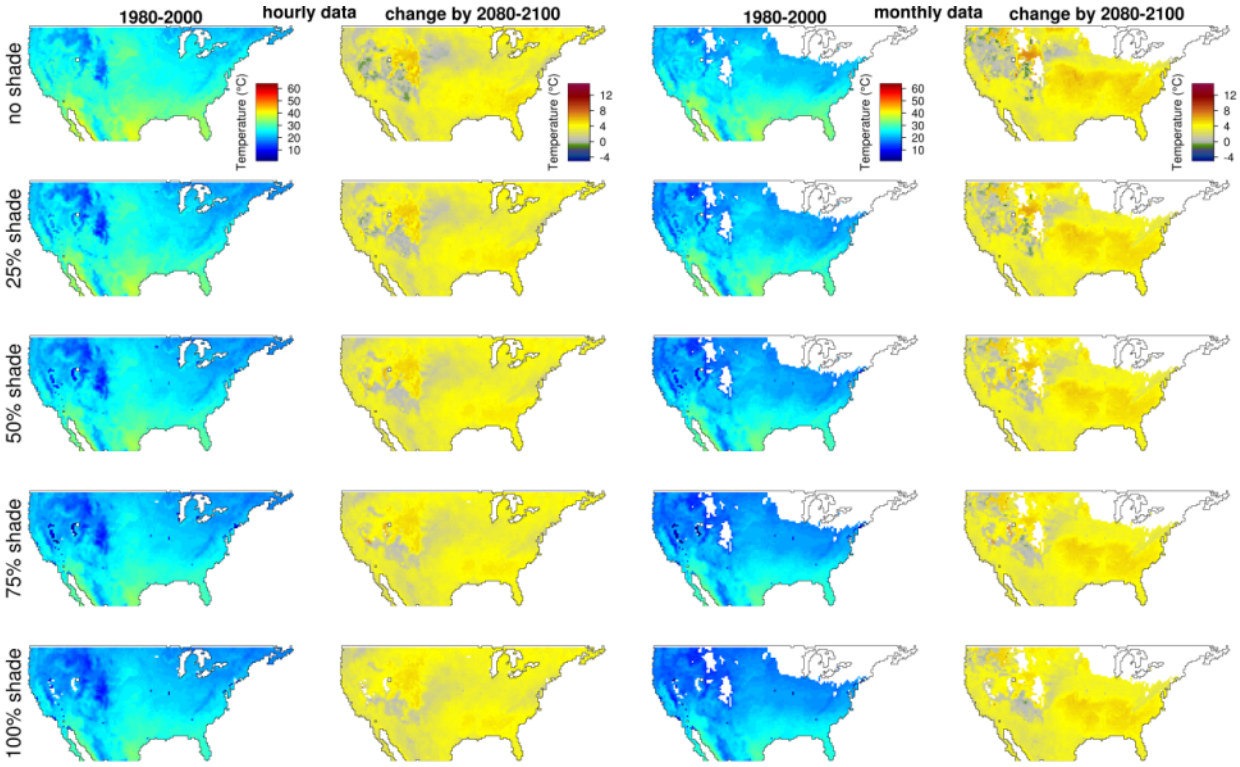

Figure S128: Maximum soil temperature during nesting under monthly and hourly data during past (1980-2000) climate and the predicted change in the future (2080-2099). Data are presented for nests laid in October at a depth of 12 cm under different shade conditions. White areas represent locations for which climate conditions did not enable enough activity to promote reproduction. Color scales are the same for figures S101-S128 to enable visual comparison between different combinations of oviposition months and nests depths.

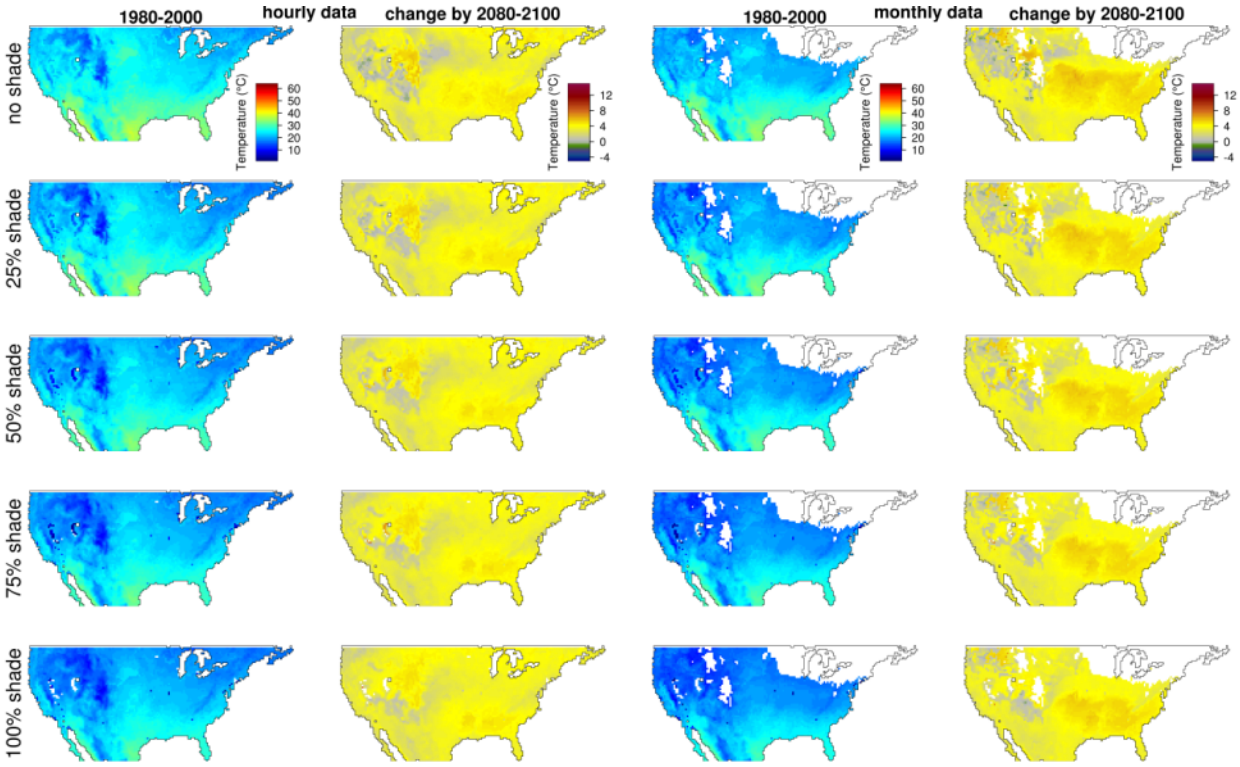

Figure S129: Probability density functions of skill scores for air temperature and specific humidity at 2 m, and wind velocities at 10 m.

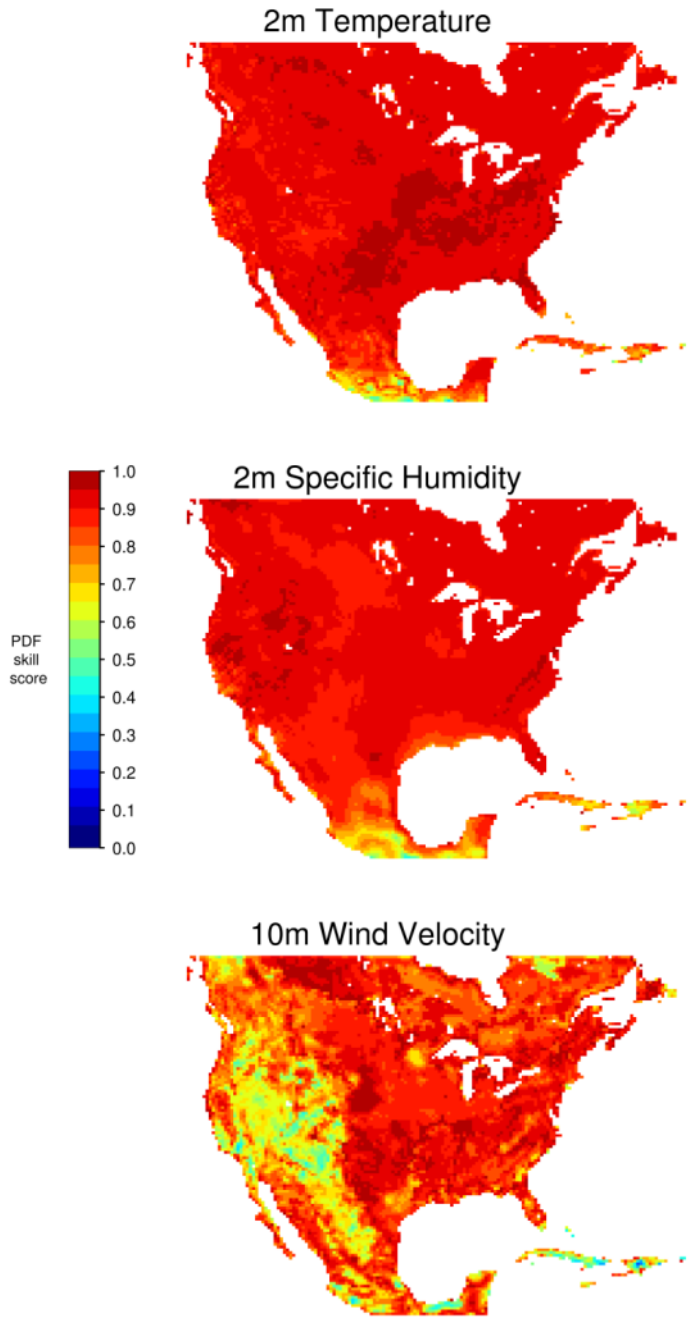

Figure S130: Frequency distributions of the probability density functions depicted in Figure S129.

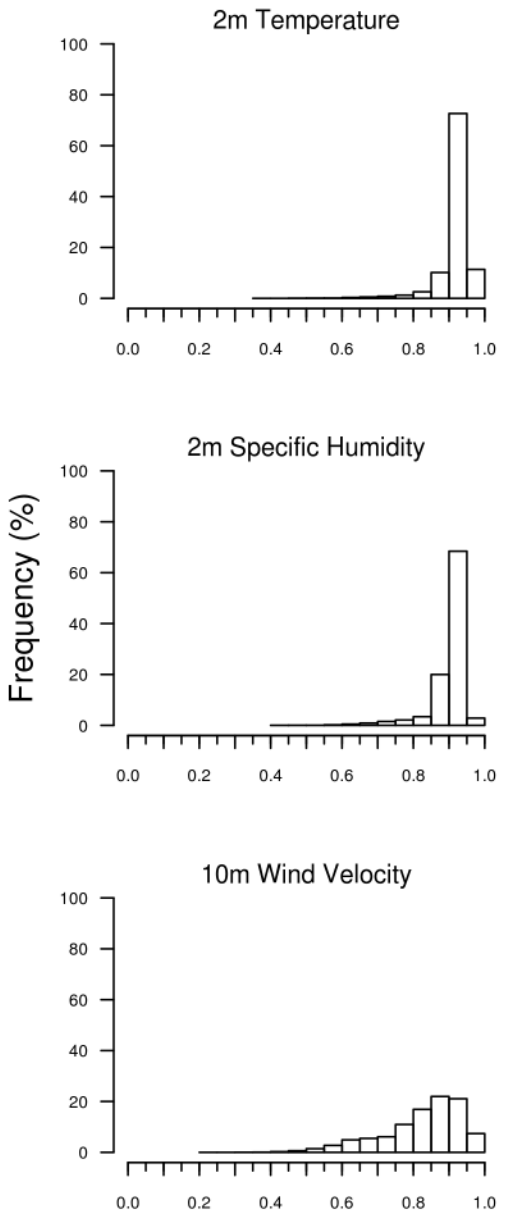

Figure S131: Probability density functions of skill scores and the biases for minimum and maximum air temperature were derived from data gathered in stations and by our microclimate simulation.

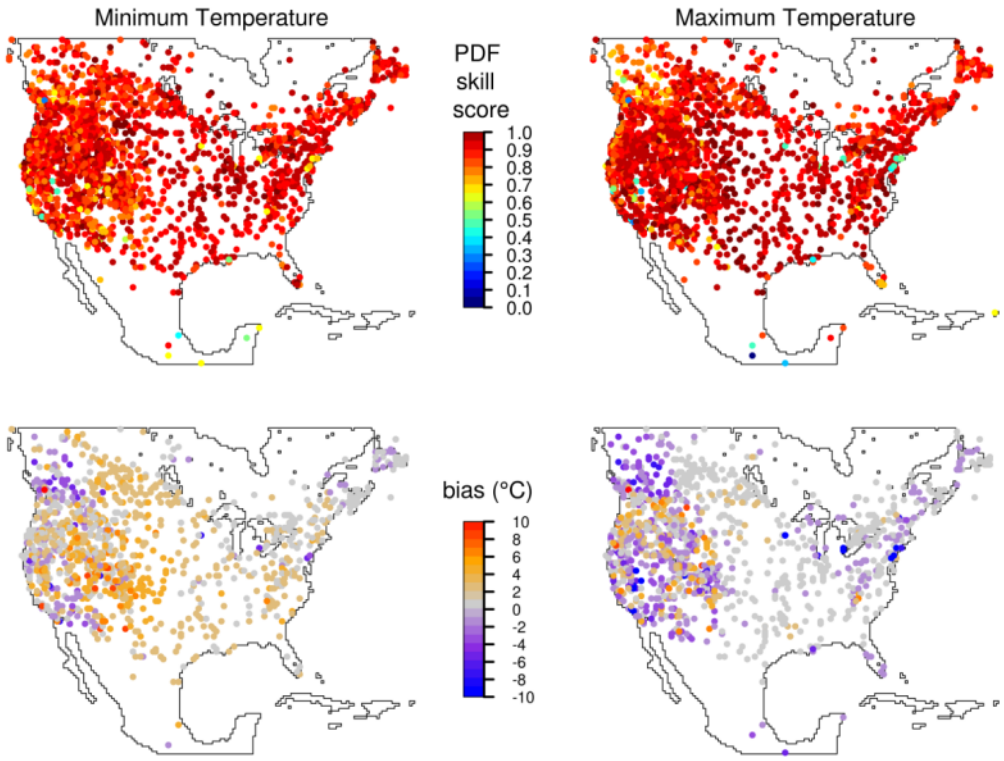

Figure S132: Probability density functions of skill scores and the biases for minimum and maximum soil temperature were derived from data gathered in stations and by our microclimate simulation.

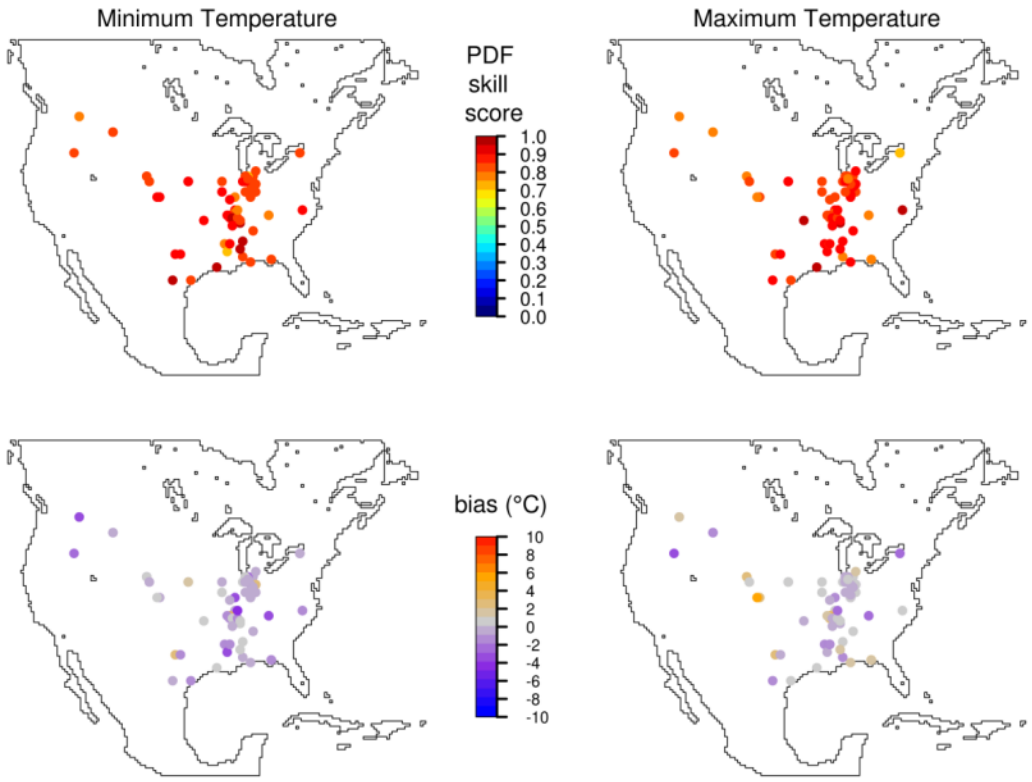

Figure S133: Temperature differences between open and fully shaded ground surfaces' minimum and maximum temperatures were derived from our microclimate simulation.

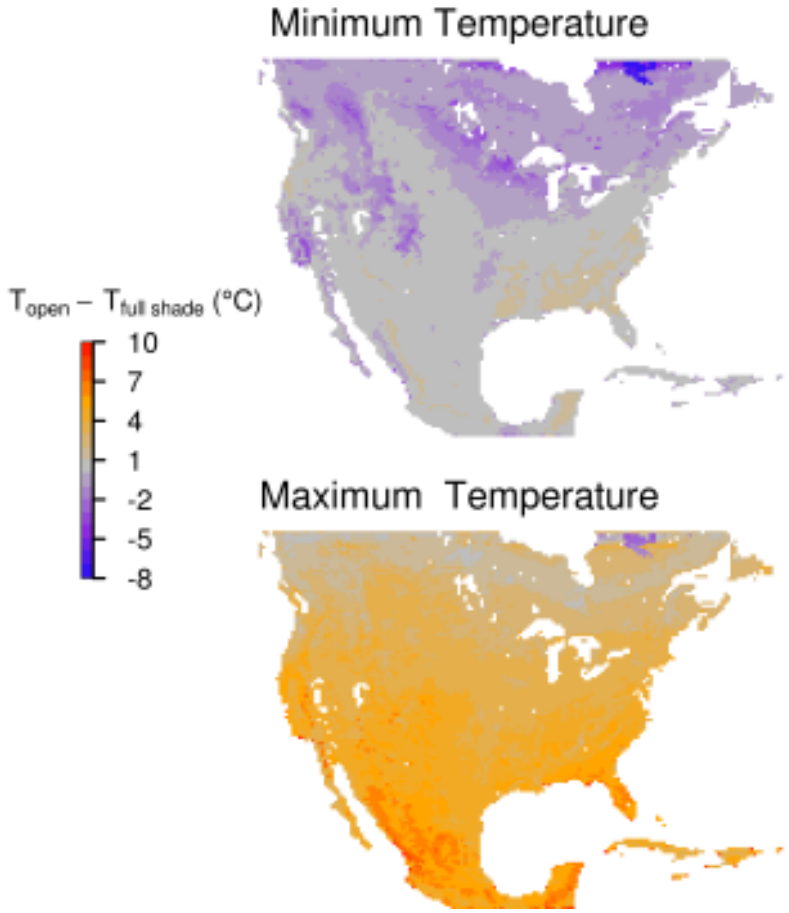

Figure S134: Frequency distributions of temperature differences between open and fully shaded ground surfaces' minimum and maximum temperatures as shown in Figure S123.